THE PATHOBIOLOGY OF PEDIATRIC B-CELL PRECURSOR ACUTE LYMPHOBLASTIC LEUKEMIA

Elisabeth M.P. Steeghs

The pathobiology of pediatric B-cell precursor acute lymphoblastic leukemia

ISBN 978-94-92801-35-7

Lay-out: Lieneke Steeghs

Cover design: Guus Gijben, proefschrift-aio.nl

Printing: Guus Gijben, proefschrift-aio.nl

The work described in this thesis was performed at the Department of Pediatric Oncology/Hematology of the Erasmus Medical Center - Sophia Children's Hospital, Rotterdam, the Netherlands. The work was funded by the Netherlands Organisation for Scientific Research (NWO), KiKa (Children Cancer Free), the Dutch Cancer Society, and SKOCR.

Printing of this thesis was financially supported by: SKOCR

THE PATHOBIOLOGY OF PEDIATRIC B-CELL PRECURSOR ACUTE LYMPHOBLASTIC LEUKEMIA

DE PATHOBIOLOGIE VAN VOORLOPER B-CEL ACUTE LYMFATISCHE LEUKEMIE BIJ KINDEREN

Proefschrift

ter verkrijging van den graad van doctor
aan de Erasmus Universiteit Rotterdam
op gezag van de rector magnificus
Prof. dr. H.A.P. Pols

en volgens besluit van het College van Promoties op

woensdag 4 juli 2018 om 11:30 uur

door

Elisabeth Maria Petronella Steeghs
geboren te Oirlo

Erasmus University Rotterdam

Promotiecommissie

Promoteren:	Prof. dr. M. L. den Boer
	Prof. dr. R. Pieters
Overige leden:	Prof. dr. H.G.P. Raaijmakers
	Prof. dr. C.M. Zwaan
	Prof. dr. J.J.C. Neefjes

TABLE OF CONTENTS

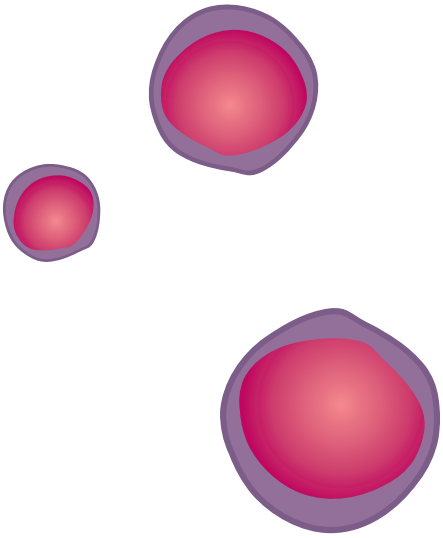

Chapter 1

GENERAL INTRODUCTION

Hematopoiesis

Hematopoietic stem cells (HSCs) give rise to all lineages of blood cells, which include thrombocytes (required for blood clotting), red blood cells (responsible for oxygen transport), and leukocytes (responsible for defense against pathogens). Importantly, HSCs also have the capacity of self-renewal and thereby the process of hematopoiesis is a lifelong process. After birth, hematopoiesis occurs mainly in the bone marrow. However, during fetal development HSCs reside in different niches, including the yolk sac, liver, and spleen.[1,2] HSCs give rise to lymphoid and myeloid progenitor cells, which further maturate (differentiate) into all blood cell types (Figure 1). During the process of differentiation, blood cells gain more functionality at the expense of their proliferative potency. These features keep the process of hematopoiesis in balance. Proliferation and differentiation are tightly controlled by different factors, including transcription factors (e.g. *IKZF1*) and micro-environmental factors (e.g. cytokines and growth factors).

Leukemia

In leukemia the process of normal hematopoiesis is disturbed. Proliferation, differentiation and cell death of the different blood cells types are no longer in balance. Disturbance of these processes result in the expansion of malignant leukocytes, also called blasts, at the expense of healthy blood cells. Leukemia can be classified based on the origin of progenitor cell, i.e. myeloid or lymphoid. Furthermore, classification is based on the onset of the disease: acute or chronic. Acute leukemia displays a fast rise and is characterized by an uncontrolled high proliferation of blasts with an immature phenotype. Chronic leukemia on the other hand has a mature phenotype. Therefore these blasts can also perform of their 'normal' functions, resulting in a more slow onset.

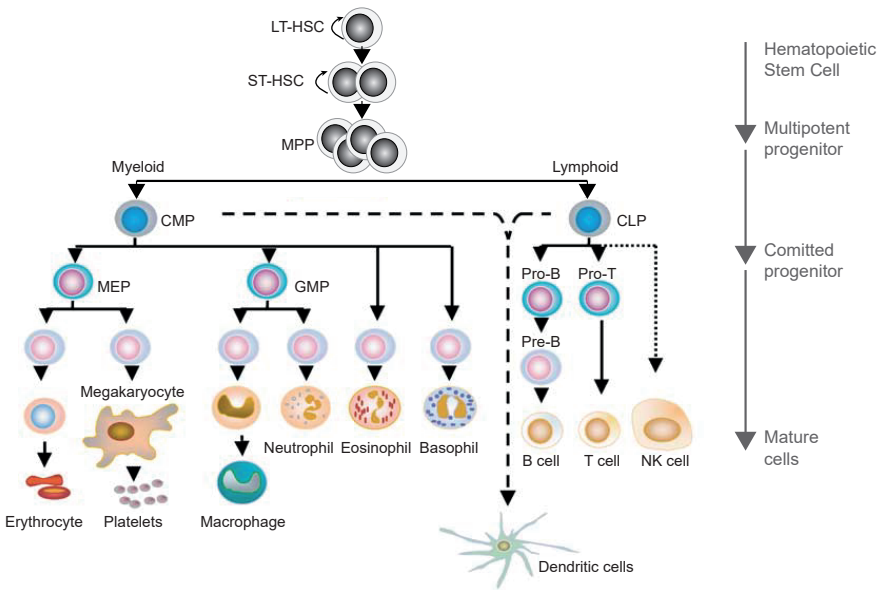

Figure 1. Schematic overview of hematopoiesis. Adapted from Larsson et al.[3]

Acute lymphoblastic leukemia (ALL) is the most common childhood malignancy. In the Netherlands approximately 125 children are diagnosed with the disease every year. Survival rates show an remarkable improve during the last decades: in the early 1960 cure rate was approximately 10% whereas nowadays approximately 90% of the patients can be cured (Figure 2). Despite this dramatic increase in outcome, this still means that one out of the ten children diagnosed with ALL cannot be cured. Pediatric ALL is heterogeneous disease, caused by the malignant transformation of either T-cell (T-ALL,~15% of the cases) or B-cell progenitors (BCP-ALL, ~85% of the cases). The scope this thesis is on pediatric BCP-ALL.

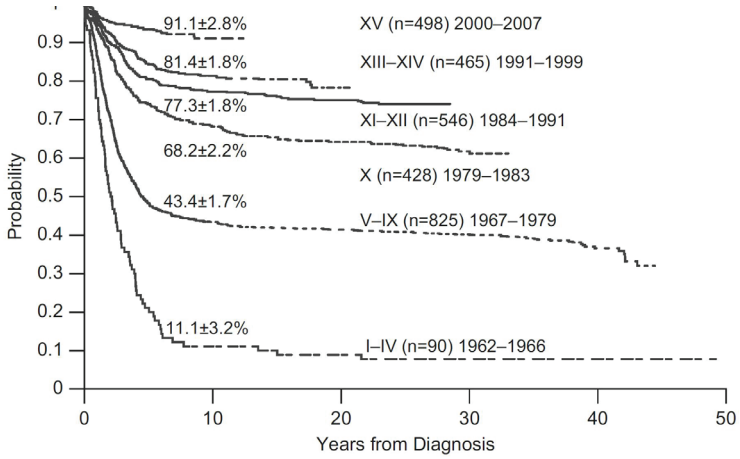

Figure 2. Survival of 2852 children with newly diagnosed ALL between 1962 and 2007.[4]

B-cell development and the bone marrow microenvironment

The bone marrow microenvironment plays a crucial role in the development and differentiation of HSCs. This niche consists of hematopoietic and non-hematopoietic cells. Mesenchymal stromal cells (MSCs), non-hematopoietic cells, play an important role in the regulation of HSC differentiation, through both cytokine secretion and direct cell-to-cell communication.[5-7] In addition, the process of maturation is regulated intracellular by transcription factors. These transcription factor create a regulatory network in which activation of the B-cell development genes is ensured and genes involved in the commitment to other lineages are silenced. Key regulators of normal B-cell development include *ERG*, *IKZF1*, *EBF1*, and *PAX5*, as shown in Figure 3.[8]

HSCs generally remain in a quiescent, dormant, state, close to the endosteal (inner) surface of the bone. Thereby they preserve self-renewing capacity and prevent stem cell exhaustion. During maturation progenitor cells migrate from the endosteal niche to the vascular niche (close to the blood vessels).[7,9] B cell maturation can be subdivided in several stages, characterized by rearrangement status of the immunoglobulin heavy and light chains. This recombination process gives rise to an extensive (unique) receptor repertoire. Additionally, migration of progenitors cells through the bone marrow microenvironment, enables interaction of these cells with different niches.

Leukemic cells also reside in the bone marrow microenvironment. During progression of leukemia, blasts spread at the expense of healthy progenitor cells. Thereby they might take advantages of niche specific signaling or manipulate their microenvironment to promote survival.[10] The importance of the bone marrow microenvironment for leukemic cells is demonstrated by the protection the niche provides against chemotherapeutic agents.[11,12] In *in vitro* assays, MSCs mimic this support of the bone marrow microenvironment.[13-17] Understanding the leukemic cells-niche interaction is important for targeting this process in the treatment of leukemia.

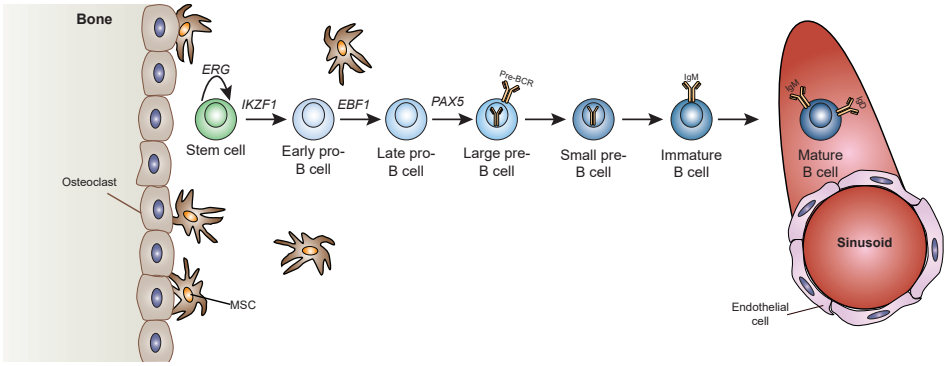

Figure 3. Schematic overview of maturation of B cells and the bone marrow microenvironment.

Pathobiology of B-cell Precursor Acute Lymphoblastic Leukemia

BCP-ALL is thought to originate from various genetic hits in progenitor B-cells, resulting in their malignant transformation. These lesions include aberrations in genes involved in B-cell development, proliferation, or survival of cells. Aberrations can be defined as point mutations, chromosomal translocations, or alterations in copy numbers affecting specific genes or even whole chromosome(s).[18]

A common mechanism underlying the pathobiology of BCP-ALL cases includes chromosomal translocations. Two segments from different chromosomes are rearranged, resulting in novel (altered) chromosomes. Consequently, genes that are located on the translocated part of the chromosomes are placed in a new environment. This can result in the fusion of two different genes, forming one new fusion gene. The t(12;21) rearrangement, a translocation between chromosome 12 and 21, is an example of a genetic aberration present in ~28% of BCP-ALL cases. The resulting *ETV6-RUNX1* fusion gene contains a part of the ETV6 gene, a nuclear phosphoprotein that is a member of the ETS family of transcription factors, fused to *RUNX1*, a transcription factor involved in lymphoid and myeloid differentiation. Other chromosomal translocations include t(9;22) and t(1;19), resulting in *BCR-ABL1* and *TCF3-PBX1* translocations, respectively. Both aberrations are detected in a minority of the BCP-ALL cases (3% and 8%, respectively). In addition, approximately 3% of the BCP-ALL cases harbors rearrangements involving the *KMT2A* gene. *KMT2A*, located on chromosome 11, can translocate to different chromosomes (e.g. chromosome 4 and 9), resulting in different fusion genes (e.g. *KMT2A-AF4*, *KMT2A-AF9*). Although this subtype is detected in a minority of BCP-ALL cases, it is a hallmark of infant ALL (age of patients below 366 days).

Chromosomal translocations predominantly contain genes involved in (regulation) of transcription. In this perspective, the *BCR-ABL1* fusion gene is an exception: the tyrosine kinase ABL1 is placed under the control of BCR promoter, resulting in a constitutively active protein tyrosine kinase. Protein tyrosine kinases are enzymes that facilitate the activation of specific proteins via the phosphorylation of select tyrosine residues in these proteins. The *BCR-ABL1* tyrosine kinase activates multiple signaling pathways, involved in proliferation and survival of cells. Unlike transcription factors, tyrosine kinases can be inhibited by precision medicines.[19] Therefore, inhibition of the *BCR-ABL1* fusion protein by specific tyrosine kinase inhibitors (e.g. imatinib) offers an attractive treatment strategy in these cases.

Besides chromosomal rearrangements, approximately 28% of the pediatric BCP-ALL cases is characterized by an increase in chromosomal copy numbers. Presence of more than 50 chromosome is a characteristic of high hyperdiploidy. The remaining group of BCP-ALL patients (~30%) involves genetically unclassified cases (B-other). Recent studies showed that a subgroup of these genetically unclassified cases have a gene expression profile that resembles the profile of *BCR-ABL1*-positive cases, although the *BCR-ABL1* translocation is absent. Therefore these cases are classified as *BCR-ABL1*-like cases.[20,21] Kinase activating lesions (other than *BCR-ABL1*) were identified in a subgroup of these *BCR-ABL1*-like patients.[22,23] For remaining *BCR-ABL1*-like and non-*BCR-ABL1*-like B-other cases, the underlying pathogenesis remains poorly understood. *BCR-ABL1*-like is present in 19% of pediatric BCP-ALL cases, whereas non-*BCR-ABL1*-like B-other BCP-ALL is detected in ~11% of the pediatric cases.

Different subtypes of BCP-ALL are associated with different treatment outcomes. *ETV6-RUNX1*-positive, high hyperdiploid, and *TCF3-PBX1*-positive cases have a favorable prognosis. non-*BCR-ABL1*-like B-other BCP-ALL is associated with an intermediate outcome. *KMT2A*-rearranged, *BCR-ABL1*-positive, and *BCR-ABL1*-like are poor prognostic subtypes (Figure 4).

Although pediatric BCP-ALL is often characterized chromosomal abnormalities, additional lesions need be present to induce overt leukemia.[18] The high frequency of *ETV6-RUNX1* translocation in cord blood samples of healthy neonates compared to the low incidence of

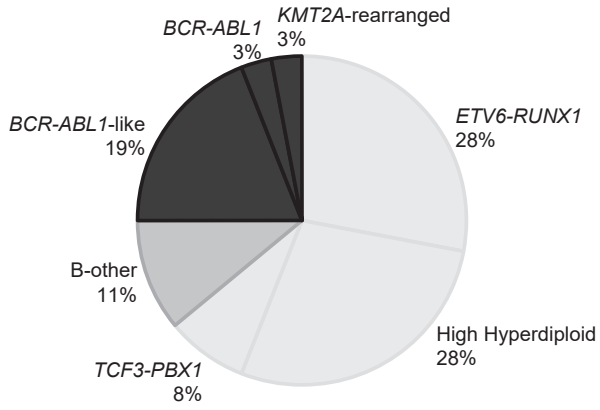

Figure 4. Genetic subtype of pediatric BCP-ALL.

pediatric *ETV6-RUNX1*-positive BCP-ALL indicates the requirement of additional genomic aberrations for the development of leukemia.[24] Copy number alterations (CNAs) in B-cell development genes (e.g. *IKZF1*, *EBF1*, *PAX5*) are an example of additional, cooperating lesions.[20,25] These aberrations affect differentiation and proliferation processes of B-cells and thereby predispose cells for malignant transformation.[26] The *BCR-ABL1* fusion gene also requires additional lesions to develop BCP-ALL, as indicated by a study in a monozygous twin. Identical *BCR-ABL1* genomic translocations were detected in neonatal blood spots of both children. However, only the twin harboring an *IKZF1* deletion developed leukemia.[27]

Taken together, pediatric BCP-ALL can be subdivided in different subtypes, which are associated with different treatment responses and long-term clinical outcome. These subtypes are often characterized by chromosomal translocations. Besides these chromosomal translocations, cooperating lesions (e.g. CNAs) are required to induce an overt leukemia.

Treatment of pediatric ALL

Chemotherapeutic agents that are currently used for the treatment of ALL are already in clinic for decades. These drugs are relative aspecific and cause adverse side-effects. The remarkable improve in outcome of BCP-ALL patients was mainly achieved by improved risk stratification and intensification of chemotherapy with these old drug. However, further intensification is not possible due to severe side effects.[4,28] Therefore, new treatment approaches are warranted.

During recent years, evidence increased that the *BCR-ABL1* fusion protein has kinase activity. Specific inhibition of this kinase offered an attractive treatment strategy and therefore led to the development of the selective ABL tyrosine kinase inhibitor imatinib mesylate.[29-31] Introduction of imatinib, combined with intensive chemotherapy, significantly improved prognosis of *BCR-ABL1*-positive patients.[32]

The treatment of newly diagnosed ALL can be divided in several phases (i.e. induction, central nervous system (CNS) prophylaxis, consolidation, intensification, and maintenance).[28] Induction therapy aims to achieve cytomorphological complete remission, meaning that <5% leukemic cells (blasts) can be detected in microscopic slide of the patient's bone marrow sample. A combination of chemotherapeutic agents is used to induce complete remission, in which glucocorticoids, asparaginase, vincristine, and sometimes anthracyclines, have an important role. After this induction therapy, patients receive consolidation therapy containing 6-mercaptopurine, cyclophosphamide, cytarabine, and methotrexate. Subsequently, patients are stratified in risk groups mainly by minimal residual disease (MRD) levels.[28,33,34] During the following intensification and maintenance phase, therapy will be reduced for patients with favorable stratification parameters (standard risk), intensified in patients with medium risk parameters, and strongly intensified in patients at high risk. A combination of chemotherapeutic agents is used to consolidate remission and prevent spread of leukemic cells to the CNS. The intensification phase contains the same drugs as the induction therapy. Finally, maintenance therapy is given for a prolonged period to avoid regrowth of residual leukemic cell, which contains thiopurines and methotrexate complemented dexamethasone and vincristine for medium and high risk patients. Moreover, high risk patients often receive a stem cell transplantation.

In conclusion, the treatment protocol of pediatric BCP-ALL can be subdivided in different phases, which aim to achieve complete remission.

Outline of the thesis

To improve the treatment of BCP-ALL, new targeted approaches are warranted. Therefore, more insight is required in the pathobiology of pediatric BCP-ALL. This thesis aimed to gain insight the pathobiology of genetically unclassified BCP-ALL cases (i.e. *BCR-ABL1*-like and non-*BCR-ABL1*-like B-other) and thereby identify new targets for precision medicines. *BCR-ABL1*-like as well as non-*BCR-ABL1*-like-B-other are large heterogeneous subtypes. The *BCR-ABL1*-like subtype is characterized by enrichment of CNAs in genes involved in B-cell development (e.g. *IKZF1*), intrachromosomal amplification of chromosome 21, and dicentric chromosome (9;20).[20,35] In addition, chromosomal translocations involving ABL (ABL1, ABL2, PDGFRB, CFS1R) or JAK (JAK2, CRLF2, EPOR) class kinases are present in a subgroup of patients.[22,23,36] Like BCR-ABL1, these fusion proteins might offer an attractive target for precision medicines. In **Chapter 2 and 3** we focused on this group of patients. The frequency of ABL or JAK class chromosomal translocations was studied in *BCR-ABL1*-like and non-*BCR-ABL1*-like B-other patients. Moreover, the clinical characteristics of these fusion gene positive patients were studied. Although ABL class inhibitors are already applied in the treatment of BCP-ALL for *BCR-ABL1*-positive cases, the effect of JAK inhibitors in BCP-ALL is less well known. In **Chapter 3**, we therefore analyzed the potency of JAK2 kinase inhibition in patients harboring *JAK2* aberrations (translocations and point mutations). Unfortunately, in only a minority (18%) of the *BCR-ABL1*-like cases tyrosine kinase translocations are detected. For the remaining group of *BCR-ABL1*-like and non-*BCR-ABL1*-like B-other patients, no druggable targets have yet been identified. To gain insights in the pathobiology of these cases, gene expression profiles were analyzed of a large cohort of BCP-ALL cases. These analyses revealed *STAP1* to be highly expressed in a subgroup of *BCR-ABL1*-like and non-*BCR-ABL1*-like B-other patients. Previous reports hint that *STAP1* is involved in the B-cell receptor (BCR) signaling cascade. Indeed pathway analysis showed an association between high expression levels of *STAP1* and precursor BCR (pre-BCR) signaling genes.[37,38] In **Chapter 4**, we studied the role of STAP1 in BCP-ALL cell survival, as well as the association between STAP1 and the pre-BCR signaling cascade. In **Chapter 5**, we studied the frequency and patterns of CNAs in genes involved in lymphoid differentiation, proliferation, cell cycle, and transcription. In this chapter we aimed to gain insight in associations between CNAs, cellular drug resistance, and clinical outcome parameters. In the final research chapter of this thesis we focused on the interaction between leukemic cells and the bone marrow micro-environment (**Chapter 6**). MSCs are key components of the process of hematopoiesis through both cytokine secretion and direct cell-to-cell communication.[5,6] In addition, MSCs protect BCP-ALL cells against chemotherapeutic agents.[13-17] Unraveling this mechanism of protection may provide novel options for therapeutic intervention.

The work presented in this thesis demonstrates the potency of precision medicines in pediatric BCP-ALL, but also shows its limitations. The findings of this thesis and its future directions are discussed in **Chapter 7** and summarized in **Chapter 8** (in English and Dutch).

REFERENCES

1. Boisset JC, Robin C. On the origin of hematopoietic stem cells: progress and controversy. Stem Cell Res. 2012;8(1):1-13.
2. Durand C, Dzierzak E. Embryonic beginnings of adult hematopoietic stem cells. Haematologica. 2005;90(1):100-108.
3. Larsson J, Karlsson S. The role of Smad signaling in hematopoiesis. Oncogene. 2005;24(37):5676-5692.
4. Pui CH, Evans WE. A 50-year journey to cure childhood acute lymphoblastic leukemia. Semin Hematol. 2013;50(3):185-196.
5. Zhang J, Niu C, Ye L, et al. Identification of the haematopoietic stem cell niche and control of the niche size. Nature. 2003;425(6960):836-841.
6. Nagasawa T. Microenvironmental niches in the bone marrow required for B-cell development. Nature Reviews Immunology. 2006;6(2):107-116.
7. Lilly AJ, Johnson WE, Bunce CM. The haematopoietic stem cell niche: new insights into the mechanisms regulating haematopoietic stem cell behaviour. Stem Cells International. 2011;2011:274564.
8. Somasundaram R, Prasad MA, Ungerback J, Sigvardsson M. Transcription factor networks in B-cell differentiation link development to acute lymphoid leukemia. Blood. 2015;126(2):144-152.
9. Park D, Sykes DB, Scadden DT. The hematopoietic stem cell niche. Frontiers in Bioscience. 2012;17:30-39.
10. Raaijmakers MH. Niche contributions to oncogenesis: emERGing concepts and implications for the hematopoietic system. Haematologica. 2011;96(7):1041-1048.
11. McMillin DW, Delmore J, WeisbERG E, et al. Tumor cell-specific bioluminescence platform to identify stroma-induced changes to anticancer drug activity. Nat Med. 2010;16(4):483-489.
12. Lane SW, Scadden DT, Gilliland DG. The leukemic stem cell niche: current concepts and therapeutic opportunities. Blood. 2009;114(6):1150-1157.
13. Polak R, de Rooij B, Pieters R, den Boer ML. B-cell precursor acute lymphoblastic leukemia cells use tunneling nanotubes to orchestrate their microenvironment. Blood. 2015.
14. Iwamoto S, Mihara K, Downing JR, Pui CH, Campana D. Mesenchymal cells regulate the response of acute lymphoblastic leukemia cells to asparaginase. J Clin Invest. 2007;117(4):1049-1057.
15. Vianello F, Villanova F, Tisato V, et al. Bone marrow mesenchymal stromal cells non-selectively protect chronic myeloid leukemia cells from imatinib-induced apoptosis via the CXCR4/CXCL12 axis. Haematologica. 2010;95(7):1081-1089.
16. Baldridge MT, King KY, Goodell MA. Inflammatory signals regulate hematopoietic stem cells. Trends Immunol. 2011;32(2):57-65.
17. Takizawa H, Boettcher S, Manz MG. Demand-adapted regulation of early hematopoiesis in infection and inflammation. Blood. 2012;119(13):2991-3002.
18. Pui CH, Robison LL, Look AT. Acute lymphoblastic leukaemia. Lancet. 2008;371(9617):1030-1043.
19. Dietel M, Johrens K, Laffert MV, et al. A 2015 update on predictive molecular pathology and its role in targeted cancer therapy: a review focussing on clinical relevance. Cancer Gene Ther. 2015;22(9):417-430.
20. Den Boer ML, van Slegtenhorst M, De Menezes RX, et al. A subtype of childhood acute lymphoblastic leukaemia with poor treatment outcome: a genome-wide classification study. Lancet Oncol. 2009;10(2):125-134.
21. Mullighan CG, Su X, Zhang J, et al. Deletion of IKZF1 and prognosis in acute lymphoblastic leukemia. N Engl J Med. 2009;360(5):470-480.
22. Roberts KG, Li Y, Payne-Turner D, et al. Targetable kinase-activating lesions in Ph-like acute lymphoblastic leukemia. N Engl J Med. 2014;371(11):1005-1015.
23. Roberts KG, Morin RD, Zhang J, et al. Genetic alterations activating kinase and cytokine receptor signaling in high-risk acute lymphoblastic leukemia. Cancer Cell. 2012;22(2):153-166.
24. Mori H, Colman SM, Xiao Z, et al. Chromosome translocations and covert leukemic clones are generated during normal fetal development. Proc Natl Acad Sci U S A. 2002;99(12):8242-8247.
25. Mullighan CG, Goorha S, Radtke I, et al. Genome-wide analysis of genetic alterations in acute lymphoblastic leukaemia. Nature. 2007;446(7137):758-764.
26. Hunger SP, Mullighan CG. Acute Lymphoblastic Leukemia in Children. N Engl J Med. 2015;373(16):1541-1552.
27. Cazzaniga G, van Delft FW, Lo Nigro L, et al. Developmental origins and impact of BCR-ABL1 fusion and IKZF1 deletions in monozygotic twins with Ph+ acute lymphoblastic leukemia. Blood. 2011;118(20):5559-5564.
28. Pieters R, de Groot-Kruseman H, Van der Velden V, et al. Successful Therapy Reduction and Intensification for Childhood Acute Lymphoblastic Leukemia Based on Minimal Residual Disease Monitoring: Study ALL10 From the Dutch Childhood Oncology Group. J Clin Oncol. 2016;34(22):2591-2601.
29. Druker BJ, Sawyers CL, Kantarjian H, et al. Activity of a specific inhibitor of the BCR-ABL tyrosine kinase in the blast crisis of chronic myeloid leukemia and acute lymphoblastic leukemia with the Philadelphia chromosome. N Engl J Med. 2001;344(14):1038-1042.
30. Mauro MJ, O'Dwyer M, Heinrich MC, Druker BJ. STI571: a paradigm of new agents for cancer therapeutics. J Clin Oncol. 2002;20(1):325-334.
31. Savage DG, Antman KH. Imatinib mesylate--a new oral targeted therapy. N Engl J Med. 2002;346(9):683-693.
32. Schultz KR, Bowman WP, Aledo A, et al. Improved early event-free survival with imatinib in Philadelphia chromosome-positive acute lymphoblastic leukemia: a children's oncology group study. J Clin Oncol. 2009;27(31):5175-5181.

33. Cave H, van der Werff ten Bosch J, Suciu S, et al. Clinical significance of minimal residual disease in childhood acute lymphoblastic leukemia. European Organization for Research and Treatment of Cancer--Childhood Leukemia Cooperative Group. N Engl J Med. 1998;339(9):591-598.
34. van Dongen JJ, Seriu T, Panzer-Grumayer ER, et al. Prognostic value of minimal residual disease in acute lymphoblastic leukaemia in childhood. Lancet. 1998;352(9142):1731-1738.
35. Geng H, Hurtz C, Lenz KB, et al. Self-enforcing feedback activation between BCL6 and pre-B cell receptor signaling defines a distinct subtype of acute lymphoblastic leukemia. Cancer Cell. 2015;27(3):409-425.
36. 36.Imamura T, Kiyokawa N, Kato M, et al. Characterization of pediatric Philadelphia-negative B-cell precursor acute lymphoblastic leukemia with kinase fusions in Japan. Blood Cancer J. 2016;6:e419.
37. Ohya K, Kajigaya S, Kitanaka A, et al. Molecular cloning of a docking protein, BRDG1, that acts downstream of the Tec tyrosine kinase. Proc Natl Acad Sci U S A. 1999;96(21):11976-11981.
38. Yokohari K, Yamashita Y, Okada S, et al. Isoform-dependent interaction of BRDG1 with Tec kinase. Biochem Biophys Res Commun. 2001;289(2):414-420.

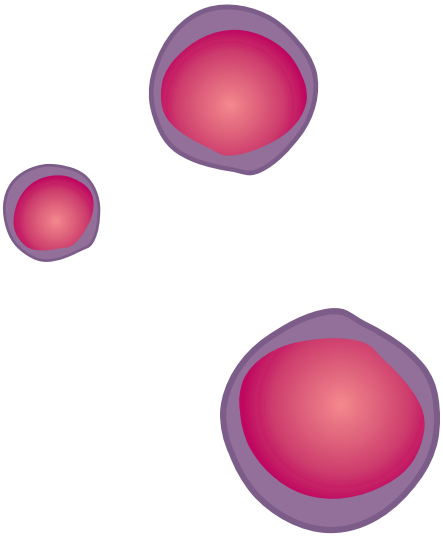

Chapter 2

TYROSINE KINASE FUSION GENES IN PEDIATRIC *BCR-ABL1*-LIKE ACUTE LYMPHOBLASTIC LEUKEMIA

Judith M. Boer, Elisabeth M.P. Steeghs, João R.M. Marchante, Aurélie Boeree, James J. Beaudoin, H. Berna Beverloo, Roland P. Kuiper, Gabriele Escherich, Vincent H.J. van der Velden, C. Ellen van der Schoot, Hester A. de Groot-Kruseman, Rob Pieters, and Monique L. den Boer

Oncotarget. 2017 Sep 16;8(52):89923-Jan 17;8(3):4618-4628.

ABSTRACT

Approximately 15% of pediatric B cell precursor acute lymphoblastic leukemia (BCP-ALL) is characterized by gene expression similar to that of *BCR-ABL1*-positive disease and unfavorable prognosis. This *BCR-ABL1*-like subtype shows a high frequency of B-cell development gene aberrations and tyrosine kinase-activating lesions. To evaluate the clinical significance of tyrosine kinase gene fusions in children with BCP-ALL, we studied the frequency of recently identified tyrosine kinase fusions, associated genetic features, and prognosis in a representative Dutch/German cohort. We identified 14 tyrosine kinase fusions among *77 BCR-ABL1*-like cases (18%) and none among *76* non-*BCR-ABL1*-like B-other cases. Novel exon fusions were identified for *RCSD1-ABL2* and *TERF2-JAK2*. *JAK2* mutation was mutually exclusive with tyrosine kinase fusions and only occurred in cases with high *CRLF2* expression. The non/late response rate and levels of minimal residual disease in the fusion-positive *BCR-ABL1*-like group were higher than in the non-*BCR-ABL1*-like B-others ($p<0.01$), and also higher, albeit not statistically significant, compared with the fusion-negative *BCR-ABL1*-like group. The 8-year cumulative incidence of relapse in the fusion-positive *BCR-ABL1*-like group (35%) was comparable with that in the fusion-negative *BCR-ABL1*-like group (35%), and worse than in the non-*BCR-ABL1*-like B-other group (17%, $p=0.07$). *IKZF1* deletions, predominantly other than the dominant-negative isoform and full deletion, co-occurred with tyrosine kinase fusions. This study shows that tyrosine kinase fusion-positive cases are a high-risk subtype of BCP-ALL, which warrants further studies with specific kinase inhibitors to improve outcome.

INTRODUCTION

Children with B-cell precursor acute lymphoblastic leukemia (BCP-ALL) with the *BCR-ABL1* fusion gene form a small patient group with a poor prognosis, which has been substantially improved in recent treatment protocols with the addition of imatinib and other tyrosine kinase inhibitors.[1,2] Approximately 15% of cases of BCP-ALL are characterized by a gene expression signature similar to that of *BCR-ABL1*-positive disease and an unfavorable prognosis.[3,4] This *BCR-ABL1*-like subtype is found in approximately 50% of so-called B-other cases, which are BCP-ALL cases negative for the sentinel cytogenetic lesions *BCR-ABL1*, *ETV6-RUNX1*, *TCF3-PBX1*, rearrangement of *MLL*, or high hyperdiploidy (51-65 chromosomes). *BCR-ABL1*-like BCP-ALL shows a high frequency of B-cell development gene aberrations, especially *IKZF1* deletions,[3-5] and tyrosine kinase activating lesions.[6,7]

Tyrosine kinase activating lesions are diverse and include tyrosine kinase fusion proteins, cytokine receptor overexpression, or activating point mutations in genes encoding kinases, cytokine receptors, or signaling molecules (recently reviewed in [8]). In our study, we focus on tyrosine kinase fusion genes because they are most similar to the well-known *BCR-ABL1* fusion gene and expected to be clonal leukemia drivers. Detection of tyrosine kinase fusions could guide targeted treatment with tyrosine kinase inhibitors and improve outcome in a similar way as currently for *BCR-ABL1*-positive patients.

Tyrosine kinases known to be involved in fusions include the ABL class kinases ABL1, ABL2, PDGFRB and CSF1R as well as the JAK class kinase JAK2. Each of these kinases has been detected in in-frame fusions with multiple 5' partner genes resulting in the expression of a constitutively active, oncogenic kinase. The number of patients without sentinel chromosomal abnormalities and the diversity of novel tyrosine kinase fusions poses a challenge to routine fusion gene detection. Previous studies have described the discovery and oncogenic potential of ABL and JAK class fusion genes and the sensitivity of patients' cells or *in vitro* cell models to tyrosine kinase inhibition.[6,7] Selection of patients for fusion detection in these studies was based on gene expression profiling indicating Philadelphia-like ALL.[6,7] A large Japanese study screened all B-other cases by transcriptome analysis or multiplexed RT-PCR for 15 fusions and found both methods similarly sensitive.[9] Other studies describe systematic screens in B-other cases by FISH or RT-PCR to detect specific tyrosine kinase fusions.[10,11]

We aimed at the detection of recently identified tyrosine kinase fusion genes in 153 B-other cases of a population-based cohort of 574 Dutch/German pediatric BCP-ALL patients at initial diagnosis to address the frequency of tyrosine kinase fusions, their clinical response characteristics, and associated genetic lesions in B-cell development genes.

RESULTS

Tyrosine kinase fusions are restricted to *BCR-ABL1*-like subtype

We identified 14 ABL/JAK class tyrosine kinase activating fusion genes among 77 *BCR-ABL1*-like cases (18%), and none among 76 non-*BCR-ABL1*-like B-other cases (Table 1; Supplemental Figure S1). We found nine tyrosine kinase fusions predictive for activated ABL signaling: 4 *EBF1-PDGFRB*, 2 *SSBP1-CSF1R*, and one each of *ZMIZ1-ABL1*, *FOXP1-ABL1*, *RCSD1-ABL2*. Five tyrosine kinase fusions are predictive for activated JAK signaling:

three *PAX5-JAK2*, one each of *BCR-JAK2* and *TERF2-JAK2*. The exons included in the fusion transcripts were the same as described previously,[6,12,13] except for *RCSD1* exon 3-*ABL2* exon 5 (Supplemental Figure S2), and *TERF2* exon 10-*JAK2* exon 19 with a deletion of the last 11 coding nucleotides of *TERF2* exon 10 (Supplemental Figure S3). All detected fusion transcripts encode in-frame fusion proteins as evaluated using ProteinPaint.[14]
Table 2 summarizes the genomic analyses of the tyrosine kinase fusion cases. All *PDGFRB*, *CSF1R* and *ABL1* fusions showed aberrant FISH patterns with the appropriate break apart FISH probes (Table 2, Supplemental Figure S4). In addition, both *ABL1* fusions showed add(9)(q34) in their karyotypes (*ABL1* is located on 9q34), together with add(10)(q21) in the *ZMIZ1-ABL1* case (*ZMIZ1* is located on 10q22), and with del(3)(p13) in the *FOXP1-ABL*1 case (*FOXP1* is located on 3p13). Two *EBF1-PDGFRB* cases showed an interstitial 5q deletion on array-CGH, one case arose by balanced t(5;5) translocation, and one case showed a more complex copy number alteration, with loss of *EBF1* exon 16 and gain of a genomic region encompassing *EBF1* exons 7-9 (Table 2; Supplemental Figure S5A-B). *EBF1* exon 16 deletion was confirmed by MLPA in the two interstitial 5q deletion cases and the complex case (Table 2). Genomic breaks were also detected in *SSBP2-CSF1R*, *BCR-JAK2* and *TERF2-JAK2* fusions (Table 2, Supplemental Figure S5C-F). Interestingly, one *SSBP2-CSF1R* fusion probably arose by chromothripsis of chromosome 5 (Supplemental Figure S5D). Finally, when we ordered the gene expression levels of the involved tyrosine kinases for the 153 B-other BCP-ALL cases, the expression in the fusion cases ranked in the top (median percentile 2.6%, range 0.7-14%; Table 2).

CRLF2 high expression and PAR1 deletions are common in both *BCR-ABL1*-like and B-other cases

High gene expression levels of the cytokine receptor *CRLF2* were found in 16% of *BCR-ABL1*-like cases, none of which overlapped with ABL/JAK class tyrosine kinase fusion cases, and also in 16% of non-*BCR-ABL1*-like B-other cases. About 50% of *CRLF2*-high cases carried a *JAK2* mutation.[15] The frequency of *CRFL2* high expression cases with a PAR1 deletion, *JAK2* mutation or both was similarly high in *BCR-ABL1*-like (9/12 cases)

Table 1. Frequency of identified tyroxine kinase fusion genes

	BCR-ABL1-like (n=77)	Remaining B-other (n=76)
ABL1/ABL2 fusion	3.9%	0%
ZMIZ1-ABL1	1	
FOXP1-ABL1	1	
RSD1-ABL2	1	
PDGFRB fusions	5.2%	0%
EBF1-PDGFRB	4	
JAK2 fusions	6.5%	0%
PAX5-JAK2	3	
BCR-JAK2	1	
TERF2-JAK2	1	
CRLF2 expression*	15.6%	15.8%
PAR1 deletion**	10.5%	10.7%

*Expression of Affymetrix U133 Plus 2.0 probe set 208303_s_at above the 90th percentile of the total BCPALL group, as described previously5. **Deletion of IL3RA and CSF2RA and retention of CRLF2 as determined by MLPA.

and B-other cases (11/12 cases (Figure 1). *CRLF2* expression had no prognostic value in this Dutch/German BCP-ALL cohort as described previously.[5]

Tyrosine kinase fusion cases are enriched for *IKZF1* deletion variants

Next, we compared the frequency of B-cell development gene lesions between the tyrosine kinase fusion-positive *BCR-ABL1*-like cases, the fusion-negative *BCR-ABL1*-like cases, and the non-*BCR-ABL1*-like B-other cases. While *IKZF1* deletions were common both in fusion-positive and fusion-negative *BCR-ABL1*-like cases (64% vs. 40%; p=0.14), *IKZF1*

Table 2. Molecular characteristics of identified tyrosine kinase fusion genes

Case	Tyrosine kinase fusion	Simplified karyotype	Array-CGH[a]	EBF1 exon 16[b]	FISH[c]	Expr rank[d]	Exons fused	Validation
R32	*EBF1-PDGFRB*	ND	deletion chr5: 149,494,702-158,058,047	0.64	PDGFRB split	1%	e15-e11	RT-PCR
A288	*EBF1-PDGFRB*	46,XY,t(2;12)(q23~24;q12)[20]/46,XY[14]	diploid	ND	PDGFRB split	5%	e14-e11	RT-PCR
A472	*EBF1-PDGFRB*	46,XY[20]	deletion chr5: 149,494,702-158,030,723; gain chr5: 158,049,831-158,428,865	0.62	PDGFRB split	4%	e15-e11	RT-PCR
A428	*EBF1-PDGFRB*	46,XY[20].ish 7(cep7,D7S522)x1,i(7)(q10)(D7S522+,cep7+,D7S522+)[13/25]	gain chr5: 158,222,469-158,428,865	0.54	PDGFRB split	6%	e15-e11	RT-PCR
A123	*SSBP2-CSF1R*	ND	small deletions typical of chromothripsis	1.0	PDGFRB split	1%	e16-e12	RT-PCR
A526	*SSBP2-CSF1R*	46,XY[10]	gain chr5: 80,740,416-149,403,322	1.1	PDGFRB split	3%	e16-e12	RT-PCR
A91	*ZMIZ1-ABL1*	47,XY,add(9)(q34),add(10)(q21),mar[9]	diploid	1.1	ABL1 split	2%	e18-e2	RT-PCR
A26	*FOXP1-ABL1*	46,XY,del(3)(p13),add(9)(q34),i(22)(q10),inc[6]	diploid	1.0	ABL1 split	14%	e27-e4	TLA; PCR
A530	*RCSD1-ABL2*	46,XY[4]/42~46,XY,inc[3]	ND	0.71	ND	1%	e3-e5	RT-PCR; TLA
A31	*PAX5-JAK2*	46,XX,del(1)(q32q42),inc[2]/46,XX[18]	diploid	0.94	ND	1%	e5-e19	RT-PCR
A286	*PAX5-JAK2*	46,XX[17]	diploid	0.81	ND	6%	e5-e19	RT-PCR
A204	*PAX5-JAK2*	ND	diploid	0.96	ND	3%	e5-e19	RT-PCR
A214	*TERF2-JAK2*	46,XY[20]	gain chr16: 67,958,182-88,690,630; deletion chr9: 593,494-5,068,342	0.95	ND	3%	e10-e19	RT-PCR; TLA
A216	*BCR-JAK2*	ND	deletion chr9: 194,193-5,068,342; gain chr9: 5,080,443-5,647,733; gain chr22: 14,513,474-21,885,107; deletion chr22: 21,898,315-22,667,667	0.91	ND	1%	e1-e17	RT-PCR; TLA

[a] Genome positions in build hg18, copy number changes shown for the genes involved in the fusion; see also Supplemental Figure S5. [b] EBF1 exon 16 copy number ratio determined by MLPA. A value below 0.75 is called as a deletion.
[c] FISH break apart probes from Cytocell were used. The centromeric PDGFRB probe overlaps with CSF1R and can be used to detect breakpoints in CSF1R as well as in PDGFRB. [d] Expr rank indicates the percentile in rank of the tyrosine kinase gene expression among 153 B-other BCP-ALL cases on Affymetrix U133 Plus 2 arrays. ND: not determined

deletions other than exon 4-7 or full deletion, including deletion of exons 1, 1-2, 1-3, 2-3, 2-7, 2-8, 4-8, 5 and 7-8, occurred more frequently in the fusion-positive compared with the fusion-negative *BCR-ABL1*-like cases (43% vs. 15%; p=0.03; Table 3). Except for deletions in *EBF1*, enriched in *EBF1-PDGFRB* fusion cases due to interstitial 5q deletion, none of the other genes detected by P335 MLPA (*PAX5*, *ETV6*, *RB1*, *BTG1*, *CDKN2A/B*, *PAR1*) showed an aberrant deletion frequency in tyrosine kinase fusion cases compared with non-*BCR-ABL1*-like B-other cases (Table 2). In the fusion-positive cases, *CDKN2A/B* deletion was less frequent than in the fusion-negative *BCR-ABL1*-like cases (14% vs. 63%, p=0.002; Table 3). Two large genomic lesions previously described to occur in *BCR-ABL1*-like BCP-ALL, dic(9;20) and intrachromosomal amplification of chromosome 21, 3, 16 were mutually exclusive with the identified tyrosine kinase fusions (Table 3).

Tyrosine kinase fusion cases show poor treatment response to induction therapy and high minimal residual disease levels

Finally, we evaluated clinical response characteristics. Of 12 tyrosine kinase fusion-positive cases with evaluable data, 5 patients did not achieve complete morphological remission at the end induction therapy; 4 of them were late responders, and one was a non-responder resulting in early death (Figure 2A). This non/late response rate at the end of induction therapy was higher in the fusion-positive cases compared with non-*BCR-ABL1*-like B-other

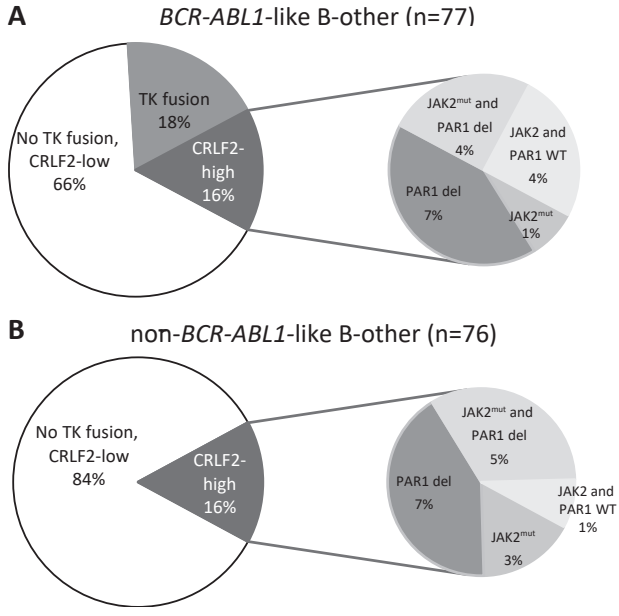

Figure 1. Distribution of tyrosine kinase fusions and *CRLF2* high expression cases

Pie diagrams showing the percentages of tyrosine kinase (TK) fusion cases and *CRLF2* high expression among (**A**) *77 BCR-ABL1*-like B-other cases, and (**B**) *76* non-*BCR-ABL1*-like B-other cases. Within the CRLF2 high expression cases, a sub-distribution of cases with *JAK2* mutation and/or PAR1 deletion is shown. In the non-*BCR-ABL1*-like B-other cases, two PAR1-deleted cases were not tested for *JAK2* mutations.

(42% vs. 7%, p=0.004) and also higher, albeit not statistically significant, compared with fusion-negative *BCR-ABL1*-like cases (42% vs. 17%, p=0.11; Table 3). Furthermore, fusion-positive cases were characterized by higher levels of minimal residual disease (MRD) compared with non-*BCR-ABL1*-like B-other cases at end of induction therapy (p=0.001) and before consolidation (p=0.002) and also, although less significant, compared with fusion-negative *BCR-ABL1*-like cases (p=0.09, p=0.04, respectively; Table 3). The 8-year cumulative incidence of relapse (CIR) in the *BCR-ABL1*-like group with tyrosine kinase

Table 3. Clinical and molecular features of ABL/JAK class tyrosine kinase fusions

		TK fusion-positive *BCR-ABL1*-like	TK fusion-negative *BCR-ABL1*-like	Fisher P TK fusion-positive vs. TK fusion-negative *BCR-ABL1*-like	Non-*BCR-ABL1*-like B-other	Fisher P TK fusion-positive vs. non-*BCR-ABL1*-like B-other
CLINICAL FEATURES						
Male		**11/14 (79%)**	**28/63 (44%)**	**0.036**	44/76 (58%)	0.23
age ≥ 10 years		7/14 (50%)	18/63 (29%)	0.2	25/76 (33%)	0.24
WBC ≥ 50x109/L		6/14 (43%)	32/63 (51%)	0.77	23/76 (30%)	0.37
NCI high risk[a]		11/14 (79%)	43/63 (68%)	0.53	42/76 (55%)	0.14
MRD TP1[a]	**High**	7/11 (64%)	17/36 (47%)		10/45 (22%)	
	Intermediate	3/11 (27%)	4/36 (11%)	0.093	5/45 (11%)	**0.001**
	Low	1/11 (9%)	15/36 (42%))		30/45 (67%	
MRD TP2[b]	**High**	4/7 (57%)	4/30 (13%)		1/34 (3%)	
	Intermediate	0/7 (0%)	3/30 (10%)	**0.037**	1/34 (3%)	**0.002**
	Low	3/7 (43%)	23/30 (77%))		32/34 (94%)	
Risk arm MR or HR		12/14 (86%)	15/36 (42%)	1	47/74 (64%)	0.13
Prednisone poor response[c]		2/7 (29%)	3/31 (10%)	0.22	3/31 (10%)	0.22
No CR after induction[d]		**5/12 (42%)**	10/58 (17%)	0.11	**5/73 (7%)**	**0.004**
MOLECULAR FEATURES						
IKZF1 deletion	**Total**	**9/14 (64%))**	25/62 (40%)	0.14	**13/73 (18%)**	**0.0009**
	Common[e]	3/14 (21%)	16/62 (26%)	1	5/73 (7%)	0.11
	Other[f]	**6/14 (43%)**	**9/62 (15%)**	**0.026**	**8/73 (11%)**	**0.009**
EBF1 deletion		**4/14 (29%)**	9/62 (15%)	0.24	**3/73 (4%)**	**0.012**
EBF1 single exon 16 del		**4/14 (29%)**	**0/62 (0%)**	**0.0008**	**0/73 (0%)**	**0.0005**
PAX5 deletion/amp		3/14 (21%)	32/62 (52%)	0.072	26/73 (36%)	0.37
ETV6 deletion		2/14 (14%)	9/62 (15%)	1	18/75 (24%)	0.73
BTG1 deletion		2/14 (14%)	1/62 (2%)	0.085	6/74 (8%)	0.61
CDKN2A/B deletion		**2/14 (14%)**	**39/62 (63%)**	**0.002**	29/75 (39%)	0.13
RB1 deletion		1/14 (7%)	6/62 (10%)	1	5/74 (7%)	1
CRLF2 high expression		0/14 (0%)	12/63 (19%)	0.11	12/76 (16%)	0.2
PAR1 deletion		0/14 (0%)	8/62 (13%)	0.34	8/75 (11%)	0.35
dic(9;20)		**0/14 (0%)**	**15/57 (26%)**	**0.031**	2/74 (3%)	1
iAMP21		0/14 (0%)	10/57 (18%)	0.19	2/74 (3%)	1

[a] NCI-Rome high risk is defined by white blood cell count (WBC) ≥_50x109/L and/or age ≥ 10 years. [b] Minimal residual disease PCR high (≥10-3), intermediate (≥10-4 and <10-3), low (<10-4); TP1, after the first induction course of chemotherapy, DCOG ALL-10 protocol day 33, ALL-9 protocol day 42, COALL day 28; TP2, before consolidation, day 79. [c] Prednisone response on day 8 ≥1.0x109 blasts/L (DCOG ALL-8/10 protocols). [d] Complete remission (CR) after induction (day 33 in DCOG ALL-9/10, day 42 in ALL-8) is defined on morphological grounds by the presence of <5% leukemic blasts and regenerating hematopoiesis. [e] Common IKZF1 deletions are defined as full deletion (exons 1-8) and deletion of exons 4-7. [f] Other IKZF1 deletions included deletion of exons 1, 1-2, 1-3, 2-3, 2-7, 2-8, 4-8, 5 and 7-8.

fusions (35% ± 16%) was comparable with the remaining *BCR-ABL1*-like group (35% ± 6%), and worse than the non-*BCR-ABL1*-like B-other group (17% ± 5%; Gray p-value 0.066; Figure 2B). Of the three relapsed fusion-positive cases, one died of relapse and two were alive at end of follow-up (6-12 months). Remarkably, the percentage of males was higher in fusion-positive than fusion-negative *BCR-ABL1*-like cases (79% vs. 44%, p=0.04; Table 3).

A

Case	Sex	Protocol	Pred	Resp	MRD TP1	MRD TP2	IKZF1 del	TK fusion
R32	M	ALL8-HR*	poor	LR	nd	nd	WT	*EBF1-PDGFRB*
A288	M	ALL10-HR*	poor	LR	high	high	DEL4-7	*EBF1-PDGFRB*
A472	M	ALL10-HR*	good	CR	high	high	WT	*EBF1-PDGFRB*
A428	M	ALL10-MR	good	unkn	high	low	DEL1-8	*EBF1-PDGFRB*
A123	F	COALL03-HR	nd	CR	int	nd	DEL1-8	*SSPB2-CSF1R*
A526	M	ALL10-HR*	good	CR	high	high	DEL2-7	*SSBP2-CSF1R*
A91	M	ALL9-SR	nd	LR	nd	nd	WT	*ZM1Z1-ABL1*
A26	M	ALL9-HR	nd	NR	nd	nd	DEL2-8	*FOXP1-ABL1*
A530	M	ALL10-HR*	good	unkn	high	high	DEL2-3	*RCSD1-ABL2*
A31	F	ALL9-HR	nd	CR	int	low	DEL1	*PAX5-JAK2*
A286	F	ALL10-SR	good	CR	low	low	WT	*PAX5-JAK2*
A204	M	COALL03-HR	nd	CR	high	nd	DEL2-7	*PAX5-JAK2*
A214	M	COALL03-HR*	nd	LR	high	nd	WT	*TERF2-JAK2*
A216	M	COALL03-HR*	nd	CR	int	nd	DEL2-3	*BCR-JAK2*

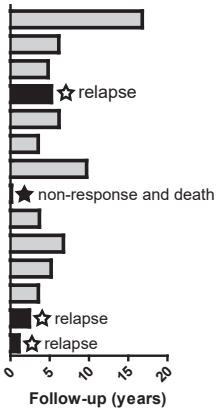

B

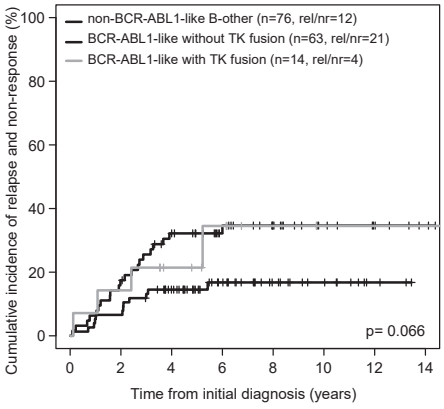

Figure 2. *BCR-ABL1*-like tyrosine kinase fusion cases

(**A**) Clinical characteristics and follow-up for the tyrosine kinase fusion cases. Barplot representing years from diagnosis to event or censoring. Treatment protocol and arm, prednison window response (Pred), morphological response after induction therapy (Resp), minimal residual disease (MRD), and deletion status of IKZF1 are shown. MRD monitoring by PCR was performed for research purposes in ALL-9 and COALL03 and for MRD-guided risk stratification in ALL-10. WT indicates no *IKZF1* deletion. For definition of Pred, Resp, and MRD see footnotes Table 3. Response 'unkn' indicates patients with low cellularity bone marrow which could not be evaluated. * Indicates patients who received bone marrow transplant, for which HR-treated cases were eligible. (**B**) Cumulative incidence of relapse and non-response curves for tyrosine kinase fusion positive *BCR-ABL1*-like cases, fusion-negative *BCR-ABL1*-like cases, and non-*BCR-ABL1*-like B-other cases. Relapse and non-response were considered as events, death as competing event. Cumulative incidence probabilities were estimated using a competing risk model, equality was tested with the Gray test.

DISCUSSION

We identified ABL/JAK class tyrosine kinase fusion genes in 14/153 (9%) of DCOG/COALL B-other cases and these fusions were restricted to the *BCR-ABL1*-like B-other subgroup. Given that these 153 cases were derived from a population-based selection of BCP-ALL[5] and that these fusions do not co-occur with other driver leukemic fusions (*BCR-ABL1*, rearranged *MLL*, *TCF3-PBX1*, *ETV6-RUNX1*), ABL/JAK class tyrosine kinase fusions cases are estimated to represent approximately 2.5% of pediatric BCP-ALL, making this heterogeneous subgroup similar in size to the *BCR-ABL1*-positive cytogenetic subtype. Although the number of cases evaluated in our study is modest, the frequency of tyrosine kinase fusion cases is similar to those reported in other cohorts: 3% ABL/JAK class fusions in a high-risk pediatric US cohort[6] and 5% ABL/JAK class fusions among Japanese pediatric B-other cases.[9]

The most comprehensive detection of novel tyrosine kinase fusion genes requires transcriptome or whole genome sequencing. These costly methods have not been applied to complete cohorts but rather to subsets of cases, for example cases selected based on Philadelphia-like gene expression or absence of sentinel chromosomal abnormalities, mostly in retrospective studies.[6,9] More targeted approaches to detect recently identified tyrosine kinase fusions include RT-PCR [9], capture-targeted sequencing[17] or targeted locus amplification (TLA) and sequencing.[18] We combined genomic information from copy number, gene expression, targeted RT-PCR, FISH, and TLA to detect tyrosine kinase fusion genes in a representative cohort of 153 BCP-ALL cases without sentinel chromosomal aberrations that were taken from a population-based cohort of 574 cases at initial diagnosis of BCP-ALL. We found tyrosine kinase fusions exclusively in the *BCR-ABL1*-like B-other group, and found them non-overlapping with two chromosomal abnormalities that were described earlier to occur in *BCR-ABL1*-like cases, iAMP21 and dic(9;20).[3] Moreover, while *CRLF2* high expression cases are present both in *BCR-ABL1*-like and non-*BCR-ABL1*-like B-others, we found that tyrosine kinase fusions and high *CRLF2* expression were mutually exclusive. The current study did not aim at discovering novel tyrosine kinase fusions, therefore there is a small probability that a sample with a novel tyrosine kinase gene is included in the tyrosine kinase fusion negative group.

Our finding that tyrosine kinase fusions are only found in patients with *BCR-ABL1*-like features, and our earlier finding that tyrosine kinase fusion cases are identified by both the St. Jude and Erasmus MC *BCR-ABL1*-like expression signatures,[16] means that a pre-screening method based on gene expression, such as the US-developed low density array, is suitable to narrow down the patient population to be screened for tyrosine kinase fusions. An alternative approach screens patients selected by poor early clinical response for tyrosine kinase fusions.[10]

We found that ABL/JAK kinase fusion cases were characterized by poor initial response to induction treatment, high MRD levels, and a higher relapse rate compared with non-*BCR-ABL1*-like B-other ALL cases but a comparable relapse rate as *BCR-ABL1*-like ALL without tyrosine kinase fusions. In correspondence, a recent Japanese study showed that the event-free survival of tyrosine kinase-activating fusion cases (albeit including *CRLF2* rearrangements) was unfavorable compared with fusion-negative BCP-ALL [9], Schwab *et al.* described that *EBF1-PDGFRB*-positive patients were MRD positive at the end of induction[10], and Roberts *et al.* described MRD positivity and inferior survival in the total group of Philadelphia-like cases. Recent protocols using MRD-based risk-directed therapy

suggest that initial poor treatment response in tyrosine kinase fusion-positive cases or the total group of Philadelphia-like cases can be overcome with intensive chemotherapy, leading to durable remission.[10,19] *Ex vivo* leukemic patients' cells with JAK and ABL class fusions were shown to be sensitive to tyrosine kinase inhibitors.[6,7,15] Promising early clinical results suggests that ABL class tyrosine kinase fusion patients respond well to ABL class inhibitors imatinib or dasatinib.[6,10,20,21] Together with our data, these reports stress the importance of prospective detection of tyrosine kinase fusions and incorporation of tyrosine kinase inhibitors in ALL treatment protocols to improve outcome.

METHODS

Patient samples

This study comprised 574 children with newly diagnosed BCP-ALL enrolled in consecutive Dutch Childhood Oncology Group trials (DCOG ALL-8, ALL-9 and ALL-10)[5,22] and German Cooperative ALL trials (COALL 06-97 and 07-03)[23,24]. These patient cohorts were described and analyzed together previously.[3,5] Written informed consent was obtained from parents or guardians and institutional review boards approved the use of excess of diagnostic material for research purposes. These studies were conducted in accordance with the Declaration of Helsinki. Mononuclear cells were collected using Lymphoprep sucrose gradient centrifugation (Nycomed Pharma, Oslo, Norway) from bone marrow aspirates and peripheral blood samples obtained prior to treatment. Where needed, mononuclear cells were enriched to >90% leukemic cells by depleting normal cells using anti-CD marker coated magnetic beads (Dynal, Oslo, Norway) as described previously.[25] DNA and total RNA were isolated using TRIzol (Invitrogen Life Technologies, Breda, the Netherlands) and quantified using a Nanodrop ND1000 (Nanodrop, Wilmington, DE). From this cohort, we focused on B-other patients, defined as patients without the sentinel chromosomal abnormalities *BCR-ABL1*, MLL rearrangements, *ETV6-RUNX1*, *TCF3-PBX1*, and high hyperdiploidy. Among the B-other cases, *BCR-ABL1*-like cases identified by hierarchical clustering of gene expression data were described previously in our cohort.[5] For 153 out of 204 B-other/*BCR-ABL1*-like cases in the cohort, tyrosine kinase fusion testing was performed (see flow chart in Supplemental Figure S1).

Tyrosine kinase fusion detection

Detection of tyrosine kinase fusion genes was performed by RT-PCR followed by Sanger sequencing for six fusion transcripts *EBF1-PDGFRB*, *PAX5-JAK2*, *NUP214-ABL1*, *RANBP2-ABL1*, *ETV6-ABL1*, *RCSD1-ABL1* and *STRN3-JAK2* described by Roberts *et al.*[7] In addition, we performed a more extensive RT-PCR panel[6] enabling detection of 30-39 fusion genes (depending on availability of material). For RT-PCR primers see Supplemental Table S1. We used targeted locus amplification for 21 cases to detect fusion genes involving *ABL1*, *PDGFRB*, *CSF1R*, *ABL2*, *TYK2*, and *JAK2* (TLA, Cergentis, Utrecht, the Netherlands).[18,26] We used break apart FISH with PDGFRB/CSF1R and ABL1 probes (Cytocell) to confirm fusions. The methods applied to each case depended on the type and amount of available patient material and is indicated in Supplemental Figure S1. For the comparison of tyrosine kinase fusion positive versus negative patients, we included 153 samples that were tested at least by the 7-fusion RT-PCR panel. For expression rank

analysis (Table 2), the Affymetrix microarray gene expression values for each tyrosine kinase gene were ranked from high to low for the 153 samples. Then the percentile rank of the fusion-positive case among the 153 samples was calculated.

Genome-wide DNA copy number arrays (array-CGH)

Copy number analysis was performed using Agilent SurePrint G3 Hmn 4x180K arrays (Agilent Technologies, Amstelveen, the Netherlands) co-hybridized with 1 µg patient DNA labeled with ULS-Cy5 and 1 µg reference genomic DNA male pool (G147A, Promega, Leiden, the Netherlands) labeled with ULS-Cy3 (Agilent Genomic DNA ULS Labeling Kit). Copy number microarray data were normalized using median log ratio in the CGHcall[27] version 2.14.0, centralized using CGHnormaliter[28] version 1.8.0, and segmented and called using CGHcall default settings (-1 for loss, 0 for diploid, 1 for gain and 2 for amplification) in R version 2.14.1.

Multiplex ligation-dependent probe amplification

The SALSA P335 ALL-IKZF1 (a3) and the SALSA P202 Multiplex Ligation-dependent Probe Amplification (MLPA) assays (MRC-Holland) were used to identify or confirm genomic lesions on the following genes: *IKZF1*, *CDKN2A*, *CDKN2B*, *ETV6*, *PAX5*, *RB1*, *BTG1* and *EBF1* as described previously.[5,29] In short, 125 ng of genomic DNA was used to generate DNA fragments with incorporated FAM nucleotides according to the manufacturer's protocol. The amplified fragments were quantified using an ABI-3130 genetic analyzer (Applied Biosystems, Carlsbad, CA). Peak intensities were normalized to the manufacturer's control probes and to a synthetic control reference generated from five normal DNA samples in the same MLPA run. A peak ratio lower than 0.75 was considered a deletion, a ratio between 0.75 and 1.3 was considered normal copy number, a ratio higher than 1.3 was considered a gain in copy number.

Targeted locus amplification

Targeted Locus Amplification (TLA) combined with deep-sequencing was used to detect fusion genes and sequence mutations in regions up to 100 kb around a pre-selected primer pair by crosslinking of physically proximal genomic sequences as described before.[16] Briefly, DNA and protein in 10-15 million viable leukemic blast cells were crosslinked in a 2% formaldehyde solution. Cells were lysed and DNA was digested with NlaIII, followed by ligation, de-crosslinking and DNA purification. DNA molecules were trimmed with NspI and ligated at a concentration of 5 ng/µl to promote intramolecular ligation to DNA fragments of approximately 2 kb. These chimeric fragments were PCR amplified, sonicated and adaptor-ligated for paired-end high-throughput Illumina sequencing. A total of 31 primer sets targeting 19 recurrently affected genes were designed and multiplexed, including the genes involved in the classical cytogenetic subtypes *MLL*, *RUNX1*, *TCF3*, and *IKZF1*, the tyrosine kinase genes *ABL1*, *ABL2*, *PDGFRB*, *CSF1R*, *JAK1*, *JAK2*, *JAK3*, *FLT3*, and *TYK2*, and the cytokine signaling genes *CRLF2*, *EPOR*, *IL7R*, *TSLP*, *SH2B3*, and *IL2RB*.[17]

Fluorescent in-situ hybridization (FISH)

FISH was performed on interface nuclei using break apart probes (Cytocell, Cambridge, UK) for *PDGFRB* and *ABL1*. The FISH probes for *PDGFRB* overlap with the neighboring *CSF1R* locus. At least 100 interphase nuclei were evaluated.

Reverse transcriptase PCR (RT-PCR)

cDNA was synthesized from 1 µg total or copy RNA using M-MLV reverse transcriptase and combined oligo-dT and pdN6 priming in 20 µl (Promega, Madison, WI). PCR was performed on 2.5 µl cDNA using Taq polymerase, MgCl2 and buffer from Applied Biosystems (Bleiswijk, Netherlands). For primer sequences see Supplemental Table S1.

Association with clinical outcome

Cumulative incidence of relapse (CIR) was estimated using a competing risks model. We considered relapse as event, and death as competing event. To test for equality of CIRs, Gray's test has been applied. The CIR probability (pCIR) with standard error was reported. Outcome analyses were performed in R 3.0.1, using the packages cmprsk version 2.2-6 [0], mstate version 0.2.6[31], and survival version 2.37-4[32].

Acknowledgements

We thank Oksana Montecchini and Alice Poropat for technical assistance.

Disclosure of Conflicts of Interest

The authors declare no conflicts of interest.

Authorship Contributions

JMB, EMPS, JRMM, JJB, HBB, AB, VHJvdV, CEvdS and RPK designed and performed experiments, and analyzed and interpreted data. RP, HAdGK and GE provided patients' characteristics and clinical outcome data. RP and MLdB conceptualized the study, and interpreted data. JMB and MLdB drafted the manuscript. The manuscript was revised and approved by all authors.

Grant Support

This work was supported by the VICI program grant 016.126.612 from Netherlands Organisation for Scientific Research (NWO), the Foundation Pediatric Oncology Center Rotterdam (SKOCR), the Dutch Cancer Society grants EMCR 2007-3718 and AMC 2008-4265, the KiKa Foundation (Kika-132 grant) and the European Union's Seventh Framework Program FP7/2007-2013 ENCCA grant HEALTH-F2-2011-261474

REFERENCES

1. Biondi A, Schrappe M, De Lorenzo P, Castor A, Lucchini G, Gandemer V, Pieters R, Stary J, Escherich G, Campbell M, Li CK, Vora A, Arico M, Rottgers S, Saha V and Valsecchi MG. Imatinib after induction for treatment of children and adolescents with Philadelphia-chromosome-positive acute lymphoblastic leukaemia (EsPhALL): a randomised, open-label, intergroup study. Lancet Oncol. 2012; 13(9):936-945.
2. Schultz KR, Carroll A, Heerema NA, Bowman WP, Aledo A, Slayton WB, Sather H, Devidas M, Zheng HW, Davies SM, Gaynon PS, Trigg M, Rutledge R, Jorstad D, Winick N, Borowitz MJ, et al. Long-term follow-up of imatinib in pediatric Philadelphia chromosome-positive acute lymphoblastic leukemia: Children's Oncology Group study AALL0031. Leukemia. 2014; 28(7):1467-1471.
3. Den Boer ML, van Slegtenhorst M, De Menezes RX, Cheok MH, Buijs-Gladdines JG, Peters ST, Van Zutven LJ, Beverloo HB, Van der Spek PJ, Escherich G, Horstmann MA, Janka-Schaub GE, Kamps WA, Evans WE and Pieters R. A subtype of childhood acute lymphoblastic leukaemia with poor treatment outcome: a genome-wide classification study. Lancet Oncol. 2009; 10:125-134.
4. Mullighan CG, Su X, Zhang J, Radtke I, Phillips LA, Miller CB, Ma J, Liu W, Cheng C, Schulman BA, Harvey RC, Chen IM, Clifford RJ, Carroll WL, Reaman G, Bowman WP, et al. Deletion of IKZF1 and prognosis in acute lymphoblastic leukemia. N Engl J Med. 2009; 360(5):470-480.
5. Van der Veer A, Waanders E, Pieters R, Willemse ME, Van Reijmersdal SV, Russel LJ, Harrison CJ, Evans WE, Van der Velden VHJ, Hoogerbrugge PM, Van Leeuwen F, Escherich G, Horstmann MA, Mohammadi Khankahdani L, Rizopoulos D, De Groot-Kruseman HA, et al. Independent prognostic value of BCR-ABL1-like signature and IKZF1 deletion, but not high CRLF2 expression, in children with B-cell precursor ALL. Blood. 2013; 122(15):2622-2629.
6. Roberts KG, Li Y, Payne-Turner D, Harvey RC, Yang YL, Pei D, McCastlain K, Ding L, Lu C, Song G, Ma J, Becksfort J, Rusch M, Chen SC, Easton J, Cheng J, et al. Targetable kinase-activating lesions in Ph-like acute lymphoblastic leukemia. N Engl J Med. 2014; 371(11):1005-1015.
7. Roberts KG, Morin RD, Zhang J, Hirst M, Zhao Y, Su X, Chen SC, Payne-Turner D, Churchman ML, Harvey RC, Chen X, Kasap C, Yan C, Becksfort J, Finney RP, Teachey DT, et al. Genetic alterations activating kinase and cytokine receptor signaling in high-risk acute lymphoblastic leukemia. Cancer Cell. 2012; 22(2):153-166.
8. Izraeli S. Beyond Philadelphia: 'Ph-like' B cell precursor acute lymphoblastic leukemias - diagnostic challenges and therapeutic promises. Curr Opin Hematol. 2014; 21(4):289-296.
9. Imamura T, Kiyokawa N, Kato M, Imai C, Okamoto Y, Yano M, Ohki K, Yamashita Y, Kodama Y, Saito A, Mori M, Ishimaru S, Deguchi T, Hashii Y, Shimomura Y, Hori T, et al. Characterization of pediatric Philadelphia-negative B-cell precursor acute lymphoblastic leukemia with kinase fusions in Japan. Blood Cancer J. 2016; 6:e419.
10. Schwab C, Ryan SL, Chilton L, Elliott A, Murray J, Richardson S, Wragg C, Moppett J, Cummins M, Tunstall O, Parker CA, Saha V, Goulden N, Vora A, Moorman AV and Harrison CJ. EBF1-PDGFRB fusion in pediatric B-cell precursor acute lymphoblastic leukemia (BCP-ALL): genetic profile and clinical implications. Blood. 2016; 127(18):2214-2218.
11. Zaliova M, Moorman AV, Cazzaniga G, Stanulla M, Harvey RC, Roberts KG, Heatley SL, Loh ML, Konopleva M, Chen IM, Zimmermannova O, Schwab C, Smith O, Mozziconacci MJ, Chabannon C, Kim M, et al. Characterization of leukemias with ETV6-ABL1 fusion. Haematologica. 2016; 101(9):1082-1093.
12. Kamps WA, van der Pal-de Bruin KM, Veerman AJ, Fiocco M, Bierings M and Pieters R. Long-term results of Dutch Childhood Oncology Group studies for children with acute lymphoblastic leukemia from 1984 to 2004. Leukemia. 2010; 24:309-319.
13. Escherich G, Horstmann MA, Zimmermann M, Janka-Schaub GE and Grp CS. Cooperative study group for childhood acute lymphoblastic leukaemia (COALL): long-term results of trials 82,85,89,92 and 97. Leukemia. 2010; 24(2):298-308.
14. Escherich G, Zimmermann M and Janka-Schaub G. Doxorubicin or daunorubicin given upfront in a therapeutic window are equally effective in children with newly diagnosed acute lymphoblastic leukemia. A randomized comparison in trial CoALL 07-03. Pediatr Blood Cancer. 2013; 60(2):254-257.
15. Den Boer ML, Harms DO, Pieters R, Kazemier KM, Göbel U, Körholz D, Graubner U, Haas RJ, Jorch NJ, Spaar HJ, Kaspers GJL, Kamps WA, Van der Does-Van den BERG A, Van Wering ER, Veerman AJP and Janka-Schaub GE. Patient stratification based on prednisolone-vincristine-asparaginase resistance profiles in children with acute lymphoblastic leukemia. J Clin Oncol. 2003; 21:3262-3268.
16. de Vree PJ, de Wit E, Yilmaz M, van de Heijning M, Klous P, Verstegen MJ, Wan Y, Teunissen H, Krijger PH, Geeven G, Eijk PP, Sie D, Ylstra B, Hulsman LO, van Dooren MF, van Zutven LJ, et al. Targeted sequencing by proximity ligation for comprehensive variant detection and local haplotyping. Nat Biotechnol. 2014; 32(10):1019-1025.
17. Kuiper RP, Van Reijmersdal SV, Simonis M, Yu J, Sonneveld E, Scheijen B, Boer JM, Boeree A, Klous P, Hoogerbrugge P, Yilmaz M, Van Leeuwen FN, Den Boer ML and Splinter E. Targeted locus amplification & next generation sequencing for the detection of recurrent and novel gene fusions for improved treatment decisions in pediatric acute lymphoblastic leukemia. Annual Meeting Abstracts Blood. 2015; 126(23):696.
18. van de Wiel MA, Kim KI, Vosse SJ, van Wieringen WN, Wilting SM and Ylstra B. CGHcall: calling aberrations for array CGH tumor profiles. Bioinformatics. 2007; 23(7):892-894.

19. van Houte BP, Binsl TW, Hettling H, Pirovano W and Heringa J. CGHnormaliter: an iterative strategy to enhance normalization of array CGH data with imbalanced aberrations. BMC Genomics. 2009; 10:401.
20. Boer JM, Koenders JE, van der Holt B, Exalto C, Sanders MA, Cornelissen JJ, Valk PJ, den Boer ML and Rijneveld AW. Expression profiling of adult acute lymphoblastic leukemia identifies a BCR-ABL1-like subgroup characterized by high non-response and relapse rates. Haematologica. 2015; 100(7):e261-264.
21. Escherich G, Zur Stadt U, Alawi M and Horstmann M. Rapid capture targeted next generation sequencing (NGS) for detection of genomic kinase- and cytokine receptor rearrangements in B-precursor acute lymphoblastic leukemia. Annual Meeting Abstracts Blood. 2015; 126(23):2609.
22. Gray RJ. cmprsk: Subdistribution Analysis of Competing Risks. R package version 22-6 2013; http://CRAN.R-project.org/package=cmprsk.
23. De Wreede LC, Fiocco M and Putter H. mstate: An R Package for the Analysis of Competing Risks and Multi-State Models. J Stat Softw. 2011; 38(7):1-30.
24. Therneau T. A Package for Survival Analysis in S. R package version 236-12. 2012.
25. Soler G, Radford-Weiss I, Ben-Abdelali R, Mahlaoui N, Ponceau JF, Macintyre EA, Vekemans M, Bernard OA and Romana SP. Fusion of ZMIZ1 to ABL1 in a B-cell acute lymphoblastic leukaemia with a t(9;10)(q34;q22.3) translocation. Leukemia. 2008; 22(6):1278-1280.
26. Ernst T, Score J, Deininger M, Hidalgo-Curtis C, Lackie P, Ershler WB, Goldman JM, Cross NC and Grand F. Identification of FOXP1 and SNX2 as novel ABL1 fusion partners in acute lymphoblastic leukaemia. Br J Haematol. 2011; 153(1):43-46.
27. Zhou X, Edmonson MN, Wilkinson MR, Patel A, Wu G, Liu Y, Li Y, Zhang Z, Rusch MC, Parker M, Becksfort J, Downing JR and Zhang J. Exploring genomic alteration in pediatric cancer using ProteinPaint. Nature Genetics. 2015; 48(1):4-6.
28. Steeghs EMP, Jerchel IS, de Goffau-Nobel W, Hoogkamer AQ, Boer JM, Boeree A, van de Ven C, Koudijs MJ, Cuppen E, De Groot-Kruseman HA, Horstmann MA, Pieters R and Den Boer ML. JAK2 aberrations in childhood precursor B cell acute lymphoblastic leukemia. Submitted.
29. Boer JM, Marchante JRM, Evans WE, Horstmann MA, Escherich G, Pieters R and Den Boer ML. BCR-ABL1-Like Cases in Pediatric Acute Lymphoblastic Leukemia: a Comparison Between DCOG/Erasmus MC and COG/St. Jude Signatures. Haematologica 2015; 100(9):e354-357.
30. Roberts KG, Pei D, Campana D, Payne-Turner D, Li Y, Cheng C, Sandlund JT, Jeha S, Easton J, Becksfort J, Zhang J, Coustan-Smith E, Raimondi SC, Leung WH, Relling MV, Evans WE, et al. Outcomes of Children With BCR-ABL1-Like Acute Lymphoblastic Leukemia Treated With Risk-Directed Therapy Based on the Levels of Minimal Residual Disease. Journal of Clinical Oncology. 2014; 32(27):3012-3020.
31. Weston BW, Hayden MA, Roberts KG, Bowyer S, Hsu J, Fedoriw G, Rao KW and Mullighan CG. Tyrosine Kinase Inhibitor Therapy Induces Remission in a Patient With Refractory EBF1-PDGFRB-Positive Acute Lymphoblastic Leukemia. Journal of Clinical Oncology. 2013; 31(25):e413-416.
32. Lengline E, Beldjord K, Dombret H, Soulier J, Boissel N and Clappier E. Successful tyrosine kinase inhibitor therapy in a refractory B-cell precursor acute lymphoblastic leukemia with EBF1-PDGFRB fusion. Haematologica. 2013; 98(11):e146-148.

SUPPLEMENTAL DATA

Supplemental Table S1. Reverse transcription PCR primers used for the detection of tyrosine kinase fusion genes

Gene fusion	Forward Primer ID	Forward sequence 5' to 3'	Reverse Primer ID	Reverse sequence 5' to 3'
ETV6-ABL1	ETV6 exon5	ggagaataatcactgcccagcgtcct	ABL1 exon 4	gccaccgtcaggctgtatttcttcc
NUP214-ABL1	NUP241 exon 20	cagtggccttggaggaaaacccagt	ABL1 exon 4	gccaccgtcaggctgtatttcttcc
RANBP2-ABL1	RANBP2 exon 16	tggttctttgcgaaatgcagattca	ABL1 exon 4	gccaccgtcaggctgtatttcttcc
RCSD1-ABL1	RCSD1 exon 3	cagccagtaaaccaacccgaaggaa	ABL1 exon 4	gccaccgtcaggctgtatttcttcc
SNX2-ABL1	SNX2 exon 3	cggaaccttctcctgcagtcacacc	ABL1 exon 4	gccaccgtcaggctgtatttcttcc
ZMIZ1-ABL1	ZMIZ1 exon 17	gaccggcagatgaaca	ABL1 exon 3	cattccccattgtgattatag
PAG1-ABL2	PAG1 exon 7	ccttcaggagaaggaaggggggagagg	ABL2 exon6	gtcgtggatgggggacacaccatag
RCSD1-ABL2	RCSD1 exon 3	cagccagtaaaccaacccgaaggaa	ABL2 exon6	gtcgtggatgggggacacaccatag
ZC3HAV1-ABL2	ZC3HAV1 exon 11	tgtcagagatccatcacctacatcca	ABL2 exon6	gtcgtggatgggggacacaccatag
SSBP2-CSF1R	SSBP2 exon 12	tcatgcctagtccagcagattcaacca	CSF1R exon 14	tggctcatgatcttcagctcggaca
MYH9-CSF1R	MYH9 exon 1	gcgggaaggcggcgaggag	CSF1R exon 14	tggctcatgatcttcagctcggaca
MEF2D-CSF1R	MEF2D exon 7	cctgcgagtcatcacttc	CSF1R exon 14	tggctcatgatcttcagctcggaca
EBF1-CSF1R	EBF1 exon 11	ccaccatcgattatggtttccagaggt	CSF1R exon 14	tggctcatgatcttcagctcggaca
ETV6-NTRK3	ETV6 exon5	ggagaataatcactgcccagcgtcct	NTRK3 exon 15	atcttgtccttggtcgggctgaggt
ATF7IP-JAK2	ATF7IP exon 12	aacccatacaaccagcaccgcctct	JAK2 exon 20	tgttgtcatgctgtagggatttcagga
BCR-JAK2	BCR exon 1	gtgccataagcggcaccggcact	JAK2 exon 18	aggcctgaaatctggttcata
EBF1-JAK2	EBF exon 14	cacgagcatgaacggatacggctct	JAK2 exon 20	tgttgtcatgctgtagggatttcagga
ETV6-JAK2	ETV6 exon 3	atggcaaagctctcctgctgctgac	JAK2 exon 20	tgttgtcatgctgtagggatttcagga
PAX5-JAK2	PAX5 exon 3	acaatgacaccgtgcctagcgtcag	JAK2 exon 19	tcaaaggcaccagaaaac
PPFIBP1-JAK2	PPFIBP1 exon 10	tgcaagatgaaaggagaaggggttga	JAK2 exon 20	tgttgtcatgctgtagggatttcagga
SSBP2-JAK2	SSBP2 exon 7	ggcacttggaggtgtcccaggaagt	JAK2 exon 20	tgttgtcatgctgtagggatttcagga
STRN3-JAK2	STRN3 exon 7	tgaaggagctggagaagcacggagt	JAK2 exon 20	tgttgtcatgctgtagggatttcagga
TPR-JAK2	TPR exon 38	tggaaatgcctcttccaaagaagttga	JAK2 exon 20	tgttgtcatgctgtagggatttcagga
TERF2-JAK2	TERF2 exon 10	tggggaaggaaactgg	JAK2 exon 20	tgttgtcatgctgtagggatttcagga
EBF1-PDGFRB	EBF1 exon 14	ccccagcagaccaactat	PDGFRB exon 12	ttccatcggatctcgtaa
TNIP1-PDGFRB	TNIP1 exon 13	aagcactgagcatccaaacc	PDGFRB exon 13	tttcatcgtggcctgagaatggctc
ZEB2-PDGFRB	ZEB2 exon 9	cccaactggagcagctactttgctga	PDGFRB exon 13	tttcatcgtggcctgagaatggctc
SSBP2-PDGFRB	SSBP2 exon 7	ggcacttggaggtgtcccaggaagt	PDGFRB exon 13	tttcatcgtggcctgagaatggctc
SSBP2-PDGFRB	SSBP2 exon 12	tcatgcctagtccagcagattcaacca	PDGFRB exon 13	tttcatcgtggcctgagaatggctc
MYB-TYK2	MYB exon 6	tcaggctccgcctacagctcaactc	TYK2 exon 19	tccgggttcacagtcaagacgtcag

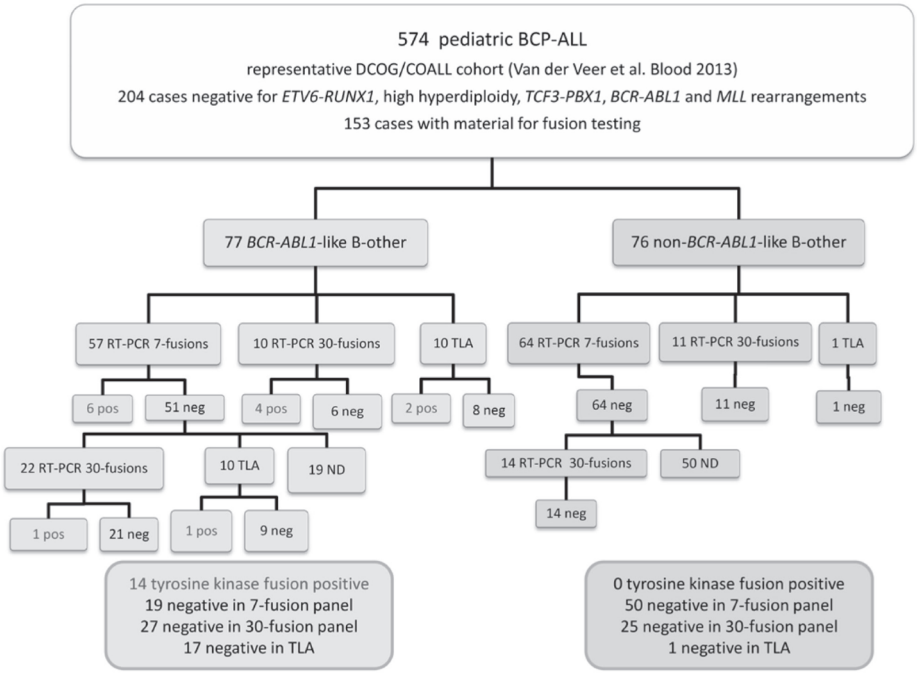

Supplemental Figure S1. Overview of cohort screened for tyrosine kinase fusion genes
Flowchart showing the number of cases tested for tyrosine kinase fusion genes using an RT-PCR panel of 7 fusions[3], an RT-PCR panel of 30 fusions[1], and targeted locus amplification for 6 kinases[4]. Boxes at the bottom summarize the number of positive and negative cases per method. ND, not determined.

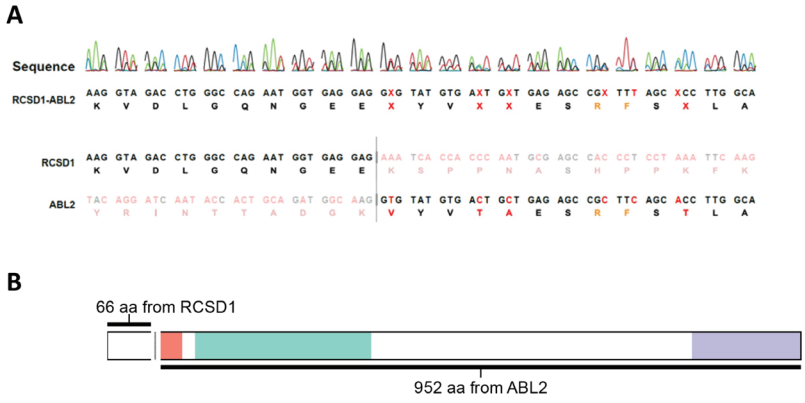

Supplemental Figure S2. Sanger sequencing and TLA fusion read of *RCSD1-ABL2* in case A530

(**A**) Sequence confirmation of the *RCSD1-ABL2* fusion by Sanger sequencing of RT-PCR product indicates fusion of RCSD1 exon 3 to ABL2 exon 5. For primers used in validation RT-PCR see Supplemental Table S1. The fusion encodes an in frame fusion protein. (**B**) Schematic representation of the in-frame *RCSD1-ABL2* fusion protein drawn in ProteinPaint[5]. (**C**) Targeted locus amplification genomic DNA fusion read showing *RCSD1* intron 3 (chr1) (red) and *ABL2* intron 4 (chr1) in green.

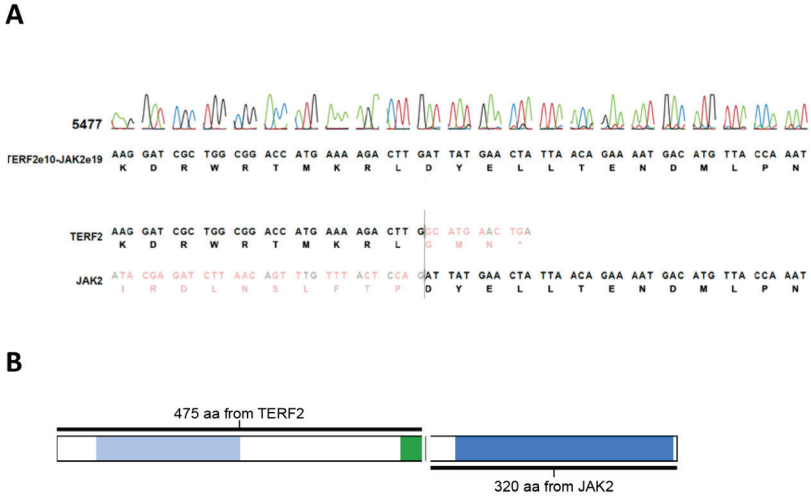

Supplemental Figure S3. Sanger sequencing of *TERF2-JAK2* in case A214

(**A**) Sequence confirmation of the *TERF2-JAK2* fusion by Sanger sequencing of RT-PCR product indicates fusion of *TERF2* exon 10 to *JAK2* exon 19. For primers used in validation RT-PCR see Supplemental Table S1. The fusion encodes an in frame fusion protein. (**B**) Schematic representation of the in-frame *TERF2-JAK2* fusion protein drawn in ProteinPaint[5].

(A) *PDGFRB* R32

83% with unbalanced pattern with one normal locus and loss of telomeric probe (Fusion, Red)

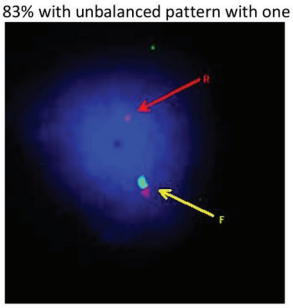

(B) *PDGFRB* A288

32% with balanced translocation and two normal loci (Fusion, Fusion, Red, Green);
56% with balanced pattern and two normal loci and an additional signal for centromeric probe (Fusion, Fusion, Red, Red, Green); also some smaller subclones present

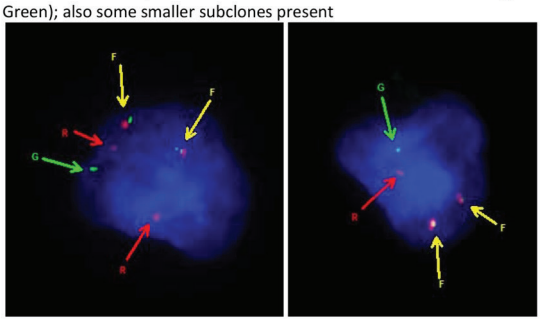

(C) *PDGFRB* A428

22% balanced pattern with one normal locus (Fusion, Red, Green);
64% balanced pattern with one normal locus and one additional signal for telomeric probe (Fusion, Red, Green, Green); some smaller subclones present (Fusion, Fusion, Red, Green; Fusion, Red, Red, Green);

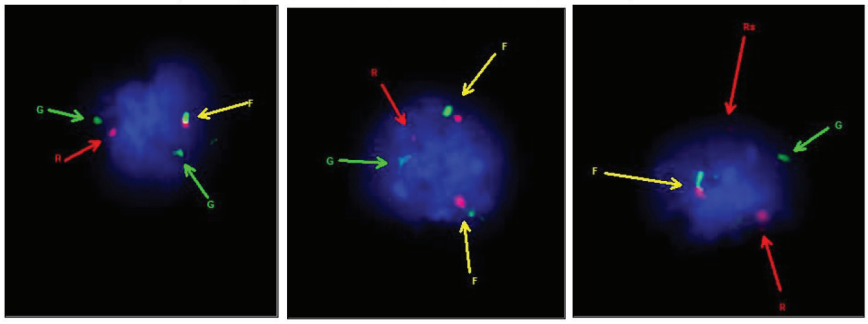

Supplemental Figure S4. FISH with *PDGFRA* break apart probes on *EBF1-PDGFRA* fusion cases.

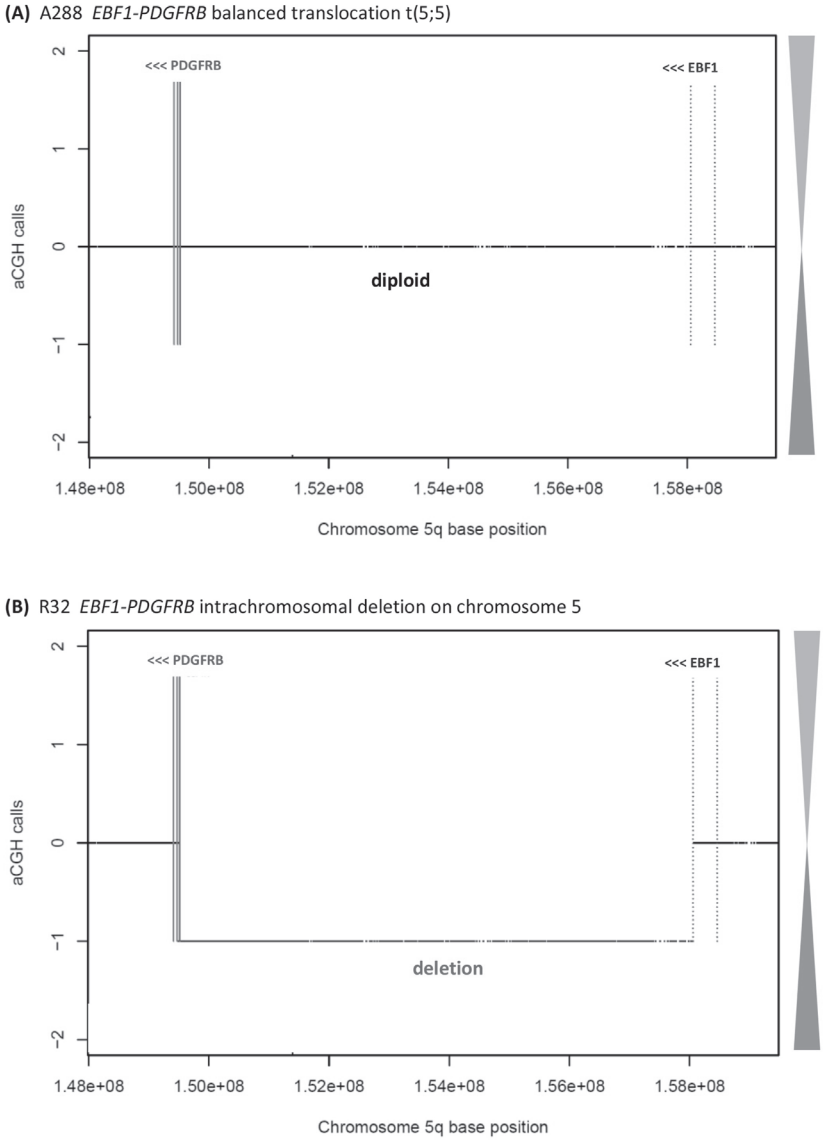

Supplemental Figure S5. Array comparative genomic hybridization 180K Agilent array data for tyrosine kinase fusion cases.

The x-axis indicates genomic location on the indicated chromosome, the y-axis shows the called array-CGH data with 0 representing two copies, 1 representing gain and -1 loss (**A-C**) or the normalized log2 ratios (**D-F**). The colored triangles on the right indicate gain (orange) and loss (blue). (**A-D**) Rearrangements involving chromosome 5. Beginning and end position of the genes involved in the tyrosine kinase fusions are indicated by colored vertical lines: purple, *CSF1R*; red, *PDGFRB*; blue, *EBF1*; light-blue, *SSBP1*. The orientation of the genes is indicated with < for minus strand and > plus strand. (**E-F**) Rearrangements resulting in JAK2 fusions. The complete chromosomes involved in the rearrangements are shown. The genes involved in the fusions are indicated in red, the breakpoint is indicated by a red arrow. The positions of the centromeres are indicated by black vertical lines. *(Continued on the next pages)*

(C) A526 *SSBP2-CSF1R* intrachromosomal duplication on chromosome 5

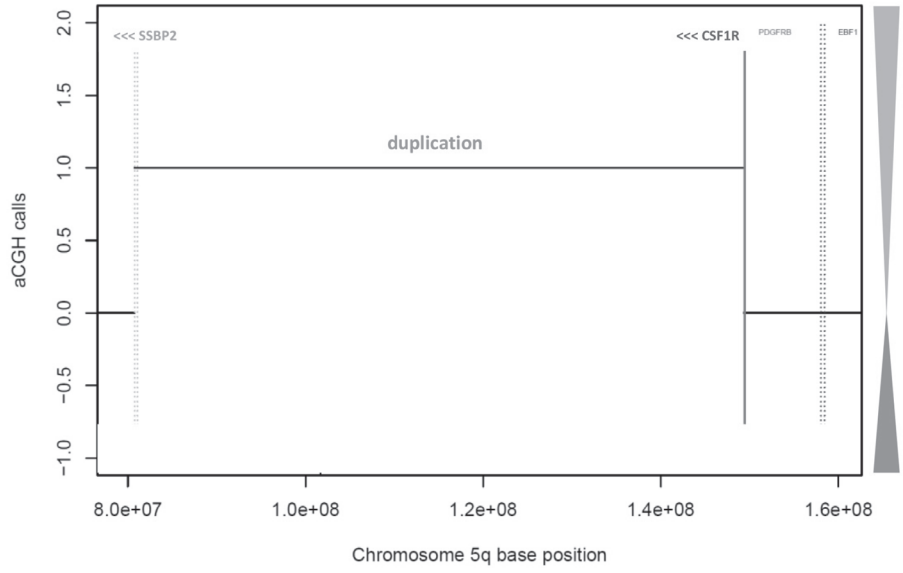

(D) A123 *SSBP2-CSF1R* resulting from chromothripsis of chromosome 5

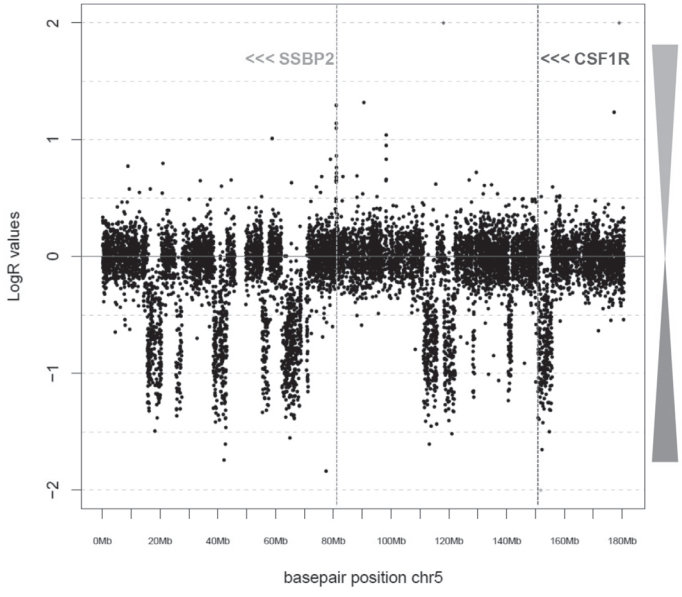

Supplemental Figure S5. Array comparative genomic hybridization 180K Agilent array data for tyrosine kinase fusion cases. ***(continued)***

(E) A216 *BCR-JAK2* fusion involving chromosomes 22 and 9

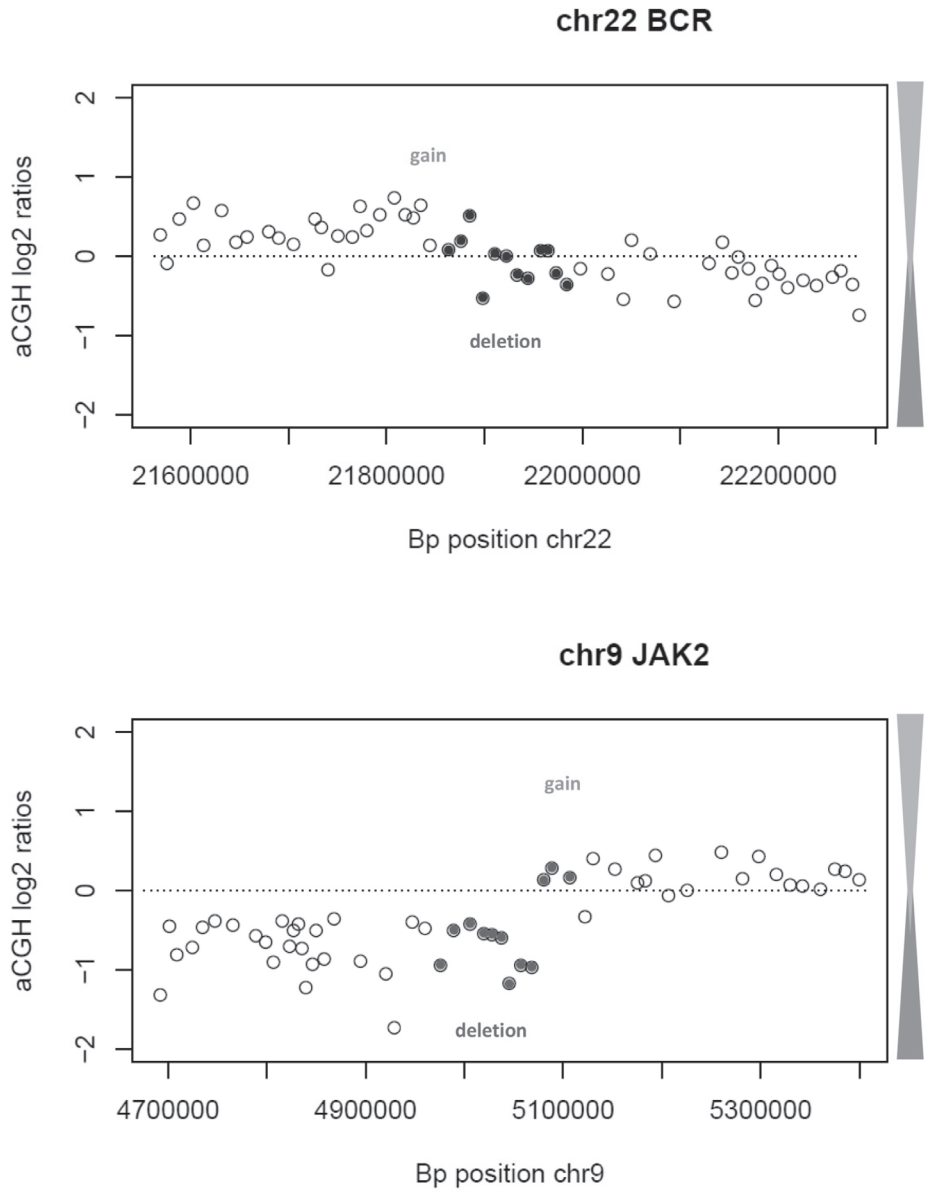

Supplemental Figure S5. Array comparative genomic hybridization 180K Agilent array data for tyrosine kinase fusion cases. ***(continued)***

(F) A214 *TERF2-JAK2* fusion involving chromosomes 16 and 9

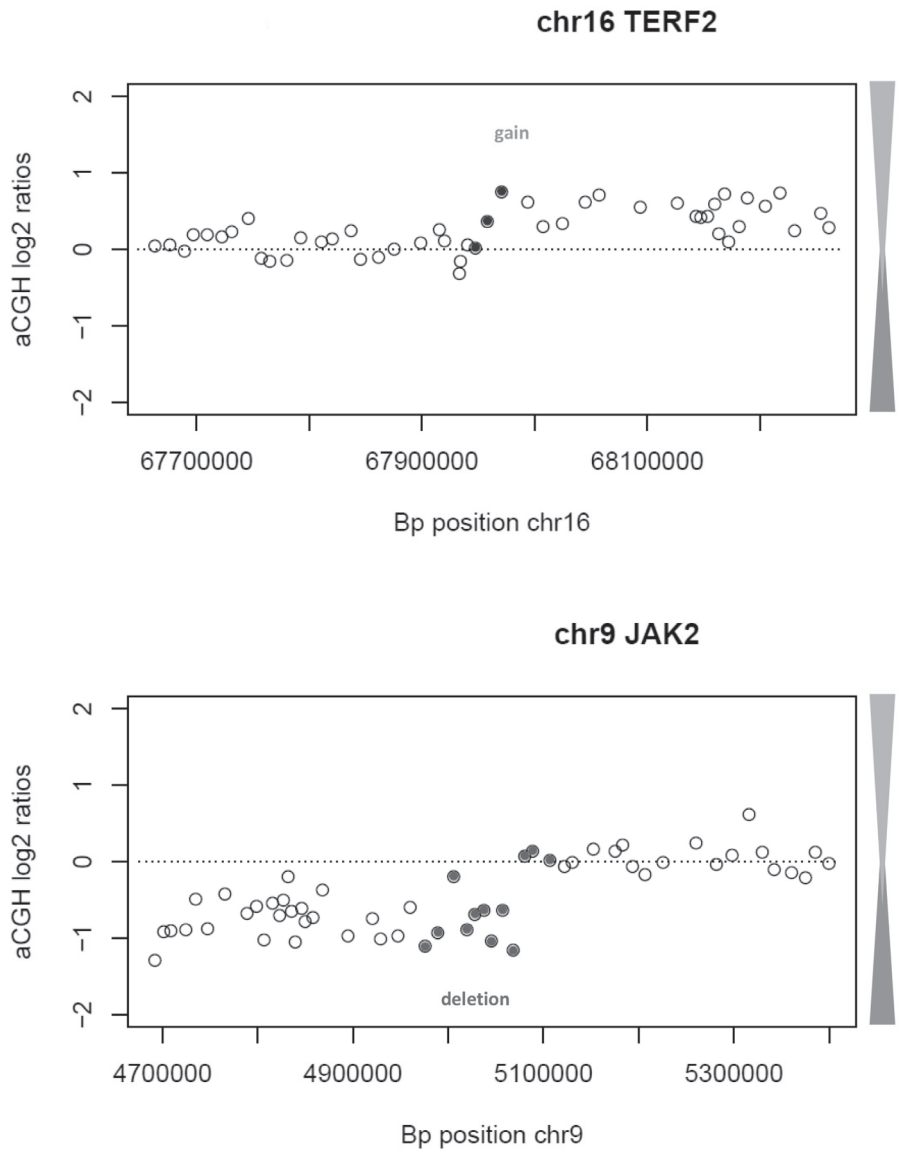

Supplemental Figure S5. Array comparative genomic hybridization 180K Agilent array data for tyrosine kinase fusion cases. ***(continued)***

REFERENCES SUPPLEMENT

1. Becksfort J, Rusch M, Chen SC, Easton J, Cheng J, et al. Targetable kinase-activating lesions in Ph-like acute lymphoblastic leukemia. N Engl J Med. 2014; 371(11):1005-1015.
2. Van der Veer A, Waanders E, Pieters R, Willemse ME, Van Reijmersdal SV, Russel LJ, Harrison CJ, Evans WE, Van der Velden VHJ, Hoogerbrugge PM, Van Leeuwen F, Escherich G, Horstmann MA, Mohammadi Khankahdani L, Rizopoulos D, De Groot-Kruseman HA, et al. Independent prognostic value of BCR-ABL1-like signature and IKZF1 deletion, but not high CRLF2 expression, in children with B-cell precursor ALL. Blood. 2013; 122(15):2622-2629.
3. Roberts KG, Morin RD, Zhang J, Hirst M, Zhao Y, Su X, Chen SC, Payne-Turner D, Churchman ML, Harvey RC, Chen X, Kasap C, Yan C, Becksfort J, Finney RP, Teachey DT, et al. Genetic alterations activating kinase and cytokine receptor signaling in high-risk acute lymphoblastic leukemia. Cancer Cell. 2012; 22(2):153-166.
4. Kuiper RP, Van Reijmersdal SV, Simonis M, Yu J, Sonneveld E, Scheijen B, Boer JM, Boeree A, Klous P, Hoogerbrugge P, Yilmaz M, Van Leeuwen FN, Den Boer ML and Splinter E. Targeted locus amplification & next generation sequencing for the detection of recurrent and novel gene fusions for improved treatment decisions in pediatric acute lymphoblastic leukemia. Annual Meeting Abstracts Blood. 2015; 126(23):696.
5. Zhou X, Edmonson MN, Wilkinson MR, Patel A, Wu G, Liu Y, Li Y, Zhang Z, Rusch MC, Parker M, Becksfort J, Downing JR and Zhang J. Exploring genomic alteration in pediatric cancer using ProteinPaint. Nat Genet. 2015; 48(1):4-6.

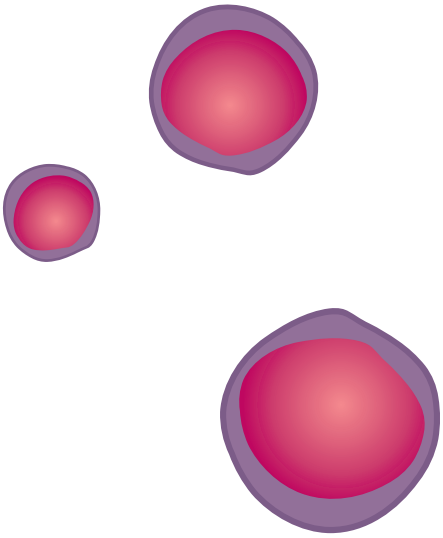

Chapter 3

JAK2 ABERRATIONS IN CHILDHOOD B-CELL PRECURSOR ACUTE LYMPHOBLASTIC LEUKEMIA

Elisabeth M.P. Steeghs, Isabel S. Jerchel*, Willemieke de Goffau-Nobel, Alex Q. Hoogkamer, Judith M. Boer, Aurélie Boeree, Cesca van de Ven, Marco J. Koudijs, Nicolle J.M. Besselink, Hester A. de Groot-Kruseman, C. Michel Zwaan, Martin A. Horstmann, Rob Pieters, and Monique L. den Boer*

**E.M.P. Steeghs and I.S. Jerchel contributed equally to this work*

Oncotarget. 2017 Sep 16;8(52):89923-89938.

ABSTRACT

JAK2 abnormalities may serve as target for precision medicines in pediatric B-cell precursor acute lymphoblastic leukemia (BCP-ALL). In the current study we performed a screening for *JAK2* mutations and translocations, analyzed the clinical outcome and studied the efficacy of two JAK inhibitors in primary BCP-ALL cells. Importantly, we identify a number of limitations of JAK inhibitor therapy.

JAK2 mutations mainly occurred in the poor prognostic subtypes *BCR-ABL1*-like and non-*BCR-ABL1*-like B-other (negative for sentinel cytogenetic lesions). *JAK2* translocations were restricted to *BCR-ABL1*-like cases. Momelotinib and ruxolitinib were cytotoxic in both *JAK2* translocated and *JAK2* mutated cells, although efficacy in *JAK2* mutated cells highly depended on cytokine receptor activation by TSLP. However, our data also suggest that the effect of JAK inhibition may be compromised by mutations in alternative survival pathways and microenvironment-induced resistance. Furthermore, inhibitors induced accumulation of phosphorylated JAK2^{Y1007}, which resulted in a profound re-activation of JAK2 signaling upon release of the inhibitors. This preclinical evidence implies that further optimization and evaluation of JAK inhibitor treatment is necessary prior to its clinical integration in pediatric BCP-ALL.

INTRODUCTION

Janus kinase 2 (JAK2) is a member of the non-receptor tyrosine kinase family and mediates intracellular signaling upon activation of cytokine receptors, which lack an intrinsic tyrosine kinase domain, such as cytokine receptor-like factor 2 (*CRLF2*). Ligand binding (e.g. TSLP for CLRF2) induces dimerization of cytokine receptors chains, resulting in activation of JAK proteins via cross-phosphorylation. JAKs activate signal transducers of transcription (STATs), which, upon dimerization, migrate to the nucleus and induce transcription of genes involved in differentiation and proliferation of hematopoietic cells.[1]

JAK2 has seven homologous domains (JH1-JH7). The JH1 and JH2 domains are C-terminally located and comprise the catalytic kinase (JH1) and pseudokinase (JH2) domain. The JH2 domain has a dual regulatory function: exerting a negative regulatory effect on the kinase domain, and facilitating JAK2 activation upon receptor activation by ligand binding.[2] The JH3-JH4 domains share homology with Src homology 2 (SH2) domains and mediate protein-protein interactions. The N-terminal located JH6 and JH7 domains, also known as the FERM domain, are required for binding of JAK2 to cytokine receptors.[1]

In pediatric BCP-ALL patients, gain of function mutations and translocations affecting *JAK2* have been identified.[3-15] Genomic translocations of *JAK2* have been observed in high-risk *BCR-ABL1*-like patients. For several of these fusion genes, constitutive JAK2 kinase activation has been demonstrated.[12-14, 16] Point mutations often occur in Down Syndrome ALL, mainly affect exon 16 (located in the pseudokinase domain), and functionally cooperate with overexpression of the type I cytokine receptor *CRLF2*.[6, 9, 10] Indeed, requirement for the interaction of mutant JAK2 with a cytokine receptor was shown in cell lines models by several groups.[6, 8, 9]

Mutations and translocations represent biologically distinct entities, but both are potential targets for precision medicines. JAK inhibitors were shown to be effective against mutant and translocated JAK2 *in vitro*.[3, 5, 7, 8, 12, 13, 16, 17] However, *in vivo* mouse studies show conflicting data and none has been reported to be curative.[13, 17-21] To date, clinical data with JAK inhibitors are scarce. The Children's Oncology Group performed a phase 1 dosing study of the JAK inhibitor ruxolitinib, but no cases harboring JAK2 activating mutations or translocations were included.[22]

Several papers have reported data with a focus on either fusion genes or mutations of *JAK2*, although often with small sample size or only in specific subtypes of BCP-ALL. Furthermore, most reports lack *ex vivo* efficacy data of JAK inhibitors in primary leukemic cells. To assess the clinical potential of JAK inhibitors in pediatric BCP-ALL, we performed a comprehensive study to determine the frequency and prognosis of *JAK2* mutations and translocations among different subtypes of childhood BCP-ALL. Furthermore, the biological efficacy of the JAK inhibitors momelotinib and ruxolitinib was studied in primary leukemic cells harboring JAK2 aberrations, and the clonal stability of *JAK2* mutations was investigated in ALL patient derived xenograft models. We show that JAK inhibitors are overall effective towards BCP-ALL cells, but also identified a number of limitations of JAK inhibitor therapy.

RESULTS

Frequency and type of *JAK2* aberrations in BCP-ALL patients

JAK2 mutation status was analyzed in 461 newly diagnosed BCP-ALL cases representing all major subtypes seen in children, with a distribution that is comparable to the general pediatric BCP-ALL population. *JAK2* exons 16, 20, 21 and 23 were examined by targeted amplicon sequencing at a median read depth of 673, 577, 711 and 944, respectively. Analyses revealed that 3.5% (16/461) of these BCP-ALL cases harbored *JAK2* mutations, which were detected in 7.6% (6/79) of *BCR-ABL1*-like cases, 11.9% (8/67) of non-*BCR-ABL1*-like B-other cases, and 1.6% (2/124) of high hyperdiploid cases. No *JAK2* mutations were detected in *KMT2A-ALL1* (0/15), *BCR-ABL1* (0/26), *ETV6-RUNX1* (0/124) or *TCF3-PBX1* (0/26) cases. The variant allele frequency (VAF) ranged from 1.0% to 56% (Figure 1A). Seven patients carried two different *JAK2* mutations, and one patient even harbored three different *JAK2* mutations. Mutations involved amino acid residue R683 in 13 of 16 mutated cases, which is an important amino acid for the JH2 domain mediated negative auto-regulation of JAK2 activity.[23] *CRLF2* overexpression was detected in 87.5% (14/16) of these cases (Figure 1A, Supplementary Figure 1). One *CRLF2* low expressing case harbored a subclonal *JAK2* mutation, suggesting that *CRLF2* overexpression might be subclonal as well. The other case harbored a *JAK2*^{R923H} with a VAF of 50 %, suggesting that this mutation in the kinase domain is not associated with *CRLF2* overexpression.

The screen for *JAK2* fusion genes was confined to 153 BCP-ALL cases, negative for sentinel BCP-ALL associated lesions (*KMT2A*-rearranged, *BCR-ABL1*, *ETV6-RUNX1*, *TCF3-PBX1*, high hyperdiploid), as *JAK2* translocations were previously reported in this group of patients.[12,13,24] No *JAK2* translocations were detected in 76 non-*BCR-ABL1*-like B-other cases, whereas in 5 of the 77 (6.5%) *BCR-ABL1*-like cases JAK2 tyrosine kinase activating fusion genes were identified. The cases involved 3 *PAX5-JAK2* cases, 1 *BCR-JAK2* case and 1 *TERF2-JAK2* case (Figure 1A). The *PAX5-JAK2* and *BCR-JAK2* fusions contained identical exons as reported before.[12,13] The *TERF2-JAK2* case displayed an in frame fusion of *TERF2* exon 10 to *JAK2* exon 19. All *JAK2* fusion genes harbored an intact JH1 kinase domain (Supplementary Figure 2). Gene expression data revealed high expression levels of *JAK2* in these cases (Supplementary Figure 3). Absence of the cytokine receptor-binding FERM domain in *JAK2* fusion protein suggests that they signal independent of a cytokine receptor.

Clinical characteristics and prognosis of patients harboring *JAK2* lesions

Ten out of sixteen (62.5%) *JAK2*-mutated patients remained in continuous complete remission at more than 5 years of follow up. The median time to relapse in the six other patients was 2.1 years [range 0.71-7.8 years]. Minimal residual disease (MRD) data were available for nine out of fourteen patients. The four patients with high MRD levels ($\geq 10^{-3}$) at day 29/33 of treatment (time point 1 of COALL and DCOG protocol, respectively) relapsed, whereas the remaining five mutated patients with low MRD levels remained in continuous complete remission (p=0.008, Fisher exact test).

Three out of the five cases harboring *JAK2* fusion genes remained in continuous complete remission at more than 5 years of follow up, whereas two cases suffered from a relapse within 2.4 years of diagnosis (Figure 1A). Both patients who relapsed were assigned to the High Risk arm of the COALL-03 study protocol because of unfavorable age (>10 years) or high white blood cell count at diagnosis (>50 WBC/nl).

A

	Patient	Protocol	Risk group	Age (years)	WBC ($x10^9$/L)	Down Syndrome	MRD (d29/d33)	Subtype	Translocation	Mutation 1 (VAF)	Mutation 2 (VAF)	Mutation 3 (VAF)	*CRLF2* status
JAK2 Mutation	A20	ALL9	HR	14	75		<10^-3	*BCR-ABL1*-like		p.R873N 40%	p.R683S 2%	p.R683G 2%	High
	A35	ALL9	NHR	1	44		NA	*BCR-ABL1*-like		p.R683T 56%	p.R683G 13%		High
	A38	ALL9	HR	6	128,8		NA	*BCR-ABL1*-like		p.R683G 32%	p.T875N 10%		High
	A129	COALL03	HR-S	4	450	Yes	NA	B-other		p.R683G 2%	p.K914E 1%		High
	A159	COALL03	HR-S	4	39		NA	High Hyperdiploid		p.R683G 1%			Low
	A160	COALL03	LR-S	3	4,3		NA	B-Other		p.R683G 24%			High
	A167	COALL03	HR-S	9	30		NA	B-other		p.D873N 10%	p.R683G 8%		High
	A178	COALL03	LR-R	7	10		≥10^-3	B-other		p.R683T 30%	p.R683G 4%		High
	A186	COALL97	HR-S	11	9,9		≥10^-3	*BCR-ABL1*-like		p.T875N 37%			High
	A251	COALL97	HR-S	7	115		NA	*BCR-ABL1*-like		p.R683G 63%			High
	A282	ALL10	SR	3	21		<10^-3	B-Other		p.R683S 25%	p.R683G 7%		High
	A315	ALL10	MR	3	3,6	Yes	<10^-3	B-Other		p.R683G 41%			High
	A359	ALL10	MR	8	390	Yes	≥10^-3	B-other		p.R683G 27%	p.R683S 25%		High
	A404	ALL10	MR	8	222,6		<10^-3	*BCR-ABL1*-like		p.R683G 26%			High
	A433	ALL10	MR	2	1,9	Yes	≥10^-3	High Hyperdiploid		p.R683G 25%			High
	A521	ALL10	MR	11	12,1		<10^-3	B-Other		p.R923H 50%			Low
JAK2 Translocation	A31	ALL9	HR	1	53,8		<10^-3	*BCR-ABL1*-like	*PAX5-JAK2*				Low
	A204	COALL03	HR-S	14	4,5		<10^-3	*BCR-ABL1*-like	*PAX5-JAK2*				Low
	A286	ALL10	SR	1	3,4		<10^-3	*BCR-ABL1*-like	*PAX5-JAK2*				Low
	A214	COALL03	HR-S	11	19,5		≥10^-3	*BCR-ABL1*-like	*TERF2-JAK2*				Low
	A216	COALL03	HR-S	5	204		<10^-3	*BCR-ABL1*-like	*BCR-JAK2*				Low

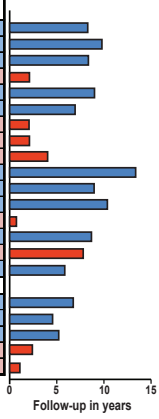

B

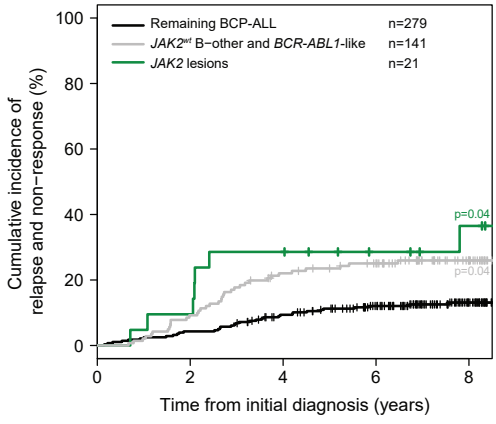

Figure 1. *JAK2* aberrations in BCP-ALL patients

(A) Type of lesions, clinical characteristics and follow-up of *JAK2* lesion positive patients. Treatment protocol and risk group assigned to each patient per protocol have been listed (HR-S: High Risk Standard. HR: High Risk. MR: Median Risk. SR: Standard Risk. LR-S: Low Risk Standard. LR-R: Low Risk Reduced. NHR: Non-High Risk). WBC indicates white blood cell count. Minimal residual disease (MRD) levels at day 29/33 of treatment of COALL and DCOG protocol, respectively. Type of translocation or mutation is listed. VAF indicates the variant allele frequency (%). *CRLF2* status indicates gene expression below (low) or above (high) the 90th percentile levels. Right panel: Bar plot represents years from diagnosis to event or last contact. In blue: cases in complete clinical remission. In red: cases with an event (relapse or death). **(B)** Cumulative incidence of relapse curves for patients with *JAK2* lesions (green line), *JAK2* wildtype *BCR-ABL1*-like and B-other cases (grey line), and *JAK2* wildtype remaining BCP-ALL cases (black line; *ETV6-RUNX1*, high hyperdiploid, *TCF3-PBX1*). Patients were treated according to ALL8, ALL9, ALL10, COALL97 or COALL03 protocol. Cumulative incidence of relapse (CIR) was estimated using a competing risk model. Relapse and non-response were considered as event, and death as competing event. Non-response was counted as event at day 79. The Gray's test was applied to test for equality of CIRs (*JAK2* lesion versus remaining BCP-ALL p=0.04; *JAK2* wildtype B-other/*BCR-ABL1*-like versus remaining BCP-ALL p=0.04).

Cumulative incidence of relapse in these *JAK2* aberrant patients did not differ from *JAK2* wildtype *BCR-ABL1*-like and B-other cases. Both displayed an unfavorable outcome compared to remaining BCP-ALL cases (p=0.04; Figure 1B). These findings underline the clinical relevance of *JAK2* lesions. Mutations and translocations represent biologically distinct entities, but both may be targetable by JAK-inhibitors.

Leukemic cells with *JAK2* lesions can be targeted by JAK inhibitors

Primary leukemic and patient-derived-xenograft (PDX) cells (Supplementary Figure 4, reference [25]) were exposed to momelotinib and ruxolitinib. *JAK2* translocated cells were more sensitive to both momelotinib and ruxolitinib compared to *JAK2* wildtype cases ($p<0.05$; Figure 2A-B, Supplementary Figure 5). *JAK2* mutated cells were less sensitive to these inhibitors than *JAK2* fusion positive cells, and were only marginally more sensitive than wildtype cells ($P<0.05$). Leukemic cells without genetic *JAK2* aberrations were resistant to ruxolitinib, but showed some sensitivity to momelotinib. Importantly, normal bone marrow mononuclear cells were resistant to both inhibitors (Supplementary Figure 5). Both JAK inhibitors effectively reduced levels of phosphorylated $STAT5^{Y694}$ and/or $STAT1^{Y701}$ (Figure 2C-D, Supplementary Figure 6).

The marginal sensitivity for both inhibitors and the low levels of phosphorylated STAT5 in *JAK2* mutated cells may be explained by lack of human TSLP ligand to activate the *CRLF2* pathway in our culture conditions. Addition of human TSLP sensitized *JAK2* mutated cells to ruxolitinib, but not to momelotinib ($p<0.01$, Figure 3A-B, Supplementary Figure 7-8). TSLP exposure did not change the efficacy of JAK inhibitors in *JAK2*-fusion positive cells, confirming cytokine-independent signaling (Figure 3C-D, Supplementary Figure 7). *JAK2* wildtype leukemic cells were not sensitized to JAK inhibitors by TSLP treatment (Figure 3E-F, Supplementary Figure 7). In the presence of TSLP both *JAK2* translocated and *JAK2* mutated cells were sensitive to JAK inhibitors (Figure 3G-H). At the protein level, TSLP exposure upregulated the levels of phosphorylated $STAT1^{Y701}$ and $STAT5^{Y694}$ in $JAK2^{R683S}$ mutated cells, whereas no effect was observed in *JAK2* fusion positive and *JAK2*-wildtype leukemic cells (Figure 3I-K, Supplementary Figure 9). Notably, TSLP triggered the phosphorylation and hence activation of the MEK/ERK pathway in $JAK2^{R683S}$ mutated cells, but not in $JAK2^{R683G}$ mutated cells (Figure 3I, 3L), suggesting that this activation is context-dependent. Phosphorylation of $STAT1^{Y701}$ and $STAT5^{Y694}$ was inhibited by momelotinib and ruxolitinib (Figure 3L).

JAK2 inhibition results in accumulation of phosphorylated JAK2

Exposure of primary leukemic cells, harboring *TERF2-JAK2* or *PAX5-JAK2*, to momelotinib and ruxolitinib resulted in accumulation of phosphorylated $JAK2^{Y1007}$ fusion proteins (Figure 2C). Wash out of both inhibitors induced a slight rebound effect with upregulation of $pSTAT1^{Y701}$ and $pSTAT5^{Y694}$ in *TERF2-JAK2* cells (Figure 4A, Supplementary Figure 10).

This rebound effect was also observed in the $JAK2^{V617F}$-positive leukemic cell line HEL (Supplemental Figure 11-12). Phosphorylated $JAK2^{Y1007}$ accumulated upon exposure to ruxolitinib. Removal of the inhibitor resulted in reactivation of JAK2 signaling, observed by a clear increase in phosphorylated $STAT5^{Y694}$ levels within 4 hours (time point 100 hours; Supplementary Figure 11A-B). The inhibitory effect of momelotinib was more transient compared to ruxolitinib, resulting in an earlier reactivation of JAK2, observed by high levels of phosphorylated $STAT5^{Y694}$ after 48 hours of momelotinib exposure (Supplemental Figure 11A).

Mesenchymal stromal cells protect against JAK inhibitors

Leukemic cells reside in the bone marrow microenvironment, where they disrupt normal hematopoietic stem cell niches.[26] This abnormal niche protects ALL cells against chemotherapy.[27,28] To study whether the bone marrow microenvironment protects against JAK inhibitors, we mimicked this niche by co-culturing PDX cells with bone marrow mesenchymal stromal cells (MSCs) derived from a leukemia patient. Survival of leukemic cells was improved in co-cultures together with MSCs compared to leukemic cells cultured without MSCs (Figure 5A). In these PDX/MSC co-cultures, JAK inhibitors decreased leukemic cell survival (Supplementary Figure 13A-G). However, leukemic cells were more resistant to ruxolitinib in PDX/MSC co-culture compared to culture without MSCs ($p<0.05$). A similar trend was observed for momelotinib (Figure 5B-C, Supplementary Figure 13H-I).

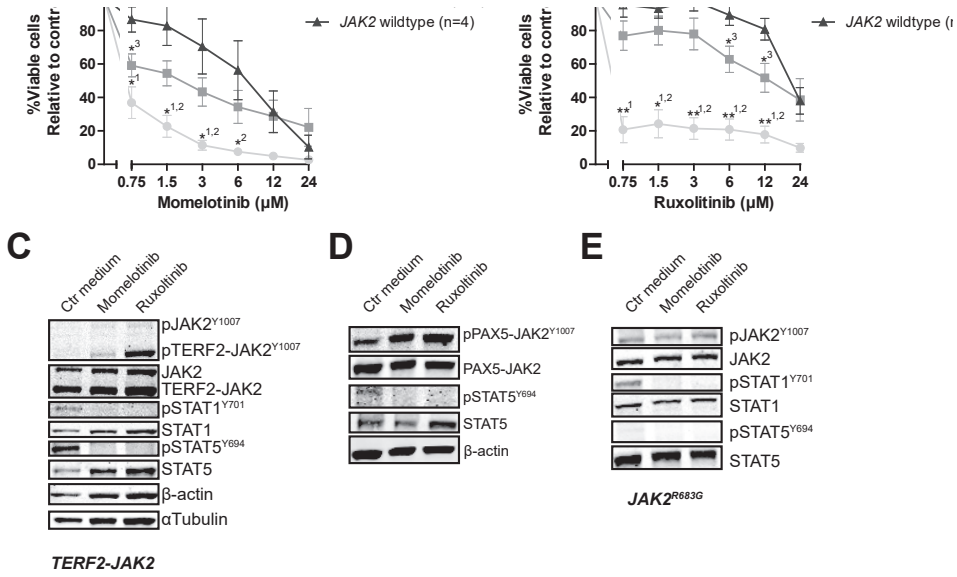

Figure 2. The efficacy of JAK inhibitors on *JAK2* translocated and mutated cells

(A-B) Leukemic (PDX or primary patient) cells were incubated for four days with to an increasing concentration range of momelotinib or ruxolitinib, after which cell viability was measured using an MTT assay. Sensitivity of exposed cells was calculated relative to vehicle treated controls. Individual samples were tested in duplicate. Mean±SEM of five *JAK2* translocated cases, six *JAK2* mutated cases and four *JAK2* wildtype cases is shown. Cell viability of samples was compared using independent sample T-test. **p≤0.01, *p≤0.05, [1]*JAK2* translocations versus *JAK2* wildtype, [2]*JAK2* translocations versus *JAK2* mutations, [3]*JAK2* mutations versus *JAK2* wildtype. **(C-E)** *TERF2-JAK2, PAX5-JAK2,* and *JAK2*^{R683G} PDX cells were exposed for four hours to vehicle control medium, 1.5 μM momelotinib or 0.75 μM ruxolitinib, after which (phosphorylated) TERF2-JAK2, PAX5-JAK2, JAK2, STAT1 and STAT5 levels were analysed using western blot (25 μg lysate).

Different outgrowth pattern in xenografts

The outgrowth patterns of primary leukemic cells (>90% blast purity) in three NSG mice per patient was determined by paired-end deep-sequencing of *JAK2* hotspot regions (exon 16, 20, 21 and 23; median read depth 554, 465, 411 and 593, respectively). PDX cells originating from a *JAK2*^{R683G} mutated case had a different VAF profile compared to the original patient sample (Figure 6A, Supplementary Figure 14A). The primary sample contained a major *JAK2*^{R683G} clone at a VAF of 63% and a minor *KRAS*^{G12D} clone at VAF 14%. In two out of three PDX samples generated, the VAF of the *JAK2*^{R683G} mutation increased to 98% (PDX1) and 99% (PDX3), whereas in the remaining PDX sample the VAF decreased to 49% (PDX2). In contrast, the *KRAS*^{G12D} mutation increased to a VAF 23% in this PDX2 sample, whereas this mutation was not detected in PDX1 and PDX3. The reduced VAF of the *JAK2* clone in PDX2 did not result in a decreased efficacy of momelotinib or ruxolitinib (Figure 6B). However, levels of pMEK1/2$^{S217/221}$ and pERK1/2$^{T202/Y204}$ in this sample were increased compared to the other two PDX samples (Figure 6C). Exposure to both JAK inhibitors did not decrease the levels of phosphorylated MEK and ERK.

Sanger sequencing of *JAK2*^{R683S} and *JAK2*^{R683T} PDX models also indicated a change in the VAF of PDX cells compared to the primary sample. In PDX cells from three NSG mice injected with *JAK2*^{R683S} cells, the A/T peak ratio at nucleotide position 2049 differed, suggesting heterogeneity in frequency of *JAK2* mutations between samples (Supplementary Figure 14B). Strikingly, two mice injected with *JAK2*^{R683T} mutated leukemic cells developed *JAK2* wildtype leukemia (Supplementary Figure 14C). Although the *JAK2* mutation was lost, *CRLF2* expression levels remained high (Supplementary Figure 14D-E). TSLP stimulation activated the JAK2 pathway signaling (Supplementary Figure 14F), but cells were not sensitive for JAK2 inhibition (Supplementary Figure 14G-H).

Figure 3. The effect of TSLP stimulation on the efficacy of JAK inhibitors .

Cells (PDX or primary ALL) were pre-incubated for 1 hour with or without 25 ng/ml TSLP, after which cells were exposed for four days to indicated concentrations of momelotinib or ruxolitinib. Cell viability was measured using an MTT assay. Sensitivity was calculated relative to vehicle treated controls. Individual samples were tested in duplicate. (**A-B**) Efficacy of momelotinib and ruxolitinib on *JAK2* mutated cells with or without TSLP pre-incubation. Mean±SEM of six independent samples is shown. (**C-D**) Efficacy of momelotinib and ruxolitinib on cells with *JAK2* translocations. Mean±SEM of two independent samples is shown. (**E-F**) Efficacy of momelotinib and ruxolitinib on *JAK2* wildtype PDX cells. Mean±SEM of three independent samples is shown. (**G-H**) Combined graph of the efficacy of momelotinib (**G**) and ruxolitinib (**H**) on TSLP stimulated cells with *JAK2* mutations (n=6), *JAK2* translocations (n=2), or *JAK2* wildtype cells (n=3). Mean±SEM of independent samples is shown. Cell viability of samples was compared using the independent sample T-test. **p≤0.01, *p≤0.05. [1]*JAK2* translocations versus *JAK2* wildtype, [2]*JAK2* wildtype versus *JAK2* mutations. (**I-K**) Western blot of *JAK2*^{R683S}, *TERF2-JAK2* and *JAK2*^{wt} PDX cells with or without TSLP stimulation (25 ng/ml for 1 hour). (**L**) *JAK2*^{R683G} cells were pre-incubated for 1 hour with or without 25 ng/ml TSLP, after which cells were exposed for four hours to vehicle control medium, 1.5 μM momelotinib or 0.75 μM ruxolitinib. Levels of (phosphorylated) JAK2, STAT1, STAT5, MEK1/2 and ERK1/2 were analysed using western blot.

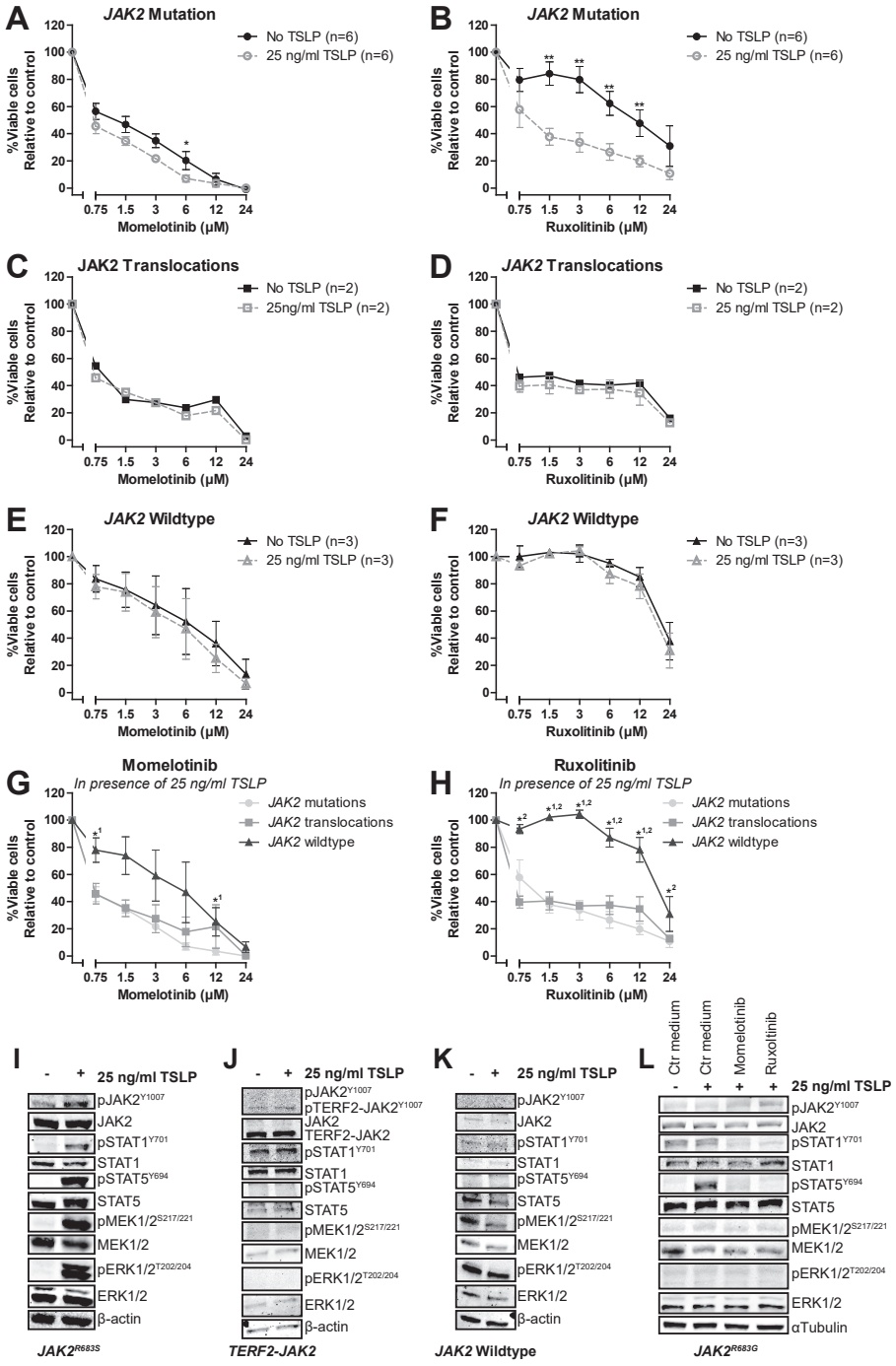
A
JAK2 Mutation
No TSLP (n=6)
25 ng/ml TSLP (n=6)
%Viable cells Relative to control
Momelotinib (µM)
B
JAK2 Mutation
Ruxolitinib (µM)
C
JAK2 Translocations
No TSLP (n=2)
25ng/ml TSLP (n=2)
D
JAK2 Translocations
25 ng/ml TSLP (n=2)
E
JAK2 Wildtype
No TSLP (n=3)
25 ng/ml TSLP (n=3)
F
JAK2 Wildtype
G
Momelotinib
In presence of 25 ng/ml TSLP
JAK2 mutations
JAK2 translocations
JAK2 wildtype
H
Ruxolitinib
I
25 ng/ml TSLP
pJAK2Y1007
JAK2
pSTAT1Y701
STAT1
pSTAT5Y694
STAT5
pMEK1/2S217/221
MEK1/2
pERK1/2T202/204
ERK1/2
β-actin
JAK2R683S
J
pJAK2Y1007
pTERF2-JAK2Y1007
TERF2-JAK2
TERF2-JAK2
K
JAK2 Wildtype
L
Ctr medium
Momelotinib
Ruxoltinib
αTubulin
JAK2R683G

DISCUSSION

This study aimed to evaluate the clinical need (frequency of lesions and prognostic value) and potential of JAK inhibitors in pediatric BCP-ALL. For this purpose pediatric BCP-ALL patients were screened for *JAK2* lesions. *JAK2* point mutations were found in 3.6% of our BCP-ALL patients, of which the majority were *JAK2*^{R683} mutations. These mutations were solely detected in *BCR-ABL1*-like, B-other and high hyperdiploid patients, but not in *KMT2A-AFF1*, *BCR-ABL1*, *ETV6-RUNX1* or *TCF3-PBX1* patients. *JAK2* translocations were detected in the poor prognostic *BCR-ABL1*-like group, but not in non-*BCR-ABL1*-like B-other cases. The prognosis of patients with *JAK2* aberrations was as poor as *JAK2* wildtype *BCR-ABL1*-like and non-*BCR-ABL1*-like B-other patients.

JAK2 mutations were not detected as frequently in our DCOG/COALL sequencing cohort as reported for COG high-risk cohorts.[5, 10] Two independent classifiers are used to describe *BCR-ABL1*-like BCP-ALL.[29-31] Differences in genetic ancestry between the American COG and European DCOG/COALL cohorts likely affected the signatures to classify patients as *BCR-ABL1*-like. Hence, genetic differences, or more specifically the lack of Hispanic/Latino cases[10, 32] might explain the lower frequencies of JAK2 mutations, as well as the difference in treatment outcome.

A targeted approach was used to detect *JAK2* translocations. All cases with high *JAK2* expression levels harbored one of the known fusion genes, making it therefore unlikely that novel fusion genes were missed.

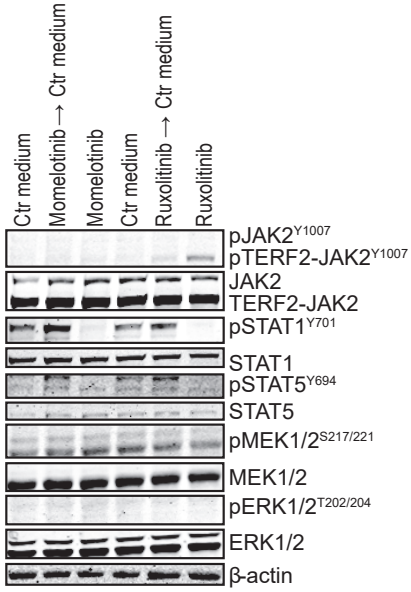

Figure 4. Accumulation of pJAK2 ^{Y1007} results in a rebound effect of JAK2

TERF2-JAK2 PDX cells were incubated for four hours with or without 1.5 μM momelotinib or 0.75 μM ruxolitinib, after which cells were washed to remove the JAK inhibitors. Half of the cells were exposed for another 1.5 hours to 1.5 μM momelotinib or 0.75 μM ruxolitinib, whereas the other cells were incubated in vehicle control (Ctr) medium. Protein expression levels were examined by western blot (25 μg lysate).

The poor outcome of cases harboring *JAK2* lesions underline the clinical relevance of activated JAK2. The therapeutic potential of JAK2 was demonstrated by efficacy of JAK inhibitors in *JAK2* mutated and *JAK2* translocated primary BCP-ALL cells. *JAK2* translocated cells were sensitive to both JAK inhibitors, independent of cytokine activation. In contrast, the efficacy of JAK inhibitors in *JAK2* mutated cells highly depended on CRLF2 activation by TSLP, which is in concordance with previous reports.[3, 5, 7, 8, 17] These results highlight the importance of TSLP in *in vitro* and *in vivo* studies involving *JAK2* mutations. Since human CRLF2 cannot be activated by mouse TSLP, conventional mouse xenograft models are not suitable to test the efficacy of ruxolitinib and other JAK inhibitors on *JAK2* mutated cells. Absence of human TSLP in ALL xenograft mouse models might therefore explain the disappointing efficacy of JAK inhibitors in *in vivo* models.[18-21] The recently engineered xenograft model which synthesizes human TSLP may overcome this limitation.[33]

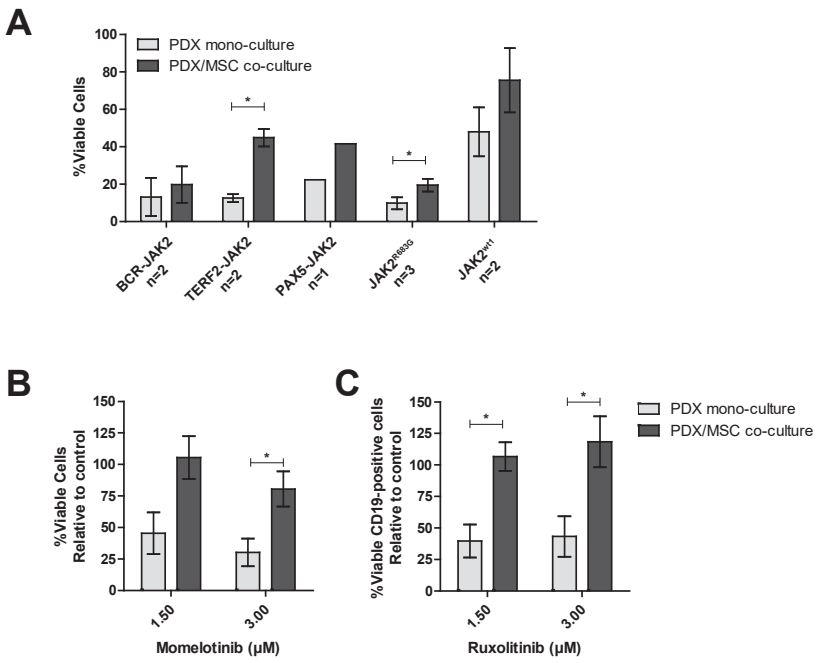

Figure 5. Efficacy of JAK inhibitors in co-culture

The response of CD19+ PDX cells, co-cultured with MSCs (hCD19$^-$), to increasing concentrations of momelotinib and ruxolitinib, was assessed after four days of culture using flow cytometry. Cells were stained with Brilliant Violet 421 anti-human CD19 antibody, FITC Annexin V, and PI. Viability was calculated relative to vehicle controls. **(A)** Survival of PDX cells in mono-culture, or PDX/MSC co-culture. Individual samples were tested in duplicate. Bars represent the mean±SEM of two *BCR-JAK2*, two *TERF2-JAK2*, one *PAX5-JAK2*, three *JAK2*^{R683G}, and two *JAK2* wildtype samples. Cell viability of samples in mono-culture versus co-culture was compared using the independent sample T-test. *p≤0.05. (**B-C**) The effect of 1.5 μM and 3.0 μM momelotinib or ruxolitinib on the viability of PDX cells with *JAK2* translocations in mono-culture, or in co-culture with primary MSCs. Mean±SEM of three *JAK2* translocated samples is shown. Cell viability of samples was compared using independent sample T-test. *p≤0.05.

Despite the need for human TSLP, we and others observed engraftment of primary *JAK2* mutated cells in NSG mice, giving rise to leukemia within months after intra-femoral injection.[18, 19, 21] This implies that the proliferation of *JAK2* mutated leukemic cells in the mouse bone marrow does not (solely) depend on CRLF2 signaling, but may be supported by activation of alternative pathways.[34, 35] This argues against targeted monotherapy, as cells might escape via an alternative pathway, such as the RAS pathway.[35, 36] This is further strengthened by a study in Down syndrome ALL, in which a switch was observed from a *JAK2* mutation at initial diagnosis to a RAS-mutation at relapse.[37] In the current study, we also observed co-occurrence of *JAK2* and *KRAS* lesions in non-Down syndrome BCP-ALL cells. More importantly, these *JAK2* and *KRAS* mutations showed different outgrowth patterns in NSG xenograft models. Co-occurrence of these mutations suggests that a combination of JAK and RAS pathway inhibitors may be more effective for *JAK2*-aberrant

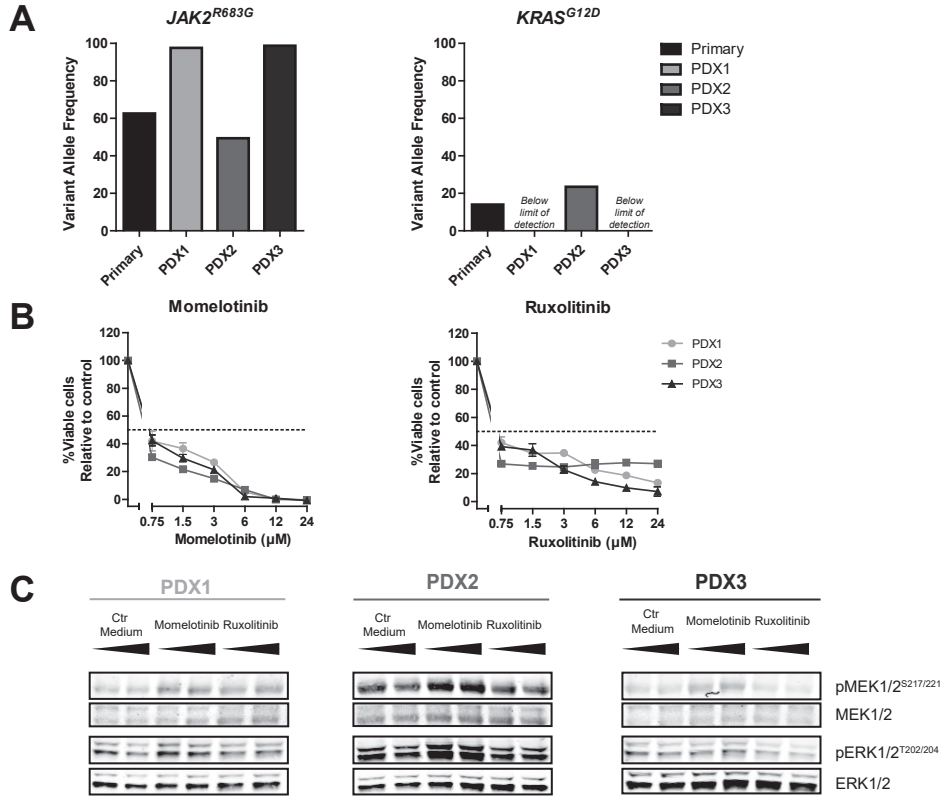

Figure 6. Outgrowth pattern of *JAK2* mutated samples in xenografts

(A) VAF of *JAK2*^{R683G} and *KRAS*^{G12D} in primary leukemic cells and three PDX samples of the same patient was determined using targeted amplicon sequencing. **(B)** PDX cells were pre-incubated for 1 hour with 25 ng/ml TSLP, after which they were exposed for four days to indicated concentrations of momelotinib or ruxolitinib in the presence of TSLP. Cell viability was measured using an MTT assay. Cell survival was calculated relative to vehicle treated controls. Samples were tested in duplicate. Mean±SD of each sample is shown. **(C)** Protein expression levels of PDX samples, exposed to 1.5 μM momelotinib or 0.75 μM ruxolitinib for four hours.

cases. Moreover our results indicate that *JAK2* mutations by itself might not be drivers of leukemic outgrowth, which is also corroborated by the outgrowth of *JAK2* wildtype leukemic cells in mice injected with *JAK2*^{R683T} cells. Taken together, these data imply that 1) the expansion properties of *JAK2* mutated leukemic cells vary, 2) other subclones (e.g. *KRAS*^{G12D}) can grow out at the expense of the major *JAK2* mutated clone, 3) *JAK2* mutations can get lost while leukemia progresses. Therefore, *JAK2* mutations are most likely secondary lesions, in contrast to *JAK2* translocations, which are primary lesions. The selection of alternative pathways indicates a potential risk for use of JAK inhibitors in *JAK2* mutated cases without detailed monitoring of the mutational status of leukemic cells in time. Interestingly, we observed a difference in the cytotoxicity of momelotinib and ruxolitinib. Both agents fully inhibited JAK/STAT signaling by downregulation of phosphorylation levels of STAT1 and STAT5. However, only momelotinib affected *JAK2* wildtype and non-TSLP stimulated *JAK2* mutated cells, regardless of activation of STAT5. Therefore, it is likely that momelotinib also affects alternative targets.[38, 39] In addition, our data revealed that exposure to JAK inhibitors, especially ruxolitinib, resulted into accumulation of phosphorylated JAK2^{Y1007}, which consequently induced a profound re-activation of downstream STAT signaling. Accumulation of phosphorylated JAK2^{Y1007} is in concordance with other reports.[20, 40-42] The rebound effect observed in the present study identifies an important limitation of these agents. As type I inhibitors bind JAK2 in its active conformation, reactivation of JAK2 may be overcome by type II inhibitors, which bind JAK2 in its inactive conformation.[17, 43] Preclinical *in vitro* and *in vivo* data indicate high efficacy of the type II inhibitor CHZ868. Clinical data of this inhibitor and other novel inhibitors are warranted. Besides studying the mechanism of action, we showed influences of the bone marrow microenvironment on the efficacy of JAK inhibitors. Microenvironment-induced resistance of leukemic cells has been reported for conventional drugs, e.g. prednisolone and asparaginase, for imatinib in *BCR-ABL1*-positive cells, and for JAK inhibitors in the present study.[44-46] These data imply that the local tumor environment can stimulate a survival program, which may provide leukemic cells a way to escape from JAK inhibitors.

Taken together, *JAK2* lesions are infrequently found in children with newly diagnosed BCP-ALL and are mainly restricted to *BCR-ABL1*-like and non-*BCR-ABL1*-like B-other cases (negative for sentinel cytogenetic lesions). Although mutations and translocations represent biologically distinct entities, both may be targetable by JAK-inhibitors. Indeed, we showed efficacy of momelotinib and ruxolitinib in both cell types. As both momelotinib and ruxolitinib have a short half-life (less than half a day), the observed rebound effect may be therapeutically of risk.[47, 48] Although it should be confirmed by functional *in vivo* studies, our data suggest that the effect of JAK inhibition may be compromised by microenvironment-induced resistance and induction of alternative survival pathways. In conclusion, JAK inhibitors may be considered to be added to, but not substitute, chemotherapy for patients with *JAK2* aberrations, especially for those at high risk of relapse due to high MRD levels upon induction therapy. Therapeutic monitoring for activation of alternative pathways (e.g. RAS) is highly recommended.

METHODS

Primary patient-derived material

Bone marrow and/or peripheral blood samples were obtained from children (1-18 years) with newly diagnosed ALL. Written informed consent was obtained from parents or guardians to use excess diagnostic material for research purposes, as approved by the institutional review board. These studies were conducted in accordance with the Declaration of Helsinki. Mononuclear cells were isolated and processed as described previously.[49] Samples were enriched towards > 90% leukemic cells by depletion of non-leukemic cells using immunomagnetic beads. The major cytogenetic subtypes were determined using fluorescent in situ hybridization, (RT-)PCR, and the 110-probeset gene expression classifier.[30] Patients were treated according to the DCOG ALL8, ALL9 or ALL10 protocol, or the COALL-06-97 and COALL-07-03 study protocols.[50-54] Patient characteristics were provided by the central study centers of DCOG (The Hague, the Netherlands) and COALL (Hamburg, Germany).

Mesenchymal stromal cells (MSCs) were isolated from the bone marrow aspirate of a *BCR-ABL1*-like patient as described previously.[55] Purity of MSCs was assessed by negativity for the hematopoietic markers CD34, CD45, and CD19, and positivity for the mesenchymal markers CD13, CD29, CD44, CD54, CD73, CD90, CD105, CD146 and CD166, as detected by flow cytometry (MACS Quant). Expression was measured using the human mesenchymal stem cell marker antibody panel (R&D Systems, Minneapolis, Minnesota, USA), and CD13-APC, CD29-APC, CD34-PE, CD54-PE, CD73-PE, IgG1-PE, and IgG1-APC (BD Biosciences, San Jose, California, USA).

Cell lines

The human erythroleukemia cell line HEL was obtained from the German Collection of Microorganisms and Cell lines (DSMZ, Braunschweig, Germany) and cultured in RPMI-1640 medium, supplemented with 10% fetal calf serum (Bodinco BV, Alkmaar, Netherlands), 100 units/ml penicillin, 100 µg/ml streptomycin and 0.125 µg/mL fungizone (Life Technologies, Bleiswijk, Netherlands). The identity of the cell line was routinely verified by DNA fingerprinting. Additionally, presence of Mycoplasma was excluded every 25 passages by PCR.

Patient-derived-xenograft cells

Primary leukemic cells were transplanted by intra-femoral injection in 7-12 weeks old female NOD.Cg-*Prkdc*^{scid}*Il2rg*^{tm1Wjl}/SzJ (NSG) mice (Charles River, Wilmington, Massachusetts, USA; three NSG mice per patient), as approved by the animal ethics committee (EMC 2863). Mice were sacrificed upon overt leukemia or 6 months after injection. Leukemic cells were isolated from bone marrow and spleen. The percentage of human leukemic cells was analyzed by flow cytometry (APC anti-human CD19, PE anti-human CD45 and FITC anti-mouse CD45; Biolegend, London, UK) and May-Grünwald-Giemsa staining. Patient-derived-xenograft cells (PDX) were enriched for > 90% human leukemic cells using anti-human-CD19 immunomagnetic beads (MACS Miltenyi, Leiden, Netherlands).

JAK2 mutations

JAK2 mutations status was analyzed in 461 BCP-ALL cases, representing the major cytogenetic subtypes (6% *BCR-ABL1*, 17% *BCR-ABL1*-like, 15% non-*BCR-ABL1*-like B-other, 27% *ETV6-RUNX1*, 27% high hyperdiploid, 3% *MLL-AF4*, 6% *TCF3-PBX1*). Genomic DNA was isolated using Trizol reagent (Life Technologies), or in some cases using the DNeasy blood and tissue kit (Qiagen) according to manufacturer's instructions, and quantified using the Qubit dsDNA Broad Range Assay Kit (Life Technologies). 100-250ng genomic DNA was used to prepare sequencing libraries according to manufacturer's instructions. Successful library preparation, correct amplicon length and concentration were assessed using the Labchip GX genomic analyzer (Caliper Life Sciences Benelux N.V.) with the HT DNA 12K Reagent Kit, Version 2. Samples were pooled equi-molarly and sequenced on an Illumina MiSeq in paired-end reads of 250bp each. The custom amplicons covered the exons 16, 20, 21 and 23 and represent the mutational hotspot region of JAK2.

Sequence reads were exported in fastq format and, aligned to the standard 1000 genomes human reference sequences (version b37, from the GATK resource bundle provided by the Broad institute, USA), using BWA version 0.7.10 and the GATK indel realigner version 3.3-0. Freebayes version 0.9.18-24, Varscan version 2.3.7, Bcftools version 1.0, and GATK version 3.3-0 were used to call single nucleotide variants. The resulting variant call format files were annotated using snpEff and snpSift version 4.1a and the dbNSFP version 2.7 database. Variants were combined and filtered based on several criteria using an in-house developed pipeline: variants were excluded if they were not located in targeted regions, were reported by only one caller, had coverage of < 100 reads, or had < 10 reads supporting the variant allele. Furthermore, variants had to occur at least once with a VAF above 2% in any sample and to be distributed equally between runs according to a chi-square test. Additionally only variants were taken into account if they were reported in the COSMIC V73 GRCh37 database, lead to an amino acid change, were unlikely to be a germline variant and not a known SNP. SNPs were defined as having a mean population frequency of ≥ 5% across the 1000Gp1 complete human population, 1000Gp1 population of European decent, and the ESP-6500 population of European decent allele frequency databases. Variants found in ≥ 10 samples with a mean and median VAF > 40% were labelled as possible germline. Sufficient coverage was crucial to detect subclonal mutations, which could be reliably detected ≥ 5% VAF in on average 91% of the cases. Detection of variants with a frequency of 1% was limited to a smaller group (26%), and is therefore a conservative estimate in the present study.

Genomic DNA of PDX cells was used to identify *JAK2* mutations in exon 16. Samples were analyzed by Baseclear B.V. using Sanger sequencing (forward primer 5'-ATGCCTCCAAATTATTATACTATCA-3', reverse primer 5'-ATCACCTCACAGTCCATG GTTAT-3').

JAK2 translocations

Presence of ten recurrently reported *JAK2* translocations was examined by RT-PCR in 153 BCP-ALL cases, negative for sentinel BCP-ALL associated lesions (n=77 *BCR-ABL1*-like, n=76 non-*BCR-ABL1*-like B-other). Total RNA was extracted from leukemic cells using Trizol reagents (Life Technologies). cDNA was synthesized using random hexamers

and oligodT primers, and M-MLV reverse transcriptase (Promega, Leiden, Netherlands). RT-PCR was performed in a final volume of 25 µl, containing 0.3 µM forward primer, 0.3 µM reverse primer, 200 µM dNTPs, 1x PCR buffer II, 4 mM MgCl2, 0.125 µl AmpliTaq DNA polymerase (Promega) and 2.5 µl cDNA. Primer sequences are shown in Supplementary Table 1. PCR products were Sanger sequenced by Baseclear B.V. (Leiden, Netherlands).

CRLF2 status

CRLF2 expression levels were determined by Affymetrix gene expression microarrays (U133 Plus 2.0; Santa Clara, California, USA), of a previously published cohort of pediatric BCP-ALL patients at initial diagnosis.[56] High CRLF2 expression levels are indicative P2RY8 CRLF2 and IGH-CRLF2 translocations in different studies, though not all cases with high CRLF2 mRNA expression levels harbor CRLF2 rearrangements.[10, 56-58] Of 406 cases, both *CRLF2* gene expression data and *JAK2* mutation status was available. Signal intensity of probeset 208303_s_at above the 90th percentile levels was classified as *CRLF2* high, as described previously.[56]

In addition, *CRLF2* expression in primary leukemic and PDX samples was determined using RT-qPCR and SYBR green. *CRLF2* expression (forward primer 5'-ACGGGGATCTCCTCTATG-3', reverse primer: 5'-GAGGCGTTGG TGTCTCT-3') was calculated relative to RSP20 expression (forward primer 5'-AAGGGCTGAGGATTTTTG-3', reverse primer 5'-CGTTGCGGCTTGTTAG-3'), using the comparative cycle time (Ct) method; $2^{-\Delta Ct}$ x 100%, whereby $\Delta C_t = Ct_{CRLF2} - Ct_{RPS20}$. RT-qPCR expression values were correlated to Affymetrix microarray data of probeset 208303_s_at.

JAK2 expression levels

JAK2 expression levels were analyzed using Affymetrix gene expression microarrays, in a previously published pediatric BCP-ALL cohort.[56] Signal intensity of probeset 205841_at was used to quantify *JAK2* gene expression.

Ex vivo drug cytotoxicity assays

Cell-intrinsic resistance towards momelotinib and ruxolitinib (Selleck Chemicals, Kirby Drive, Houston, USA) was evaluated as described previously.[49] Briefly, leukemic cells were exposed to a concentration range (24µM to 750nM) of these compounds for four days and cytotoxicity was quantified using 3-(4,5-dimethylthiazol-2-yl)-2,5-diphenyltetrazolium bromide (MTT). For TSLP stimulation, cells were pre-incubated for 1 hour with 25 ng/ml TSLP (R&D systems, Oxon, UK). In addition to single cell cultures, leukemic cells (1×10^6 cells) were co-cultured with primary MSCs (5×10^4 cells) for four days in a 24 well plate in the presence of a dilution series of momelotinib and ruxolitinib. Cell survival was quantified using flow cytometry (MACSQuant, FlowJo 10.0.8r1), and cells were stained with Brilliant Violet 421 anti-human CD19 antibody (Biolegend), FITC Annexin V (Biolegend), and Propidium Iodide (PI; Invitrogen, Bleiswijk, Netherlands), as described previously.[44]

Western blotting

Leukemic cells were lysed in lysis buffer supplemented with freshly added protease and phosphatase inhibitors. 25µg (BCA method; Thermo Scientific) lysate was loaded on 10% mini protean precast gels (BioRad, Veenendaal, Netherlands), and transferred to a nitrocellulose membrane (Biorad). Primary antibody incubation was performed according to manufacturer's protocol. Anti-JAK2 (#3230), anti-phospho-JAK2^{Y1007} (#4406), anti-phospho-STAT5^{Tyr694} (#9351), anti-phospho-STAT1^{Tyr701} (#9167), anti-Stat1 (#9175), anti-phospho-MEK1/2$^{Ser217/221}$ (#9154), anti-MEK1/2 (#4694), anti-phospho-Erk1/2$^{T202/Y204}$ (#4370), anti-Erk1/2 (#91078), and anti-αTubulin (#2144) were obtained from Cell Signaling Technology (Danvers, Massachusetts, USA). Anti-β-actin (ab6276) was obtained from Abcam (Cambridge, UK), and anti-STAT5 (sc-835) from Santa Cruz (Heidelberg, Germany). Blots were stained with secondary antibodies (IRDye 680RD- or 800CW-labelled anti-rabbit and IRDye 680RD- or 800CW-labelled anti-mouse; Li-Cor Biosciences, Leusden, Netherlands) and scanned using the Odyssey infrared imaging system (Li-Cor Biosciences). To reprobe membranes, they were stripped in NewBlot Nitrocellulose stripping buffer (Li-Cor Biosciences) according to manufacturer's protocol. *BCR-JAK2*, *PAX5-JAK2* and *TERF2-JAK2* proteins were separated from wildtype *JAK2* based on size (~94, 57, 95 and 125 kDa, respectively).

Statistics

Cumulative incidence of relapse (CIR) was estimated using a competing risk model. Relapse and non-response (counted at day 79) were considered as event, and death as competing event. The Gray's test was applied to test for equality of CIRs.[59] Outcome analyses were performed in R 3.0.1, using the packages cmprsk version 2.2-7[60], mstate version 0.2.7[61], and survival version 2.37-4[62].

Acknowledgements

We thank Ies Nijman, Annelies Smouters and Edwin Cuppen (University Medical Centre Utrecht) for their help in setting up the sequencing experiments and analysis pipeline.
This work was supported by the VICI program grant 016.126.612 from Netherlands Organization for Scientific Research (NWO), the Dutch Cancer Society grants AMC 2008-4265 and EMCR 2014-6998, the Kika Foundation (grant 132 and 161), the Pediatric Oncology Foundation Rotterdam (KOCR), and by the Centre for Personalized Cancer Treatment, which is a collaboration between all University Medical Cancer Centres and the Netherlands Cancer Institute Amsterdam and is supported by grants from KWF/Alpe d'Huzes and Nuts/Ohra.

Authorship Contributions

EMPS and ISJ designed and performed experiments, and analyzed and interpreted data. MJK designed deep sequencing primers. ISJ and NJMB performed deep sequencing. ISJ, AQH and JMB analyzed and interpreted deep sequence data. EMPS and WGN performed *ex vivo* experiments and analyzed data. EMPS, AB and CvdV collected PDX samples. EMPS and AB performed PCR reactions for Sanger sequencing analyses. RP, HAdGK, CMZ and MH provided clinical characteristics and clinical outcome data, and

interpreted data. MLdB designed the study and interpreted data. EMPS, ISJ and MLdB drafted the manuscript. The manuscript was revised and approved by all authors.

Disclosure of Conflicts of Interest

The authors declare no conflicts of interest.

REFERENCES

1. Smith CA and Fan G. The saga of JAK2 mutations and translocations in hematologic disorders: pathogenesis, diagnostic and therapeutic prospects, and revised World Health Organization diagnostic criteria for myeloproliferative neoplasms. Hum Pathol. 2008; 39(6):795-810.
2. Saharinen P and Silvennoinen O. The pseudokinase domain is required for suppression of basal activity of Jak2 and Jak3 tyrosine kinases and for cytokine-inducible activation of signal transduction. J Biol Chem. 2002; 277(49):47954-47963.
3. Bercovich D, Ganmore I, Scott LM, Wainreb G, Birger Y, Elimelech A, Shochat C, Cazzaniga G, Biondi A, Basso G, Cario G, Schrappe M, Stanulla M, Strehl S, Haas OA, Mann G, et al. Mutations of JAK2 in acute lymphoblastic leukaemias associated with Down's syndrome. Lancet. 2008; 372(9648):1484-1492.
4. Russell LJ, Capasso M, Vater I, Akasaka T, Bernard OA, Calasanz MJ, Chandrasekaran T, Chapiro E, Gesk S, Griffiths M, Guttery DS, Haferlach C, Harder L, Heidenreich O, Irving J, Kearney L, et al. Deregulated expression of cytokine receptor gene, CRLF2, is involved in lymphoid transformation in B-cell precursor acute lymphoblastic leukemia. Blood. 2009; 114(13):2688-2698.
5. Mullighan CG, Zhang J, Harvey RC, Collins-Underwood JR, Schulman BA, Phillips LA, Tasian SK, Loh ML, Su X, Lu W, Devidas M, Atlas SR, Chen IM, Clifford RJ, Gerhard DS, Carroll WL, et al. JAK mutations in high-risk childhood acute lymphoblastic leukemia. Proc Natl Acad Sci U S A. 2009; 106(23):9414-9418.
6. Mullighan CG, Collins-Underwood JR, Phillips LA, Loudin MG, Liu W, Zhang J, Ma J, Coustan-Smith E, Harvey RC, Willman CL, Mikhail FM, Meyer J, Carroll AJ, Williams RT, Cheng J, Heerema NA, et al. Rearrangement of CRLF2 in B-progenitor- and Down syndrome-associated acute lymphoblastic leukemia. Nat Genet. 2009; 41(11):1243-1246.
7. Kearney L, Gonzalez De Castro D, Yeung J, Procter J, Horsley SW, Eguchi-Ishimae M, Bateman CM, Anderson K, Chaplin T, Young BD, Harrison CJ, Kempski H, So CW, Ford AM and Greaves M. Specific JAK2 mutation (JAK2R683) and multiple gene deletions in Down syndrome acute lymphoblastic leukemia. Blood. 2009; 113(3):646-648.
8. Yoda A, Yoda Y, Chiaretti S, Bar-Natan M, Mani K, Rodig SJ, West N, Xiao Y, Brown JR, Mitsiades C, Sattler M, Kutok JL, DeAngelo DJ, Wadleigh M, Piciocchi A, Dal Cin P, et al. Functional screening identifies CRLF2 in precursor B-cell acute lymphoblastic leukemia. Proc Natl Acad Sci U S A. 2010; 107(1):252-257.
9. HertzBerg L, Vendramini E, Ganmore I, Cazzaniga G, Schmitz M, Chalker J, Shiloh R, Iacobucci I, Shochat C, Zeligson S, Cario G, Stanulla M, Strehl S, Russell LJ, Harrison CJ, Bornhauser B, et al. Down syndrome acute lymphoblastic leukemia, a highly heterogeneous disease in which aberrant expression of CRLF2 is associated with mutated JAK2: a report from the International BFM Study Group. Blood. 2010; 115(5):1006-1017.
10. Harvey RC, Mullighan CG, Chen IM, Wharton W, Mikhail FM, Carroll AJ, Kang H, Liu W, Dobbin KK, Smith MA, Carroll WL, Devidas M, Bowman WP, Camitta BM, Reaman GH, Hunger SP, et al. Rearrangement of CRLF2 is associated with mutation of JAK kinases, alteration of IKZF1, Hispanic/Latino ethnicity, and a poor outcome in pediatric B-progenitor acute lymphoblastic leukemia. Blood. 2010; 115(26):5312-5321.
11. Tirado CA, Chen W, Huang LJ, Laborde C, Hiemenz MC, Valdez F, Ho K, Winick N, Lou Z and Koduru P. Novel JAK2 rearrangement resulting from a t(9;22)(p24;q11.2) in B-acute lymphoblastic leukemia. Leuk Res. 2010; 34(12):1674-1676.
12. Roberts KG, Li Y, Payne-Turner D, Harvey RC, Yang YL, Pei D, McCastlain K, Ding L, Lu C, Song G, Ma J, Becksfort J, Rusch M, Chen SC, Easton J, Cheng J, et al. Targetable kinase-activating lesions in Ph-like acute lymphoblastic leukemia. N Engl J Med. 2014; 371(11):1005-1015.
13. Roberts KG, Morin RD, Zhang J, Hirst M, Zhao Y, Su X, Chen SC, Payne-Turner D, Churchman ML, Harvey RC, Chen X, Kasap C, Yan C, Becksfort J, Finney RP, Teachey DT, et al. Genetic alterations activating kinase and cytokine receptor signaling in high-risk acute lymphoblastic leukemia. Cancer Cell. 2012; 22(2):153-166.
14. Cuesta-Dominguez A, Ortega M, Ormazabal C, Santos-Roncero M, Galan-Diez M, Steegmann JL, Figuera A, Arranz E, Vizmanos JL, Bueren JA, Rio P and Fernandez-Ruiz E. Transforming and tumorigenic activity of JAK2 by fusion to BCR: molecular mechanisms of action of a novel BCR-JAK2 tyrosine-kinase. PLoS One. 2012; 7(2):e32451.
15. Boer JM, Steeghs EM, Marchante JR, Boeree A, Beaudoin JJ, Beverloo HB, Kuiper RP, Escherich G, van der Velden VH, van der Schoot CE, de Groot-Kruseman HA, Pieters R and den Boer ML. Tyrosine kinase fusion genes in pediatric BCR-ABL1-like acute lymphoblastic leukemia. Oncotarget. 2017; 8(3):4618-4628.
16. Schinnerl D, Fortschegger K, Kauer M, Marchante JR, Kofler R, Den Boer ML and Strehl S. The role of the Janus-faced transcription factor PAX5-JAK2 in acute lymphoblastic leukemia. Blood. 2015; 125(8):1282-1291.
17. Wu SC, Li LS, Kopp N, Montero J, Chapuy B, Yoda A, Christie AL, Liu H, Christodoulou A, van Bodegom D, van der Zwet J, Layer JV, Tivey T, Lane AA, Ryan JA, Ng SY, et al. Activity of the Type II JAK2 Inhibitor CHZ868 in B Cell Acute Lymphoblastic Leukemia. Cancer Cell. 2015; 28(1):29-41.
18. Suryani S, Bracken LS, Harvey RC, Sia KC, Carol H, Chen IM, Evans K, Dietrich PA, Roberts KG, Kurmasheva RT, Billups CA, Mullighan CG, Willman CL, Loh ML, Hunger SP, Houghton PJ, et al. Evaluation of the in vitro and in vivo efficacy of the JAK inhibitor AZD1480 against JAK-mutated acute lymphoblastic leukemia. Mol Cancer Ther. 2015; 14(2):364-374.
19. Maude SL, Tasian SK, Vincent T, Hall JW, Sheen C, Roberts KG, Seif AE, Barrett DM, Chen IM, Collins JR, Mullighan CG, Hunger SP, Harvey RC, Willman CL, Fridman JS, Loh ML, et al. Targeting

JAK1/2 and mTOR in murine xenograft models of Ph-like acute lymphoblastic leukemia. Blood. 2012; 120(17):3510-3518.

20. Weigert O, Lane AA, Bird L, Kopp N, Chapuy B, van Bodegom D, Toms AV, Marubayashi S, Christie AL, McKeown M, Paranal RM, Bradner JE, Yoda A, Gaul C, Vangrevelinghe E, Romanet V, et al. Genetic resistance to JAK2 enzymatic inhibitors is overcome by HSP90 inhibition. J Exp Med. 2012; 209(2):259-273.
21. Tasian SK, Teachey DT, Li Y, Shen F, Harvey RC, Chen IM, Ryan T, Vincent TL, Willman CL, Perl AE, Hunger SP, Loh ML, Carroll M and Grupp SA. Potent efficacy of combined PI3K/mTOR and JAK or ABL inhibition in murine xenograft models of Ph-like acute lymphoblastic leukemia. Blood. 2017; 129(2):177-187.
22. Loh ML, Tasian SK, Rabin KR, Brown P, Magoon D, Reid JM, Chen X, Ahern CH, Weigel BJ and Blaney SM. A phase 1 dosing study of ruxolitinib in children with relapsed or refractory solid tumors, leukemias, or myeloproliferative neoplasms: A Children's Oncology Group phase 1 consortium study (ADVL1011). Pediatr Blood Cancer. 2015; 62(10):1717-1724.
23. Li F, Guo HY, Wang M, Geng HL, Bian MR, Cao J, Chen C, Zeng LY, Wang XY and Wu QY. The effects of R683S (G) genetic mutations on the JAK2 activity, structure and stability. Int J Biol Macromol. 2013; 60:186-195.
24. Imamura T, Kiyokawa N, Kato M, Imai C, Okamoto Y, Yano M, Ohki K, Yamashita Y, Kodama Y, Saito A, Mori M, Ishimaru S, Deguchi T, Hashii Y, Shimomura Y, Hori T, et al. Characterization of pediatric Philadelphia-negative B-cell precursor acute lymphoblastic leukemia with kinase fusions in Japan. Blood Cancer J. 2016; 6:e419.
25. Schmitz M, Breithaupt P, Scheidegger N, Cario G, Bonapace L, Meissner B, Mirkowska P, Tchinda J, Niggli FK, Stanulla M, Schrappe M, Schrauder A, Bornhauser BC and Bourquin JP. Xenografts of highly resistant leukemia recapitulate the clonal composition of the leukemogenic compartment. Blood. 2011; 118(7):1854-1864.
26. Colmone A, Amorim M, Pontier AL, Wang S, Jablonski E and Sipkins DA. Leukemic cells create bone marrow niches that disrupt the behavior of normal hematopoietic progenitor cells. Science. 2008; 322(5909):1861-1865.
27. McMillin DW, Delmore J, WeisBerg E, Negri JM, Geer DC, Klippel S, Mitsiades N, Schlossman RL, Munshi NC, Kung AL, Griffin JD, Richardson PG, Anderson KC and Mitsiades CS. Tumor cell-specific bioluminescence platform to identify stroma-induced changes to anticancer drug activity. Nat Med. 2010; 16(4):483-489.
28. Lane SW, Scadden DT and Gilliland DG. The leukemic stem cell niche: current concepts and therapeutic opportunities. Blood. 2009; 114(6):1150-1157.
29. Boer JM, Marchante JR, Evans WE, Horstmann MA, Escherich G, Pieters R and Den Boer ML. BCR-ABL1-like cases in pediatric acute lymphoblastic leukemia: a comparison between DCOG/Erasmus MC and COG/St. Jude signatures. Haematologica. 2015; 100(9):e354-357.
30. Den Boer ML, van Slegtenhorst M, De Menezes RX, Cheok MH, Buijs-Gladdines JG, Peters ST, Van Zutven LJ, Beverloo HB, Van der Spek PJ, Escherich G, Horstmann MA, Janka-Schaub GE, Kamps WA, Evans WE and Pieters R. A subtype of childhood acute lymphoblastic leukaemia with poor treatment outcome: a genome-wide classification study. Lancet Oncol. 2009; 10(2):125-134.
31. Mullighan CG, Su X, Zhang J, Radtke I, Phillips LA, Miller CB, Ma J, Liu W, Cheng C, Schulman BA, Harvey RC, Chen IM, Clifford RJ, Carroll WL, Reaman G, Bowman WP, et al. Deletion of IKZF1 and prognosis in acute lymphoblastic leukemia. N Engl J Med. 2009; 360(5):470-480.
32. Hicks C, Miele L, Koganti T, Young-Gaylor L, Rogers D, Vijayakumar V and Megason G. Analysis of Patterns of Gene Expression Variation within and between Ethnic Populations in Pediatric B-ALL. Cancer informatics. 2013; 12:155-173.
33. Francis OL, Milford TA, Martinez SR, Baez I, Coats JS, Mayagoitia K, Concepcion KR, Ginelli E, Beldiman C, Benitez A, Weldon AJ, Arogyaswamy K, Shiraz P, Fisher R, Morris CL, Zhang XB, et al. A novel xenograft model to study the role of TSLP-induced CRLF2 signals in normal and malignant human B lymphopoiesis. Haematologica. 2016; 101(4):417-426.
34. Ma X, Edmonson M, YErgeau D, Muzny DM, Hampton OA, Rusch M, Song G, Easton J, Harvey RC, Wheeler DA, Ma J, Doddapaneni H, Vadodaria B, Wu G, Nagahawatte P, Carroll WL, et al. Rise and fall of subclones from diagnosis to relapse in pediatric B-acute lymphoblastic leukaemia. Nat Commun. 2015; 6:6604.
35. Vesely C, Frech C, Eckert C, Cario G, Mecklenbrauker A, Zur Stadt U, Nebral K, Kraler F, Fischer S, Attarbaschi A, Schuster M, Bock C, Cave H, von StackelBerg A, Schrappe M, Horstmann MA, et al. Genomic and transcriptional landscape of P2RY8-CRLF2-positive childhood acute lymphoblastic leukemia. Leukemia. 2017.
36. Winter PS, Sarosiek KA, Lin KH, Meggendorfer M, Schnittger S, Letai A and Wood KC. RAS signaling promotes resistance to JAK inhibitors by suppressing BAD-mediated apoptosis. Science signaling. 2014; 7(357):ra122.
37. Nikolaev SI, Garieri M, Santoni F, Falconnet E, Ribaux P, Guipponi M, Murray A, Groet J, Giarin E, Basso G, Nizetic D and Antonarakis SE. Frequent cases of RAS-mutated Down syndrome acute lymphoblastic leukaemia lack JAK2 mutations. Nat Commun. 2014; 5:4654.
38. Zhu Z, Aref AR, Cohoon TJ, Barbie TU, Imamura Y, Yang S, Moody SE, Shen RR, Schinzel AC, Thai TC, Reibel JB, Tamayo P, Godfrey JT, Qian ZR, Page AN, Maciag K, et al. Inhibition of KRAS-driven tumorigenicity by interruption of an autocrine cytokine circuit. Cancer discovery. 2014; 4(4):452-465.
39. Asshoff M, Petzer V, Warr MR, Haschka D, Tymoszuk P, Demetz E, Seifert M, Posch W, Nairz M, Maciejewski P, Fowles P, Burns CJ, Smith G, Wagner KU, Weiss G, Whitney JA, et al. Momelotinib inhibits ACVR1/ALK2, decreases hepcidin production, and ameliorates anemia of chronic disease in rodents. Blood. 2017; 129(13):1823-1830.

40. Haan S, Wuller S, Kaczor J, Rolvering C, Nocker T, Behrmann I and Haan C. SOCS-mediated downregulation of mutant Jak2 (V617F, T875N and K539L) counteracts cytokine-independent signaling. Oncogene. 2009; 28(34):3069-3080.
41. Hart S, Goh KC, Novotny-Diermayr V, Hu CY, Hentze H, Tan YC, Madan B, Amalini C, Loh YK, Ong LC, William AD, Lee A, Poulsen A, Jayaraman R, Ong KH, Ethirajulu K, et al. SB1518, a novel macrocyclic pyrimidine-based JAK2 inhibitor for the treatment of myeloid and lymphoid malignancies. Leukemia. 2011; 25(11):1751-1759.
42. Grandage VL, Everington T, Linch DC and Khwaja A. Go6976 is a potent inhibitor of the JAK 2 and FLT3 tyrosine kinases with significant activity in primary acute myeloid leukaemia cells. Br J Haematol. 2006; 135(3):303-316.
43. Meyer SC and Levine RL. Molecular pathways: molecular basis for sensitivity and resistance to JAK kinase inhibitors. Clin Cancer Res. 2014; 20(8):2051-2059.
44. Polak R, de Rooij B, Pieters R and den Boer ML. B-cell precursor acute lymphoblastic leukemia cells use tunneling nanotubes to orchestrate their microenvironment. Blood. 2015; 126(21):2404-2414.
45. Iwamoto S, Mihara K, Downing JR, Pui CH and Campana D. Mesenchymal cells regulate the response of acute lymphoblastic leukemia cells to asparaginase. J Clin Invest. 2007; 117(4):1049-1057.
46. Vianello F, Villanova F, Tisato V, Lymperi S, Ho KK, Gomes AR, Marin D, Bonnet D, Apperley J, Lam EW and Dazzi F. Bone marrow mesenchymal stromal cells non-selectively protect chronic myeloid leukemia cells from imatinib-induced apoptosis via the CXCR4/CXCL12 axis. Haematologica. 2010; 95(7):1081-1089.
47. Shilling AD, Nedza FM, Emm T, Diamond S, McKeever E, Punwani N, Williams W, Arvanitis A, Galya LG, Li M, Shepard S, Rodgers J, Yue TY and Yeleswaram S. Metabolism, excretion, and pharmacokinetics of [14C]INCB018424, a selective Janus tyrosine kinase 1/2 inhibitor, in humans. Drug Metab Dispos. 2010; 38(11):2023-2031.
48. Tyner JW, Bumm TG, Deininger J, Wood L, AichBerger KJ, Loriaux MM, Druker BJ, Burns CJ, Fantino E and Deininger MW. CYT387, a novel JAK2 inhibitor, induces hematologic responses and normalizes inflammatory cytokines in murine myeloproliferative neoplasms. Blood. 2010; 115(25):5232-5240.
49. Den Boer ML, Harms DO, Pieters R, Kazemier KM, Gobel U, Korholz D, Graubner U, Haas RJ, Jorch N, Spaar HJ, Kaspers GJ, Kamps WA, Van der Does-Van den Berg A, Van Wering ER, Veerman AJ and Janka-Schaub GE. Patient stratification based on prednisolone-vincristine-asparaginase resistance profiles in children with acute lymphoblastic leukemia. J Clin Oncol. 2003; 21(17):3262-3268.
50. Escherich G, Zimmermann M, Janka-Schaub G and CoALL study group. Doxorubicin or daunorubicin given upfront in a therapeutic window are equally effective in children with newly diagnosed acute lymphoblastic leukemia. A randomized comparison in trial CoALL 07-03. Pediatr Blood Cancer. 2013; 60(2):254-257.
51. Veerman AJ, Kamps WA, van den Berg H, van den Berg E, Bokkerink JP, Bruin MC, van den Heuvel-Eibrink MM, Korbijn CM, Korthof ET, van der Pal K, Stijnen T, van Weel Sipman MH, van Weerden JF, van Wering ER, van der Does-van den Berg A and Dutch Childhood Oncology G. Dexamethasone-based therapy for childhood acute lymphoblastic leukaemia: results of the prospective Dutch Childhood Oncology Group (DCOG) protocol ALL-9 (1997-2004). Lancet Oncol. 2009; 10(10):957-966.
52. Escherich G, Troger A, Gobel U, Graubner U, Pekrun A, Jorch N, Kaspers G, Zimmermann M, zur Stadt U, Kazemier K, Pieters R, Den Boer ML, Horstmann M, Janka GE and CoALL study group. The long-term impact of in vitro drug sensitivity on risk stratification and treatment outcome in acute lymphoblastic leukemia of childhood (CoALL 06-97). Haematologica. 2011; 96(6):854-862.
53. Kamps WA, Bokkerink JP, Hakvoort-Cammel FG, Veerman AJ, Weening RS, van Wering ER, van Weerden JF, Hermans J, Slater R, van den Berg E, Kroes WG and van der Does-van den Berg A. BFM-oriented treatment for children with acute lymphoblastic leukemia without cranial irradiation and treatment reduction for standard risk patients: results of DCLSG protocol ALL-8 (1991-1996). Leukemia. 2002; 16(6):1099-1111.
54. Pieters R, de Groot-Kruseman H, Van der Velden V, Fiocco M, van den Berg H, de Bont E, Egeler RM, Hoogerbrugge P, Kaspers G, Van der Schoot E, De Haas V and Van Dongen J. Successful Therapy Reduction and Intensification for Childhood Acute Lymphoblastic Leukemia Based on Minimal Residual Disease Monitoring: Study ALL10 From the Dutch Childhood Oncology Group. J Clin Oncol. 2016; 34(22):2591-2601.
55. van den Berk LC, van der Veer A, Willemse ME, Theeuwes MJ, Luijendijk MW, Tong WH, van der Sluis IM, Pieters R and den Boer ML. Disturbed CXCR4/CXCL12 axis in paediatric precursor B-cell acute lymphoblastic leukaemia. Br J Haematol. 2014; 166(2):240-249.
56. van der Veer A, Waanders E, Pieters R, Willemse ME, Van Reijmersdal SV, Russell LJ, Harrison CJ, Evans WE, van der Velden VH, Hoogerbrugge PM, Van Leeuwen F, Escherich G, Horstmann MA, Mohammadi Khankahdani L, Rizopoulos D, De Groot-Kruseman HA, et al. Independent prognostic value of BCR-ABL1-like signature and IKZF1 deletion, but not high CRLF2 expression, in children with B-cell precursor ALL. Blood. 2013; 122(15):2622-2629.
57. Cario G, Zimmermann M, Romey R, Gesk S, Vater I, Harbott J, Schrauder A, Moericke A, Izraeli S, Akasaka T, Dyer MJ, Siebert R, Schrappe M and Stanulla M. Presence of the P2RY8-CRLF2 rearrangement is associated with a poor prognosis in non-high-risk precursor B-cell acute lymphoblastic leukemia in children treated according to the ALL-BFM 2000 protocol. Blood. 2010; 115(26):5393-5397.
58. Chen IM, Harvey RC, Mullighan CG, Gastier-Foster J, Wharton W, Kang H, Borowitz MJ, Camitta BM, Carroll AJ, Devidas M, Pullen DJ, Payne-Turner D, Tasian SK, Reshmi S, Cottrell CE, Reaman GH, et al. Outcome modeling with CRLF2, IKZF1, JAK, and minimal residual disease

in pediatric acute lymphoblastic leukemia: a Children's Oncology Group study. Blood. 2012; 119(15):3512-3522.
59. Fine JP and R.J. G. A Proportional Hazards Model for the Subdistribution of a Competing Risk. Journal of the American Statistical Association. 1999; 94(446):496-509.
60. Gray RJ. cmprsk: Subdistribution Analysis of Competing Risks. R package version 22-6 2013; http://CRAN.R-project.org/package=cmprsk.
61. De Wreede LC, Fiocco M and Putter H. mstate: An R Package for the Analysis of Competing Risks and Multi-State Models. J Stat Softw. 2011; 38(7):1-30.
62. Therneau T. A Package for Survival Analysis in S. R package version 236-12. 2012.

SUPPLEMENTAL DATA

Supplementary Table 1: RT-PCR primers used for the dectetion of *JAK2* translocations

Gene fusion	Forward Primer ID	Forward sequence (5'to 3')	Reverse Primer ID	Reverse sequence (5'to 3')
ATF7IP-JAK2	ATF7IP exon 12	aacccatacaaccagcaccgcctct	JAK2 exon 20	tgttgtcatgctgtagggatttcagga
BCR-JAK2	BCR exon 1	gtgccataagcggcaccggcact	JAK2 exon18	aggcctgaaatctggttcata
EBF1-JAK2	EBF1exon 14	cacgagcatgaacggatacggctct	JAK2 exon 20	tgttgtcatgctgtagggatttcagga
ETV6-JAK2	ETV6 exon 3	atggcaaagctctcctgctgctgac	JAK2 exon 20	tgttgtcatgctgtagggatttcagga
PAX5-JAK2	PAX5 exon 3	acaatgacaccgtgcctagcgtcag	JAK2 exon 19	tcaaaggcaccagaaaac
PPFIBP1-JAK2	PPFIBP1 exon 10	tgcaagatgaaaggagaaggggttga	JAK2 exon 20	tgttgtcatgctgtagggatttcagga
SSBP2-JAK2	SSBP2 exon 7	ggcacttggaggtgtcccaggaagt	JAK2 exon 20	tgttgtcatgctgtagggatttcagga
STRN3-JAK2	STRN3 exon 7	tgaaggagctggagaagcacggagt	JAK2 exon 20	tgttgtcatgctgtagggatttcagga
TPR-JAK2	TPR exon 38	tggaaatgcctcttccaaagaagttga	JAK2 exon 20	tgttgtcatgctgtagggatttcagga
TERF2-JAK2	TERF2 exon 10	tggggaaggaaactgg	JAK2 exon 20	tgttgtcatgctgtagggatttcagga

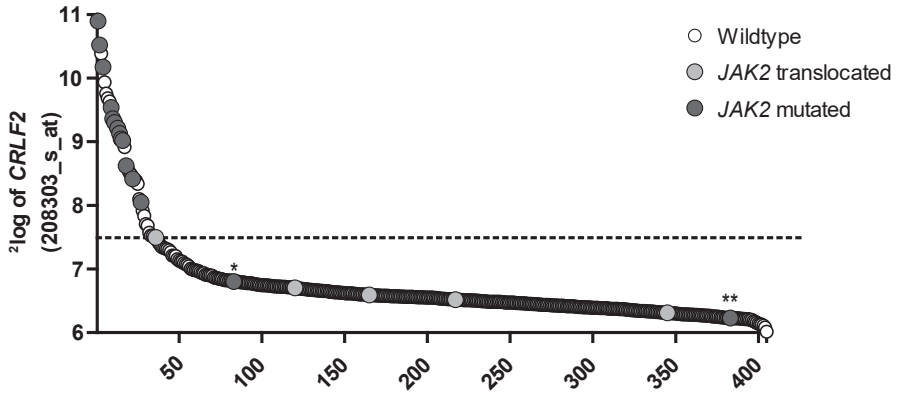

Supplementary Figure 1. *CRLF2* expression values
^{2}log expression levels of Affymetrix probeset 205841_at in 405 pediatric BCP-ALL cases, which were tested for *JAK2* aberrations. * represents patient A159. ** represents patient A521.

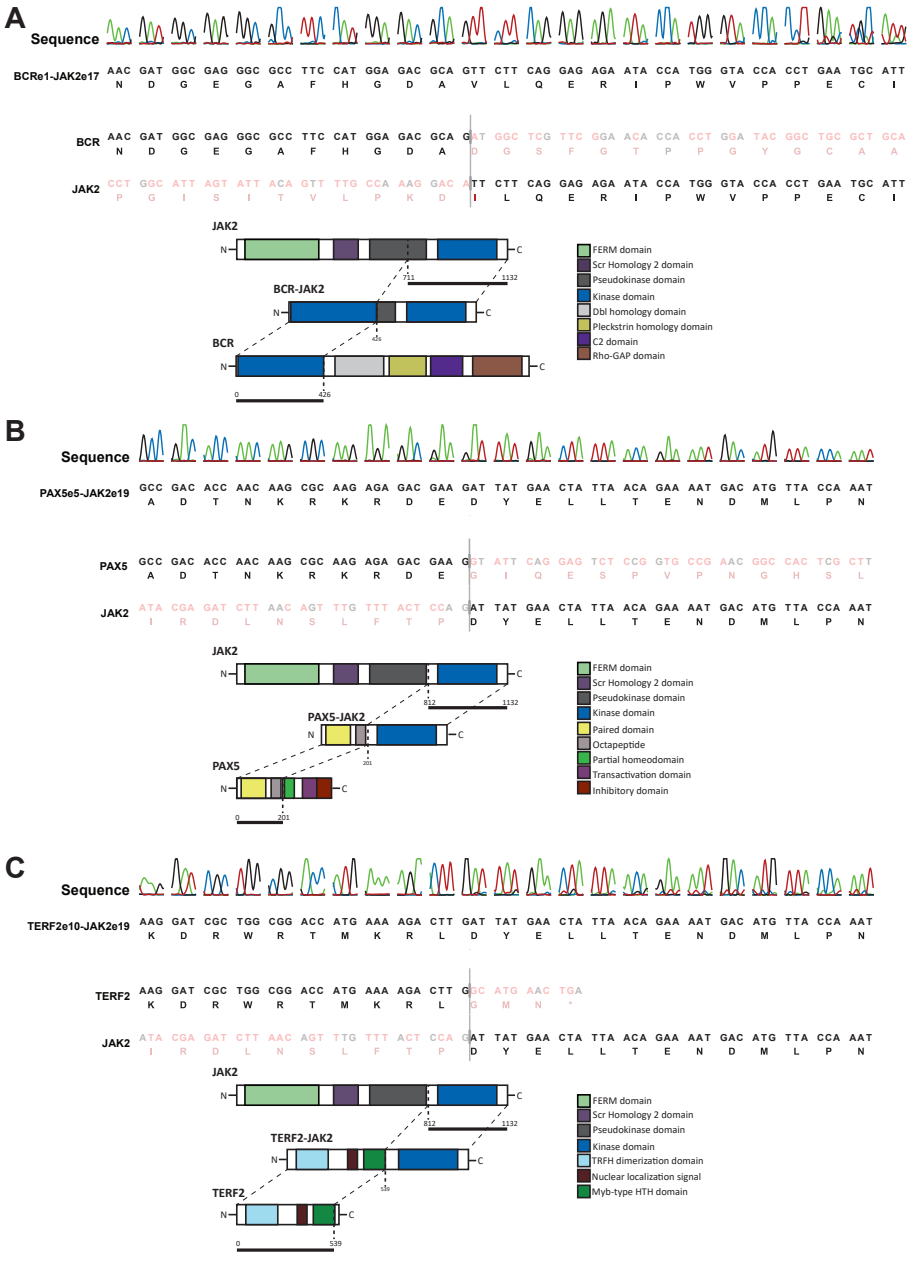

Supplementary Figure 2. Sequencing results of *JAK2* translocations
(A-C) Presence of fusion genes was examined on cDNA level using RT-PCR, followed by Sanger sequencing to detect *BCR-JAK2*, *PAX5-JAK2* and *TERF2-JAK2* translocations.

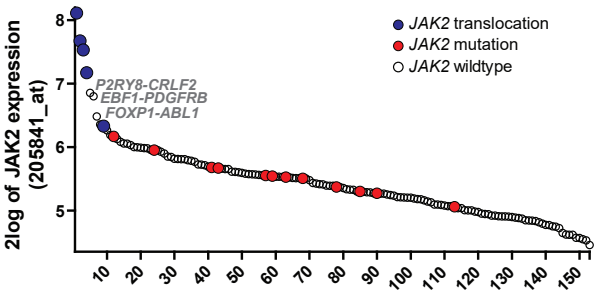

Supplementary Figure 3. *JAK2* expression values
^{2}log expression levels of Affymetrix probeset 205841_at in 77 *BCR-ABL1*-like and 76 B-other cases, which were tested for *JAK2* translocations. JAK2 mutation status is also indicated. Information was added to the three cases with high *JAK2* expression levels, without *JAK2* translocations.

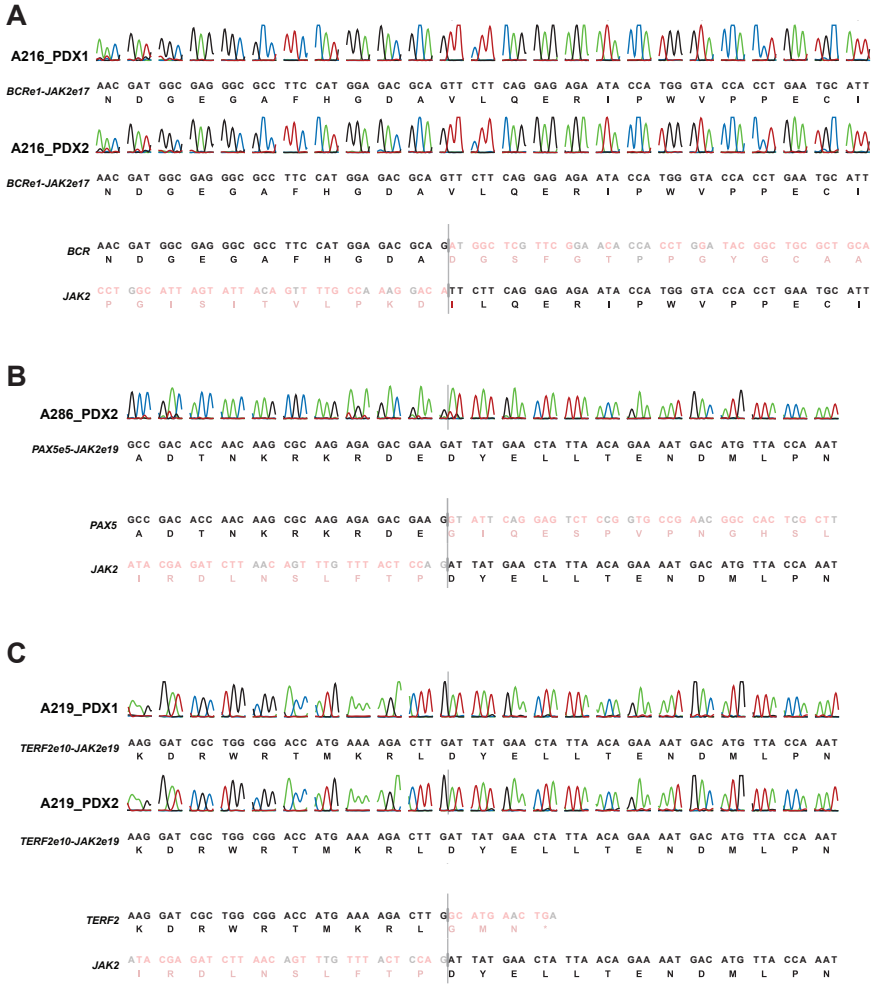

Supplementary Figure 4. *JAK2* aberrations in PDX cells
(A-C) Presence of *JAK2* translocation in PDX cells was validated on cDNA level using Sanger sequencing of cDNA.

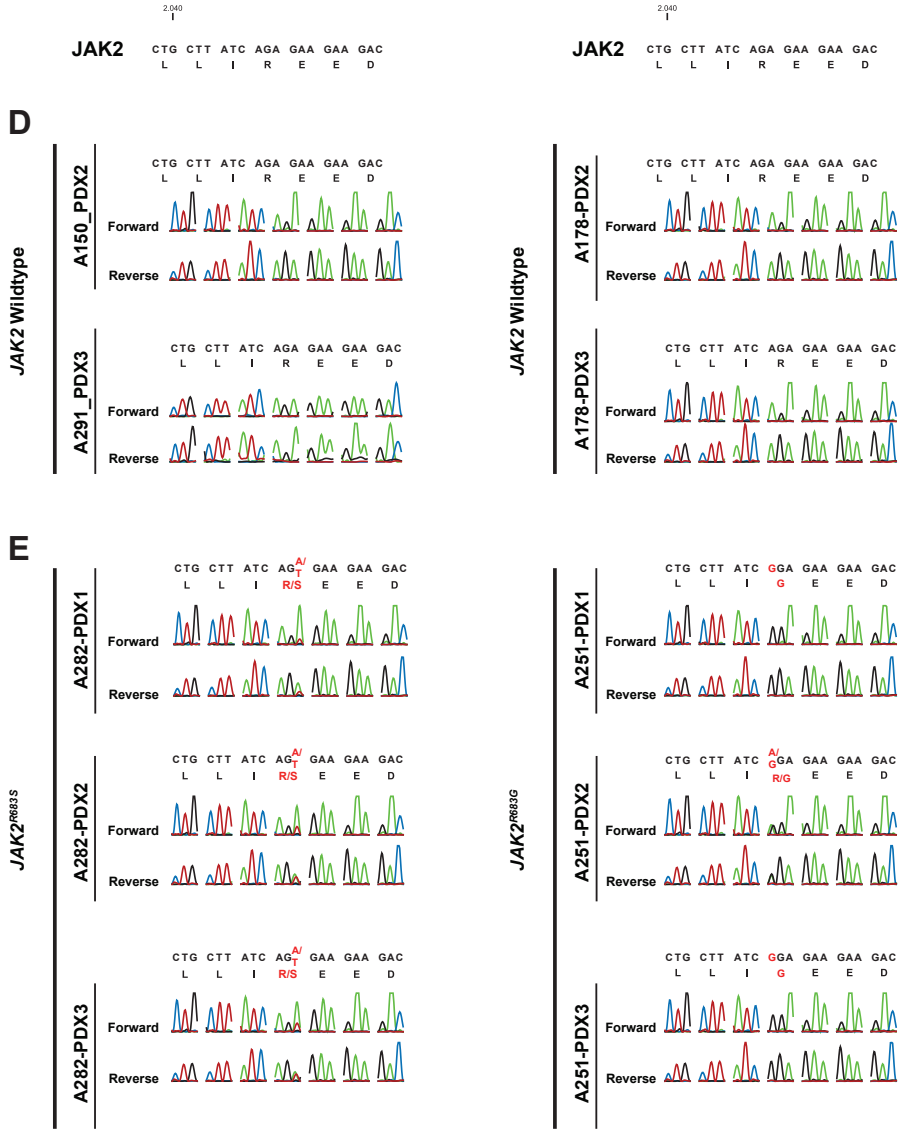

Supplementary Figure 4 continued. *JAK2* aberrations in PDX cells (continued)
(D-E) Genomic DNA of PDX cells was used to identify the absence **(D)** or presence **(E)** of *JAK2* mutations in exon 16.

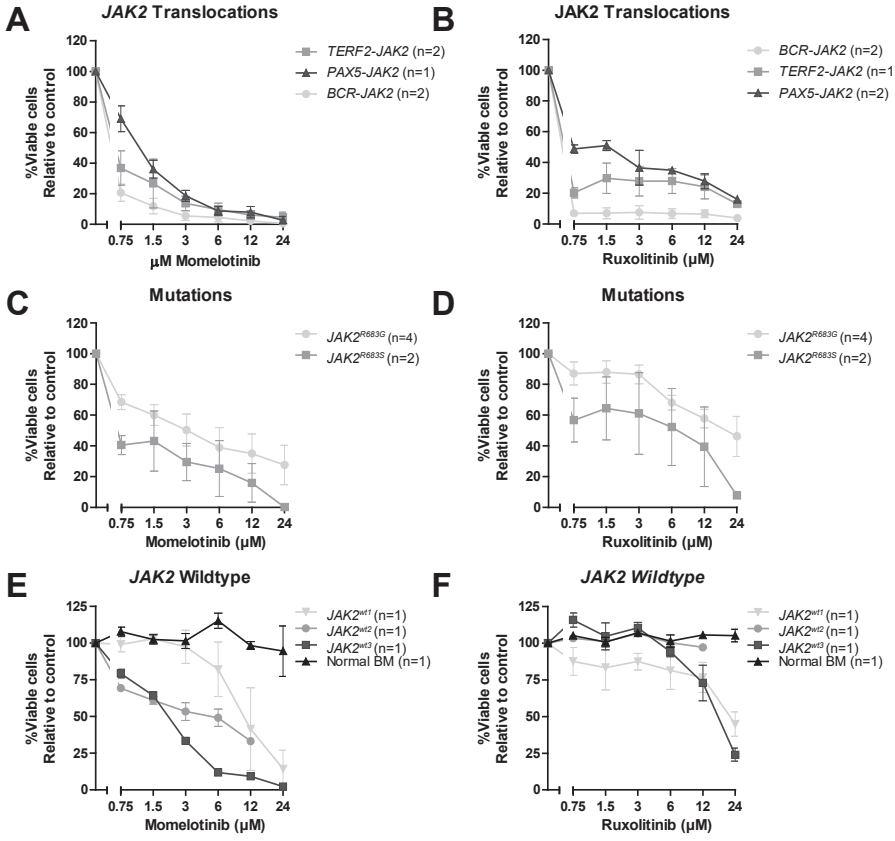

Supplementary Figure 5. The efficacy of JAK inhibitors on JAK2 translocated and mutated cells per type of aberration

Leukemic (PDX or primary patient) cells were incubated for four days to indicated concentrations of momelotinib or ruxolitinib, after which viability was measured using an MTT assay. Sensitivity of exposed cells was calculated relative to vehicle treated controls. Individual samples were tested in duplicate. Data derived from samples with identical *JAK2* lesions were grouped for analyses. **(A-B)** Efficacy of momelotinib and ruxolitinib on PDX cells with *JAK2* translocations: *BCR-JAK2* (n=2), *TERF2-JAK2* (n=2) and *PAX5-JAK2* (n=1). Mean±SD of individual samples (in duplicate) are shown. **(C-D)** Efficacy of momelotinib and ruxolitinib on *JAK2* mutated cells: $JAK2^{R683G}$ (n=4) and $JAK2^{R683S}$ (n=2) Mean±SEM of individual samples is depicted. **(E-F)** Efficacy of momelotinib and ruxolitinib on *JAK2* wildtype PDX cells and normal bone marrow cells. Mean±SD of individual samples (in duplicate) are shown. **(H-I)** Efficacy of momelotinib and ruxolitinib on Down syndrome and non-Down syndrome $JAK2^{R683G}$ cells. Mean±SD of individual samples (in duplicate) are shown.

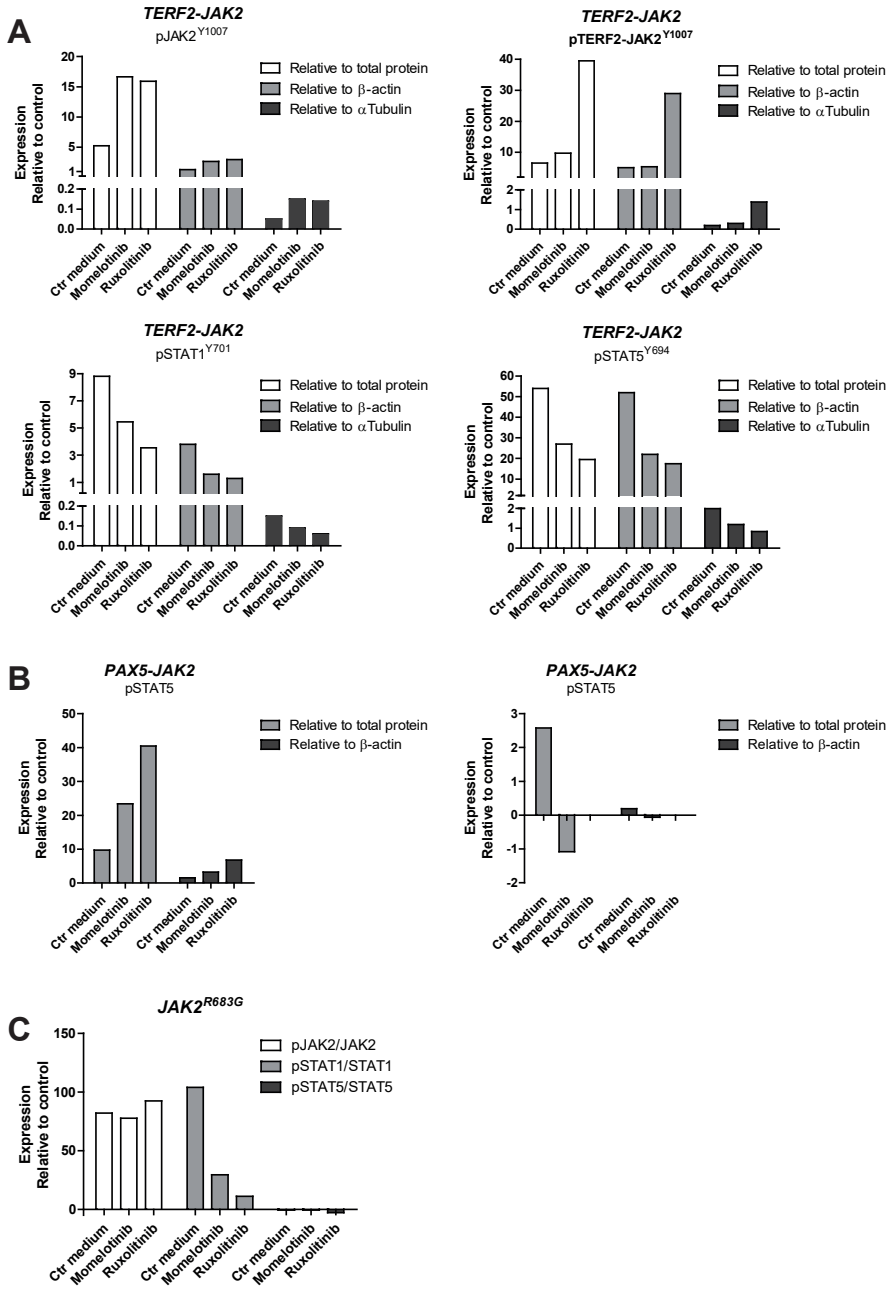

Supplementary Figure 6. Quantified expression levels western blots Figure 2
(A-C) *TERF2-JAK2, PAX5-JAK2* and *JAK2*^{R683G} PDX cells were exposed for four hours to vehicle control medium, 1.5 μM momelotinib or 0.75 μM ruxolitinib, after which (phosphorylated) TERF2-JAK2, PAX5-JAK2, JAK2, STAT1 and STAT5 levels were analyzed using western blot (25 μg lysate). Expression levels of phospho-proteins were quantified relative to total protein or loading control.

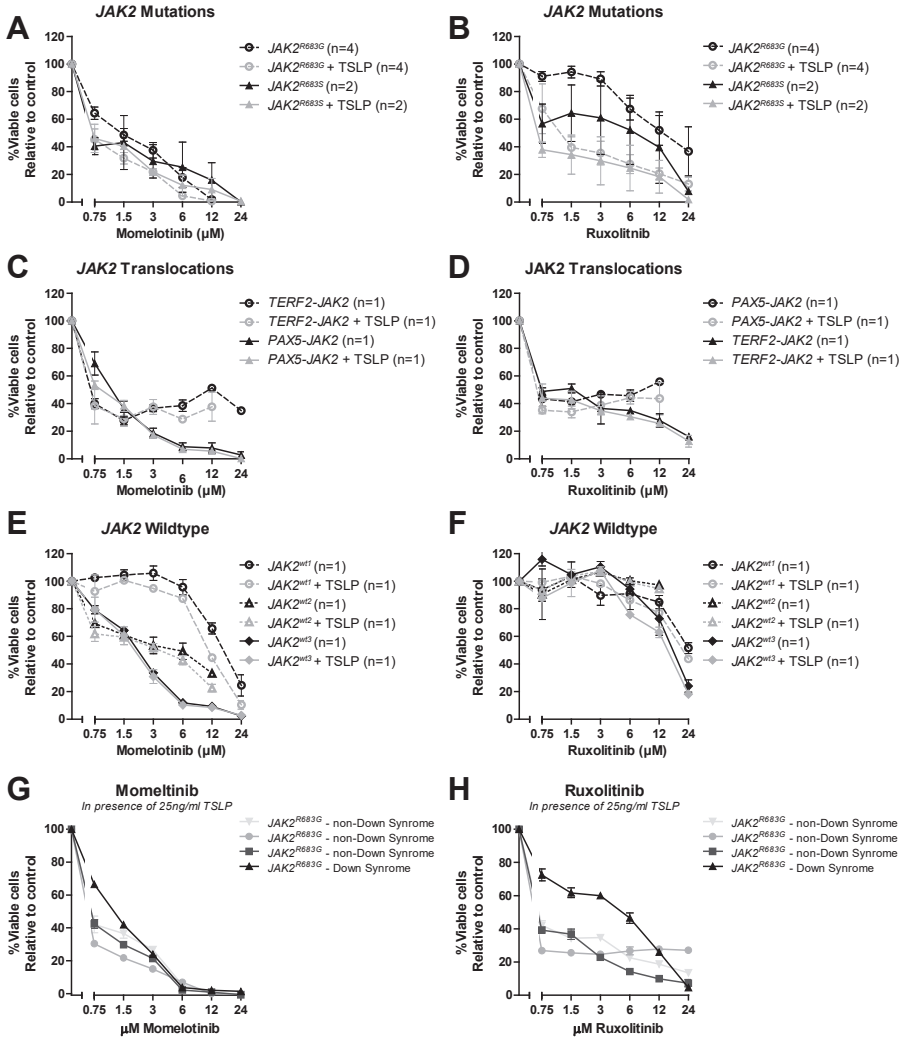

Supplementary Figure 7. The effect of TSLP stimulation on the efficacy of JAK inhibitors per type of aberration

Leukemic (PDX or primary patient) cells were pre-incubated for 1 hour without or with 25 ng/ml TSLP, after which they were exposed for four days to indicated concentrations of momelotinib or ruxolitinib. Viability was measured using an MTT assay. Sensitivity was calculated relative to vehicle treated controls. Individual samples were tested in duplicate. **(A-B)** Efficacy of momelotinib and ruxolitinib on *JAK2* mutated samples with or without TSLP pre-incubation: Mean±SEM four *JAK2*^{R683G} and two *JAK2*^{R683S} samples is shown. **(C-D)** Efficacy of momelotinib and ruxolitinib on cells with JAK2 translocations (n=2). Mean±SD of sample duplicates from a *TERF2-JAK2* and *PAX5-JAK2* sample are shown. **(E-F)** Efficacy of momelotinib and ruxolitinib on *JAK2* wildtype PDX cells (n=3). Mean±SD of sample duplicates are shown.

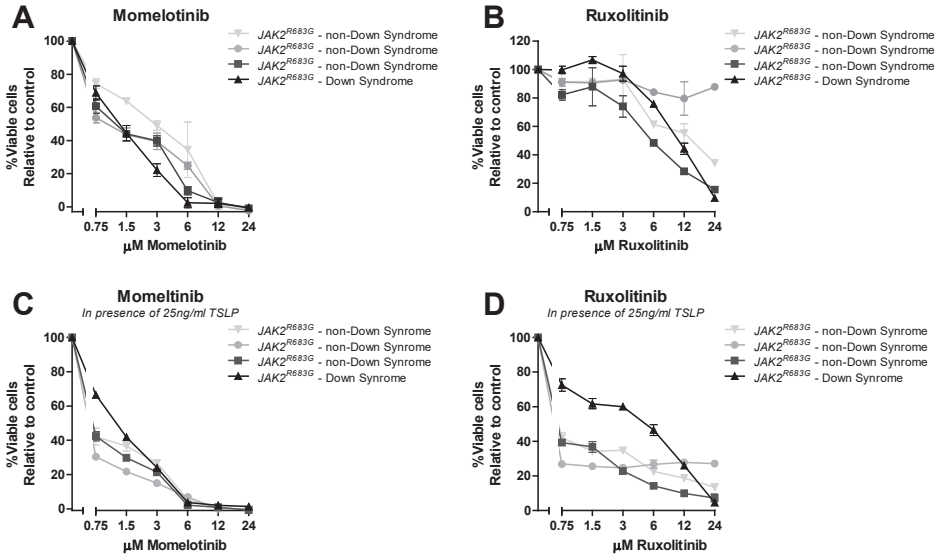

Supplementary Figure 8. Down syndrome and the efficacy of JAK inhibitors on *JAK2* mutated cells

Cells were exposed for four days to indicated concentrations of momelotinib or ruxolitinib. Viability was measured using an MTT assay. Sensitivity of exposed cells was calculated relative to vehicle treated controls. Individual samples were tested in duplicate. Mean±SD of sample duplicates is shown.

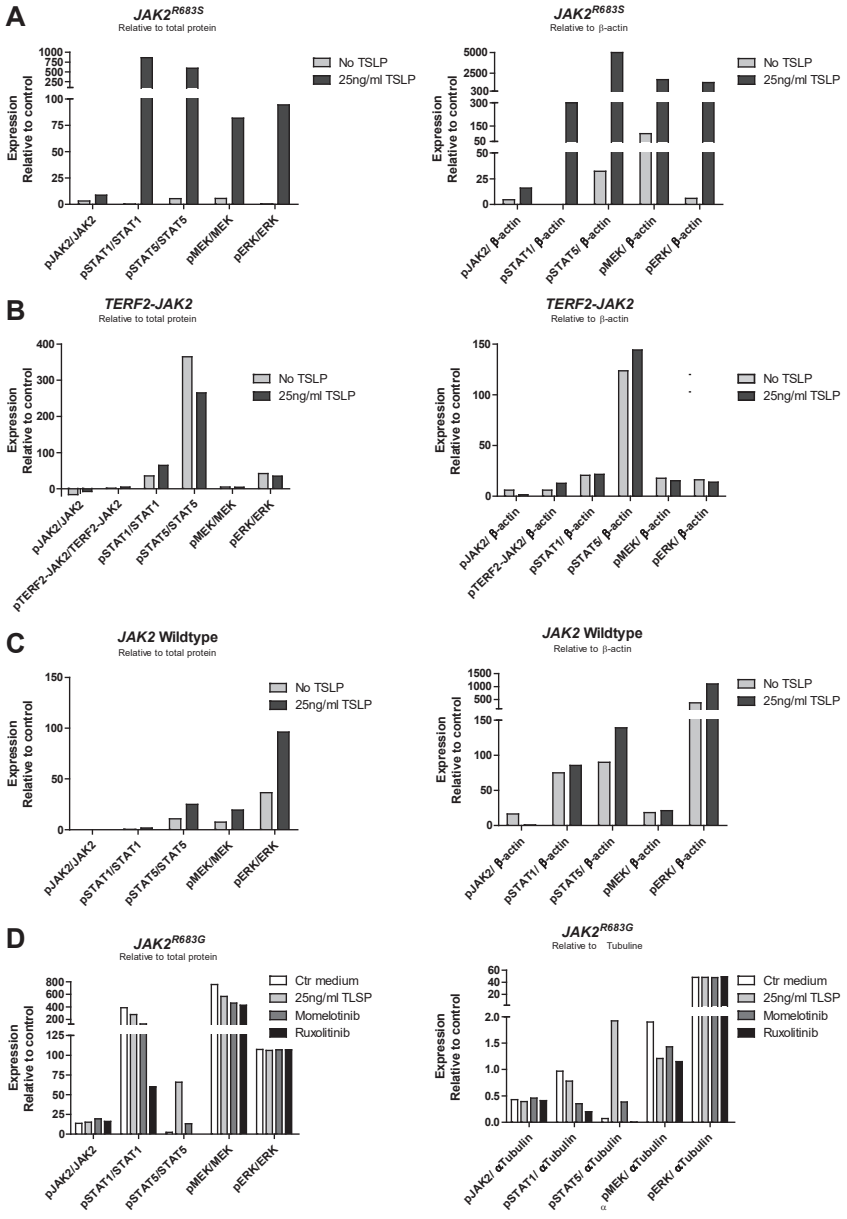

Supplementary Figure 9. Quantified expression levels western blots Figure 3

(**A-C**) Western blot of *JAK2*^{R683S}, *TERF2-JAK2* and *JAK2*^{wt} PDX cells with or without TSLP stimulation (25 ng/ml for 1 hour). Expression levels of phospho-proteins were quantified relative to total protein or loading control (β-actin). (**D**) *JAK2*^{R683G} cells were pre-incubated for 1 hour with or without 25 ng/ml TSLP, after which cells were exposed for four hours to vehicle control medium, 1.5 μM momelotinib or 0.75 μM ruxolitinib. Levels of (phosphorylated) JAK2, STAT1, STAT5, MEK1/2 and ERK1/2 were analyzed using western blot. Expression levels of phospho-proteins were quantified relative to total protein or loading control (α-Tubulin).

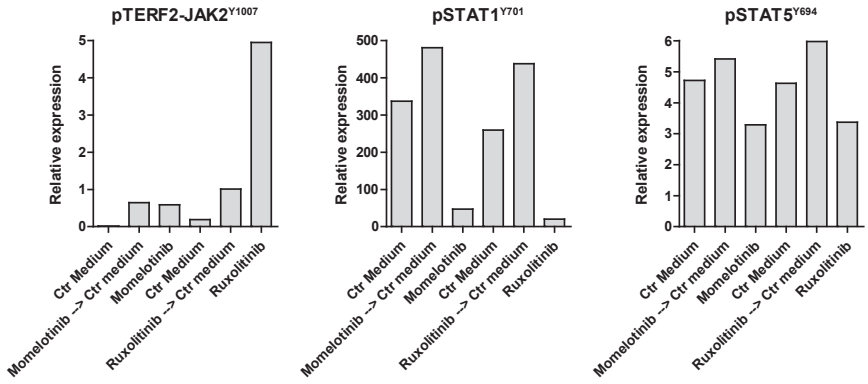

Supplementary Figure 10. Quantified expression levels western blots Figure 4
TERF2-JAK2 PDX cells were incubated for four hours with or without 1.5 µM momelotinib or 0.75 µM ruxolitinib, after which cells were washed to remove the JAK inhibitors. Half of the cells were exposed for another 1.5 hours to 1.5 µM momelotinib or 0.75 µM ruxolitinib, whereas the other cells were incubated in vehicle control (Ctr) medium. Protein expression levels were examined by western blot (25 µg lysate). Expression levels of phospho-proteins were quantified relative to total protein.

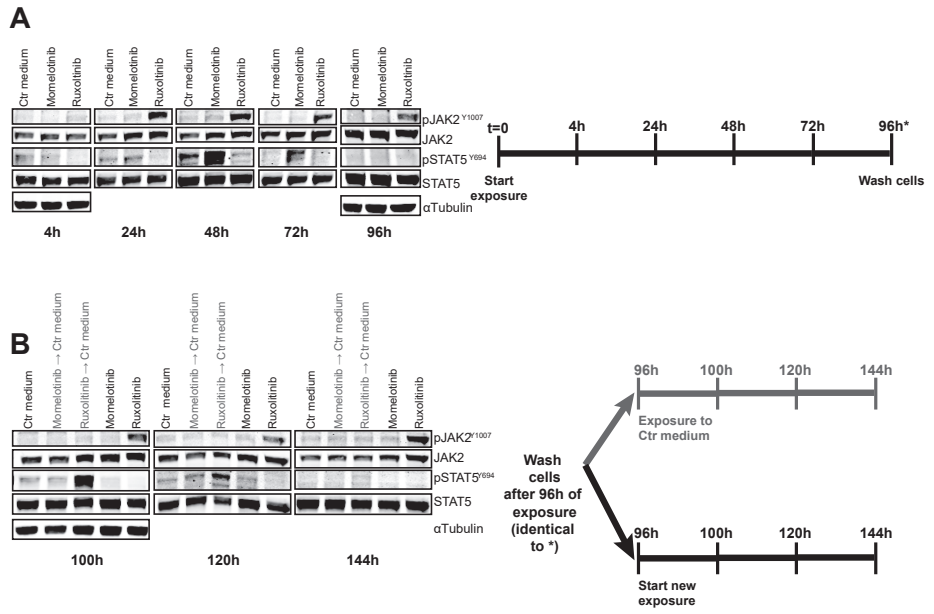

Supplementary Figure 11. Accumulation of pJAK2 Y1007 results in a rebound effect of JAK2
(A) HEL cells were incubated with or without 1.5 µM momelotinib or 0.75 µM ruxolitinib for 4 hours, 24 hours, 48 hours, 72 hours and 96 hours, after which cells were lysed and protein expression levels were examined using western blot (25 µg lysate). **(B)** After 96 hours of exposure to JAK inhibitors (indicated by * in panel A), cells were washed in normal culture medium, to remove momelotinib and ruxolitinib. Subsequently, half of the cells were incubated with 1.5 µM momelotinib or 0.75 µM ruxolitinib for another 4 hours, or 24 hours, whereas the remaining cells were incubated in vehicle control (Ctr) medium. Protein expression levels were examined using western blot (25 µg lysate).

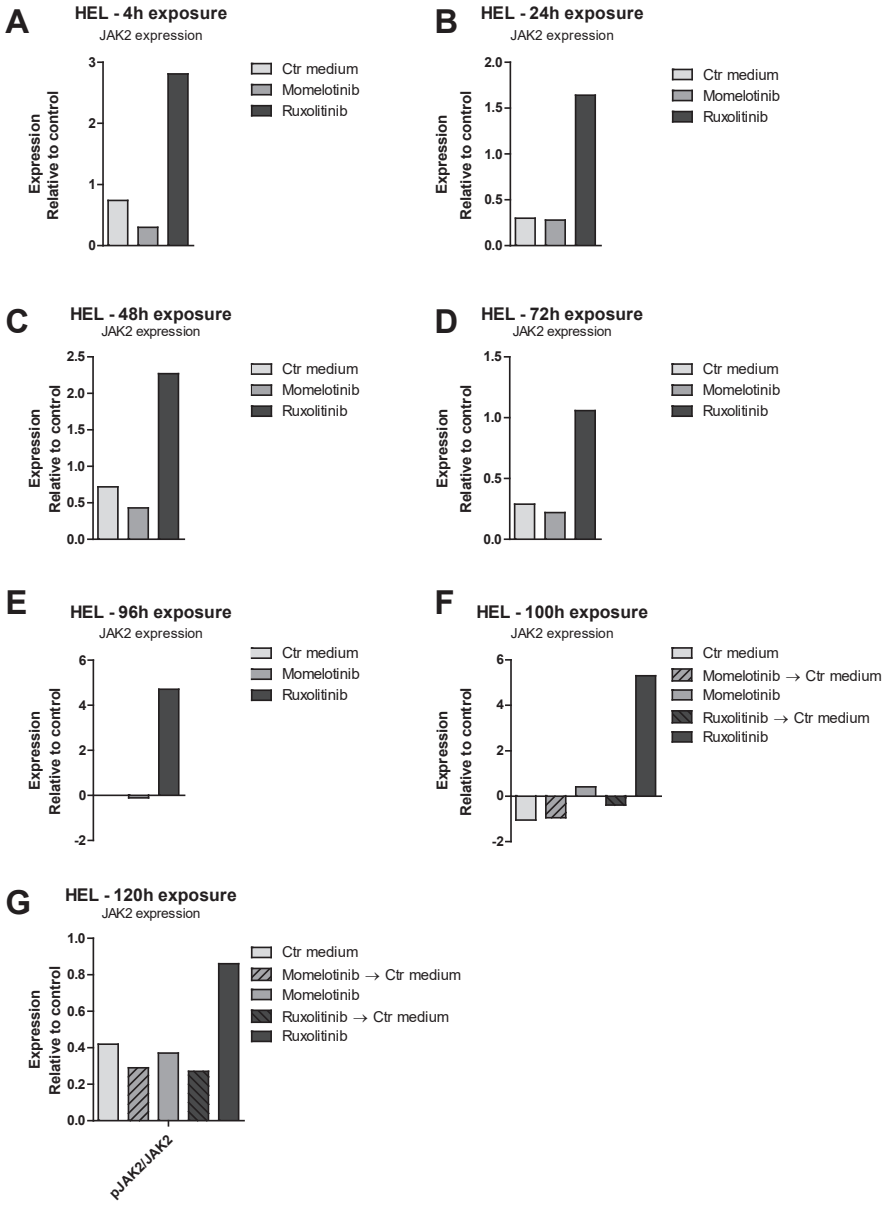

Supplementary Figure 12. Quantified expression levels western blots Supplementary Figure 8 (continued on next page)

(A-N) HEL cells were incubated with or without 1.5 μM momelotinib or 0.75 μM ruxolitinib for 4 hours, 24 hours, 48 hours, 72 hours and 96 hours. After 96 hours of exposure to JAK inhibitors, cells were washed in normal culture medium, to remove momelotinib and ruxolitinib. Subsequently, half of the cells were incubated with 1.5 μM momelotinib or 0.75 μM ruxolitinib for another 4 hours, or 24 hours, whereas the remaining cells were incubated in vehicle control (Ctr) medium. Protein expression levels were examined using western blot (25 μg lysate). Expression levels of phospho-proteins were quantified relative to total protein.

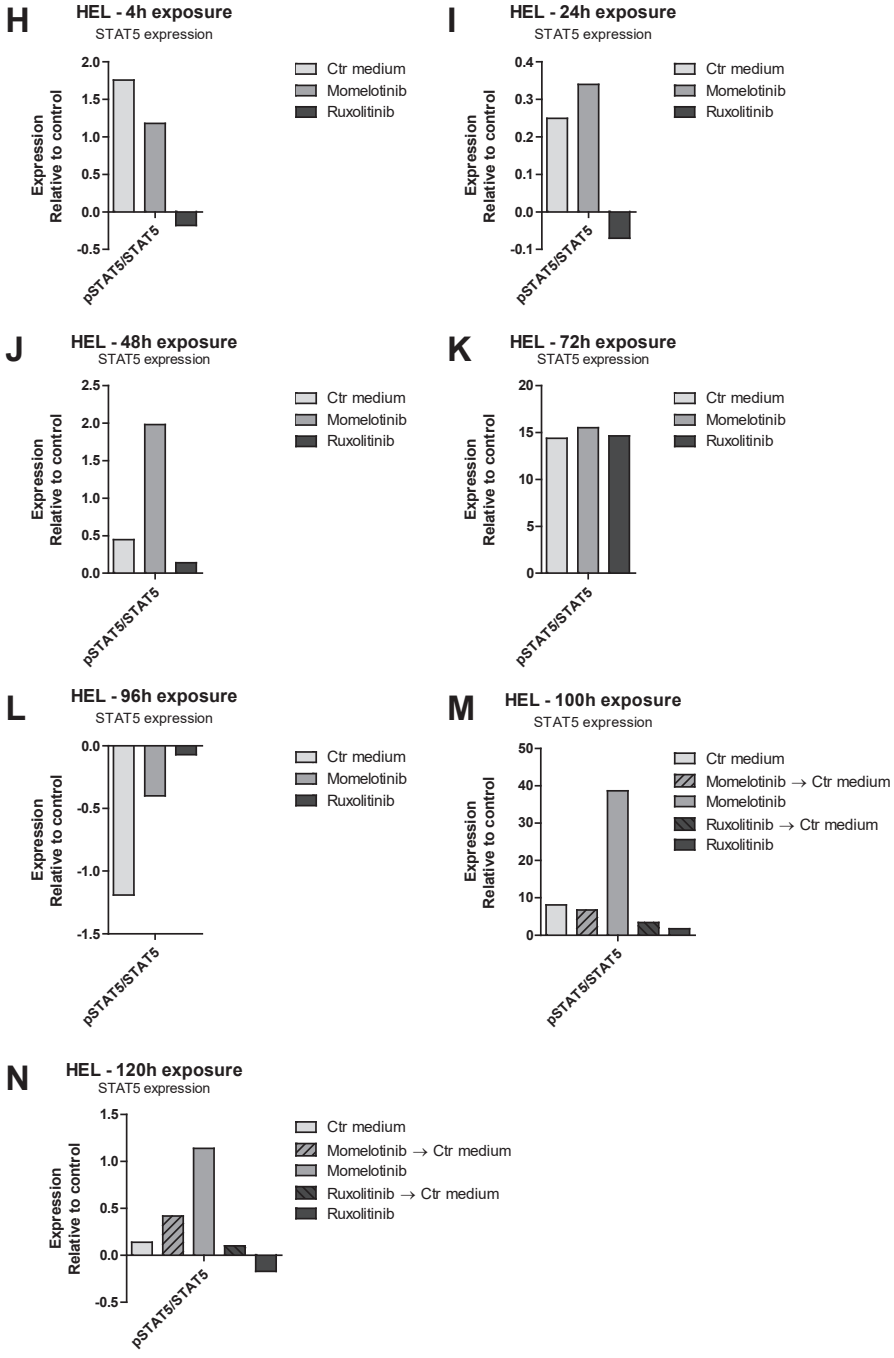

Supplementary Figure 12. Quantified expression levels western blots Supplementary Figure 8 (continued)

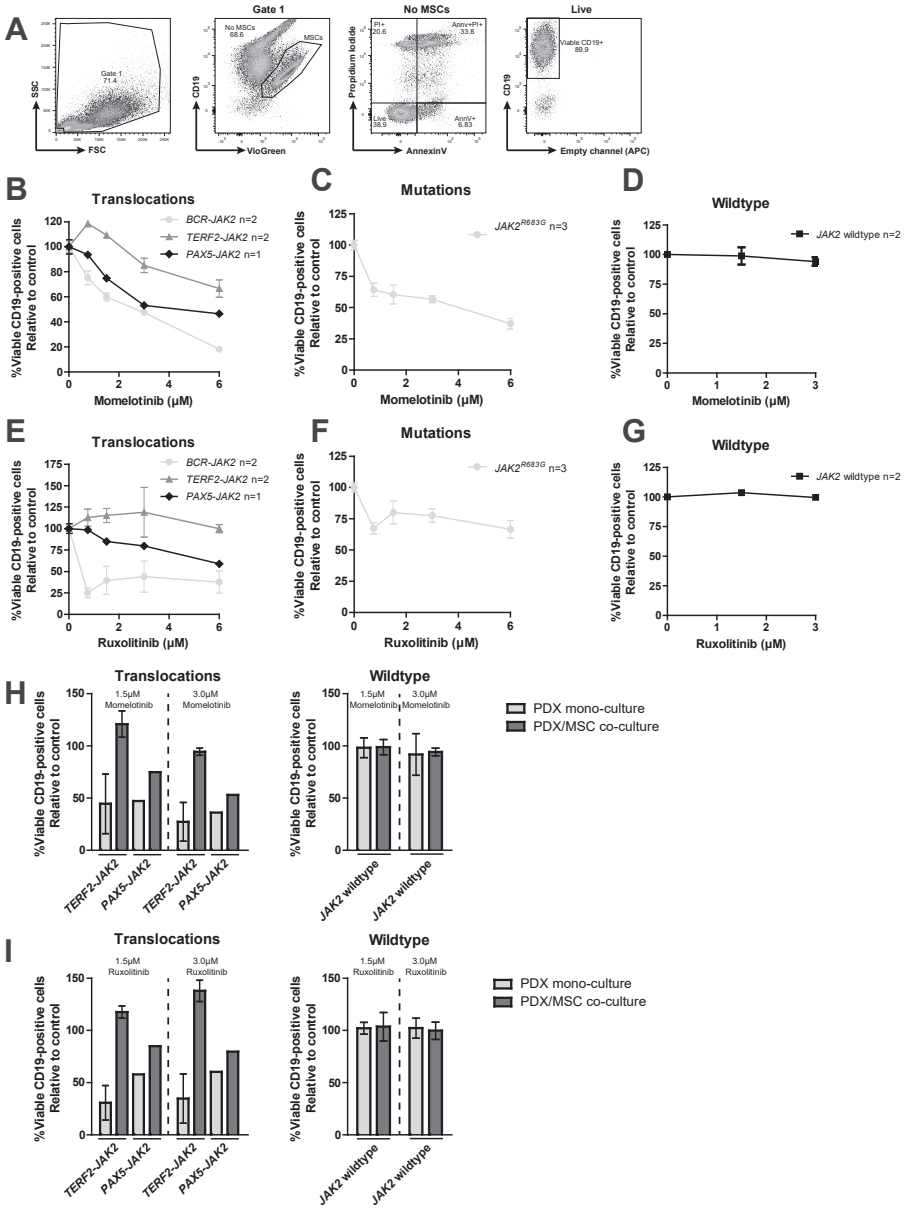

Supplementary Figure 13. The efficacy of JAK inhibitors in PDX/MSC co-cultures

The response of PDX cells (CD19+) co-cultured with MSCs (CD19-) to increasing concentrations of momelotinib and ruxolitinib was assessed after four days of culture using flow cytometry. Viability was calculated relative to untreated controls. Mean±SEM is shown. **(A)** Gating strategy. **(B-G)** Percentage of viable PDX cells being *JAK2* translocated (*BCR-JAK2* n=2; *TERF2-JAK2* n=2; *PAX5-JAK2* n=1), *JAK2* mutated (*JAK2*^{R683G} n=3), or *JAK2* wildtype cells (*JAK2* wildtype n=2), co-cultured with patient MSCs, after four days exposure to momelotinib and ruxolitinib. **(H-I)** The effect of 1.5 μM and 3.0 μM momelotinib or ruxolitinib on the viability of *JAK2* translocated PDX cells in mono-culture, or in co-culture with patient MSCs. *TERF2-JAK2* n=2; *PAX5-JAK2* n=1, *JAK2* wildtype n=2.

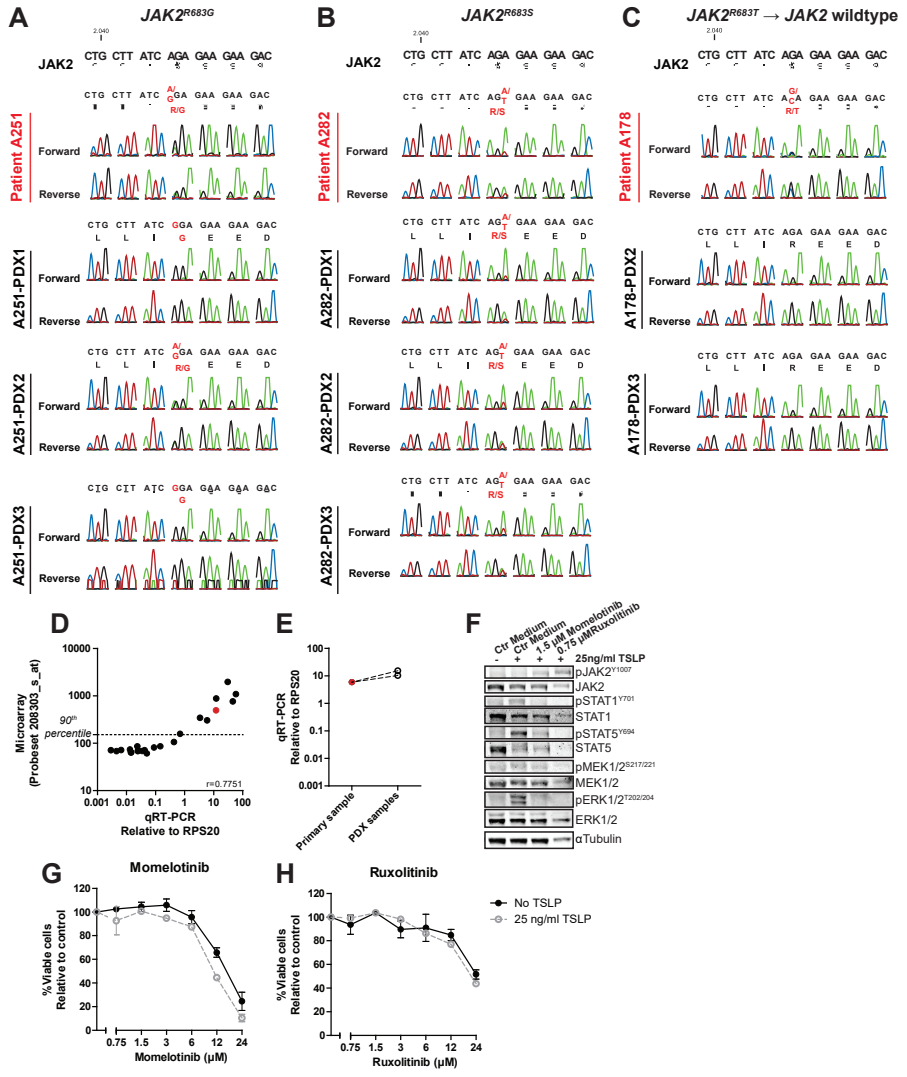

Supplementary Figure 14. *JAK2* mutations in primary leukemic and PDX cells

(**A-C**) Primary patient cells (A251, A282, and A178) were injected intra-femoral into three NSG mice per patient. After engraftment, leukemic cells were harvested from these mice (PDX1, PDX2, and PDX3). Genomic DNA was used to identify *JAK2* mutations in exon 16 (forward primer 5'-ATGCCTCCAAATTATTATACTATCA-3', reverse primer 5'-ATCACCTCACAGTCCA TGGTTAT-3') in these PDX cells and primary leukemic cells, using Sanger sequencing. (**D**) *CRLF2* expression in primary leukemic samples was determined using qRT-PCR and SYBR green. qRT-PCR expression values were correlated to Affymetrix microarray data of probeset 208303_s_at. Spearman correlation coefficient is reported. (**E**) *CRLF2* expression levels in the primary leukemic and PDX samples was determined using qRT-PCR. *CRLF2* expression was calculated relative to RSP20 expression levels. (**F**) *JAK2* wildtype cells were incubated for 1h with 25 ng/ml TSLP. Effect of TSLP on protein expression levels was examined using western blotting. (**G-H**) *JAK2* wildtype cells were exposed for four days to indicated concentrations of momelotinib or ruxolitinib. Viability was measured using an MTT assay, after which cell survival was calculated relative to vehicle treated controls. Mean±SD of duplicates are shown.

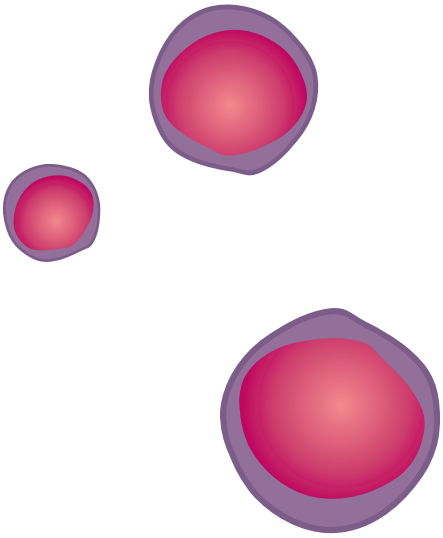

Chapter 4

HIGH *STAP1* EXPRESSION IN *DUX4*-REARRANGED CASES IS NOT SUITABLE AS THERAPEUTIC TARGET IN PEDIATRIC B-CELL PRECURSOR ACUTE LYMPHOBLASTIC LEUKEMIA

Elisabeth M.P. Steeghs, Marjolein Bakker, Alex Q. Hoogkamer, Judith M. Boer, Quirine J. Hartman, Femke Stalpers, Gabriele Escherich, Valerie de Haas, Hester A. de Groot-Kruseman, Rob Pieters, and Monique L. den Boer

Scientific Reports. 2018. Jan 12;8(1):693.

ABSTRACT

Approximately 25% of the pediatric B-cell precursor acute lymphoblastic leukemia (BCP-ALL) cases are genetically unclassified. More thorough elucidation of the pathobiology of these genetically unclassified (B-other) cases may identify novel treatment options.

We analyzed gene expression profiles of 572 pediatric BCP-ALL cases, representing all major ALL subtypes. High expression of *STAP1*, an adaptor protein downstream of the B-cell receptor (BCR), was identified in *BCR-ABL1*-like and non-*BCR-ABL1*-like B-other cases. Limma analysis revealed an association between high expression of *STAP1* and BCR signaling genes. However, *STAP1* expression and pre-BCR signaling were not causally related: cytoplasmic Igμ levels were not abnormal in cases with high levels of *STAP1* and stimulation of pre-BCR signaling did not induce *STAP1* expression. To elucidate the role of STAP1 in BCP-ALL survival, expression was silenced in two human BCP-ALL cell lines. Knockdown of *STAP1* did not reduce the proliferation rate or viability of these cells, suggesting that *STAP1* is not a likely candidate for precision medicines. Moreover, high expression of *STAP1* was not predictive for an unfavorable prognosis of *BCR-ABL1*-like and non-*BCR-ABL1*-like B-other cases. Remarkably, *DUX4*-rearrangements and intragenic *ERG* deletions, were enriched in cases harboring high expression of *STAP1*.

INTRODUCTION

Acute lymphoblastic leukemia (ALL) is the most common malignancy diagnosed in children. Survival rates have improved during the last decades and nowadays is approaching 90%. This dramatic increase in survival was achieved mostly because of risk-adjusted treatment, therapy intensification, and stem cell transplantations.[1] B-cell precursor ALL (BCP-ALL) can be subdivided in different genetic subtypes, which have different long-term clinical outcome. However, approximately 25% of the BCP-ALL cases lack sentinel genetic aberrations (*KMT2A*-rearrangements, *BCR-ABL1*, *ETV6-RUNX1*, *TCF-PBX1*, high hyperdiploidy) and are classified as 'B-other'. We and others showed that part of this B-other group has a gene expression profile similar to that of *BCR-ABL1*-positive ALL cases, and is associated with an unfavorable clinical outcome.[2,3] Although these patients are known to lack the *BCR-ABL1* fusion gene, the underlying pathobiology of this subtype remains poorly understood. Cases are enriched for copy number alterations (CNAs) in genes involved in B-cell development, intrachromosomal amplification of chromosome 21, dicentric chromosome (9;20), and a subgroup of cases harbors kinase activating lesions.[2-7] Likewise, the remaining non-*BCR-ABL1*-like B-other cases are a very heterogeneous group. Only very recently, chromosomal translocations involving *DUX4*, *ZNF384*, and *MEF2D* were identified in these non-*BCR-ABL1*-like B-other cases.[8-10] Although kinase activating lesions offer a potentive attractive target for precision medicine, for the remaining group of *BCR-ABL1*-like and non-*BCR-ABL1*-like B-other cases, no druggable targets have yet been identified.

BCP-ALL cells are immature B-cells in which differentiation is arrested at early immature stages. The precursor B-cell receptor (pre-BCR), an immature immunoglubulin (Igμ) heavy chain with 'surrogate' light-chain components, is involved in the expansion and maturation of pre-B cells. For a short period of time, in-frame rearranged V_HDJ_H gene segments are expressed to pass the pre-BCR checkpoint. In absence of this expression, pre-B cells are eliminated by programmed cell death.[11,12] Malignant pre-B cells can evade this pre-B cell checkpoint via activation of alternative pathways.[12] In mature B-cells PI3K-AKT signaling can rescue BCR deficient cells.[13] Signaling of pre-BCR and mature BCR are largely similar.[14] Targeting BCR signaling is an attractive treatment strategy in mature B-cell malignancies and is also being explored in BCP-ALL.[15-20]

Advanced understanding of the pathobiology of genetically unclassified BCP-ALL cases may identify novel treatment options. To identify dysregulated genes in these cases, we analyzed gene expression profiles in leukemia cells of cohort of BCP-ALL patients at initial diagnosis.[21] High expression levels of the adapter protein signal transducing adaptor family member 1 (*STAP1*) were identified in a subgroup of *BCR-ABL1*-like and non-*BCR-ABL1*-like B-other patients. STAP1 is a relatively unknown protein, consisting out of Peckstrin homology (PH) domains and unique Src homology 2 (SH2) domains, suggesting that STAP1 recruits signaling proteins to receptor tyrosine kinases.[22,23] *STAP1* is reported to be a docking protein downstream of Tec protein tyrosine kinase (TEC), which is involved in BCR signaling.[24,25] In addition, reports show enriched expression in hematopoietic stem cells and a potential role of STAP1 in microglia activation has been suggested.[26,27] The current study aimed to establish the therapeutic potential of inhibiting STAP1 in the subset of BCP-ALL cases that express high levels of *STAP1*.

METHODS

A detailed description of all methods can be found in the supplement.

Processing of primary patient material

Bone marrow and/or peripheral blood samples were obtained from children (1-18 years) with newly diagnosed ALL. Written informed consent was obtained from parents or guardians to use excess of diagnostic material for research purposes, as approved by the Medical Ethics Committee of the Erasmus Medical Center, The Netherlands. Studies were conducted in accordance with the Declaration of Helsinki. Mononuclear cells were isolated using Lymphoprep gradient separation and the leukemic blast percentage was determined microscopically by May-Grünwald Giemsa stained cytospin preparations, as described previously.[28] Samples were enriched to >90% leukemic cells by depleting normal cells, using anti-CD marker coated magnetic beads, i.e. anti CD3, anti-CD14, anti-CD15, anti-CD33, and/or H1 beads (IQ Products, Groningen, The Netherlands) combined with pan mouse IgG dynabeads (Invitrogen, Bleiswijk, Netherlands). Primary leukemic cells were maintained in RPMI-1640 Dutch modification (Life Technologies, Breda, Netherlands) supplemented with 20% fetal calf serum (Integro, Zaandam, Netherlands), with 0.1% insulin-transferrin-sodium selenite (Sigma Aldrich, Zwijndrecht, Netherlands), 0.4 mM glutamine (Invitrogen), 0.25 µg/ml gentamycine (Thermo Scientific, Breda, Netherlands), 100 IU/ml penicillin (Thermo Scientific), 100 µg/ml streptomycin (Thermo Scientific), 0.125 µg/ml fungizone (Thermo Scientific).
Patients were treated according to the Dutch Childhood Oncology Group ALL8, ALL9, ALL10 protocol, or the COALL-06-97 and COALL-07-03 study protocols.[29-33] The major subtypes (high hyperdiploid (51-65 chromosomes), *ETV6-RUNX1*, *TCF3-PBX1*, *KMT2A*-rearranged, *BCR-ABL1*) were determined using fluorescent in situ hybridization and RT-PCR by reference laboratories. Cases negative for these lesions were classified as B-other. Among these B-other cases, *BCR-ABL1*-like cases were identified using the 110-probeset gene expression classifier.[2] In addition, immunophenotyping was performed, including cytoplasmic Igµ (CyIgµ) expression. Samples containing more than 30% leukemic cells expressing CyIgµ were labelled as CyIgµ-positive.

Cell lines

The human BCP-ALL cell lines Nalm6 and Kasumi-2 were obtained from the German Collection of Microorganisms and Cell lines (DSMZ, Braunschweig, Germany). Cells were cultured in RPMI-1640 medium, supplemented with 10% fetal calf serum (Bodinco BV, Alkmaar, Netherlands), 100 units/ml penicillin, 100 µg/ml streptomycin and 0.125 µg/mL fungizone (Life Technologies). The identity of cell line was routinely verified by DNA fingerprinting. The B-other cell line Nalm6 expressed high levels of *STAP1* and *TCF3-PBX1* positive Kasumi-2 cells had low expression levels of *STAP1*. For stimulation experiments, cells were exposed to 1µg anti-IgM F(ab')2 (SouthernBiotech, Birmingham, AL, USA).

STAP1 expression status

Microarrays (Affymetrix U133 Plus 2 Santa Clara, California, USA) were analyzed of a previously published cohort of 572 BCP-ALL patients at initial diagnosis (GSE13351),[21] in

which all major ALL subtypes were represented (*BCR-ABL1*-positive n=24, *BCR-ABL1*-like B-other n=92, non-*BCR-ABL1*-like B-other n=113, *ETV6-RUNX1*-positive n=172, high hyperdiploid n=141, *KMT2A*-rearranged n=11, *TCF3-RUNX1*-positive n=19). Gene expression profiles of *BCR-ABL1*-like and non-*BCR-ABL1*-like B-other samples were compared to remaining BCP-ALL cases, using Limma R Package (version 3.26.9) in R 3.0.1. *BCR-ABL1*-like and non-*BCR-ABL1*-like B-other cases with signal intensity values of both *STAP1* probesets (220059_at and 1554343_a_at) above the 80th percentile of *BCR-ABL1*-like and non-*BCR-ABL1*-like B-other cases were classified as *STAP1*-high (see also Fig. 1A). Remaining *BCR-ABL1*- like and non-*BCR-ABL1*-like B-other cases were classified as *STAP1*-low.

Quantitative reverse transcription PCR (RT-qPCR)

mRNA expression levels of *STAP1* and *RPS20* were quantified using real-time PCR analysis on an ABI Prism 7700 sequence detection system (PE Applied Biosystems). RNA was extracted using the RNeasy mini kit (Qiagen, Hilden, Germany), after which cDNA was synthesized. *STAP1* and *RPS20* mRNA levels were quantified by incorporation of SYBR Green (Thermo Scientific) by quantitative real-time PCR, using *STAP1*-specific primers (5'-ccaggaaaggttaaagattact-3' and 5'-ttccccactttctgtgtt-3') and RPS20-specific primers (5'-aagggctgaggatttttg-3' and 5'-cgttgcggcttgttag-3'). Relative *STAP1* mRNA levels as percentage of RPS20 levels were calculated using the comparative cycle time (Ct) method; $2^{-\Delta Ct}$ x 100%, whereby $\Delta Ct = Ct_{STAP1} - CT_{RPS20}$.

Transfection, virus production and transduction

To knockdown *STAP1* expression, four pLKO.1-puro Mission® vectors (Sigma-Aldrich) containing a short hairpin RNA (shRNA) targeting *STAP1* (TRCN0000065083, TRCN0000065084, TRCN0000065085, TRCN0000065087; shRNA-1, shRNA-2, shRNA-3, shRNA-4, respectively) were used. The Mission ® pLKO.1-puro Non-Mammalian shRNA Control Plasmid DNA (SHC002) and Mission® pLKO.1-puro Luciferase shRNA Control Plasmid DNA (SHC007) were used as scrambled control vectors (NSC-1 and NSC-2, respectively).

Vectors were transfected in HEK293T cells, using XtremeGene, 3.7 µg psPAX2 (Addgene plasmid 12260; Addgene, Cambridge, MA, USA), 1.6 µg pMD2.G (Addgene plasmid 12259) and 10.7 µg of one of the pLKO.1 puro Mission® vectors. The second and third day after transfection virus was harvested and concentrated using ultracentrifugation for 2 hours at 32.000 rpm and 4°C. Concentrated virus was aliquoted and stored at -80°C. Leukemic cells were spin-infected and puromycin selection was initiated 24 hours after transduction. Transduction efficiency was determined using a titration range. After 48 hours of puromycin selection (1 µg/ml) cell viability was measured using flow cytometry (MACSQuant) and propidium iodide (PI; Invitrogen). Viability of transduced cells as percentage of viability of non-transduced cells was defined as the transduction efficacy. Proliferation was measured for 5 days using flow cytometry (MACSQuant) and PI staining. At day 5, viability was quantified using Annexin V (Biolegend, London, UK) and PI staining.

Ex vivo drug resistance

Ex vivo cytotoxicity of prednisolone, vincristine, L-asparaginase, daunorubicin, 6-mercaptopurine and 6-thiguanine in primary samples was evaluated using 3-(4,5-dimethylthiazolyl-2)-2,5-diphenyltetrazolium bromide (MTT), as previously described.[28] After four days of culture, viability was quantified by measuring the optical density values after 6 hours of incubation with MTT. LC50 values were compared using the Mann-Whitney U test. *In vitro* cytotoxicity of prednisolone, ibrutinib and rapamycin in cell lines was evaluated using 3-(4,5-dimethylthiazolyl-2)-5-(3-carboxymethoxyphenyl)-2-(4-sulfophenyl)-2H-tetrazolium; MTS) and phenazine methosulfate (PMS). Cells were exposed to a dilution series of agents (prednisolone: 0.06 to 250 µg/mL; ibrutinib: 0.16 to 40 µM; rapamycin: 4 nM to 40 µM) in a 96 wells plate for four days at 37°C and 5% CO_2, after which viability was quantified.

Multiplexed fluorescent bead-based immunoassay (Luminex)

Cells were lysed in RIPA buffer (ThermoFisher Scientific) with freshly added protease and phosphatase inhibitors. Protein concentration was determined using the BCA method (Thermo Scientific). Expression of 17 proteins was determined in 10µg lysate, using a fluorescent bead-based immunoassay (multi-pathway magnetic bead 9-plex and the 8-plex human Src family kinase kit; Merck Millipore, Amsterdam, Netherlands) according to the manufacturer's protocol. GAPDH beads (Merck Millipore) were used as internal reference for each sample.

Multiplex Ligation-Dependent Probe Amplification (MLPA)

To identify genomic lesions in *IKZF1*, *CDKN2A*, *CDKN2B*, *ETV6*, *PAX5*, *RB1*, *BTG1*, *EBF1*, and PAR1 (*CSF2RA/IL3RA/CRLF2*), the SALSA P335 ALL-*IKZF1* (a3) and the SALSA P202 Multiplex Ligation-dependent Probe Amplification (MLPA) assays (MRC-Holland, Amsterdam, Netherlands) were used as described previously.4,21,34 A peak ratio < 0.75 was used to determine deletions, 0.75 ≤ peak ratio ≤ 1.3 for normal copy number, and peak ratio > 1.3 for gain. Loss of either *CDKN2A* or *CDKN2B* was coded as *CDKN2A/B* deletion and intragenic amplifications of *PAX5* were coded as aberration.

Genome-wide DNA copy number arrays (array-CGH)

To identify *ERG* deletions, genome-wide DNA copy number arrays were performed as described previously.[4] Briefly, Agilent SurePrint G3 Hmn 4x180K arrays (Agilent Technologies, Amstelveen, the Netherlands) were co-hybridized with 1 µg patient DNA labeled with ULS-Cy5 and 1 µg reference genomic DNA male pool (G147A, Promega, Leiden, the Netherlands) labeled with ULS-Cy3 (Agilent Genomic DNA ULS Labeling Kit). Using median log ratios, data were normalized using the CGHcall35 version 2.14.0, centralized using CGHnormaliter36 version 1.8.0, and segmented and called using CGHcall default settings (-1 for loss, 0 for diploid, 1 for gain and 2 for amplification) in R version 2.14.1.

Clinical characteristics and statistics

To identify whether copy number alterations (CNAs), clinical characteristics or CyIgμ expression were depleted or enriched in cases harboring high expression levels of *STAP1*, the Fisher's exact test in R (version 3.2.1) was applied. Cumulative incidence of relapse (CIR) was estimated using a competing risk model and significance was determined using the Gray's test. Relapse and non-response (counted at day 79 of therapy) were considered as events and death as competing event. Event-free survival (EFS) probabilities were estimated using cox regression and compared using the Wald test. Relapse, non-response, secondary malignancies and death were counted as events. Outcome analyses were performed in R (version 3.2.1), using the packages cmprsk version 2.2-7 [37], mstate version 0.2.7 [38], and survival version 2.37-4 [39]. Five-year EFS and CIR are reported.

SNP arrays

Genome-wide human SNP arrays 6.0 (Affymetrix) were performed according to the manufacturer's protocol. Raw probe values were extracted from CEL files and processed with the R package aroma.affymetrix version 3.1.0. Samples were compared to reference values, which was the average of 53 diploid BCP-ALL and T-ALL samples. To correct for bias introduced by differences in GC content of DNA fragments, the R package ArrayTV version 1.12.0 was used. To compare the logR values of the copy numbers between samples a centralization step was performed, using the R package CGHnormaliter version 1.28.0. Data were called using CGHcall version 2.36.0 default settings (-2 for double loss, -1 for loss, 0 for diploid, 1 for gain and 2 for amplification) in R version 3.3.3.

RNAseq

mRNA was extracted from total RNA and amplified using random hexamer primers. Further Library construction was done using a strand-specific protocol. Sequencing was performed on a HiSeq 2000 producing 151bp paired-end reads with a median library size of 50 million read pairs per sample. Fastq-files with paired-end data were aligned to the GRCh37 reference sequence using STAR 2.5.0b. Read counts were determined with HTSeq-count version 0.6.1p1. To determine *DUX4* expression, the fastq-files were aligned to the DNA sequence of the gene ENSG00000259128.1 plus 200bp down- and upstream. *DUX4*-partner genes were identified using NCBI blast, in which unknown sequences after the breakpoint were aligned.[40]

RESULTS

Discriminative expression profile of *STAP1* in *BCR-ABL1*-like and B-other cases

To identify differentially expressed genes in *BCR-ABL1*-like and non-*BCR-ABL1*-like B-other cases, microarrays were performed of a representative pediatric BCP-ALL cohort of 572 cases at initial diagnosis.[21] Limma analyses revealed *STAP1* to be the probeset with the highest fold-change in *BCR-ABL1*-like and non-*BCR-ABL1*-like B-other patients compared to remaining BCP-ALL cases (fold change = 2.88, adjusted p-value < 0.0001; Supplementary Table S1). Strikingly, this elevated expression was characteristic for a subset of patients reflecting about 20% of *BCR-ABL1*-like and non-*BCR-ABL1*-like B-other cases (Fig. 1A, henceforth: *STAP1*-high cases). The remaining *BCR-ABL1*-like and non-

BCR-ABL1-like B-other cases (henceforth: *STAP1*-low) had *STAP1* expression levels comparable to those observed in other ALL subtypes and mononuclear bone marrow cells of healthy controls (Supplementary Fig. S1). Microarray results were validated using RT-qPCR (Fig. 1B, Supplementary Fig. S1). Subsequently, we analyzed which genes were associated with high expression levels of *STAP1*. Limma analyses revealed 8894 probesets to be differentially expressed between *STAP1*-high and *STAP1*-low cases (adjusted p-value < 0.05; Supplementary Table S2). Ingenuity pathway analysis was performed to identify pathways associated with these differentially expressed genes. EIF2 signaling, mTOR signaling, regulation of eIF4 and p70S6K signaling, B cell receptor signaling (BCR), and AMPK signaling included the top five differentially regulated canonical pathways (Supplementary Fig. S1). Identification of the BCR signaling pathway was a striking observation, as *STAP1* is reported to be a docking protein downstream of TEC in this pathway.[24,25] Since the signaling pathways activated by pre-BCR and mature BCR are highly overlapping,[14] we hypothesized a similar function for STAP1 in the downstream signaling cascade of the pre-BCR. Taken together, the association between STAP1 and the BCR signaling cascade may suggest an activated pre-BCR signaling pathway in a subset of *BCR-ABL1*-like and non-*BCR-ABL1*-like B-other cases. This hypothesis was further explored since it may offer a targeted treatment strategy for these cases.[17-20]

High levels of *STAP1* and pre-BCR signaling are not causally connected

We studied whether high levels of *STAP1* associated with high expression of the pre-BCR complex. To determine in-frame rearrangements of immunoglobulin heavy chain V_HDJ_H gene segments (indicative for a functional pre-BCR), cytoplasmic Igμ (CyIgμ) levels were measured in 142 *BCR-ABL1*-like and non-*BCR-ABL1*-like B-other cases. 14 of the 32 (44%) *STAP1*-high cases showed positivity (> 30% CyIgμ+ cells) compared with 31 of the 110 (28%) *STAP1*-low cases (Fisher exact test. p=0.13). This result suggests that *STAP1*-high and *STAP1*-low cases do not differ in the number of pre-BCR positive cells.

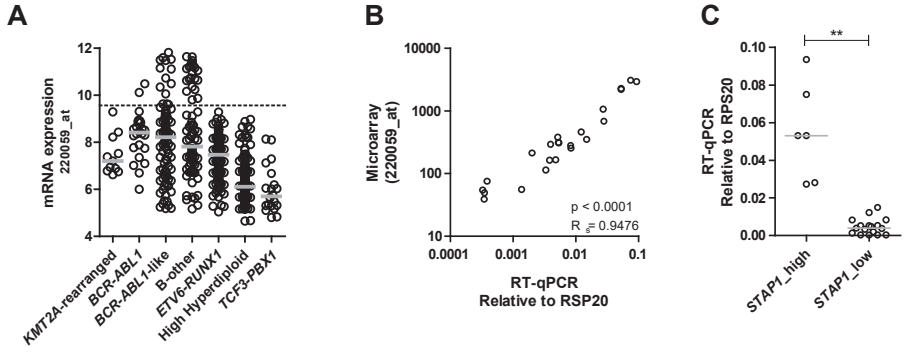

Figure 1. Discriminative expression of STAP1 in *BCR-ABL1*-like and B-other cases.
(A) 2log expression levels of Affymetrix probeset 220059_at in 572 BCP-ALL cases. The dotted line represents the 80th percentile of *BCR-ABL1*-like and B-other cases. Grey lines represent the median expression values of subtype groups. **(B)** Microarray expression levels were validated using RT-qPCR, as shown by a high spearman correlation coefficient. **(C)** Expression values of *STAP1* in 6 *STAP1*-high and 17 *STAP1*-low cases detected by RT-qPCR. Independent samples T-test. The grey lines represent the median of the *STAP1*-high and the *STAP1*–low group. Mann-Whitney U test. ** p<0.01.

In addition, we examined whether *STAP1* expression itself may be induced by pre-BCR signaling. Therefore, the BCP-ALL cell lines Nalm6 and Kasumi-2 (high and low *STAP1* expression, respectively) were stimulated for 4 days with 1µg anti-IgM antibody. To confirm activation of pre-BCR signaling by the anti-IgM antibody, phosphorylation levels of AKT^{Ser473} were analyzed (Supplementary Fig. S2). Stimulation of the pre-BCR did not increase *STAP1* expression levels in the *STAP1*-high cell line Nalm6. In the *STAP1*-low cell line Kasumi-2 only a slight increase was detected in time (~1.3-1.6 fold; Fig. 2). Taken together, these results suggest that high levels of *STAP1* and pre-BCR signaling are not causally connected.

Silencing of *STAP1* does not affect cell viability and drug sensitivity

To elucidate the role of *STAP1* in BCP-ALL survival, *STAP1* expression was silenced by four different shRNAs in the BCP-ALL cell lines Nalm6 and Kasumi-2. The knockdown efficiency at mRNA level ranged from 50-80% for both cell lines and was confirmed on protein level (Fig. 3A, Supplementary Fig. S3-4). Three out of four shRNA constructs did not alter the proliferation rate and viability of Nalm6 cells, despite effective knockdown. Only shRNA-2 reduced those parameters in Nalm6 cells, but not in Kasumi-2 cells (Fig. 3B). Seven days after transduction, the majority of leukemic cells remained alive in both cell lines and in all knockdown conditions (Fig. 3C). These data suggest that *STAP1* is not essential for the survival of BCP-ALL cells.

Next, we studied whether silencing of *STAP1* affected sensitivity for inhibitors of pre-BCR (ibrutinib) and mTOR signaling (rapamycin), and the ALL spearhead drug prednisolone. Silencing of *STAP1* did not alter the sensitivity to these compounds in the Nalm6 or Kasumi-2 cell lines (Fig. 4). To elucidate in which other signaling pathway STAP1 may be involved, the phosphorylation status of 17 proteins covering multi-signaling pathways was examined (Fig. 5). Silencing *STAP1* did not alter the phosphorylated levels/ activation of Src-family, PI3K, Ras, Stat, JNK, p38 and NFκB kinase signaling members, nor of the reported *STAP1* target in Ramos cells, i.e. phosphorylated level of $CREB^{Ser133}$.[25] Taken together, *STAP1* inhibition did not affect the survival and proliferation of the BCP-ALL

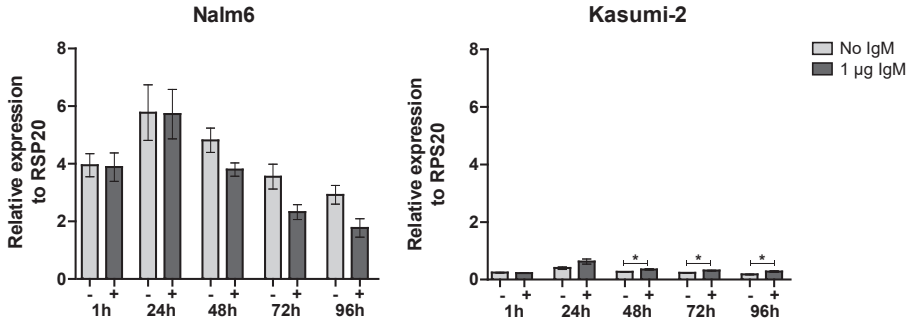

Figure 2. Pre-BCR signaling and STAP1 expression

The BCP-ALL cell lines Nalm6 and Kasumi-2 were stimulated with 1 µg anti-IgM for 1, 24, 48, 72 or 96 hours. Expression levels of STAP1 were examined using RT-qPCR. Linear values normalized to *RPS20* expression are shown. Mean±SEM of three independent experiment. Independent samples T test. * $p<0.05$.

cell lines Nalm6 and Kasumi-2 or the phosphorylated levels of downstream signaling molecules, nor did knockdown result into sensitization for prednisolone or signaling inhibitors (ibrutinib and rapamycin).

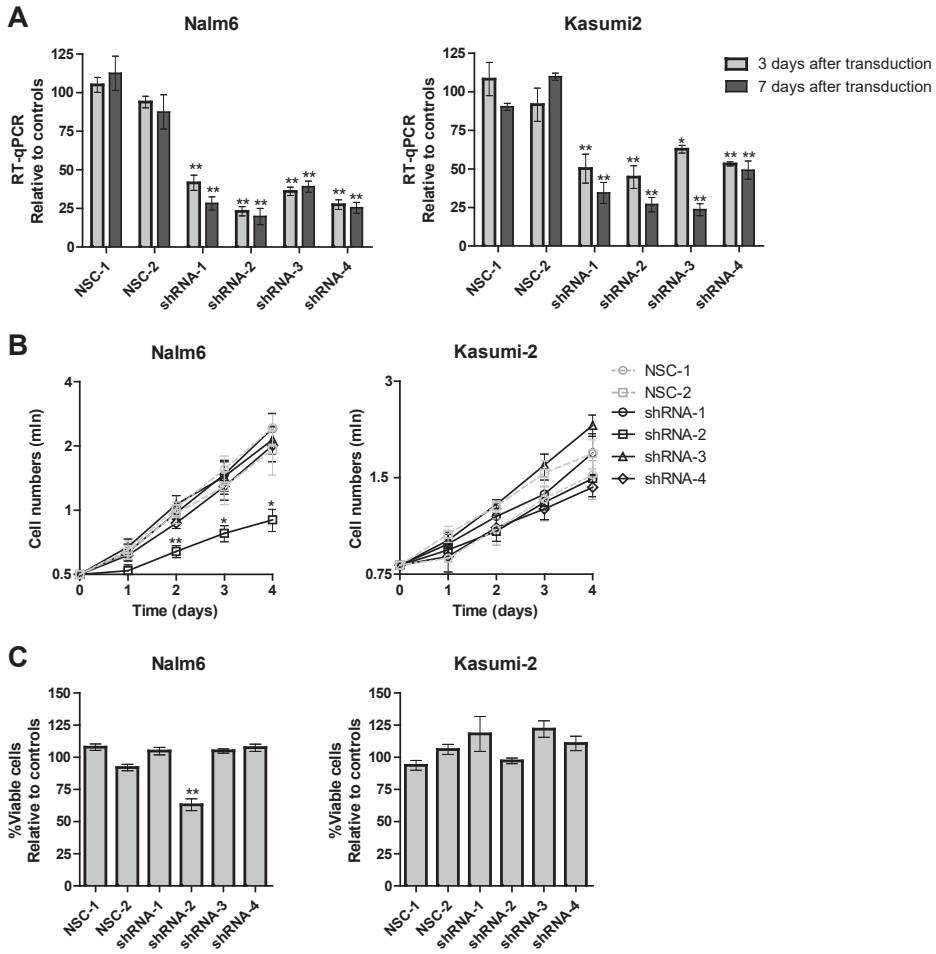

Figure 3. STAP1 knockdown does not affect leukemic cells survival.
Nalm6 and Kasumi-2 cells were transduced via spin-infection with shRNAs targeting *STAP1* or scrambled control vectors. Values represent mean±SEM of four independent experiments. Independent sample T test. ** p<0.01; *p<0.05. (**A**) Knockdown efficacy was determined three and seven days after transduction using RT-qPCR. *STAP1* expression relative to *RPS20* was calculated. Relative expression values towards the two scrambled controls are depicted. (**B**) Proliferation of Nalm6 and Kasumi-2 cells was measured for four days. At day 0 (3 days after transduction) cells were plated at equivalent concentrations. The next four days cell concentrations were detected using the MACSQuant and PI staining. Cell numbers (x10^6) are shown on the y-axis. (**C**) Seven days after transduction, viability of the cells was determined using AnnexinV and PI staining. Viability relative to scrambled control samples is shown.

Aberrations in B-cell development genes and clinical characteristics

Genes involved in B-cell development are frequently altered in *BCR-ABL1*-like patients.[2,3] Therefore, frequencies of lesions in genes involved in lymphoid differentiation, proliferation, cell cycle, and transcription were studied in *STAP1*-high and *STAP1*-low *BCR-ABL1*-like and non-*BCR-ABL1*-like B-other cases. Copy number alterations affecting *EBF1*, PAR1, and *ETV6* were virtually absent in *STAP1*-high cases compared to a frequency ranging from 10.9-22.4% in *STAP1*-low cases (Fisher exact test, $p<0.05$; Table 1). More strikingly, high expression of *STAP1* was associated with intragenic deletion of the ETS transcription

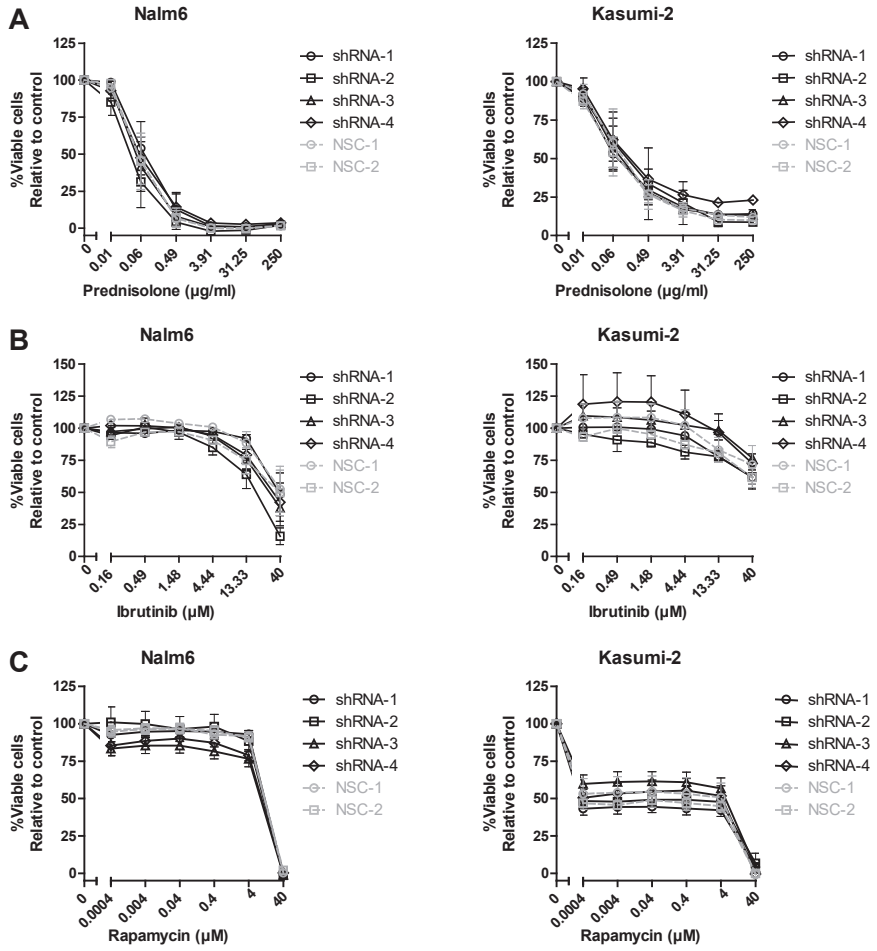

Figure 4. *STAP1* knockdown does not sensitize cells towards prednisolone, ibrutinib or rapamycin.

(**A-C**) The efficacy of prednisolone (**A**), ibrutinib (**B**), and rapamycin (**C**) was tested in Nalm6 and Kasumi 2 cells, in which *STAP1* was silenced. Three days after transduction, Nalm6 and Kasumi-2 cells were exposed to a concentration range of the indicated compounds. After four days, viability was quantified using an MTS assay. Values represent mean±SEM of four independent experiments of Nalm6 and three independent experiments of Kasumi-2.

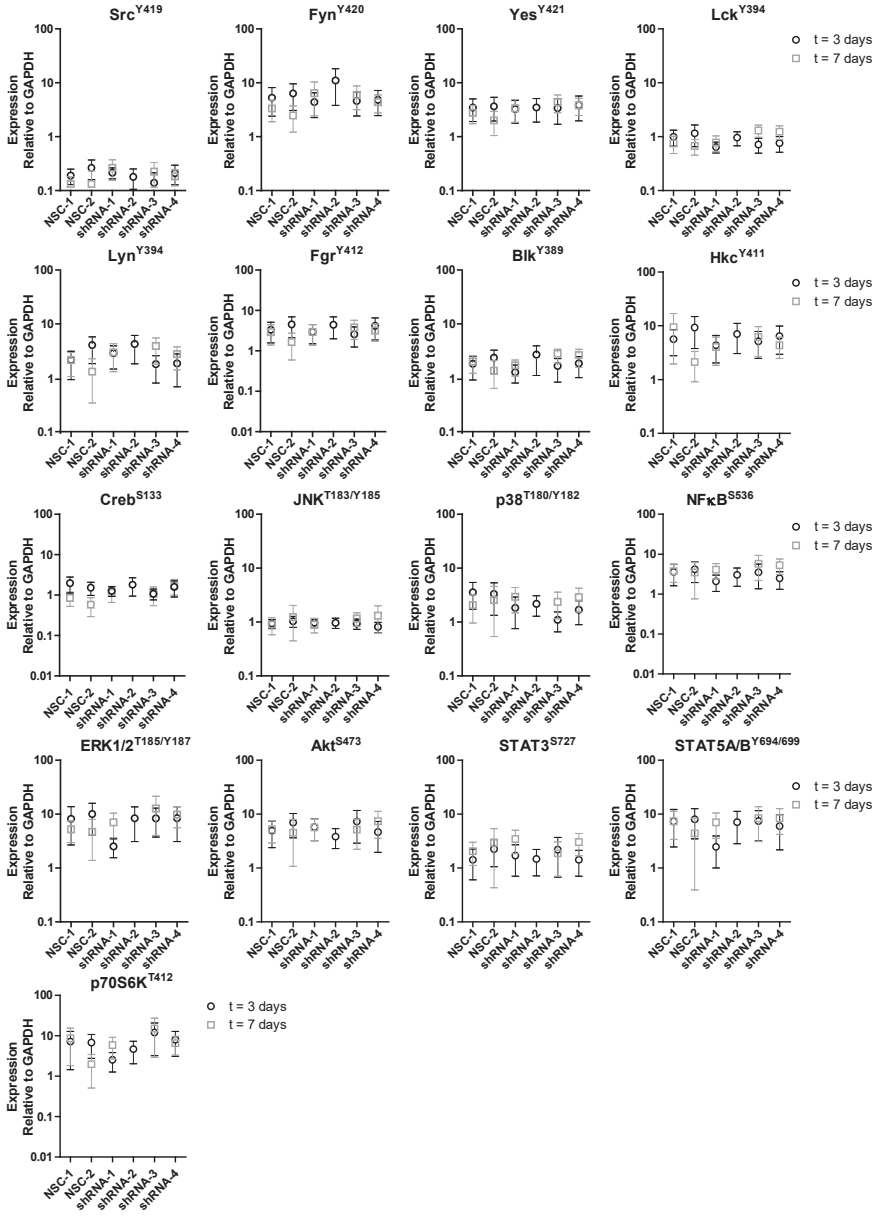

Figure 5. STAP1 knockdown does not affect common signaling pathways.

Expression of 17 proteins was determined using a fluorescent bead-based immunoassay in Nalm6 cells after knockdown of STAP1. Fluorescent intensity values relative to GAPDH are depicted. Expression was measured three and seven days after transduction. Infection and selection for stably transduced cells required three days. Subsequently, proliferation, viability and MTS assays were initiated, which took four days. mRNA and protein expression levels were examined after selection (day 3) and at the end of these functional experiments (day 7). At day 7, not enough material was available of Nalm6 cells, which were transduced with shRNA-2. Values represent mean±SEM of four independent experiments at three days after transduction and three independent experiments at seven days after transduction.

Table 1: Copy Number Alterations in B-cell development genes

	STAP1 high cases		*STAP1* low cases				
	Number	Percentage	Number	Percentage	P-value	Odds Ratio	95% Confidence Interval
***IKZF1* deletion**	8/36	22.2	58/156	37.2	0.120		
***EBF1* deletion**	0/36	0.0	17/156	10.9	0.046	0.00	0.00-1.00
***PAX5* aberration**	10/36	27.8	69/156	44.2	0.091	0.49	0.20-1.13
***CDKN2A/B* deletion**	15/36	41.7	77/156	49.4	0.460		
***RB1* deletion**	1/36	2.8	14/156	9.0	0.310		
***BTG1* deletion**	1/36	2.8	10/156	6.4	0.690		
***ETV6* deletion**	1/36	2.8	35/156	22.4	0.004	0.10	0.00-0.64
PAR1 deletion	0/36	0.0	19/156	12.2	0.027	0.00	0.000.87
***ERG* deletion**	8/29	27.6	1/131	0.8	3.80E-06	47.68	5.91-2183.65

factor *ERG*: 27.6% (8/29) in *STAP1*-high cases compared to 0.8% (1/133) in *STAP1*-low cases ($p < 0.0001$, odds ratio = 47.7; Table 1). Deletions of *ERG* are associated with a favorable prognosis in genetically unclassified high-risk pediatric BCP-ALL.[41-43] The five-year CIR and EFS of *STAP1*-high and *STAP1*-low *BCR-ABL1*-like and non-*BCR-ABL1*-like B-other cases did not significantly differ in our cohort, although *STAP1*-high cases showed a trend for a more favorable outcome (Fig. 6A-B). *STAP1*-high cases had a higher median age (Mann-Whitney U test; p=0.013; 9 years, range 2-16) than *STAP1*-low cases (6 years, range 1-18). Remaining clinical characteristics, i.e. white blood cell count, *in vivo* prednisolone response at day 8, gender, and MRD levels did not differ (Supplementary Table S3). In addition, *ex vivo* cytotoxicity of prednisolone, vincristine, daunorubicin, l-asparaginase, 6-thioguanine, 6-mercaptopurine was measured in primary leukemic cells. No difference in cytotoxicity of these compounds was observed in *STAP1*-high and *STAP1*-low *BCR-ABL1*-like and non-*BCR-ABL1*-like B-other cells (Fig. 6C-H).

Interestingly, *ERG* deletions were very recently shown to be a hallmark of a newly identified BCP-ALL subtype, involving rearrangements of the double homeobox transcription factor *DUX4*.[8-10,44] The association between high *STAP1* levels and *ERG* deletions prompted us to investigate the presence of *DUX4* rearrangements in our cases. To this aim, we screened an independent BCP-ALL cohort (n=2 *KMT2A*-rearranged, n=1 *BCR-ABL1*, n=21 B-other, n=17 *ETV6-RUNX1*, n=21 high hyperdiploid) for *DUX4*-rearrangements and *ERG* deletions. Four *DUX4*-rearranged cases were detected in the B-other group, of which two showed high expression levels of *STAP1* (Fig. 7). None of these *DUX4*-rearranged cases or remaining B-other cases harbored an *ERG* deletion. In addition, we analyzed the association between *STAP1*, *ERG*, and *DUX4* using a publically available dataset of 304 BCP-ALL cases.[10,45] Similar to the observation made in our own patients, *DUX4*-rearranged cases displayed higher levels of *STAP1* mRNA (Supplementary Fig. S6), which was independent of intragenic *ERG* deletions.

Taken together, high expression of *STAP1* is not associated with (long-term) clinical outcome parameters or *ex vivo* drug resistance. However, the *STAP1*-high group is enriched for *DUX4*-rearrangements and intragenic *ERG* deletions.

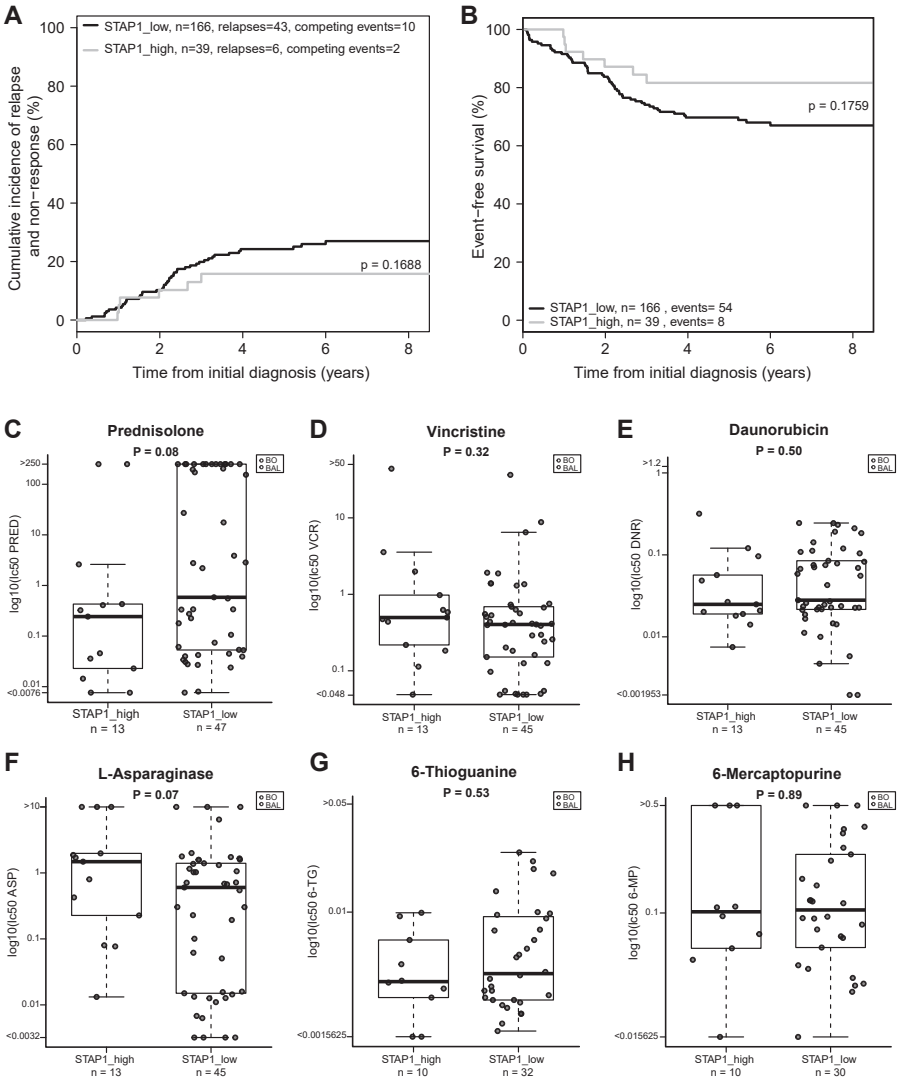

Figure 6. *Ex vivo* drug response and outcome is not affected by *STAP1* overexpression.
(**A-B**) The association between high expression levels of *STAP1*, and cumulative incidence of relapse (CIR) and event-free-survival (EFS) was examined. Patients were stratified according to treatment protocol (i.e. COALL-97 or -03, or the DCOG protocols ALL8, ALL9, or ALL10). CIR was estimated using a competing risk model with relapse and non-response as event and death as competing event. The Gray's test was applied. Relapse, non-response, secondary malignancies and death were considered as events for EFS. EFS rates were determined using Cox regression, and compared using the Wald test. (**C-H**) Leukemic cells were exposed for four days to an increasing concentration range of prednisolone (µg/ml), vincristine (µg/ml), L-asparaginase (IU/ml), daunorubicin (µg/ml), 6-mercaptopurine (µg/ml), and 6-thioguanine (µg/ml). Cell survival was measured using an MTT assay. To compare LC50-values, the Mann-Whitney U test was applied. BO = non-*BCR-ABL1*-like B-other BCP-ALL cases. BAL = B*CR-ABL1*-like BCP-ALL cases.

DISCUSSION

The aim of the current study was to assess the potential of STAP1 as a therapeutic target in BCP-ALL cases. High expression of *STAP1* was detected in a subset of *BCR-ABL1*-like and non-*BCR-ABL1*-like B-other patients. Interference with *STAP1* did not induce cell death or block proliferation, nor did it make cells more sensitive to BTK (ibrutinib) and mTOR (rapamycin) inhibitors. In addition, high expression levels of *STAP1* were not associated with a poor five-year EFS, high MRD levels, or *ex vivo* resistance to chemotherapeutic

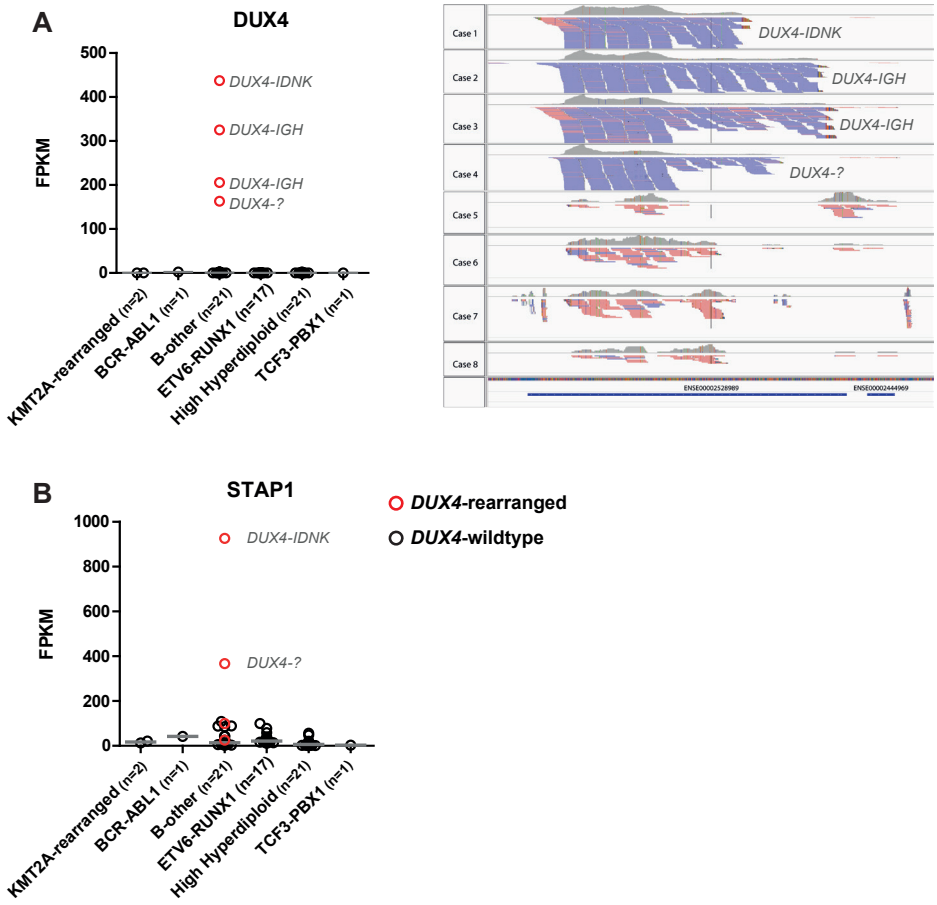

Figure 7. *STAP1* expression and *DUX4*-rearrangements

RNAseq analyses were used to determine *DUX4* and *STAP1* expression levels in an independent BCP-ALL cohort (n=2 *KMT2A*-rearranged, n=1 *BCR-ABL1*, n=21 B-other, n=17 *ETV6 RUNX1*, n=21 high hyperdiploid). Fastq-files with paired-end data were aligned to one *DUX4* gene and the *STAP1* GRCh37 reference sequence using STAR 2.5.0b. Read counts were determined with HTSeq-count version 0.6.1p1. Grey lines represent the median expression values. (**A**) *DUX4* expression values are depicted as Fragments Per Kilobase per Million mapped (FPKM). *DUX4*-partner genes were identified using NCBI blast, in which unknown sequences after the breakpoint were aligned.[40] DUX4-alignement of 4 DUX4-rearranged cases and 4 non-*DUX4*-rearranged B-other cases is shown. (**B**) *STAP1* expression values are depicted as FPKM.

drugs that are traditionally used in the treatment of BCP-ALL. Taken together, these results suggest that *STAP1* is not a likely target for precision medicines in childhood ALL.

STAP1 is a relatively unknown gene. A potential role for the protein in neuronal apoptosis and degeneration has been suggested.[26] However, involvement of the protein in cancer thus far remains elusive. We studied the gene expression profiles of *STAP1*-high BCP-ALL cases. The observed association between high expression of *STAP1* and BCR signaling is in concordance with the few reports suggesting that *STAP1* is a docking protein downstream of the BCR.[24,25] Targeting the BCR pathway is an effective treatment strategy for mature B-cell malignancies and this approach is also being explored in BCP-ALL.[15-20] The overlap in downstream molecules involved in pre-BCR and BCR signaling,[14] prompted us to investigate the connection between *STAP1* expression and the pre-BCR pathway. However, CyIgμ expression (indicative for a functional pre-BCR) was not enriched in *STAP1*-high cases, and stimulation of leukemic cell lines with IgM only marginally induced expression *STAP1* in one cell line. In addition, silencing of *STAP1* did not reduce the proliferation rate and viability of leukemic cells in the majority of shRNAs tested. Strikingly, knockdown of *STAP1* did also not affect phosphorylation levels of marker proteins involved in pre-BCR signaling (SRC) or other signaling pathway (PI3K, Ras, Stat, JNK, p38, NFκB), which are important for proliferation and survival of cells. In addition, silencing of *STAP1* did not affect the phosphorylated levels of CREB, which is a downstream target of *STAP1* in the Ramos/Burkitt lymphoma cell line.[25] The question remains regarding the signaling pathway in which *STAP1* is involved. Nevertheless, our results imply that *STAP1* is not an oncogenic driver and that the high expression is most likely a consequence of another transforming event.

Interestingly, we observed intragenic deletions of the transcription factor *ERG* in a part of the *STAP1*-high cases. The proto-oncogene *ERG* is a regulator of hematopoiesis, including B-cell development,[46,47] and is implicated in the pathogenesis of Ewing sarcoma, prostate cancer, and acute myeloid leukemia.[48-50] Recently, *ERG* deletions were shown to be a hallmark of a novel identified subtype of BCP-ALL, i.e. *DUX4*-rearranged ALL.[8-10] *DUX4* encodes a double homeobox transcription factor and is located within the D4Z4 macrosatellite repeat array on 4q35 and 10q26. This pro-apoptotic gene is normally expressed in germline and testis cells, but epigenetically silenced in somatic cells.[51,52] *DUX4*-fusion proteins, but not wildtype *DUX4*, were shown to have oncogenic potential in NIH3T3 fibroblasts.[9] The pathway induced by *DUX4*-rearrangements is yet unknown. In the present work we show that high expression of *STAP1* is characteristic for *DUX4*-rearranged cases (Fig. *7*, Supplementary Fig S6). The association between *STAP1* and *DUX4* was independent of *ERG* deletions. Therefore, upregulation of *STAP1* may be a consequence of the oncogenic signaling pathway induced in *DUX4*-rearranged cases which is independent of concomitant *ERG* deletions. Further unraveling of the signaling pathway downstream of *DUX4* will be crucial for the development of targeted treatment strategies for this genetic BCP-ALL subtype.

Acknowledgements

This work was supported by the VICI program grant 016.126.612 from Netherlands Organisation for Scientific Research (NWO), the Dutch Cancer Society grants AMC 2008-4265 and EMCR 2014-6998, the Kika Foundation (grant 132 and 161) and the Pediatric Oncology Foundation Rotterdam.
This work was supported in part by US NIH Center for Precision Medicine of Leukemia grant P50 GM115279, and we thank William Evans, Jun Yang, and Kristine Crews of St. Jude Children's Research Hospital for the RNAseq analyses.

Author Contributions Statement

EMPS designed and performed experiments, and analyzed and interpreted data. MB, QH, and FS performed experiments. AQH analyzed SNP arrays and RNAseq data. JMB designed experiments and interpreted data. RP, HAdGK, VdH, and GE provided clinical characteristics, clinical outcome data, and interpreted data. RP and MLdB conceptualized the study, and interpreted data. EMPS and MLdB drafted the manuscript. The manuscript was revised and approved by all authors.

Disclosure of Conflicts of Interest

The authors declare that they have no competing interests.

REFERENCES

1. Pui, C. H. & Evans, W. E. A 50-year journey to cure childhood acute lymphoblastic leukemia. Seminars in hematology 50, 185-196, doi:10.1053/j.seminhematol.2013.06.007 (2013).
2. Den Boer, M. L. et al. A subtype of childhood acute lymphoblastic leukaemia with poor treatment outcome: a genome-wide classification study. Lancet Oncol 10, 125-134, doi:S1470-2045(08)70339-5 [pii] 10.1016/S1470-2045(08)70339-5 (2009).
3. Mullighan, C. G. et al. Deletion of IKZF1 and prognosis in acute lymphoblastic leukemia. The New England journal of medicine 360, 470-480, doi:10.1056/NEJMoa0808253 (2009).
4. Boer, J. M. et al. Tyrosine kinase fusion genes in pediatric BCR-ABL1-like acute lymphoblastic leukemia. Oncotarget 8, 4618-4628, doi:10.18632/oncotarget.13492 (2017).
5. Imamura, T. et al. Characterization of pediatric Philadelphia-negative B-cell precursor acute lymphoblastic leukemia with kinase fusions in Japan. Blood cancer journal 6, e419, doi:10.1038/bcj.2016.28 (2016).
6. Roberts, K. G. et al. Targetable kinase-activating lesions in Ph-like acute lymphoblastic leukemia. The New England journal of medicine 371, 1005-1015, doi:10.1056/NEJMoa1403088 (2014).
7. Roberts, K. G. et al. Genetic alterations activating kinase and cytokine receptor signaling in high-risk acute lymphoblastic leukemia. Cancer cell 22, 153-166, doi:10.1016/j.ccr.2012.06.005 (2012).
8. Lilljebjorn, H. et al. Identification of ETV6-RUNX1-like and DUX4-rearranged subtypes in paediatric B-cell precursor acute lymphoblastic leukaemia. Nature communications 7, 11790, doi:10.1038/ncomms11790 (2016).
9. Yasuda, T. et al. Recurrent DUX4 fusions in B cell acute lymphoblastic leukemia of adolescents and young adults. Nat Genet 48, 569-574, doi:10.1038/ng.3535 (2016).
10. Zhang, J. et al. Deregulation of DUX4 and ERG in acute lymphoblastic leukemia. Nat Genet 48, 1481-1489, doi:10.1038/ng.3691 (2016).
11. Rickert, R. C. New insights into pre-BCR and BCR signalling with relevance to B cell malignancies. Nature reviews. Immunology 13, 578-591, doi:10.1038/nri3487 (2013).
12. Eswaran, J. et al. The pre-B-cell receptor checkpoint in acute lymphoblastic leukaemia. Leukemia 29, 1623-1631, doi:10.1038/leu.2015.113 (2015).
13. Srinivasan, L. et al. PI3 kinase signals BCR-dependent mature B cell survival. Cell 139, 573-586, doi:10.1016/j.cell.2009.08.041 (2009).
14. Herzog, S., Reth, M. & Jumaa, H. Regulation of B-cell proliferation and differentiation by pre-B-cell receptor signalling. Nature reviews. Immunology 9, 195-205, doi:nri2491 [pii] 10.1038/nri2491 (2009).
15. Lee, C. S., Rattu, M. A. & Kim, S. S. A review of a novel, Bruton's tyrosine kinase inhibitor, ibrutinib. Journal of oncology pharmacy practice : official publication of the International Society of Oncology Pharmacy Practitioners 22, 92-104, doi:10.1177/1078155214561281 (2016).
16. Wang, Y., Zhang, L. L., Champlin, R. E. & Wang, M. L. Targeting Bruton's tyrosine kinase with ibrutinib in B-cell malignancies. Clinical pharmacology and therapeutics 97, 455-468, doi:10.1002/cpt.85 (2015).
17. Wiestner, A. The role of B-cell receptor inhibitors in the treatment of patients with chronic lymphocytic leukemia. Haematologica 100, 1495-1507, doi:10.3324/haematol.2014.119123 (2015).
18. Kim, E. et al. Ibrutinib inhibits pre-BCR+ B-cell acute lymphoblastic leukemia progression by targeting BTK and BLK. Blood 129, 1155-1165, doi:10.1182/blood-2016-06-722900 (2017).
19. Muschen, M. Rationale for targeting the pre-B-cell receptor signaling pathway in acute lymphoblastic leukemia. Blood 125, 3688-3693, doi:10.1182/blood-2015-01-567842 (2015).
20. Kohrer, S. et al. Pre-BCR signaling in precursor B-cell acute lymphoblastic leukemia regulates PI3K/AKT, FOXO1 and MYC, and can be targeted by SYK inhibition. Leukemia 30, 1246-1254, doi:10.1038/leu.2016.9 (2016).
21. van der Veer, A. et al. Independent prognostic value of BCR-ABL1-like signature and IKZF1 deletion, but not high CRLF2 expression, in children with B-cell precursor ALL. Blood 122, 2622-2629, doi:blood-2012-10-462358 [pii] 10.1182/blood-2012-10-462358 (2013).
22. Huang, H. et al. Defining the specificity space of the human SRC homology 2 domain. Mol Cell Proteomics 7, 768-784, doi:10.1074/mcp.M700312-MCP200 (2008).
23. Kaneko, T. et al. Loops govern SH2 domain specificity by controlling access to binding pockets. Sci Signal 3, ra34, doi:10.1126/scisignal.2000796 (2010).
24. Ohya, K. et al. Molecular cloning of a docking protein, BRDG1, that acts downstream of the Tec tyrosine kinase. Proceedings of the National Academy of Sciences of the United States of America 96, 11976-11981 (1999).
25. Yokohari, K. et al. Isoform-dependent interaction of BRDG1 with Tec kinase. Biochemical and biophysical research communications 289, 414-420, doi:10.1006/bbrc.2001.6008 (2001).
26. Stoecker, K. et al. Induction of STAP-1 promotes neurotoxic activation of microglia. Biochemical and biophysical research communications 379, 121-126, doi:10.1016/j.bbrc.2008.12.021 (2009).
27. Masuhara, M. et al. Molecular cloning of murine STAP-1, the stem-cell-specific adaptor protein containing PH and SH2 domains. Biochemical and biophysical research communications 268, 697-703, doi:10.1006/bbrc.2000.2223 (2000).
28. Den Boer, M. L. et al. Patient stratification based on prednisolone-vincristine-asparaginase resistance profiles in children with acute lymphoblastic leukemia. J Clin Oncol 21, 3262-3268, doi:10.1200/JCO.2003.11.031 (2003).
29. Escherich, G., Zimmermann, M., Janka-Schaub, G. & CoALL study group. Doxorubicin or daunorubicin given upfront in a therapeutic window are equally effective in children with newly diagnosed acute lymphoblastic leukemia. A randomized comparison in trial CoALL 07-03. Pediatr Blood Cancer 60, 254-257, doi:10.1002/pbc.24273 (2013).

30. Veerman, A. J. et al. Dexamethasone-based therapy for childhood acute lymphoblastic leukaemia: results of the prospective Dutch Childhood Oncology Group (DCOG) protocol ALL-9 (1997-2004). Lancet Oncol 10, 957-966, doi:S1470-2045(09)70228-1 [pii] 10.1016/S1470-2045(09)70228-1 (2009).
31. Escherich, G. et al. The long-term impact of in vitro drug sensitivity on risk stratification and treatment outcome in acute lymphoblastic leukemia of childhood (CoALL 06-97). Haematologica 96, 854-862, doi:haematol.2010.039735 [pii] 10.3324/haematol.2010.039735 (2011).
32. Kamps, W. A. et al. BFM-oriented treatment for children with acute lymphoblastic leukemia without cranial irradiation and treatment reduction for standard risk patients: results of DCLSG protocol ALL-8 (1991-1996). Leukemia 16, 1099-1111, doi:10.1038/sj.leu.2402489 (2002).
33. Pieters, R. et al. Successful Therapy Reduction and Intensification for Childhood Acute Lymphoblastic Leukemia Based on Minimal Residual Disease Monitoring: Study ALL10 From the Dutch Childhood Oncology Group. J Clin Oncol 34, 2591-2601, doi:10.1200/JCO.2015.64.6364 (2016).
34. Boer, J. M. et al. Expression profiling of adult acute lymphoblastic leukemia identifies a BCR-ABL1-like subgroup characterized by high non-response and relapse rates. Haematologica 100, e261-264, doi:10.3324/haematol.2014.117424 (2015).
35. van de Wiel, M. A. et al. CGHcall: calling aberrations for array CGH tumor profiles. Bioinformatics 23, 892-894, doi:10.1093/bioinformatics/btm030 (2007).
36. van Houte, B. P., Binsl, T. W., Hettling, H., Pirovano, W. & Heringa, J. CGHnormaliter: an iterative strategy to enhance normalization of array CGH data with imbalanced aberrations. BMC genomics 10, 401, doi:10.1186/1471-2164-10-401 (2009).
37. Gray, R. J. cmprsk: Subdistribution Analysis of Competing Risks. R package version 2.2-6. http://CRAN.R-project.org/package=cmprsk (2013).
38. De Wreede, L. C., Fiocco, M. & Putter, H. mstate: An R Package for the Analysis of Competing Risks and Multi-State Models. J Stat Softw 38, 1-30 (2011).
39. Therneau, T. A Package for Survival Analysis in S. R package version 2.36-12. (2012).
40. Altschul, S. F., Gish, W., Miller, W., Myers, E. W. & Lipman, D. J. Basic local alignment search tool. Journal of molecular biology 215, 403-410, doi:10.1016/S0022-2836(05)80360-2 (1990).
41. Harvey, R. C. et al. Identification of novel cluster groups in pediatric high-risk B-precursor acute lymphoblastic leukemia with gene expression profiling: correlation with genome-wide DNA copy number alterations, clinical characteristics, and outcome. Blood 116, 4874-4884, doi:10.1182/blood-2009-08-239681 (2010).
42. Clappier, E. et al. An intragenic ERG deletion is a marker of an oncogenic subtype of B-cell precursor acute lymphoblastic leukemia with a favorable outcome despite frequent IKZF1 deletions. Leukemia 28, 70-77, doi:10.1038/leu.2013.277 (2014).
43. Zaliova, M. et al. ERG deletion is associated with CD2 and attenuates the negative impact of IKZF1 deletion in childhood acute lymphoblastic leukemia. Leukemia 28, 182-185, doi:10.1038/leu.2013.282 (2014).
44. Liu, Y. F. et al. Genomic Profiling of Adult and Pediatric B-cell Acute Lymphoblastic Leukemia. EBioMedicine 8, 173-183, doi:10.1016/j.ebiom.2016.04.038 (2016).
45. Zhou, X. et al. Exploring genomic alteration in pediatric cancer using ProteinPaint. Nat Genet 48, 4-6, doi:10.1038/ng.3466 (2016).
46. Reddy, E. S. & Rao, V. N. erg, an ets-related gene, codes for sequence-specific transcriptional activators. Oncogene 6, 2285-2289 (1991).
47. Loughran, S. J. et al. The transcription factor Erg is essential for definitive hematopoiesis and the function of adult hematopoietic stem cells. Nat Immunol 9, 810-819, doi:ni.1617 [pii] 10.1038/ni.1617 (2008).
48. Sorensen, P. H. et al. A second Ewing's sarcoma translocation, t(21;22), fuses the EWS gene to another ETS-family transcription factor, ERG. Nat Genet 6, 146-151, doi:10.1038/ng0294-146 (1994).
49. Kumar-Sinha, C., Tomlins, S. A. & Chinnaiyan, A. M. Recurrent gene fusions in prostate cancer. Nat Rev Cancer 8, 497-511, doi:nrc2402 [pii] 10.1038/nrc2402 (2008).
50. Marcucci, G. et al. Overexpression of the ETS-related gene, ERG, predicts a worse outcome in acute myeloid leukemia with normal karyotype: a Cancer and Leukemia Group B study. J Clin Oncol 23, 9234-9242, doi:10.1200/JCO.2005.03.6137 (2005).
51. van Geel, M. et al. Genomic analysis of human chromosome 10q and 4q telomeres suggests a common origin. Genomics 79, 210-217, doi:10.1006/geno.2002.6690 S0888754302966905 [pii] (2002).
52. Kowaljow, V. et al. The DUX4 gene at the FSHD1A locus encodes a pro-apoptotic protein. Neuromuscular disorders : NMD 17, 611-623, doi:10.1016/j.nmd.2007.04.002 (2007).

SUPPLEMENTARY METHODS

Microarray data analysis

Gene expression profiles of *BCR-ABL1*-like and non-*BCR-ABL1*-like B-other *STAP1*-high and *STAP1*-low samples were compared, using Limma R Package (version 3.26.9) in R 3.0.1. To identify canonical pathways that were more significantly different, Ingenuity Pathway Analysis software was used (IPA; Ingenuity Systems Inc., Redwood City, CA).

Western Blotting

Leukemic cells were lysed in lysis buffer supplemented with freshly added protease and phosphatase inhibitors. 25µg (BCA method; Thermo Scientific) lysate was loaded on 10% mini protean precast gels (BioRad, Veenendaal, Netherlands), and transferred to a nitrocellulose membrane (Biorad). Primary antibody incubation was performed according to manufacturer's protocol. Anti-pAKT^{Ser473} and anti-αTubulin (#2144) were obtained from Cell Signaling Technology (Danvers, Massachusetts, USA). Anti-STAP1 (H00026228-M01) was obtained from Abnova (Aachen, Germany) and anti-β-actin (ab6276) was obtained from Abcam (Cambridge, UK). Blots were stained with secondary antibodies (IRDye 680RD- or 800CW-labelled anti-rabbit and IRDye 680RD- or 800CW-labelled anti-mouse; Li-Cor Biosciences, Leusden, Netherlands) and scanned using the Odyssey infrared imaging system (Li-Cor Biosciences).

Ex vivo drug resistance

Ex vivo cytotoxicity of prednisolone, vincristine, L-asparaginase, daunorubicin, 6-mercaptopurine, and 6-thiguanine in primary samples was evaluated using 3-(4,5-dimethylthiazolyl-2)-2,5-diphenyltetrazolium bromide (MTT). Cells were exposed to increasing concentrations of chemotherapeutic agents (prednisolone: 0.008 to 250 µg/mL; vincristine: 0.05 to 50 µg/mL; L asparaginase: 0.003 to 10 IU/mL; daunorubicin: 0.002 to 2 µg/ml, 6-mercaptopurine: 0.015625 to 0.5 µg/ml, and 6-thioguanine: 0.001625 to 0.0.05 µg/ml) at 37°C and 5% CO_2. After four days of culture, the percentage of leukemic cells in control wells without chemotherapeutic agents was determined. Moreover, the optical density values of all wells was measured using a spectrophotometer after 6 hours of incubation with MTT. Samples were included if control wells harbored more than 70% leukemic cells and an optical density higher than 0.050 arbitrary units (adjusted for blank values). The concentration of drug lethal to 50% of the cells (LC50) was calculated. LC50 values were compared using the Mann-Whitney U test. *In vitro* cytotoxicity of prednisolone, ibrutinib and rapamycin in cell lines was evaluated using 3-(4,5-dimethylthiazolyl-2)-5-(3-carboxymethoxyphenyl)-2-(4-sulfophenyl)-2H-tetrazolium; MTS) and phenazine methosulfate (PMS). Cells were exposed to a dilution series of agents (prednisolone: 0.06 to 250 µg/mL; ibrutinib: 0.16 to 40 µM; rapamycin: 4 nM to 40 µM) in a 96 wells plate for four days at 37°C and 5% CO_2, after which viability was quantified as described above.

Multiplex Ligation-Dependent Probe Amplification (MLPA)

To identify genomic lesions in *IKZF1*, *CDKN2A*, *CDKN2B*, *ETV6*, *PAX5*, *RB1*, *BTG1*, *EBF1*, and PAR1 (*CSF2RA/IL3RA/CRLF2*), the SALSA P335 ALL-IKZF1 (a3) and the SALSA P202 Multiplex Ligation-dependent Probe Amplification (MLPA) assays (MRC-Holland, Amsterdam, Netherlands) were used as described previously.[1-3] Briefly, to generate DNA fragments with incorporated FAM nucleotides, 125 ng gDNA was used according to the manufacturer's protocol. Amplified fragments were quantified using an ABI-3130 genetic analyzer (Applied Biosystems, Carlsbad, CA). Manufacturer's control probes and a synthetic control reference, generated from five normal DNA samples in the same MLPA run, were used to normalize peak intensities (peak ratio < 0.75 for deletions, 0.75 ≤ peak ratio ≤ 1.3 for normal copy number, peak ratio > 1.3 for gain). Loss of either *CDKN2A* or *CDKN2B* was coded as *CDKN2A/B* deletion and intragenic amplifications of *PAX5* were coded as deletions.

SNP arrays

Genome-wide human SNP arrays 6.0 (Affymetrix) were performed to determine copy number and SNP genotype status according to the manufacturer's protocol. Raw probe values were extracted from CEL files and processed with the R package aroma.affymetrix version 3.1.0. This package contains a method to prepare the raw data for analysis using the CRMA v2 method. Arrays were processed individually to reduce the effects of probe crosstalk, nucleotide-position probe sequence and fragment-length. In addition, probe summarization, including copy number values from the SNP probesets, were acquired. Samples were compared to a reference values, which was the average of 53 diploid BCP-ALL and T-ALL samples. Copy number arrays can contain a very large bias between probes caused by differences in GC content of DNA fragments. This bias is likely introduced by the many amplification steps used in the protocols for the arrays. We corrected for this bias using the R package ArrayTV version 1.12.0. To compare the logR values of the copy numbers between samples a centralization step was performed, using the R package CGHnormaliter version 1.28.0. Data were called using CGHcall version 2.36.0 default settings (-2 for double loss, -1 for loss, 0 for diploid, 1 for gain and 2 for amplification) in R version 3.3.3.

To determine the specificity and sensitivity of these SNP arrays, data were compared to array-CGH and MLPA data. The methods is excellent to call large copy number changes (larger than 1Kb, if many probes are present). However, it is difficult to see deletion of a single exon even in a large exon.

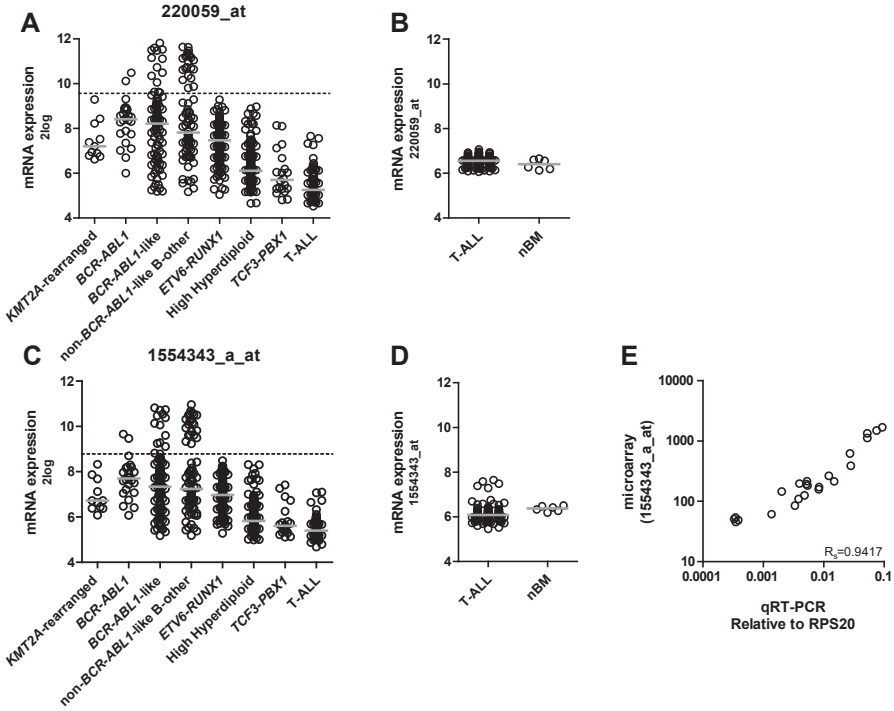

F

Ingenuity canonical pathways	Overlapping genes	P-value
EIF2 Signaling	66.5% (129/194)	2.18E-21
mTor Signaling	58.8% (117/199)	1.08E-13
Regulation of eIF4 and p70S6K Signaling	59.9% (94/157)	6.50E-12
B Cell Receptor Signaling	54.6% (101/185)	1.68E-09
AMPK Signaling	52.4% (99/189)	4.10E-08

Supplemental Figure 1. Discriminative expression of STAP1 in *BCR-ABL1*-like and B-other cases

(A-B) ^{2}log expression levels of Affymetrix probeset 220059_at in 572 BCP-ALL and 80 T-cell ALL (T ALL) cases. The dotted line represents the 80th percentile of *BCR-ABL1*-like and B-other cases (**A**). Expression levels of nBM (n=6) samples were determined in another microarray batch, in which also T ALL samples (n=105) were present (**B**). Grey lines represent the median expression values. (**C-E**) ^{2}log expression levels of Affymetrix probeset 1554343_a_at in 654 BCP-ALL cases. The dotted line represents the 80th percentile of *BCR-ABL1*-like and B-other cases (**C**). Expression levels of nBM samples were determined in another microarray batch, in which also T-ALL samples were present (**D**). Grey lines represent the median expression values. Microarray expression levels were validated using qRT-PCR. Correlation between microarray values of probeset 1554343_a_at and qRT-PCR values is depicted by the spearman coefficient of correlation (**E**). (**F**) Ingenuity pathway analysis software (Qiagen) was used to identify differentially regulated pathways between *STAP1*-high and *STAP1*-low *BCR-ABL1*-like and B-other cases was performed. Limma was applied to unravel different expressed probeset. Adjusted p-values below 0.05 were used to perform analysis.

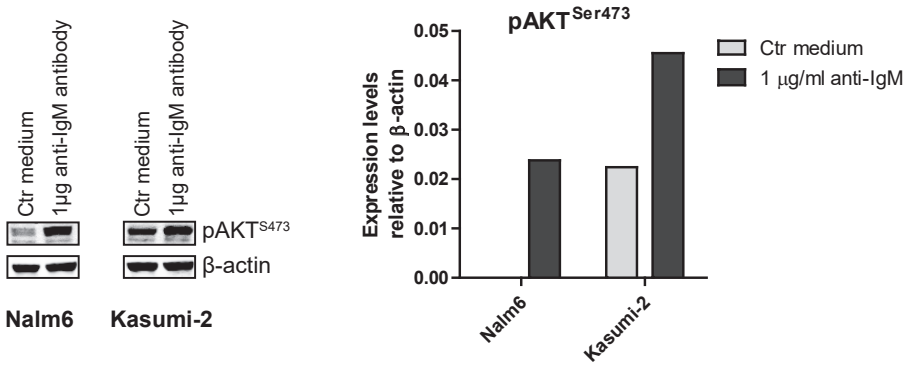

Supplemental Figure 2. Stimulation of pre-BCR signaling

Nalm6 and Kasumi-2 cells were stimulated for 1 hour with 1 µg/ml anti-IgM. Phosphorylation levels of $pAKT^{Ser473}$ were detected using western blotting, to confirm the stimulatory effect of the anti-IgM antibody. Expression levels relative to β-actin are depicted.

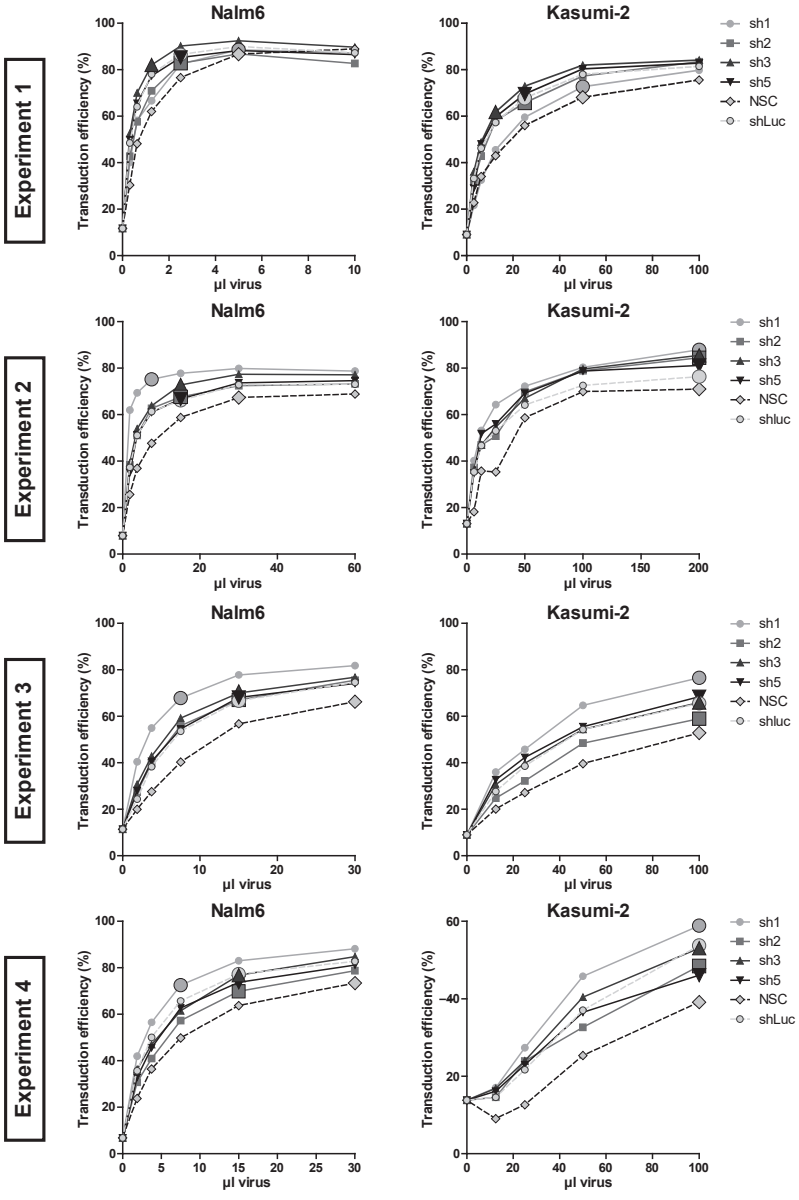

Supplemental Figure 3. Virus titration to determine the amount of virus required to infect 80% of cells.

Nalm6 and Kasumi-2 cells were exposed to indicated dilution series of virus. Cells were transduced via spin-infection. Puromycin selection (1 µg/ml) was initiated 24 hours after infection. After 48 hours of selection, cell viability was assessed using flow cytometry. PI staining was used to discriminate viable from dead cells. Transduction efficacy was calculated: (%viability of transduced cells)/(%viability of non-transduced cells)*100%. Obtained values of four independent experiments are depicted in graphs. The virus amounts used for subsequent experiments are indicated by enlarged symbols.

A

	Clone ID	Target sequence	Target region
shRNA-1	TRCN0000065083	CCAAGAATCAAGCACTACAAA	Exon 7
shRNA-2	TRCN0000065084	GCTCTACCTTTGTACTTTGAA	Exon 1
shRNA-3	TRCN0000065085	GCCTGGTAGTGACAGTAGAAA	Exon 6
shRNA-4	TRCN0000065087	CCTGTAACACTCCCAAACCTT	Exon 7/8

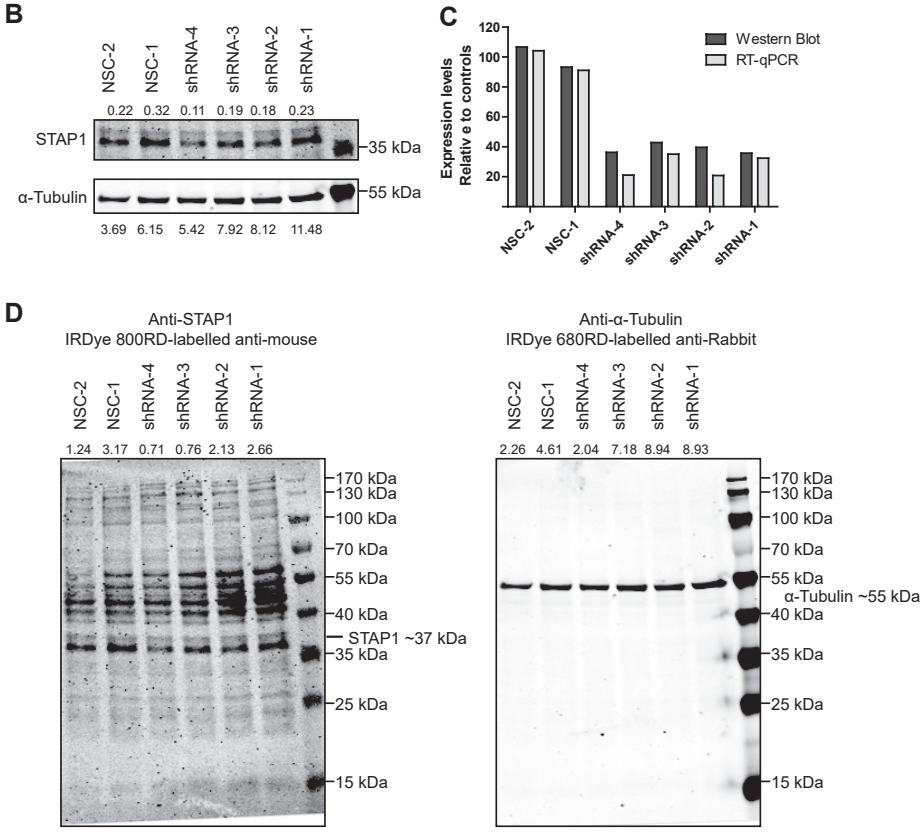

Supplemental Figure 4. Silencing of STAP1 in BCP-ALL cell lines.
Nalm6 and Kasumi-2 cells were transduced via spin-infection with shRNAs targeting STAP1 or scrambled control vectors. (**A**) Target sequences and regions of the shRNAs are depicted in the Table. (**B**) Western blot analysis of 15µg lysate of Nalm6 samples, which was collected 3 days after transduction. The blot was probed overnight with anti-STAP1 (mouse) and anti-αTubulin (rabbit). Protein expression was visualized using secondary antibodies (IRDye 680RD-labelled anti-rabbit and IRDye 800CW-labelled anti-mouse) and scanned using the Odyssey infrared imaging system (Li-Cor Biosciences). The cropped blot is shown, and the full length blot is depicted in panel d. Quantified expression levels are depicted above band. (**C**) Knockdown efficacy of the different shRNAs determined on protein level (western blot) and mRNA level (RT-qPCR), 3 days after transduction. Expression levels of STAP1 were normalized towards house-keeping genes (α-Tubulin and RPS20). Relative expression values towards the two scrambled controls are depicted. (**D**) Full western blot image of cropped image that are depicted in panel b.

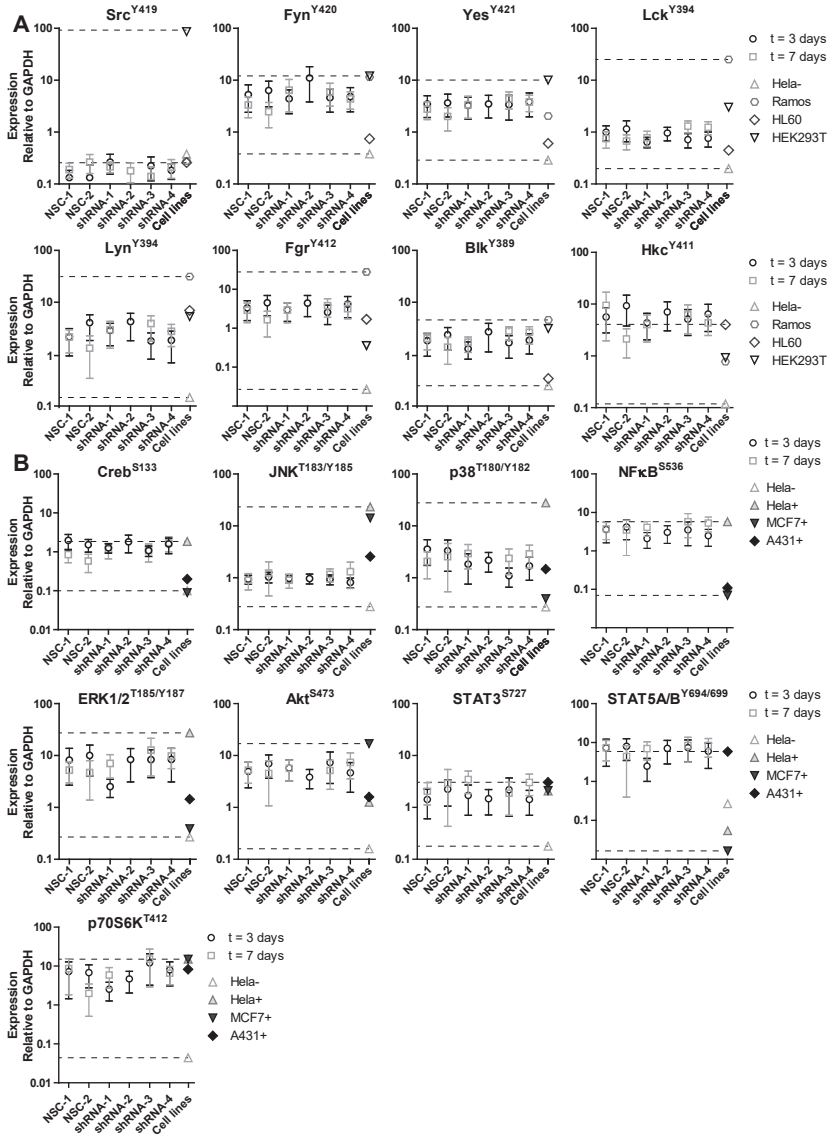

Supplemental Figure 5. Fluorescent bead-based immunoassay.

Expression of 17 proteins was determined using a fluorescent bead-based immunoassay in Nalm6 cells after knockdown of *STAP1*. Fluorescent intensity values relative to GAPDH are depicted. Expression was measured three and seven days after transduction. At day 7, not enough material was available of Nalm6 cells, which were transduced with shRNA-2. Values represent mean±SEM of four independent experiments at three days after transduction and three independent experiments at seven days after transduction. In addition, positive and negative cell line samples were included to validate the assay and antibodies. For the 8-plex human Src family kinase kit control samples included Hela-unstimulated lysate, Ramos-Pervanadate lysate, HL60- Pervanadate lysate, and HEK293 serum. For the multi-pathway magnetic bead 9-plex control samples included HeLa-unstimulated lysate, HeLa-TNFα/ Calyculin lysate, A431-EGF lysate, MCF7-IGF1 lysate.

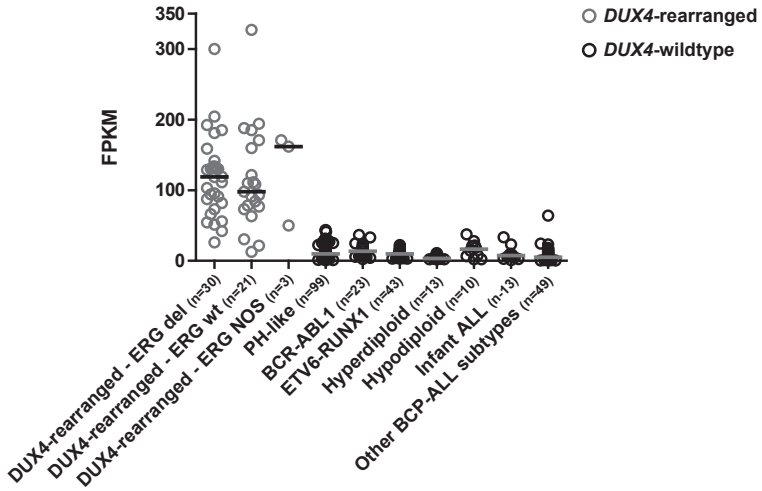

Supplemental Figure 6. *STAP1* expression and *DUX4*-rearrangemets.
STAP1 expression levels in 304 BCP-ALL cases, obtained ProteinPaint.[4,5] Fragments Per Kilobase per Million mapped (FPKM) expression values are depicted on the y-axis. Lines represent the median expression values. NOS = not other specified.

4

SUPPLEMENTAL REFERENCES

1. van der Veer, A. et al. Independent prognostic value of BCR-ABL1-like signature and IKZF1 deletion, but not high CRLF2 expression, in children with B-cell precursor ALL. Blood 122, 2622-2629, doi:blood-2012-10-462358 [pii] 10.1182/blood-2012-10-462358 (2013).
2. Boer, J. M. et al. Tyrosine kinase fusion genes in pediatric BCR-ABL1-like acute lymphoblastic leukemia. Oncotarget 8, 4618-4628, doi:10.18632/oncotarget.13492 (2017).
3. Boer, J. M. et al. Expression profiling of adult acute lymphoblastic leukemia identifies a BCR-ABL1-like subgroup characterized by high non-response and relapse rates. Haematologica 100, e261-264, doi:10.3324/haematol.2014.117424 (2015).
4. Zhou, X. et al. Exploring genomic alteration in pediatric cancer using ProteinPaint. Nat Genet 48, 4-6, doi:10.1038/ng.3466 (2016).
5. Zhang, J. et al. Deregulation of DUX4 and ERG in acute lymphoblastic leukemia. Nat Genet 48, 1481-1489, doi:10.1038/ng.3691 (2016).

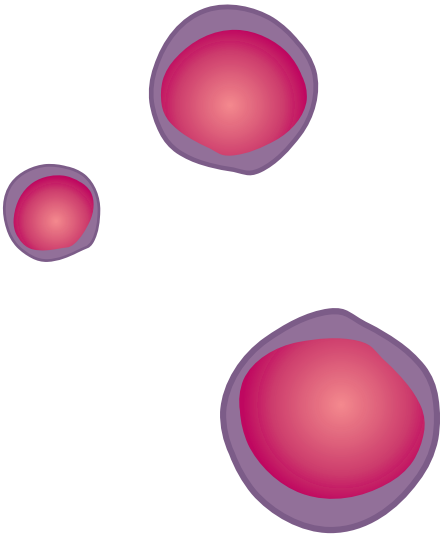

Chapter 5

CNAs IN B-CELL DEVELOPMENT GENES, CLINICAL OUTCOME, AND DRUG RESISTANCE IN PEDIATRIC BCP-ALL

Elisabeth M.P. Steeghs, Judith M. Boer, Alex Q. Hoogkamer, Aurélie Boeree, Valerie de Haas, Hester A. de Groot-Kruseman, Martin A. Horstmann, Gabriele Escherich, Rob Pieters, and Monique L. den Boer

Submitted

ABSTRACT

Pediatric B-cell precursor acute lymphoblastic leukemia (BCP-ALL) is associated with a high frequency of copy number alterations (CNAs), mostly deletions, in genes involved in B-cell development, cell cycle, and cytokine receptors (henceforth: B-cell development genes). We performed an explorative study to gain insight in the association between CNAs in these B-cell development genes, clinical outcome parameters, and cellular drug resistance.

CNAs in *IKZF1*, EBF1, *PAX5*, *CDKN2A/B*, *RB1*, *BTG1*, *ETV6*, and/or the PAR1 region were detected in 71% of newly diagnosed pediatric BCP-ALL cases. The distribution and clinical relevance of the CNAs in these eight genes was highly subtype-dependent. In the DCOG-ALL10 cohort, only loss of *IKZF1* associated as single marker with unfavorable outcome parameters and cellular drug resistance. Deletion of *IKZF1* was connected to high minimal residual disease (MRD) levels after induction therapy, an unfavorable long-term prognosis, and *ex vivo* resistance to prednisolone and thiopurines. This cellular drug resistance depended on the genetic subtype of the BCP-ALL cells: extreme prednisolone resistance (~1500-fold) was observed in primary *IKZF1*-deleted high hyperdiploid cells, while thiopurine resistance (~1.7-fold) was predominantly detected in primary *BCR-ABL1*-like and non-*BCR-ABL1*-like B-other *IKZF1*-deleted cells. These results indicate that the biological consequence of CNAs in B-cell development genes depends on the concomitant oncogenic driving lesion present in leukemic cells. Therefore, the genetic context in which lesions occur should be taken into account for risk stratification of patients with BCP-ALL and functional studies focusing on potential causes of cellular drug resistance.

INTRODUCTION

Acute lymphoblastic leukemia (ALL) is the most common cancer diagnosed in children. The introduction of risk-adjusted treatment protocols has significantly improved survival rates, which nowadays is approaching 90% survival.[1-3] Outcome of B-cell precursor ALL (BCP-ALL) differs by genetic subtype, i.e. *ETV6-RUNX1*, high hyperdiploid, and *TCF3-PBX1* cases have favorable prognosis, whereas *BCR-ABL1*, and *KMT2A*-rearranged BCP-ALL is associated with an unfavorable treatment outcome.[3] Approximately 25% of the patients has a genetically unclassified disease, which is defined as 'B-other'. This heterogeneous group can be subdivided in *BCR-ABL1*-like patients and non-*BCR-ABL1*-like B-other patients.[4,5] Within the *BCR-ABL1*-like subtype intrachromosomal amplification of chromosome 21, dicentric chromosome (9;20), and kinase activating lesions are reported.[4-9] In non *BCR-ABL1*-like B-other cases chromosomal translocations involving *DUX4*, *ZNF384*, and *MEF2D* were identified.[10-12] In addition to the major classifying abnormalities, secondary aberrations have been observed, including copy number alterations (CNAs) in genes involved in B-cell development (e.g. *IKZF1*, *EBF1*, *PAX5*, ETV6), cell cycle and proliferation (e.g. *CDKN2A/B*, *RB1*, *BTG1*), and cytokine receptors (e.g. *CRLF2*).[4, 5, 8, 9, 13-16] Interestingly, some of these genetic lesions (e.g. *IKZF1*) were shown to predict clinical outcome.[5, 14, 17] The Dutch Childhood Oncology Group (DCOG) implemented *IKZF1* status as risk factor in the ongoing DCOG-ALL11 protocol. In addition, risk stratification strategies were designed by integration of CNA profiles and genetic subtypes.[18, 19]

Cellular drug resistance is an important cause of relapse. *Ex vivo* drug resistance at diagnosis is associated with high risk of early treatment failures.[20-22] In addition, BCP-ALL cells at relapse are more resistant towards glucocorticoids, L-asparaginase, anthracyclines, and thiopurines.[23] *IKZF1* deletions are reported to mediate resistance towards glucocorticoids, but the relationship between remaining CNAs and cellular drug resistance is yet unknown.[24-26] Therefore, we performed an explorative study, which aimed to gain insight in associations between CNAs, cellular drug resistance and clinical outcome.

METHODS

Processing of primary patient material

Bone marrow and/or peripheral blood samples were obtained from children (1-18 years) with newly diagnosed ALL. Written informed consent was obtained from parents or guardians to use excess of diagnostic material for research purposes, as approved by the institutional review board. These studies were conducted in accordance with the Declaration of Helsinki. Mononuclear cells were isolated using Lymphoprep gradient separation and the leukemic blast percentage was determined microscopically by May-Grünwald Giemsa stained cytospin preparations, as described previously.[20] Samples were enriched to over 90% purity of leukemic cells by depletion of non-leukemic cells using immunomagnetic beads. Primary leukemic cells were maintained in RPMI-1640 Dutch modification supplemented with 20% fetal calf serum (Integro), with 0.1% insulin-transferrin-sodium selenite (Sigma), 0.4 mM glutamine (Invitrogen), 0.25 µg/ml gentamycine (Gibco), 100 IU/ml penicillin (Gibco), 100 µg/ml streptomycin (Gibco), 0.125 µg/ml fungizone (Gibco).

The major cytogenetic subtypes, i.e. high hyperdiploid (>50 chromosomes), *ETV6-RUNX1*, *TCF3-PBX1*, *KMT2A*-rearranged, *BCR-ABL1*, *BCR-ABL1*-like and B-other (negative for all before mentioned genomic lesions), were determined using fluorescent in situ hybridization and (RT-)PCR. The 110-probeset gene expression classifier was used to identify *BCR-ABL1*-like cases.[4] Patients were treated according to the Dutch Childhood Oncology Group (DCOG)-ALL8, -ALL9, -ALL10 or -EsPhALL protocol, or the COALL-06-97 and COALL-07-03 study protocols.[3, 27-29] Patient characteristics were provided by the central study centers of DCOG, The Hague, the Netherlands and COALL, Hamburg, Germany.

Multiplex Ligation-Dependent Probe Amplification

To identify genomic lesions in *IKZF1*, *CDKN2A*, *CDKN2B*, *ETV6*, *PAX5*, *RB1*, *BTG1*, *EBF1* and PAR1 (CSF2RA/IL3RA/*CRLF2*), the SALSA P335 ALL-*IKZF1* (a3) and the SALSA P202 Multiplex Ligation-dependent Probe Amplification (MLPA) assays (MRC-Holland, Amsterdam, Netherlands) were used as described previously.[14] In short, DNA fragments with incorporated FAM nucleotides were generated using 125 ng of genomic DNA, according to the manufacturer's protocol. To quantify the amplified fragments, an ABI-3130 genetic analyzer (Applied Biosystems, Carlsbad, CA) was used. The manufacturer's control probes were used to normalize peak intensities, as well as a synthetic control reference generated from five normal DNA samples in the same MLPA run (normal copy number = 0.75 ≤ peak ratio ≤ 2.0; deletions = peak ratio < 0.75; gain = peak ratio > 2.0). A deletion was defined by a peak ratio below 0.75 for at least one MLPA-probe per gene. *CDKN2A/B* deletions included loss of either *CDKN2A* or *CDKN2B*. The effect of intragenic amplifications and/or deletions in *PAX5* were analyzed within one group, as they were predicted to be functionally equivalent.[18, 30] Loss of the PAR1 region was defined by deletion of both *IL3RA* and *CSF2RA* probes while expression of the *CRLF2* and *SHOX* AREA probes was maintained. MLPA analyses were performed in 515 BCP-ALL cases, representing the major genetic subtypes in childhood ALL, i.e. 3.9% (20/515) *BCR-ABL1*, 17.3% (89/515) *BCR-ABL1*-like, 20.2% (104/515) non-*BCR-ABL1*-like B-other, 28.7% (148/515) *ETV6-RUNX1*, 24.5% (126/515) high hyperdiploid, 1.6% (8/515) *KMT2A*-rearranged, 3.9% (20/515) *TCF3-PBX1*.

Clinical characteristics and statistics

To identify whether CNAs were underrepresented or enriched in a subtype, the Fisher's exact test was applied using R software (version 3.2.1). Obtained odds ratios (ORs), 95% confidence interval, and p-values are reported. The Fisher's exact test was also applied to compare minimal residual disease (MRD) levels after induction and first consolidation therapy between patients groups with CNAs and wildtype patients. Cumulative incidence of relapse (CIR) was estimated using a competing risk model and significance was determined using the Gray's test. Relapse and non-response (counted as event at day 79) were considered as event, with death as competing event. Event-free survival (EFS) probabilities were estimated using cox regression and compared using the Wald test. Relapse, non-response, secondary malignancies and death were counted as events. Outcome analyses were performed in R (version 3.2.1), using the packages cmprsk version 2.2-7[44], mstate version 0.2.7[45], and survival version 2.38-4[46]. Five-year EFS and CIR are reported. A multivariate Cox proportional hazard analysis was performed in SPSS version

22 to determine the independent prognostic value of risk factors. The DCOG-ALL10 trial is the most recently completed nationwide trial in which patients were risk-stratified by minimal residual disease (MRD) levels and for whom sufficient long-term follow-up data were available. Therefore, we restricted the analysis of associations between CNA and clinical response parameters (MRD, clinical outcome) to this cohort. In addition, the genetic subtypes are represented with a distribution that is comparable to the general pediatric BCP-ALL population (excluding *BCR-ABL1*-positive cases since these patients are eligible for the EsPhALL protocol), i.e.12.2% *BCR-ABL1*-like, 13.9% non-*BCR-ABL1*-like B-other, 33.5% *ETV6-RUNX1*, 32.7% high hyperdiploid, 2.0% *KMT2A*-rearranged, and 5.7% *TCF3-PBX1* positive cases.

Ex vivo drug resistance assays

Ex vivo cytotoxicity of prednisolone, vincristine, L-asparaginase, daunorubicin, 6-mercaptopurine and 6-thioguanine was evaluated using 3-(4,5-dimethylthiazolyl-2)-2,5-diphenyltetrazolium bromide (MTT), as previously described.[20] In brief, cells were exposed to a concentration range of chemotherapeutics (prednisolone: 0.008 to 250 µg/mL; vincristine: 0.05 to 50 µg/mL; L-asparaginase: 0.003 to 10 IU/mL; daunorubicin: 0.002 to 2 µg/ml; 6-mercaptopurine: 15.6 to 500 µg/ml; and 6-thioguanine: 1.56 to 500 µg/ml) in a 96 wells plates for four days at 37°C and 5% CO_2. After four days of culture, samples were included if control wells harbored more than 70% leukemic cells and an optical density higher than 0.050 arbitrary units (adjusted for blank values). The concentration of drug lethal to 50% of the cells (LC50) was calculated. LC50-values were compared by the Mann-Whitney U test and adjusted for tied ranks if applicable.

RESULTS

A pediatric BCP-ALL cohort of 515 newly diagnosed cases, representing all major ALL subtypes, was screened for CNAs in eight genes involved in transcription of lymphoid genes and the differentiation and proliferation of precursor B-cells (henceforth: B-cell development genes). In total, 71% of the pediatric BCP-ALL cases harbored one or more CNAs in these B-cell development genes (Figure 1). The CNA frequency differed between genetic BCP-ALL subtypes. The percentage of CNAs was the highest in *BCR-ABL1*-like cases and the lowest in *TCF3-PBX1* cases (Supplementary Figure 1A).

CNAs in B-cell transcription factors

IKZF1

Deletions of the transcription factor *IKZF1* were detected in 20% of the BCP-ALL cases. This frequency differed between subtypes: *IKZF1* deletions were enriched in *BCR-ABL1* (65%) and *BCR-ABL1*-like (44%) cases, whereas deletions were low or absent in *ETV6-RUNX1* (3%) and *TCF3-PBX1* (0%), respectively (Figure 1A; Supplementary Figure 1B). In addition, 76% (78/102) of the cases with an *IKZF1* deletion harbored CNAs in additional genes, which mainly involved *PAX5* and *CDKN2A/B* (Figure 2). This co-occurrence was subtype dependent: a strong association (OR>2, p<0.001) was observed in *BCR-ABL1*, *BCR-ABL1*-like and B-other cases, whereas in high hyperdiploid cases *IKZF1* deletions mainly occurred independent of CNAs in *PAX5* and/or *CDKN2A/B*.

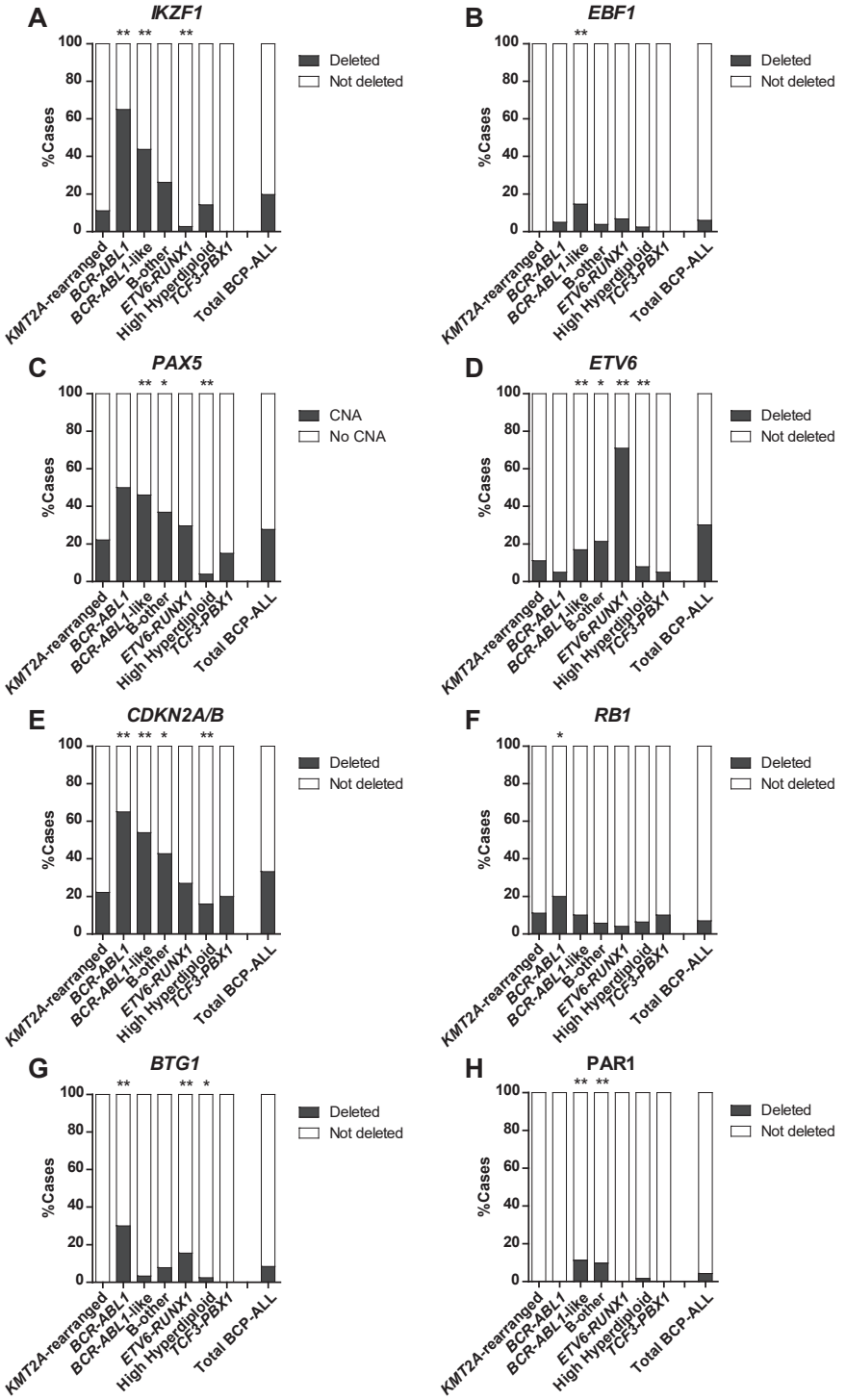
A
IKZF1
B
EBF1
C
PAX5
D
ETV6
E
CDKN2A/B
F
RB1
G
BTG1
H
PAR1
%Cases
Deleted
Not deleted
CNA
No CNA
KMT2A-rearranged
BCR-ABL1
BCR-ABL1-like
B-other
ETV6-RUNX1
High Hyperdiploid
TCF3-PBX1
Total BCP-ALL

IKZF1-deleted cases more often showed high MRD levels ($\geq 10^{-3}$) after induction therapy (TP1; p=0.013), and intermediate MRD levels ($10^{-4} \leq$ MRD $< 10^{-3}$) after the first consolidation course (TP2; p=0.028), compared to *IKZF1*-wildtype cases (Figure 3A). This association could be predominantly attributed to high MRD levels in *BCR-ABL1*-like and B-other cases, but was not observed in high hyperdiploid or *ETV6-RUNX1* cases (Supplementary Figure 3). In addition, *IKZF1*-deleted cases more often suffered from a non-response or relapse compared to *IKZF1*-wildtype cases (5-year CIR: 30.4% versus 9.0%; p<0.001; Figure 4A-B), confirming previous findings.[5, 14, 17] An *IKZF1* deletion was an independent risk factor in a multivariate Cox proportional hazard model, including prednisolone response at day 8 of treatment and MRD levels after induction and first consolidation course (Supplementary Table 1). In addition, *IKZF1* remained a predictor of a poor outcome in the medium risk (MR) treatment group of the DCOG-ALL10 cohort (Figure 4B). These observations indicate that the poor long-term clinical outcome of *IKZF1*-deleted cases is not caused by the association of *IKZF1* with current risk stratification factors based upon early treatment response.

As cellular drug resistance might underlie this poor outcome, we examined the *ex vivo* efficacy of chemotherapeutic agents that are commonly used during induction and consolidation therapy. Primary BCP-ALL cells harboring *IKZF1* deletions were more resistant to prednisolone and thiopurines compared to *IKZF1* wildtype cells (p<0.05; Figure 5A-B). Resistance against these agents was subtype dependent, as visualized in Figure 5B: prednisolone resistance was predominantly observed in high hyperdiploid cells (~1500-fold, p=0.009), whereas thiopurine resistance (6-thioguanine (1.6 fold, p=0.011) and 6-mercaptopurine (1.7 fold, p<0.001)) was mainly identified in *IKZF1*-deleted *BCR-ABL1*-like and B-other cells (Figure 5B). Moreover, in high hyperdiploid cells deletion of *IKZF1* was predictive for L-asparaginase resistance (Supplementary Figure 7A).

EBF1

The transcription factor *EBF1* was deleted in a minority (6%) of the BCP-ALL cases (Figure 1B). Deletions were enriched in *BCR-ABL1*-like cases (15%), but absent in *KMT2A*-rearranged and *TCF3-PBX1* cases (Figure 1B). Cases that harbored an *EBF1* deletion showed a trend towards higher MRD levels after induction therapy compared to non-*EBF1* deleted cases (OR=5.16, p=0.057; Figure 3B). However, power was low to study the association with cellular drug resistance, as drug resistance data were only available for six *EBF1*-deleted cases.

Figure 1. CNA landscape of B-cell development genes in the different subtypes of pediatric BCP-ALL.

CNA profile of 515 newly diagnosed pediatric BCP-ALL patients, representing all major BCP-ALL subtypes, was determined using MLPA. Association between CNAs and subtypes was studied using the Fisher Exact test. The frequency of specific CNAs per subtype is shown. CNAs tested included *IKZF1* (**A**), *EBF1* (**B**), *PAX5* (**C**), *ETV6* (**D**), *CDKN2A/B* (**E**), *RB1* (**F**), *BTG1* (**G**), PAR1 (**H**).

**p≤0.01, *p≤0.05. del = deletion

PAX5

CNAs of the transcription factor *PAX5* were observed in 28% of the BCP-ALL cases (Figure 1C). CNAs were detected throughout all BCP-ALL subtypes, although the frequency was relatively high in *BCR-ABL1* (50%) and *BCR-ABL1*-like (46%) cases (Figure 1C). The strong co-occurrence of *PAX5* and *CDKN2A/B* CNAs (Figure 2, OR=6.36, p<0.001) is likely caused by the high frequency of chromosome 9p deletions observed in these cases[31]; the chromosome arm on which *PAX5* and *CDKN2A/B* are located. Despite of the strong association between *PAX5* CNAs and *IKZF1* deletions (Figure 2, OR=2.94, p<0.001), CNAs in *PAX5* were not predictive for high MRD levels (Figure 3C) nor a poor prognosis in pediatric BCP-ALL cases (Figure 4A). Strikingly, leukemic cells harboring CNAs in *PAX5* showed an increased sensitivity (~5.1 fold, p=0.008) to prednisolone compared to *PAX5*-wildtype cells (Figure 5C). This difference in sensitivity was only significant (p=0.031) in *ETV6-RUNX1* cases, but a similar pattern was also observed in the remaining BCP-ALL subtypes (Figure 5C). Interestingly, this association depended on the *IKZF1* status: cells with both an *IKZF1* deletion and a CNA in *PAX5* were equally sensitive to prednisolone as *IKZF1* and *PAX5* wildtype cells, whereas cells with only an *IKZF1* deletion were more resistant to prednisolone (Supplementary Figure 7B). These results suggest that CNAs in *PAX5* might compensate for prednisolone resistance induced by loss of *IKZF1*.

A

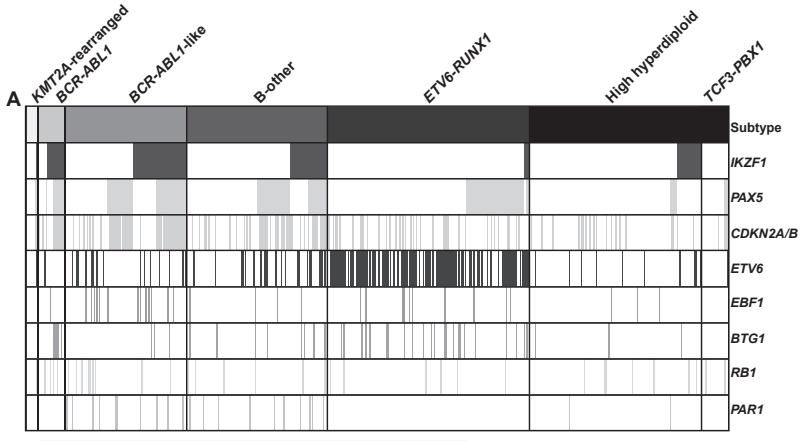

B

	Odds Ratio	P-value
IKZF1 + PAX5	2.94	<0.001
IKZF1 + CDKN2A/B	2.18	0.001
IKZF1 + BTG1	2.63	0.005
EBF1 + BTG1	5.38	<0.001
EBF1 + PAR1	3.82	0.0037
PAX5 + CDKN2A/B	6.36	<0.001
PAX5 + PAR1	2.73	0.026
BTG1 + ETV6	2.66	0.00

Figure 2. Co-occurence of CNAs in B-cell development genes in the different BCP-ALL subtypes. (**A**) Heatmap of CNA profile of 515 newly diagnosed pediatric BCP-ALL patients, representing the major BCP-ALL subtypes. CNAs are shown per subtype. Colors indicate presence of a CNA and absence of CNAs is shown in white. The heatmap is sorted on IKZF1 deletions followed by CNAs in PAX5. Each column represents an individual patient. (**B**) The co-occurrence between the different CNAs in all BCP-ALL cases was calculated using the Fisher Exact test. Odds ratios and p-values of significant associations are shown.

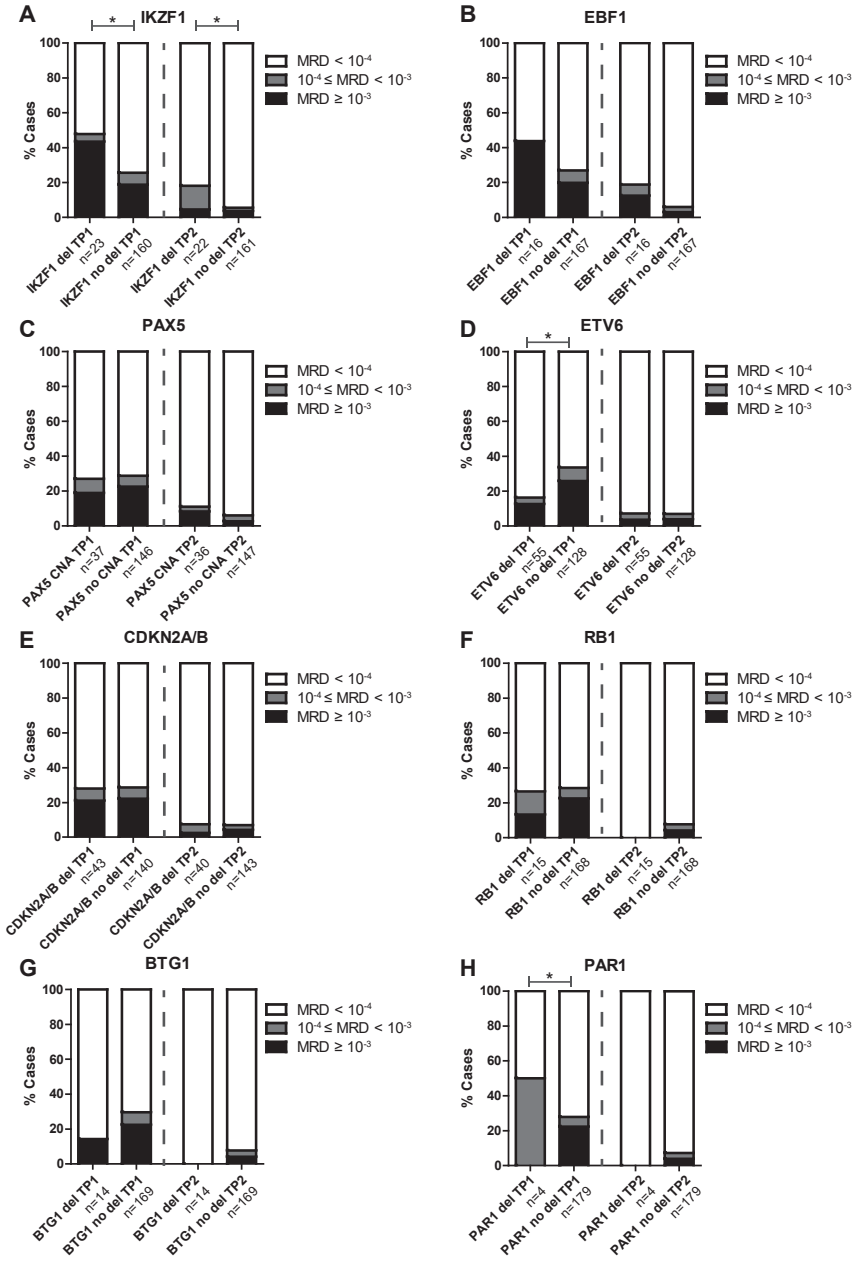

Figure 3. The association between CNAs and MRD levels after induction therapy and the first consolidation course in newly diagnosed BCP-ALL.

MRD levels of DCOG-ALL10 treated BCP-ALL cases (all risk groups) after induction (TP1; n=183) and first consolidation course (TP2; n=183). The percentage of cases with high ($\geq 10^{-3}$), medium ($10^{-4} \leq$ MRD $< 10^{-3}$), and undetectable MRD levels ($<10^{-4}$) is depicted per CNA. The Fisher's Exact test was applied to study associations between CNAs and MRD levels.

**p≤0.01, *p≤0.05. del = deletion.

A **The prognostic value of CNAs in the DCOG-ALL10 cohort (all risk groups)**

	Patients all risk groups (n)	CIR rate (SE)	P-value	EFS rate (SE)	P-value
IKZF1 no deletion	180	9.0 (2.3)	**< 0.001**	88.2 (2.5)	**0.001**
IKZF1 deletion	30	30.4 (9.9)		66.3 (9.8)	
EBF1 no deletion	192	11.9 (2.5)		85.5 (2.7)	
EBF1 deletion	18	11.5 (7.9)		83.0 (9.0)	
PAX5 no CNA	165	10.6 (2.6)		85.8 (2.8)	
PAX5 CNA	44	17.1 (6.1)		83.3 (6.0)	
ETV6 no deletion	151	12.1 (2.8)		83.8 (3.1)	
ETV6 deletion	59	11.1 (4.4)		88.9 (4.4)	
CDKN2A/B no deletion	160	10.4 (2.6)		87.1 (2.8)	
CDKN2A/B deletion	50	16.6 (5.5)		79.3 (5.9)	
RB1 no deletion	194	10.7 (2.4)	0.093	86.7 (2.6)	0.057
RB1 deletion	16	25.6 (11.5)		68.2 (11.8)	
BTG1 no deletion	193	11.9 (2.5)		85.6 (2.7)	
BTG1 deletion	17	11.8 (8.1)		82.4 (9.3)	
PAR1 no deletion	206	12.1 (2.4)		84.9 (2.6)	
PAR1 deletion	4	0.0 (0.0)		100 (0.0)	

B

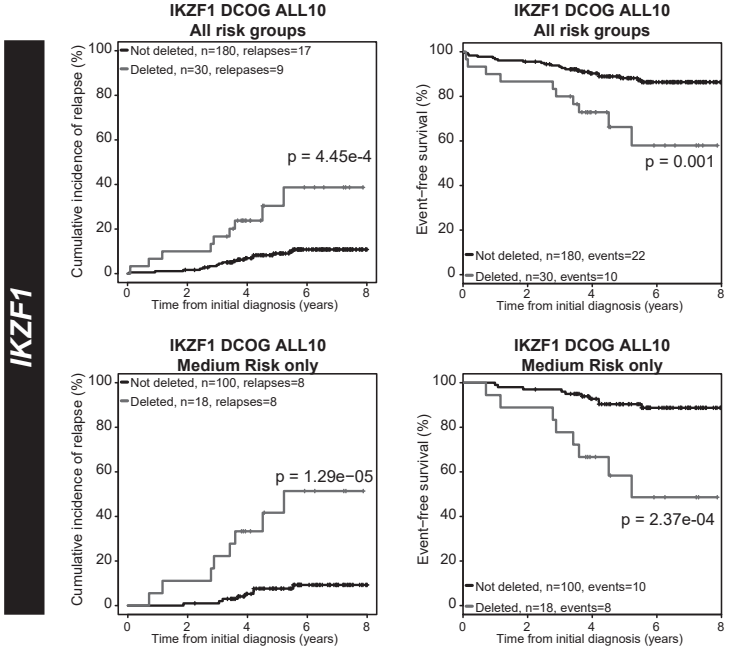

Figure 4. Prognostic value of CNAs in DCOG-ALL10 treated cases.
(A) The association between CNAs in all risk groups and cumulative incidence of relapse (CIR) and event free-survival (EFS) was examined. BCP-ALL patients (n=210) were treated according to DCOG-ALL10 protocol. CIR was estimated using a competing risk model. Relapse and non-response were considered as event, and death as competing event. To test equality of the CIRs, the Gray's test was applied. Non response, relapse, and death were considered as events for EFS. EFS rates were determined using Cox regression, and compared using the Wald test. For reliable test results, groups should contain at least 5 cases. **(B)** CIR and EFS curves of cases without or with an *IKZF1* deletion. Curves contain either all risk groups, or the medium risk arm only.

ETV6

Deletions of the transcription factor *ETV6* were detected in all BCP-ALL subtypes, but were especially enriched in *ETV6-RUNX1* cases (71%; Figure 1D). After induction therapy (TP1), *ETV6*-deleted cases more often showed low ($<10^{-4}$) MRD levels compared to *ETV6*-wildtype cases (Figure 3D; OR=2.6, p=0.02). However, this association was subtype dependent: in *BCR-ABL1*-like and B-other cases an adverse association between *ETV6* deletions and MRD levels was observed (Supplementary Figure 2). Prognosis of cases with loss of *ETV6* was not different compared to *ETV6*-wildtype cases (Figure 4). *ETV6*-deleted cells appeared to be more sensitive to prednisolone (~3.2 fold, p=0.046), and more resistant to vincristine (~1.8 fold, p<0.01) and daunorubicin (~1.9 fold, p=0.028). Remarkably, loss of the wildtype *ETV6* allele in *ETV6-RUNX1*-positve cells associated with a high sensitivity to vincristine instead of resistance (p=0.013, Figure 5D), suggesting that associations of vincristine resistance differ between genetic subtypes of ALL. Moreover, deletion of *ETV6* was associated with L-asparaginase resistance in high hyperdiploid cells and high 6-thioguanine sensitivity in *ETV6-RUNX1* cells (Supplementary Figure 7C).

CNAs in cell cycle and proliferation genes

CDKN2A/B

Deletions of the cell cycle regulators *CDKN2A* and/or *CDKN2B* were often observed (33%) in the pediatric BCP-ALL cohort (Figure 1E). Similar to *PAX5*, the deletions in *CDKN2A/B* were found in all BCP-ALL subtypes, but were especially enriched in *BCR-ABL1* (65%, OR=3.95, p=0.003), *BCR-ABL1*-like (54%, OR=2.88, p<0.001), and B-other cases (OR=1.67, p=0.026). No association with clinical outcome parameters or cellular drug resistance was observed (Figure 3-5).

RB1

The cell cycle regulator *RB1* was deleted in a minority (~7%) of the BCP-ALL cases (Figure 1F) and deletions were detected in all BCP-ALL subtypes. Within the DCOG-ALL10 cohort, *RB1*-deleted cases showed a trend towards a poor event free survival (5- year EFS: 68.2% versus 86.7%, p=0.057), which was caused by an unfavorable response in the medium risk (MR) treatment group (5-year EFS: 46.9% versus 88.3%, p=0.003; Supplementary Figure 6A). No association with MRD levels or cellular resistance to the tested drug panel was observed (Figure 5).

BTG1

The anti-proliferative gene *BTG1* was deleted in a minority (~8%) of the BCP-ALL cases. No deletions were detected in *KMT2A*-rearranged or *TCF3-PBX1* cases, whereas the highest frequency was observed in *BCR-ABL1* (30%) and *ETV6-RUNX1* (16%) cases (Figure 1G). Four out of five *BTG1*-deleted *BCR-ABL1*-like and B-other cases also harbored an *IKZF1* deletion. These four cases all experienced an event and only the patient with wildtype *IKZF1* remained in remission (Supplementary Figure 6B). This finding underlines an earlier report, in which a cooperative effect of *BTG1* and *IKZF1* lesions in leukemogenesis was observed.[26]

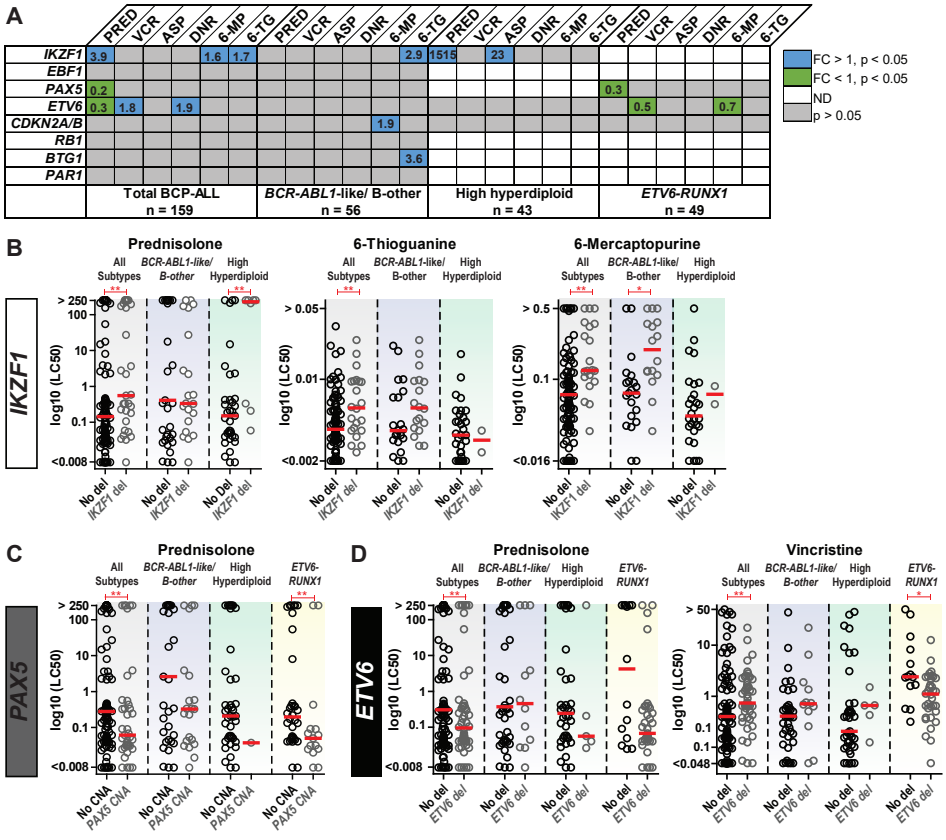

Figure 5. The association between CNAs and the *ex vivo* cellular drug response.

(A) Leukemic cells were incubated for four days with a concentration range of prednisolone (µg/ml), vincristine (µg/ml), L-asparaginase (IU/ml), daunorubicin (µg/ml), 6-mercaptopurine (µg/ml), and 6 thioguanine (µg/ml), after which cell viability was measured using an MTT assay. The Mann-Whitney U test was applied to compare LC50-values. No association is depicted in grey, resistance in blue ($p < 0.05$, fold induction (FI) > 1), sensitive in green ($p < 0.05$, FI < 1), and not determined in white. The number of cases that were tested for prednisolone is depicted, and represent the maximum number of cases. For reliable test results, groups should contain at least 5 cases. Results are depicted for all risk groups and for *BCR-ABL1*-like/ B-other cells, high hyperdiploid cells, and *ETV6-RUNX1* cells. **(B)** LC50 values for prednisolone (µg/ml), 6-thiogunanine (µg/ml), and 6-mercaptopurine (µg/ml) of cases without or with *IKZF1* deletion. Columns include all BCP-ALL subtypes (grey), *BCR-ABL1*-like/ B-other cells (blue), and high hyperdiploid cells (green). **(C)** LC50 values for prednisolone (µg/ml) of cases without or with *PAX5* CNAs. Columns include all BCP-ALL subtypes (grey), *BCR-ABL1*-like/ B-other cells (blue), high hyperdiploid cells (green), and *ETV6-RUNX1* cells (yellow). **(D)** LC50 values for prednisolone (µg/ml), vincristine (µg/ml), and daunorubicin (µg/ml) of primary leukemic cells without or with *ETV6* deletion. Columns include all BCP-ALL subtypes (grey), *BCR-ABL1*-like/ B-other cells (blue), high hyperdiploid cells (green), and *ETV6-RUNX1* cells (yellow).

* $p < 0.05$, ** $p < 0.01$; Mann-Whitney U test.

CNAs in cytokine receptors

PAR1

Deletions in the pseudoautosomal region 1 (PAR1) were the least prevalent (~4%) in this pediatric BCP-ALL cohort. CNAs in this region indicate presence of interstitial deletions or a translocation, which both induce overexpression of *CRLF2*.[32] Deletions of the PAR1 region were detected in *BCR-ABL1*-like (11%), B-other (10%), and high hyperdiploid cases (2%), but not in remaining BCP-ALL subtypes (Figure 1H). Unfortunately, power was lacking to reliable study the association between deletions in the PAR1 region, MRD levels, clinical prognosis, and cellular drug resistance.

Taken together, with the exception of loss of the *IKZF1* gene, none of the CNAs in the remaining B-cell development genes strongly associates with clinical outcome and cellular drug resistance as single marker. Our results show that the clinical value of CNAs in B-cell development genes is highly context dependent and differs between the diverse oncogenic drivers of pediatric BCP-ALL.

DISCUSSION

BCP-ALL cases harbor various genetic aberrations in genes involved in lymphoid maturation, cell cycle regulators, tumor suppressors, and tyrosine kinases. We performed an explorative study to gain insight in the association between CNAs in B-cell development genes, MRD levels, long-term prognosis, and cellular drug resistance. Interestingly, the distribution and clinical relevance of these CNAs was subtype-dependent. A high frequency of CNAs in these B-cell development genes was found in the poor prognostic subtypes *BCR-ABL1*, *BCR-ABL1*-like and B-other. Cooperative lesions may favor the aggressive phenotype of a leukemia, such as exemplified by the synergistic effect between loss of *IKZF1* and the *BCR-ABL1* fusion gene in leukemogenesis[33], and the antagonizing effect of *IKZF1* deletions in the response to imatinib.[34] In contrast, the prognosis of *ETV6-RUNX1*, *DUX4*-rearranged, and ERG-deleted BCP-ALL is probably not affected by *IKZF1* deletions, but numbers with *IKZF1* deletions in these subtypes are low.[11, 12, 15, 35, 36] These observations indicate that the genetic context influences the functional effect of CNAs in B-cell development genes. The importance of the genetic context is exemplified by the fact that isolated deletions of *BTG1* do not affect cellular drug resistance or the prognosis of BCP-ALL cases, whereas all four patients with concomitant loss of *BTG1* and *IKZF1* experienced an event. Moreover, combined loss *BTG1* and *IKZF1* was shown to enhance glucocorticoid resistance.[26] In contrast to *BTG1-IKZF1* synergy, we observed that CNAs in *PAX5* may counteract the effect of an *IKZF1* deletion on prednisolone resistance. Various combinations of cooperative lesions may therefore have different effects on the pathobiology of B cell precursor ALL cells.

In the present study we observed an association between deletion of *IKZF1* and prednisolone resistance, especially in high hyperdiploid cells. These results are in concordance with other studies, which indicate that there is a direct association between *IKZF1* and glucocorticoid-induced cell death.[24, 37] *IKZF1* functions as a metabolic gatekeeper and consequently loss of *IKZF1* results in increased intracellular ATP and glucose levels.[37] Interestingly, we previously observed a direct relation between an increased glycolytic rate and prednisolone resistance in primary BCP-ALL cells.[38, 39] In these leukemic cells, inhibition of glycolysis restored the efficacy of prednisolone.[39] Hence, inhibition of

glycolysis might also be a potential treatment strategy to re-sensitize *IKZF1*-deleted cells to prednisolone and should be explored in more detail in future studies, also in the context of *BTG1* and *PAX5* CNAs.

In contrast to high hyperdiploid cells, deletion of *IKZF1* did not affect prednisolone sensitivity in primary *BCR-ABL1*-like and B-other ALL cells, suggesting that additional factors (e.g. differentiation stage, oncogenic drivers) are important for the functional effect of a deletion of the *IKZF1* gene in these type of cells. Instead of prednisolone resistance, we observed thiopurines resistance in these *BCR-ABL1*-like and B-other ALL cells. Thiopurine resistance might be caused by deficiencies in the DNA mismatch repair system and indeed DNA repair genes were reported to be downregulated in *IKZF1*-deleted cells.[40, 41] Interestingly, this characteristic might offer opportunities to target these leukemic cells via the DNA mismatch repair apparatus, e.g. by PARP inhibitors. The mechanism of thiopurines resistance and the condition of the DNA mismatch apparatus in these leukemic cells therefore requires further investigation.

Besides *IKZF1*, deletion of *RB1* was predictive for a poor outcome in the MR-risk group of the DCOG ALL10 cohort. *RB1* deletions are known to be enriched in poor prognostic iAMP21 and hypodiploid cases, which might explain the unfavorable outcome of *RB1*-deleted cases.[13, 42, 43] However, the unfavorable outcome could not be explained by or cellular resistance against induction therapy drugs.

In conclusion, results obtained in the present study revealed that, with the exception of an *IKZF1* deletion, none of the remaining CNAs as single marker associated both with an unfavorable clinical prognosis and cellular drug resistance. Our results indicate that the biological and clinical importance of CNAs in B-cell development genes (and presumably also other genetic aberrations) is highly context dependent and differs between the diverse oncogenic drivers of pediatric BCP-ALL. Functional studies that focus on potential causes of cellular drug resistance should therefore take the oncogenic driver and additional genetic aberrations into account.

Acknowledgements

The authors thank all members of the Pediatric Oncology research laboratory of the Erasmus MC for their help in processing leukemic cell samples and performing *ex vivo* cytotoxicity assays. In addition, we would like to thank Arian van der Veer for performing the MLPA experiments.

This work was supported by the VICI program grant 016.126.612 from Netherlands Organisation for Scientific Research (NWO), the Dutch Cancer Society grants AMC 2008-4265 and EMCR 2014-6998, the Kika Foundation (grant 132 and 161) and the Pediatric Oncology Foundation Rotterdam.

Authorship Contributions

EMPS, AHQ and JMB analyzed and interpreted data. AB performed experiments. RP, HAdGK, VdH, MAH, and GE provided clinical characteristics, clinical outcome data, and interpreted data. RP and MLdB conceptualized the study, and interpreted data. EMPS and MLdB drafted the manuscript. The manuscript was revised and approved by all authors.

Disclosure of Conflicts of Interest

The authors declare no conflicts of interest.

REFERENCES

1. Moorman AV. The clinical relevance of chromosomal and genomic abnormalities in B-cell precursor acute lymphoblastic leukaemia. Blood reviews. 2012 May;26(3):123-35.
2. Pui CH, Robison LL, Look AT. Acute lymphoblastic leukaemia. Lancet. 2008 Mar 22;371(9617):1030-43.
3. Pieters R, de Groot-Kruseman H, Van der Velden V, Fiocco M, van den Berg H, de Bont E, et al. Successful Therapy Reduction and Intensification for Childhood Acute Lymphoblastic Leukemia Based on Minimal Residual Disease Monitoring: Study ALL10 From the Dutch Childhood Oncology Group. J Clin Oncol. 2016 Aug 01;34(22):2591-601.
4. Den Boer ML, van Slegtenhorst M, De Menezes RX, Cheok MH, Buijs-Gladdines JG, Peters ST, et al. A subtype of childhood acute lymphoblastic leukaemia with poor treatment outcome: a genome-wide classification study. Lancet Oncol. 2009 Feb;10(2):125-34.
5. Mullighan CG, Su X, Zhang J, Radtke I, Phillips LA, Miller CB, et al. Deletion of IKZF1 and prognosis in acute lymphoblastic leukemia. N Engl J Med. 2009 Jan 29;360(5):470-80.
6. Boer JM, Steeghs EM, Marchante JR, Boeree A, Beaudoin JJ, Beverloo HB, et al. Tyrosine kinase fusion genes in pediatric BCR-ABL1-like acute lymphoblastic leukemia. Oncotarget. 2017 Jan 17;8(3):4618-28.
7. Imamura T, Kiyokawa N, Kato M, Imai C, Okamoto Y, Yano M, et al. Characterization of pediatric Philadelphia-negative B-cell precursor acute lymphoblastic leukemia with kinase fusions in Japan. Blood cancer journal. 2016 May 13;6:e419.
8. Roberts KG, Li Y, Payne-Turner D, Harvey RC, Yang YL, Pei D, et al. Targetable kinase-activating lesions in Ph-like acute lymphoblastic leukemia. N Engl J Med. 2014 Sep 11;371(11):1005-15.
9. Roberts KG, Morin RD, Zhang J, Hirst M, Zhao Y, Su X, et al. Genetic alterations activating kinase and cytokine receptor signaling in high-risk acute lymphoblastic leukemia. Cancer Cell. 2012 Aug 14;22(2):153-66.
10. Lilljebjorn H, Henningsson R, Hyrenius-Wittsten A, Olsson L, Orsmark-Pietras C, von Palffy S, et al. Identification of ETV6-RUNX1-like and DUX4-rearranged subtypes in paediatric B-cell precursor acute lymphoblastic leukaemia. Nature communications. 2016 Jun 06;7:11790.
11. Yasuda T, Tsuzuki S, Kawazu M, Hayakawa F, Kojima S, Ueno T, et al. Recurrent DUX4 fusions in B cell acute lymphoblastic leukemia of adolescents and young adults. Nat Genet. 2016 May;48(5):569-74.
12. Zhang J, McCastlain K, Yoshihara H, Xu B, Chang Y, Churchman ML, et al. Deregulation of DUX4 and ERG in acute lymphoblastic leukemia. Nat Genet. 2016 Dec;48(12):1481-9.
13. Moorman AV. New and emerging prognostic and predictive genetic biomarkers in B-cell precursor acute lymphoblastic leukemia. Haematologica. 2016 Apr;101(4):407-16.
14. van der Veer A, Waanders E, Pieters R, Willemse ME, Van Reijmersdal SV, Russell LJ, et al. Independent prognostic value of BCR-ABL1-like signature and IKZF1 deletion, but not high CRLF2 expression, in children with B-cell precursor ALL. Blood. 2013 Oct 10;122(15):2622-9.
15. Harvey RC, Mullighan CG, Wang X, Dobbin KK, Davidson GS, Bedrick EJ, et al. Identification of novel cluster groups in pediatric high-risk B-precursor acute lymphoblastic leukemia with gene expression profiling: correlation with genome-wide DNA copy number alterations, clinical characteristics, and outcome. Blood. 2010 Dec 2;116(23):4874-84.
16. Boer JM, van der Veer A, Rizopoulos D, Fiocco M, Sonneveld E, de Groot-Kruseman HA, et al. Prognostic value of rare IKZF1 deletion in childhood B-cell precursor acute lymphoblastic leukemia: an international collaborative study. Leukemia. 2016 Jan;30(1):32-8.
17. Kuiper RP, Waanders E, van der Velden VH, van Reijmersdal SV, Venkatachalam R, Scheijen B, et al. IKZF1 deletions predict relapse in uniformly treated pediatric precursor B-ALL. Leukemia. 2010 Jul;24(7):1258-64.
18. Moorman AV, Enshaei A, Schwab C, Wade R, Chilton L, Elliott A, et al. A novel integrated cytogenetic and genomic classification refines risk stratification in pediatric acute lymphoblastic leukemia. Blood. 2014 Aug 28;124(9):1434-44.
19. Gupta SK, Bakhshi S, Kumar L, Kamal VK, Kumar R. Gene copy number alteration profile and its clinical correlation in B-cell acute lymphoblastic leukemia. Leuk Lymphoma. 2017 Feb;58(2):333-42.
20. Den Boer ML, Harms DO, Pieters R, Kazemier KM, Gobel U, Korholz D, et al. Patient stratification based on prednisolone-vincristine-asparaginase resistance profiles in children with acute lymphoblastic leukemia. J Clin Oncol. 2003 Sep 01;21(17):3262-8.
21. Kaspers GJ, Pieters R, Van Zantwijk CH, Van Wering ER, Van Der Does-Van Den Berg A, Veerman AJ. Prednisolone resistance in childhood acute lymphoblastic leukemia: vitro-vivo correlations and cross-resistance to other drugs. Blood. 1998 Jul 01;92(1):259-66.
22. Pieters R, Huismans DR, Loonen AH, Hahlen K, van der Does-van den Berg A, van Wering ER, et al. Relation of cellular drug resistance to long-term clinical outcome in childhood acute lymphoblastic leukaemia. Lancet. 1991 Aug 17;338(8764):399-403.
23. Klumper E, Pieters R, Veerman AJ, Huismans DR, Loonen AH, Hahlen K, et al. In vitro cellular drug resistance in children with relapsed/refractory acute lymphoblastic leukemia. Blood. 1995 Nov 15;86(10):3861-8.
24. Marke R, Havinga J, Cloos J, Demkes M, Poelmans G, Yuniati L, et al. Tumor suppressor IKZF1 mediates glucocorticoid resistance in B-cell precursor acute lymphoblastic leukemia. Leukemia. 2016 Jul;30(7):1599-603.
25. Imamura T, Yano M, Asai D, Moriya-Saito A, Suenobu SI, Hasegawa D, et al. IKZF1 deletion is enriched in pediatric B-cell precursor acute lymphoblastic leukemia patients showing prednisolone resistance. Leukemia. 2016 Aug;30(8):1801-3.

26. Scheijen B, Boer JM, Marke R, Tijchon E, van Ingen Schenau D, Waanders E, et al. Tumor suppressors BTG1 and IKZF1 cooperate during mouse leukemia development and increase relapse risk in B-cell precursor acute lymphoblastic leukemia patients. Haematologica. 2017 Mar;102(3):541-51.
27. Escherich G, Zimmermann M, Janka-Schaub G, CoALL study group. Doxorubicin or daunorubicin given upfront in a therapeutic window are equally effective in children with newly diagnosed acute lymphoblastic leukemia. A randomized comparison in trial CoALL 07-03. Pediatr Blood Cancer. 2013 Feb;60(2):254-7.
28. Veerman AJ, Kamps WA, van den Berg H, van den Berg E, Bokkerink JP, Bruin MC, et al. Dexamethasone-based therapy for childhood acute lymphoblastic leukaemia: results of the prospective Dutch Childhood Oncology Group (DCOG) protocol ALL-9 (1997-2004). Lancet Oncol. 2009 Oct;10(10):957-66.
29. Escherich G, Troger A, Gobel U, Graubner U, Pekrun A, Jorch N, et al. The long-term impact of in vitro drug sensitivity on risk stratification and treatment outcome in acute lymphoblastic leukemia of childhood (CoALL 06-97). Haematologica. 2011 Jun;96(6):854-62.
30. Familiades J, Bousquet M, Lafage-Pochitaloff M, Bene MC, Beldjord K, De Vos J, et al. PAX5 mutations occur frequently in adult B-cell progenitor acute lymphoblastic leukemia and PAX5 haploinsufficiency is associated with BCR-ABL1 and TCF3-PBX1 fusion genes: a GRAALL study. Leukemia. 2009 Nov;23(11):1989-98.
31. Schwab CJ, Chilton L, Morrison H, Jones L, Al-Shehhi H, Erhorn A, et al. Genes commonly deleted in childhood B-cell precursor acute lymphoblastic leukemia: association with cytogenetics and clinical features. Haematologica. 2013 Jul;98(7):1081-8.
32. Russell LJ, Capasso M, Vater I, Akasaka T, Bernard OA, Calasanz MJ, et al. Deregulated expression of cytokine receptor gene, CRLF2, is involved in lymphoid transformation in B-cell precursor acute lymphoblastic leukemia. Blood. 2009 Sep 24;114(13):2688-98.
33. Virely C, Moulin S, Cobaleda C, Lasgi C, Alberdi A, Soulier J, et al. Haploinsufficiency of the IKZF1 (IKAROS) tumor suppressor gene cooperates with BCR-ABL in a transgenic model of acute lymphoblastic leukemia. Leukemia. 2010 Jun;24(6):1200-4.
34. van der Veer A, Zaliova M, Mottadelli F, De Lorenzo P, Te Kronnie G, Harrison CJ, et al. IKZF1 status as a prognostic feature in BCR-ABL1-positive childhood ALL. Blood. 2014 Mar 13;123(11):1691-8.
35. Clappier E, Auclerc MF, Rapion J, Bakkus M, Caye A, Khemiri A, et al. An intragenic ERG deletion is a marker of an oncogenic subtype of B-cell precursor acute lymphoblastic leukemia with a favorable outcome despite frequent IKZF1 deletions. Leukemia. 2014 Jan;28(1):70-7.
36. Enshaei A, Schwab CJ, Konn ZJ, Mitchell CD, Kinsey SE, Wade R, et al. Long-term follow-up of ETV6-RUNX1 ALL reveals that NCI risk, rather than secondary genetic abnormalities, is the key risk factor. Leukemia. 2013 Nov;27(11):2256-9.
37. Chan LN, Chen Z, Braas D, Lee JW, Xiao G, Geng H, et al. Metabolic gatekeeper function of B-lymphoid transcription factors. Nature. 2017 Feb 23;542(7642):479-83.
38. Holleman A, Cheok MH, den Boer ML, Yang W, Veerman AJ, Kazemier KM, et al. Gene-expression patterns in drug-resistant acute lymphoblastic leukemia cells and response to treatment. N Engl J Med. 2004 Aug 5;351(6):533-42.
39. Hulleman E, Kazemier KM, Holleman A, VanderWeele DJ, Rudin CM, Broekhuis MJ, et al. Inhibition of glycolysis modulates prednisolone resistance in acute lymphoblastic leukemia cells. Blood. 2009 Feb 26;113(9):2014-21.
40. Chouchana L, Fernandez-Ramos AA, Dumont F, Marchetti C, Ceballos-Picot I, Beaune P, et al. Molecular insight into thiopurine resistance: transcriptomic signature in lymphoblastoid cell lines. Genome medicine. 2015;7(1):37.
41. Iacobucci I, Iraci N, Messina M, Lonetti A, Chiaretti S, Valli E, et al. IKAROS deletions dictate a unique gene expression signature in patients with adult B-cell acute lymphoblastic leukemia. PloS one. 2012;7(7):e40934.
42. Harrison CJ, Moorman AV, Schwab C, Carroll AJ, Raetz EA, Devidas M, et al. An international study of intrachromosomal amplification of chromosome 21 (iAMP21): cytogenetic characterization and outcome. Leukemia. 2014 May;28(5):1015-21.
43. Holmfeldt L, Wei L, Diaz-Flores E, Walsh M, Zhang J, Ding L, et al. The genomic landscape of hypodiploid acute lymphoblastic leukemia. Nat Genet. 2013 Mar;45(3):242-52.
44. Gray, R. J. cmprsk: Subdistribution Analysis of Competing Risks. R package version 2.2-6. http://CRAN.R-project.org/package=cmprsk (2013).
45. De Wreede, L. C., Fiocco, M. & Putter, H. mstate: An R Package for the Analysis of Competing Risks and Multi-State Models. J Stat Softw 38, 1-30 (2011).
46. Therneau, T. A Package for Survival Analysis in S. R package version 2.36-12. (2012).

SUPPLEMENTARY DATA

Supplementary Table 1: COX multivariate analysis of risk factors within the DCOG-ALL10 cohort

		Cox multivariate model		
	Number of patients	p-value	HR	95% CI
IKZF1	30/210	0.003	3.406	1.523 - 7.618
PRED response	11/204	0.153	2.529	0.709 -9.024
MRD TP1	41/210	0.067	2.08	0.951 - 4.548
MRD TP2	8/210	0.503	0.495	0.063 - 3.883

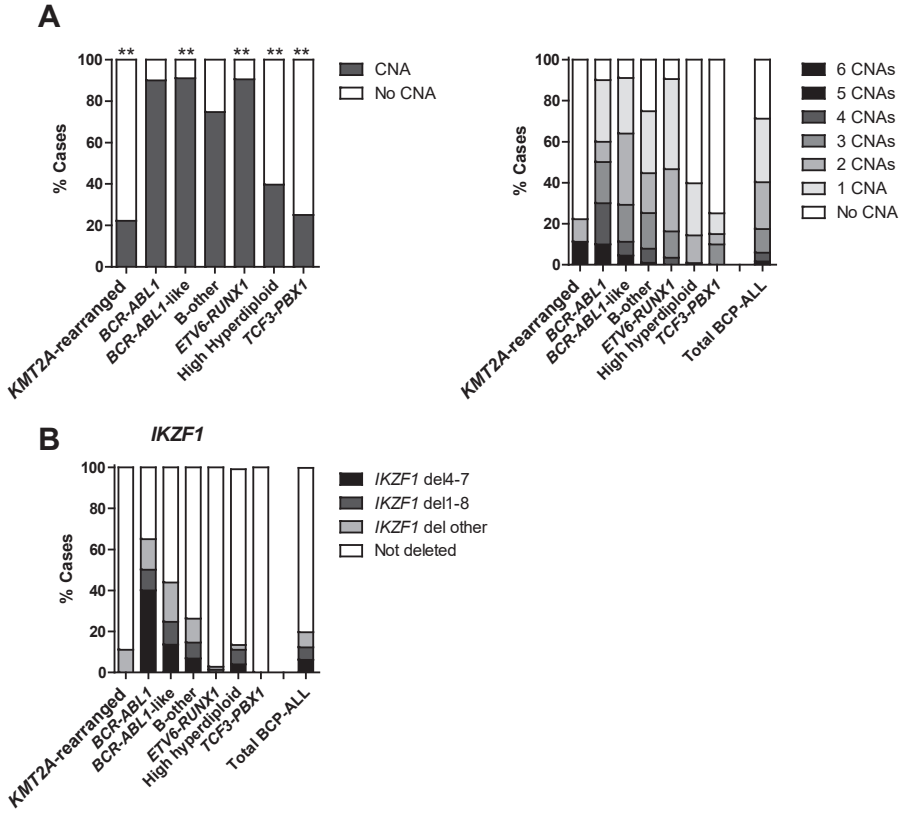

Supplementary Figure 1. CNA landscape of B-cell development genes in the different subtypes of pediatric BCP ALL.

CNA profile of 515 newly diagnosed pediatric BCP-ALL patients, representing the major BCP-ALL subtypes, was determined using MLPA. **(A)** The frequency of any CNA (*IKZF1, EBF1, PAX5, CDKN2A/B, RB1, BTG1, ETV6*, and/or PAR1) is shown per subtype. One CNA was sufficient to be quantified as altered. **p≤0.01 **(B)** The association between *IKZF1* deletions and BCP-ALL subtypes. *IKZF1* deletions are depicted as deletion of exon 4-7, deletions of exon 1-8, or remaining deletions.

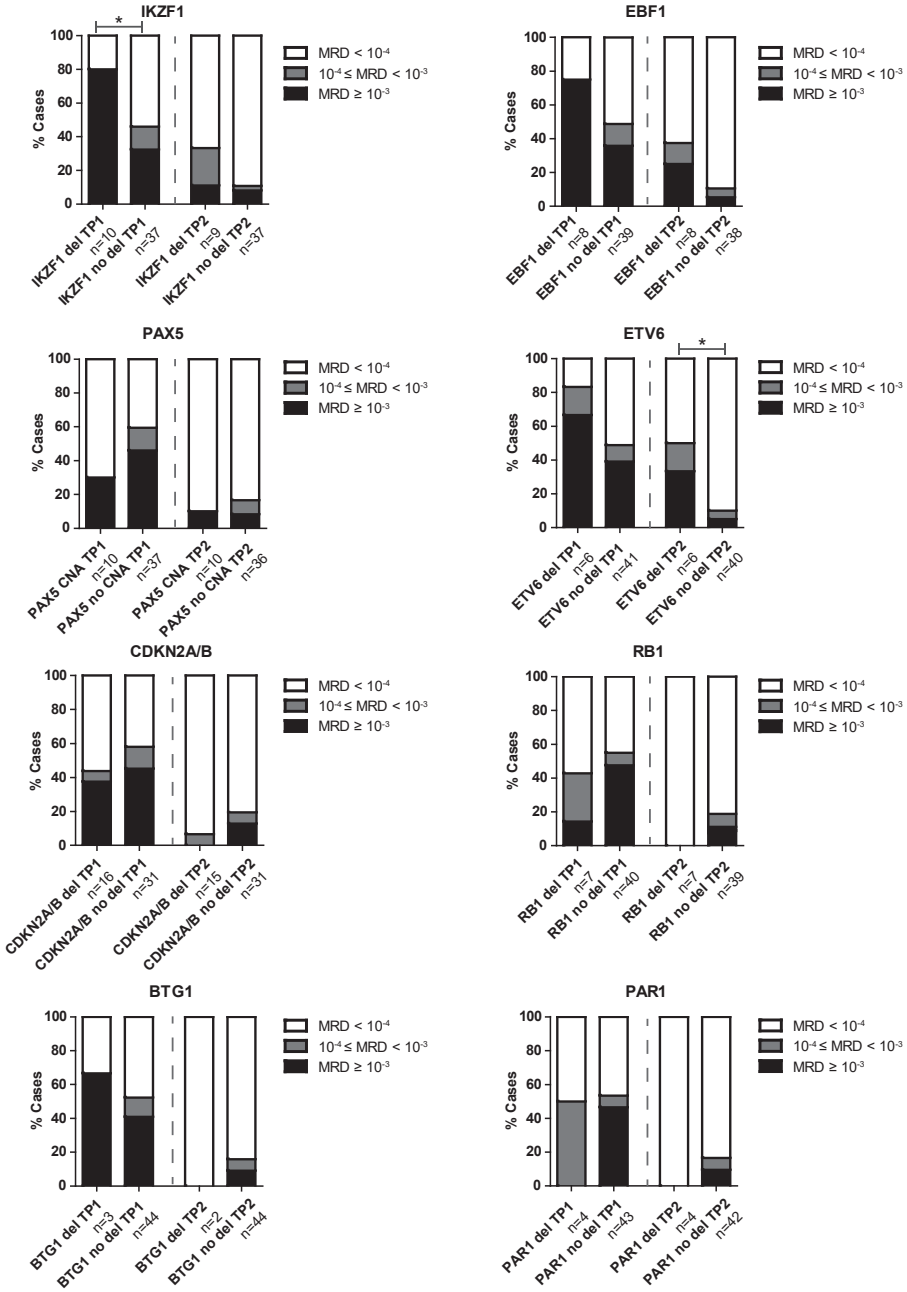

Supplementary Figure 2. The association between CNAs and MRD levels after induction therapy and the first consolidation course in *BRC-ABL1*-like and B-other patients.

MRD levels of DCOG-ALL10 treated *BCR-ABL1*-like and non-*BCR-ABL1*-like B-other cases after induction (TP1; n=47) and first consolidation course (TP2; n=46). The percentage of cases with high ($\geq 10^{-3}$), medium ($10^{-4} \leq$ MRD $< 10^{-3}$), and undetectable MRD levels ($<10^{-4}$) is depicted per CNA. Fisher's Exact test. **p≤0.01, *p≤0.05. del = deletion.

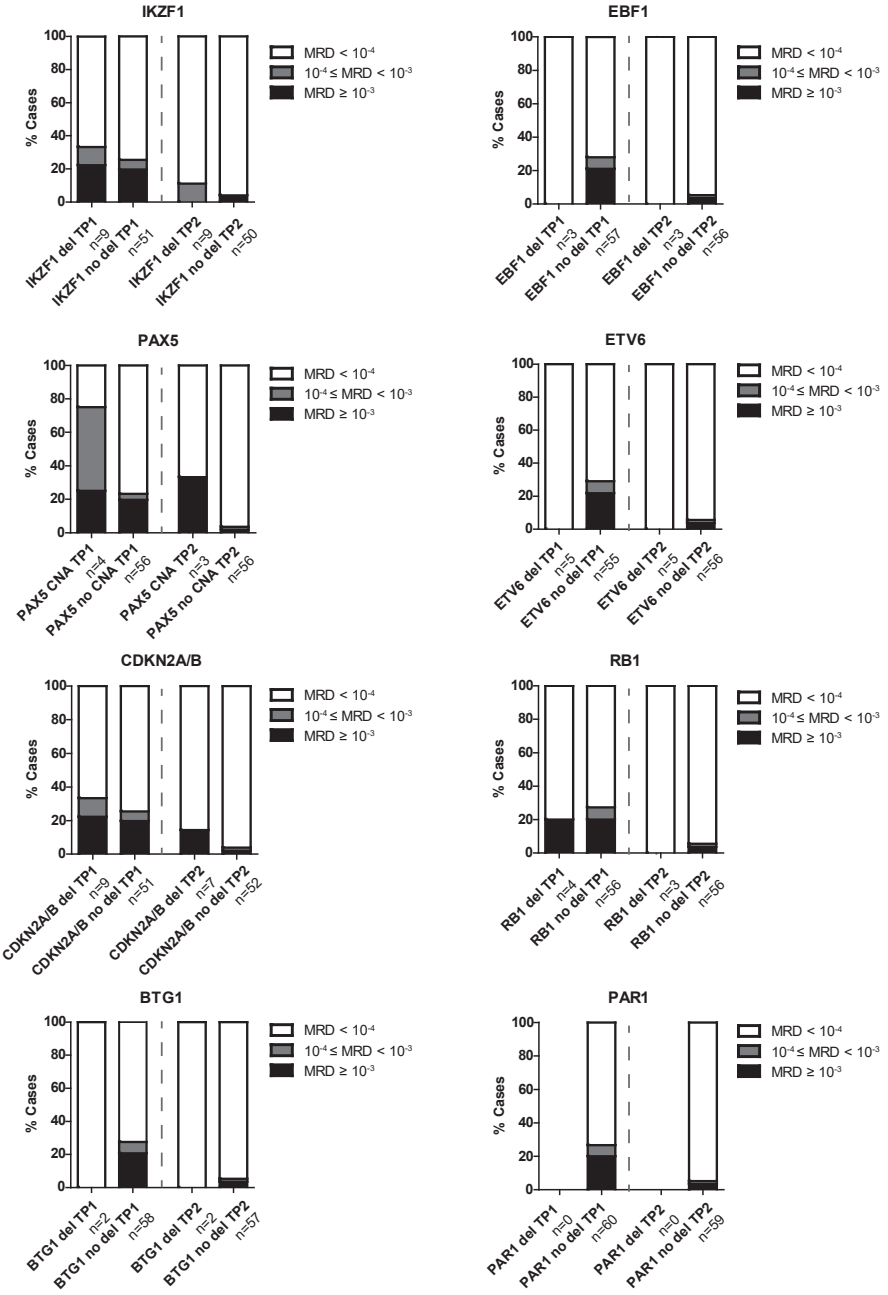

Supplementary Figure 3. The association between CNAs and MRD levels after induction therapy and the first consolidation course in high hyperdiploid patients.

MRD levels of DCOG-ALL10 treated high hyperdiploid cases after induction (TP1; n=60) and first consolidation course (TP2; n=59). The percentage of cases with high ($\geq 10^{-3}$), medium ($10^{-4} \leq$ MRD $< 10^{-3}$), and undetectable MRD levels ($<10^{-4}$) is depicted per CNA. Fisher's Exact test. **p≤0.01, *p≤0.05. del = deletion.

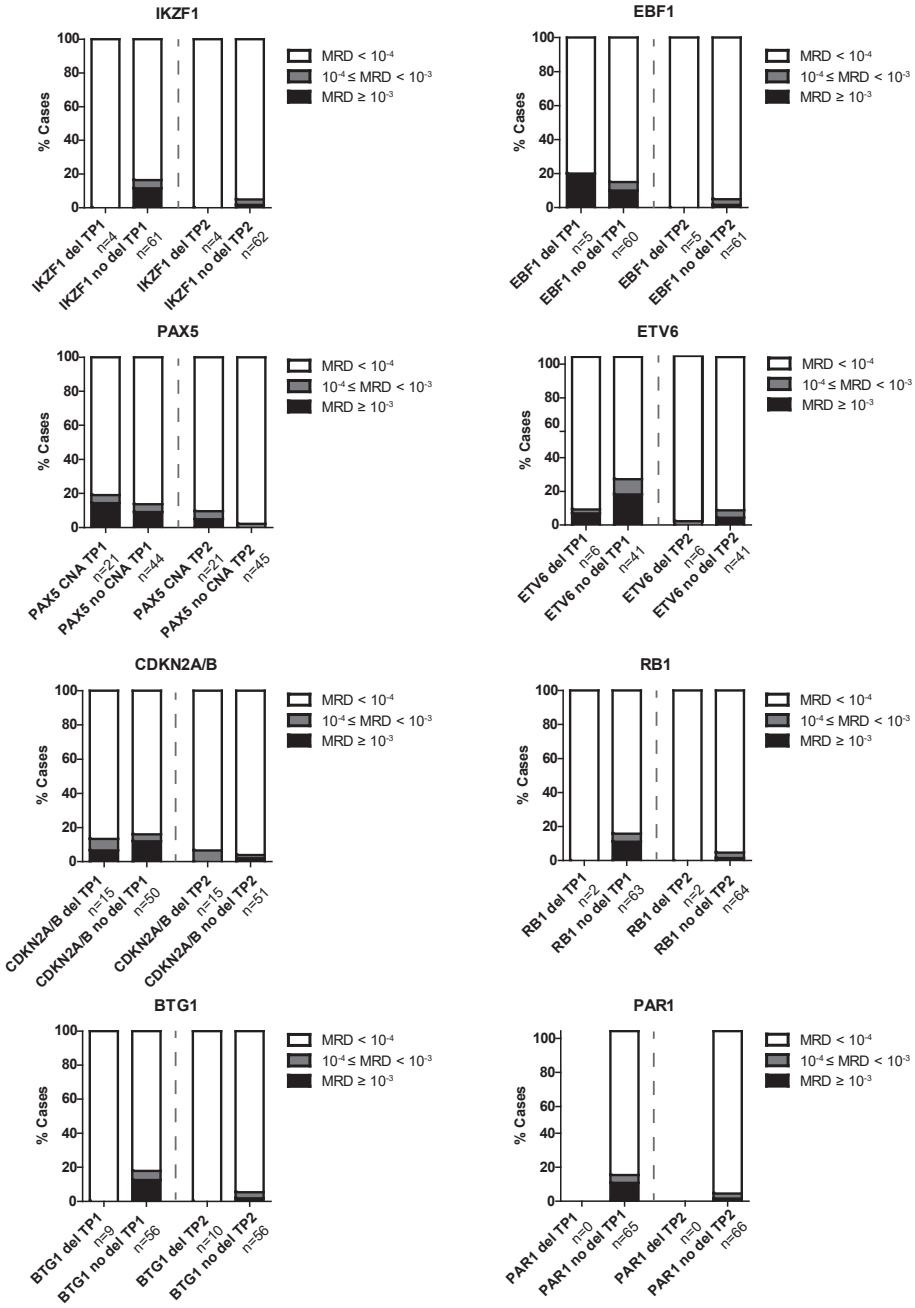

Supplementary Figure 4. The association between CNAs and MRD levels after induction therapy and the first consolidation course in *ETV6-RUNX1* patients.

MRD levels of DCOG-ALL10 treated *ETV6-RUNX1* cases after induction (TP1; n=65) and first consolidation course (TP2; n=66). The percentage of cases with high (≥10^{-3}), medium (10^{-4} ≤ MRD < 10^{-3}), and undetectable MRD levels (<10^{-4}) is depicted per CNA. Fisher's Exact test. **p≤0.01, *p≤0.05. del = deletion.

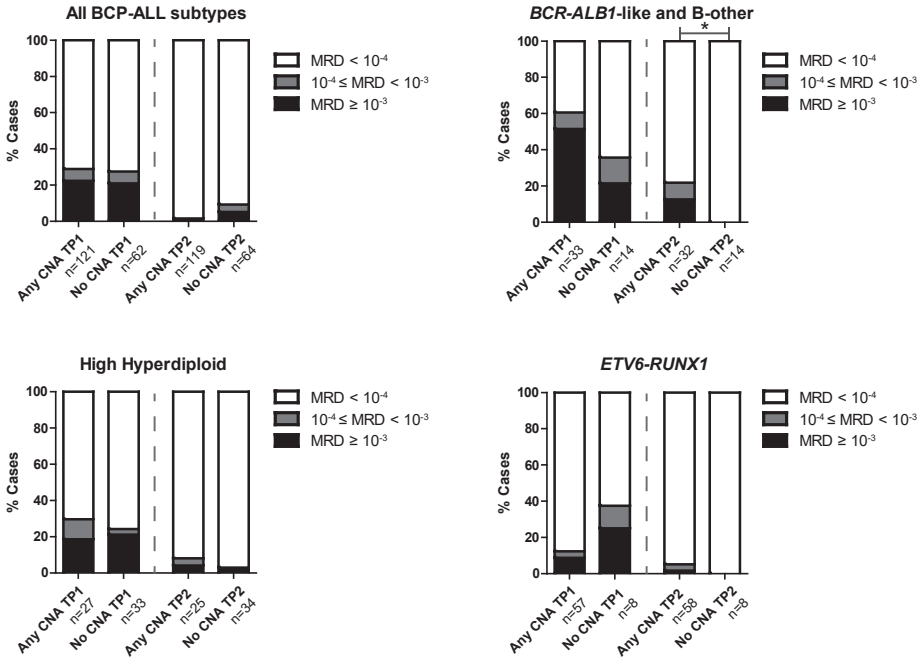

Supplementary Figure 5. The association between any CNA and MRD levels after induction therapy and the first consolidation course.

MRD levels of DCOG-ALL10 treated BCP-ALL cases after induction (TP1; n=183) and first consolidation course (TP2; n=183). The MRD levels of cases with any or no CNA are depicted for all subtypes, *BCR-ABL1*-like and non-*BCR-ABL1*-like B-other, high hyperdiploid, and *ETV6-RUNX1*.

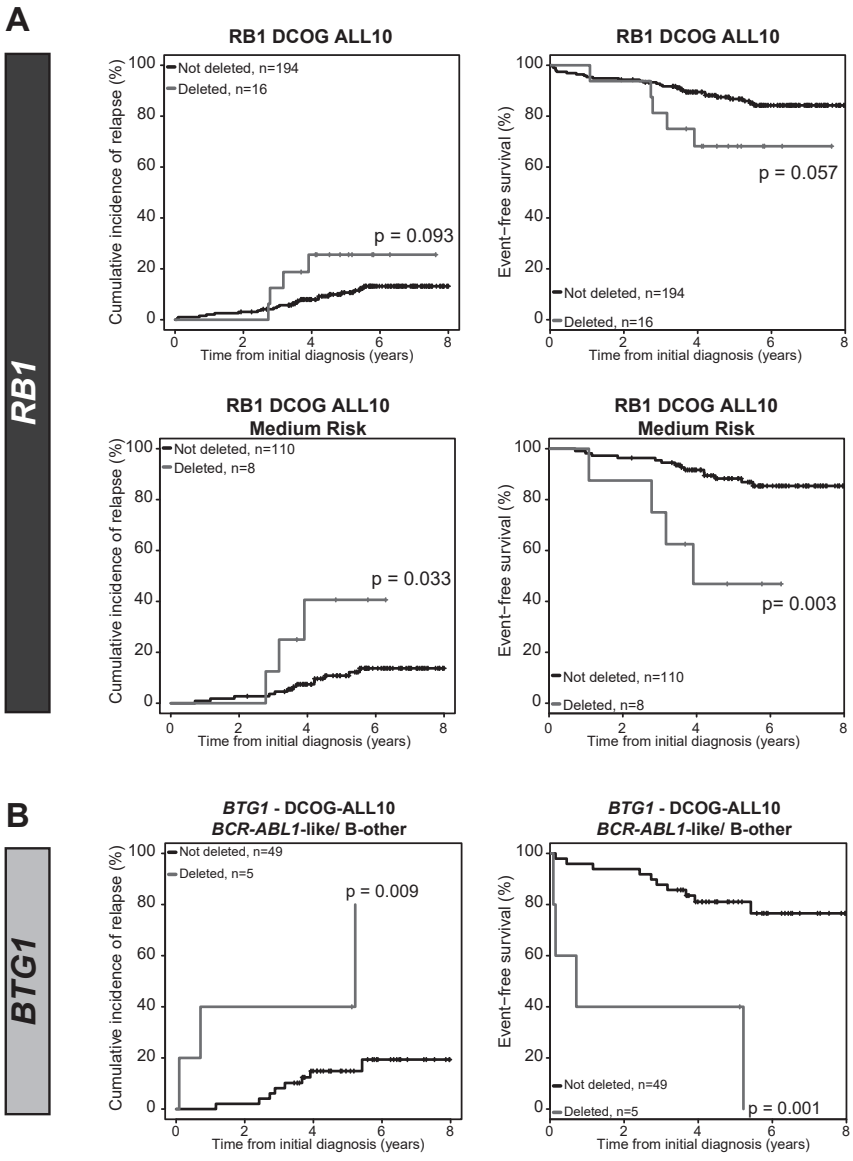

Supplementary Figure 6. Prognostic value of CNAs in DCOG-ALL10 treated cases.
The association between CNAs and cumulative incidence of relapse (CIR) or event-free-survival (EFS) was examined. Patients were treated according to DCOG-ALL10 protocol. CIR was estimated using a competing risk model. Relapse and non-response were considered as event, and death as competing event. To test equality of the CIRs, the Gray's test was applied. Non-response, relapse, and death were considered as events for EFS. EFS rates were determined using Cox regression, and compared using the Wald test. (**A**) CIR and EFS curves of cases without or with a *RB1* deletion. Curves contain either all risk groups, or the medium risk arm only. (**B**) CIR and EFS curves of *BCR-ABL1*-like and non-*BCR-ABL1*-like B-other cases without or with *BTG1* deletions.

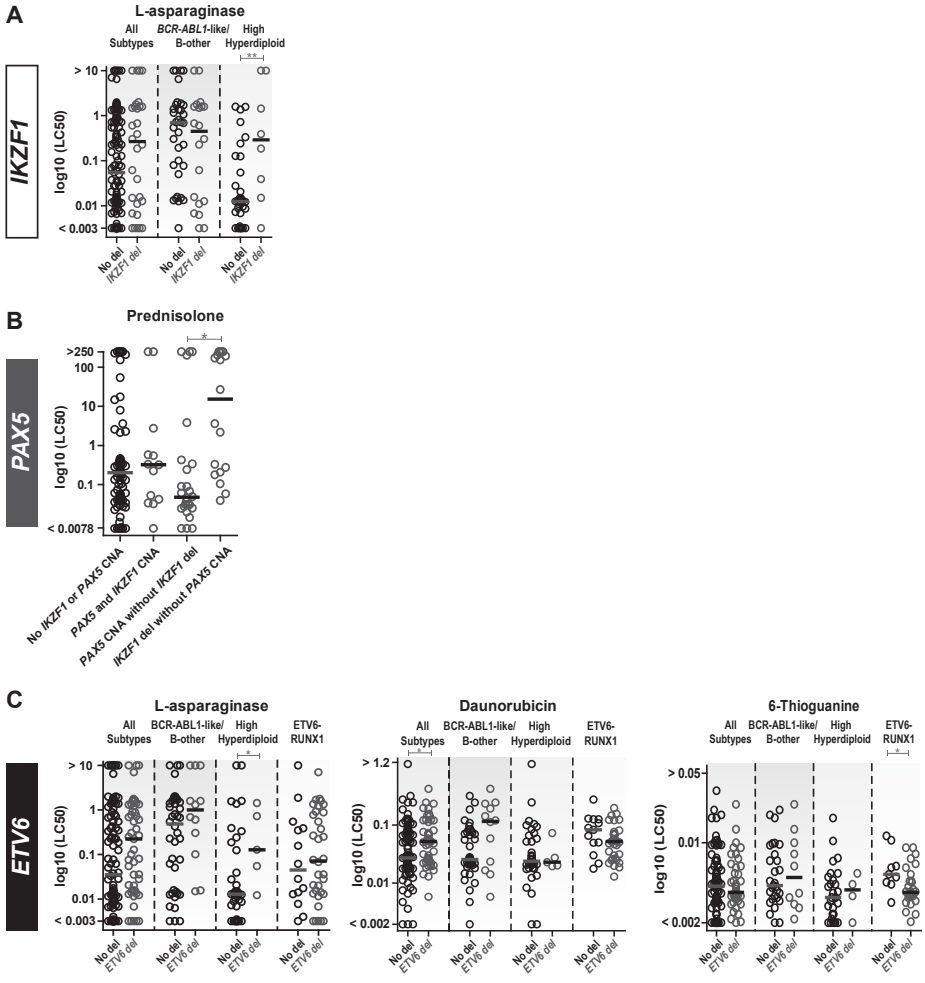

Supplementary Figure 7. Cellular drug response and CNAs.

Leukemic cells were incubated for four days with an increasing concentration range of prednisolone (µg/ml), vincristine (µg/ml), L-asparaginase (IU/ml), daunorubicin (µg/ml), 6-mercaptopurine (µg/ml), and 6-thioguanine (µg/ml), after which cell viability was measured using an MTT assay. Association between indicated CNAs and *ex vivo* cytotoxicity was studied. The Mann-Whitney U test was applied to compare LC50-values. * $p < 0.05$, ** $p < 0.01$ (**A**) LC50 values of L-asparaginase (IU/ml) of primary leukemic cells without or with *IKZF1* deletion. Columns include all BCP-ALL subtypes, *BCR-ABL1*-like/ B-other cells, and high hyperdiploid cells. (**B**) LC50 values of prednisolone (µg/ml) of primary leukemic cells without an *IKZF1* or *PAX5* CNA, with *IKZF1* and *PAX5* CNA, a *PAX5* CNA without an *IKZF1* del, or *IKZF1* an del without a *PAX5* CNA. (**C**) LC50 values of L-asparaginase (IU/ml) and 6-thiogunanine (µg/ml) of primary leukemic cells without or with *ETV6* deletion. Columns include all BCP-ALL subtypes, *BCR-ABL1*-like/ B-other cells, high hyperdiploid cells, and *ETV6-RUNX1*-positive cells.

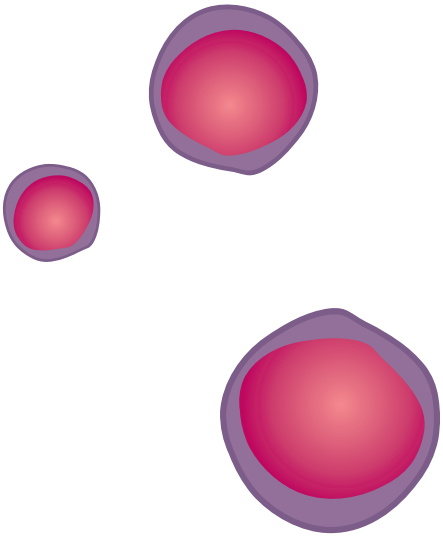

Chapter 6

B-CELL PRECURSOR ACUTE LYMPHOBLASTIC LEUKEMIA CELLS MANIPULATE MESENCHYMAL STROMAL CELLS

Elisabeth M.P. Steeghs, Roel Polak, Bob de Rooij, Lieke C.J. van den Berk, Judith M. Boer, Cesca van de Ven, Femke Stalpers, Marjolein Bakker, Rob Pieters, and Monique L. den Boer

Work in progress

ABSTRACT

B-cell precursor acute lymphoblastic leukemia (BCP-ALL) cells reside in the bone marrow, where mesenchymal stromal cells (MSCs) support many of their functions. Unraveling the role of the bone marrow niche in pediatric BCP-ALL may provide novel options for therapeutic intervention. The present study aimed to unravel whether MSCs derived from pediatric BCP-ALL patients at initial diagnosis (leukemic-MSCs) differ from MSCs derived from healthy pediatric donors (control-MSCs). Therefore, we studied their supportive properties and gene expression profiles.

Co-culture experiments of BCP-ALL cells and MSCs revealed that survival of BCP-ALL cells is significantly increased upon co-culture compared to survival in mono-culture. Both control-MSCs and leukemic-MSCs provided a similar survival benefit. Strikingly, gene expression profiles of MSCs were significantly changed after co-culture with BCP-ALL cells. Each BCP-ALL sample induced a characteristic gene expression change, which was consistent between different MSCs. The interferon/STAT1 pathway was most commonly induced. In order to study the persistence of the gene expression changes, MSCs were cultured for approximately 14 days without leukemic cells. Microarray analysis of 86 primary MSCs revealed only marginal differences in gene expression between leukemic-MSCs and control-MSCs, which disappeared in MSCs derived from BCP-ALL patients at time of remission. Hence, results suggest that BCP-ALL cells drive gene expression changes in MSCs, which convert back to normal upon elimination of leukemic cells.

In conclusion, leukemic-MSCs are intrinsically not different from control-MSCs. Instead, BCP-ALL cells enforce a pro-inflammatory expression profile in MSCs, which coincides with an increased viability of BCP-ALL cells.

INTRODUCTION

The effect of chemotherapy is often studied on the cancer cell as a single entity. However, the tumor microenvironment has a profound effect on the growth and survival of cancer cells and targeting of this niche might therefore offer an attractive treatment strategy.[1-5] The tumor niche consists of cancer cells and a supporting framework, including mesenchymal stromal cells (MSCs), fibroblasts, endothelial cells, pericytes and a variety of inflammatory cells.[2, 6] Chemokines such as IL-6, IL-1β, and SDF-1α are secreted to promote MSC migration toward this niche.[1, 2, 7] However, the role of MSCs in the initiation and progression of cancer remains unclear. MSCs have been reported to exert stimulatory (e.g. induce proliferation) as well as inhibitory (e.g. induce apoptosis) effects on cancer cells.[1, 8, 9] Unraveling the role of the tumor niche in cancer may provide novel options for therapeutic intervention.

Acute lymphoblastic leukemia (ALL) is the most common childhood malignancy and arises from malignant transformation of either B- or T-cell progenitors. B-cell precursor ALL (BCP-ALL) accounts for approximately 85% of cases and can be further subdivided in genetic subtypes, such as *BCR-ABL1*, *ETV6-RUNX1*, *TCF3-PBX1*, or *KMT2A*-rearranged ALL.[10] Leukemic cells reside in the bone marrow microenvironment, where they hijack the normal hematopoietic stem cell niches to create a leukemic niche.[11] Importance of the bone marrow microenvironment for leukemic cells is demonstrated by the protection that the niche provides against chemotherapeutic agents.[12, 13] In *in vitro* assays MSCs mimic this protective effect.[14-19] Unraveling the mechanism of protection may provide novel options for therapeutic intervention. Therefore, research is focused on the interaction between MSCs and leukemic cells.[19-23] We recently showed that MSCs and BCP-ALL cells communicate via tunneling nanotubes.[14] Disruption of this interaction inhibited leukemogenesis and re-sensitized BCP-ALL cells to prednisolone.[14] These results point to an important role of MSCs in ALL. We therefore questioned whether MSCs derived from pediatric BCP-ALL patients differ from MSCs obtained from healthy pediatric controls. To address this, the supportive properties of these MSCs were compared as well as their gene expression profiles.

METHODS

Processing of primary patient material

Bone marrow and/or peripheral blood samples were obtained from children (1-18 years) with newly diagnosed ALL. Written informed consent was obtained from parents or guardians to use excess of diagnostic material for research purposes, as approved by the institutional review board. These studies were conducted in accordance with the Declaration of Helsinki. Mononuclear cells were isolated and processed as described previously.[24] Samples were enriched to over 90% purity of leukemic cells by depletion of non-leukemic cells using immunomagnetic beads. Primary leukemic cells were maintained in RPMI-1640 Dutch modification (Life Technologies, Breda, Netherlands) supplemented with 20% fetal calf serum (Integro, Zaandam, Netherlands), with 0.1% insulin-transferrin-sodium selenite (Sigma-Aldrich, Zwijndrecht, Netherlands), 0.4 mM glutamine (Invitrogen, Bleiswijk, Netherlands), 0.25 µg/ml gentamycine (Thermo Scientific, Breda, Netherlands), 100 IU/ml penicillin (Thermo Scientific), 100 µg/ml streptomycin (Thermo Scientific), 0.125 µg/ml fungizone (Thermo Scientific).

The major cytogenetic subtypes, i.e. high hyperdiploid (51-65 chromosomes), *ETV6-RUNX1*, *TCF3-PBX1*, *KMT2A*-rearranged, *BCR-ABL1*, *BCR-ABL1*-like and B-other (negative for all before mentioned genomic lesions), were determined using fluorescent in situ hybridization, (RT-)PCR and a 110-probeset gene expression classifier (to identify *BCR-ABL1*-like cases).[25]

Isolation and expansion of BM-MSC

Bone marrow (BM) aspirates were collected from children with newly diagnosed BCP-ALL (leukemic-MSCs), after 79 days of induction and consolidation treatment (remission-MSCs), relapsed BCP-ALL (relapse-MSCs) or from children with healthy bone marrow (control-MSCs). Written informed consent was obtained from parents or guardians to use excess of diagnostic material for research purposes, as approved by the institutional review board. MSCs were isolated from these aspirates as described previously.[26] Briefly, BM aspirates were seeded in MSC expansion medium (DMEM low glucose medium (Life Technologies), 15% FCS (Integro), fungizone (Invitrogen), gentamycin (Invitrogen), freshly supplemented with 0.1 mM ascorbic acid (Sigma-Aldrich) and 1 ng/ml basic fibroblast growth factor (bFGF; Serotec, Kidlington, UK). Non-adherent cells were removed after 24 hours. After a maximum of 10 days, MSC colonies were harvested using trypsin (Thermo Scientific). Cells were further expanded for one or two additional passages in order to isolate RNA (Trizol, Invitrogen, Bleiswijk, Netherlands) and freeze cells in liquid nitrogen for future experiments. MSCs were negative for the hematopoietic markers (CD14, CD34, CD45; BD Biosciences, San Jose, CA, USA), and positive for the mesenchymal markers (CD13, CD29, CD54, CD73, and CD166; BD Biosciences) as detected by flow cytometry (BD Accuri C6 Plus). Multi-lineage potential was confirmed for adipocyte (Oil Red O staining), osteocyte (Alizarin Red S staining), and chondrocyte (Col2a/Thionine/Alcian Blue staining) differentiation (Figure S1).

Cell viability assays

Primary BCP-ALL cells ($1*10^6$ cells) were co-cultured with or without MSCs ($5*10^4$ cells) for two or five days in a 24 well plate at 37°C and 5% CO_2. To analyze BCP-ALL cell viability, cells were stained with Brilliant Violet 421 anti-human CD19 antibody (Biolegend San Diego, CA, USA), FITC Annexin V (Biolegend), and propidium iodide (PI; Invitrogen). Cell viability was quantified using flow cytometry (MACSQuant). Within the MSC-negative fraction, the percentage of AnnexinVneg/PIneg/CD19pos cells was determined using FlowJo 10.0.8r1, as described previously.[14]

Fluorescent Activated Cell Sorting

Primary BCP-ALL cells ($5*10^6$ cells) from four different patients (n=2 *ETV6-RUNX1* (ALL sample 2 and 3), n=2 B-other (ALL sample 1 and 4) were co-cultured with primary MSCs ($2.25*10^5$ cells) derived from six different donors (n=2 control-MSCs, n=4 leukemic-MSCs (n=2 derived from *ETV6-RUNX1* patients, n=2 derived from B-other patients)) in a 6 well plate at 37°C and 5% CO_2. After 40 hours of culture, BCP-ALL cells and MSCs were separated using fluorescent-activated cell sorting (FACS; BD FACSCanto). Cells were stained with Brilliant Violet 421 anti-human CD19 (Biolegend), Brilliant Violet 421 anti-human CD45 antibody (Biolegend), and PI. MSCs and BCP-ALL cells were separated

based on size in the FSC/SSC plot, after which we selected for viable ($PI^{negative}$) cells. CD19 and CD45 negativity was the final gating strategy applied to select for MSCs. RNA of sorted MSCs was isolated using the RNeasy mini kit (Qiagen, Hilden, Germany). RNA quality of one MSC sample was poor and therefore not included for microarray analyses.

Microarrays

RNA was extracted using either Trizol (Invitrogen), or the RNeasy mini kit (Qiagen), according to the manufacturer's protocol. RNA quality and integrity was analyzed using the 2100 Bioanalyzer (Agilent, Amstelveen, Netherlands). Good quality RNA (RIN > 6.9) was labeled, fragmented, and linearly amplified with the Affymetrix GeneChip 3'IVT Express Kit (Santa Clara, CA, USA), according to the manufacturer's protocol. Fragmented, amplified RNA was hybridized on Affymetrix U133 Plus 2.0 GeneChip arrays for 16 hours. Arrays were washed and stained using the GeneChip Fluidics Station 450, and scanned using the Affymetrix GeneChip Scanner 3000. Affymetrix Microarray Suite version 5.0 was used to assess gene-expression values. Expression signals were scaled to the target intensity of 500 and log transformed. Arrays were variance stabilization and normalization 2 (VSN2) normalized.[27] To identify differentially expressed probesets Limma R Package (version 3.26.9) was used in R 3.0.1. Principal component analyses were performed in Partek Genomic Suite 6.6. The data in this paper have been submitted at Gene Expression Omnibus[28] and are accessible through GEO Series accession numbers GSE101454 and GSE101425.

Quantitative RT-PCR (RT-qPCR)

STAT1, *IFI6* and *IFITM1* mRNA levels were quantified by incorporation of SYBR Green (Thermo Scientific, Breda, Netherlands) by RT-qPCR. For this purpose the following primer pairs were used: 5'-acccaatccagatgtctatg-3' and 5'-ttttgcatttgaagtcatattc-3' (*STAT1*), 5'-aggccctgaccttcat-3' and 5'-cagggcaccaatattacc-3' (*IFI6*), and 5'-ccaccgtgatcaaca tcc-3' and 5'-ccccgtttttcctgtattatc-3' (*IFITM1*), and 5'-gtcggagtcaacggatt-3' and 5'-aag cttcccgttctcag-5' (*GAPDH*). Relative mRNA levels as percentage of *GAPDH* levels were calculated using the comparative cycle time (Ct) method; $2^{-\Delta Ct}$ x 100%, with $\Delta Ct = Ct_{gene} - Ct_{GAPDH}$.

Multiplexed fluorescent bead-based immunoassay (Luminex) and ELISA

Primary leukemic cells were co-cultured with primary MSCs at 37°C and 5% CO_2. After two or five days of culture supernatant was collected. To remove cell debris, supernatant was centrifuged. The concentration of 64 cytokines/chemokines was analyzed using a fluorescent bead-based immunoassay (Luminex Human Cytokine/Chemokine Panel I and II; Merck Millipore, Amsterdam, Netherlands) according to the manufacturer's protocol. For ELISA assays, MSCs were cultured for two days in the presence of 10pg or 10ng IFNα (Clone: MMHAR-2; PBL Assay Science; Piscataway, NJ, USA). Supernatant was collected and IP-10 secretion was determined using an ELISA assay (R&D Systems, Minneapolis, MN, USA), according to the manufacturer's protocol.

Transfection, virus production and transduction

To silence the expression of *STAT1* in MSCs, three pLKO.1-puro Mission® vectors (Sigma-Aldrich) were used, containing a short hairpin RNA (shRNA) targeting *STAT1*

(TRCN0000004264 (shRNA-3), TRCN0000004265 (shRNA-2) and TRCN0000004267 (shRNA-1)). The Mission ® pLKO.1-puro Non-Mammalian shRNA Control Plasmid DNA (SHC002; NSC-2) and Mission® pLKO.1-puro Luciferase shRNA Control Plasmid DNA (SHC007; NSC-1) were used as scrambled controls. Vectors were transfected in 70-80% confluent HEK293T cells, using X-tremeGene 9 DNA transfection reagent (Roche, Woerden, Netherlands), 3.7 µg psPAX2 (Addgene plasmid 12260; Addgene, Cambridge, MA, USA), 1.6 µg pMD2.G (Addgene plasmid 12259) and 10.7 µg of one of the pLKO.1-puro Mission® vectors. The second and third day after transfection virus was harvested and concentrated using ultracentrifugation for 2 hours at 32.000rpm and 4°C (Optima L-90K Ultracentrifuge; Beckman Coulter, Woerden, Netherlands). Concentrated virus was aliquoted and stored at -80°C. MSCs were transduced by spin-infection. To select for stable transduced cells, puromycin selection was used.

Western Blotting

Cells were lysed in RIPA lysis buffer (Thermo Scientific) with freshly added protease and phosphatase inhibitors. Protein concentration was determined using the BCA method (Thermo Scientific). After denaturation, 15µg protein was loaded on a 10% mini protean precast gel (BioRad) and proteins were separated by electrophoresis. Proteins were transferred to a nitrocellulose membrane and membranes were blocked in 5% milk for 1 hour at room temperature. Primary antibody incubation was performed according to manufacturer's protocol. Anti-phospho-STAT1^{Tyr701} (#9167), anti-STAT1 (#9176) and anti-αTubulin (#2144) were obtained from Cell Signaling Technology (Danvers, MA, USA). Blots were stained with secondary antibodies (IRDye 680RD- or 800CW-labeled anti-rabbit and IRDye 680RD- or 800CW-labeled anti-mouse (Li-Cor Biosciences, Leusden, Netherlands) for 1 hour at room temperature. Blots were evaluated using the Odyssey infrared imaging system (Li-Cor Biosciences).

RESULTS

MSCs derived from leukemia patients and healthy controls both support the survival of ALL cells

Previously we observed that primary MSCs support the viability of primary ALL cells.[14] We questioned whether support given by MSCs derived from pediatric BCP-ALL patients at initial diagnosis (leukemic-MSCs) differs from that of MSCs derived from healthy pediatric donors (control-MSCs). The percentage of viable leukemic cells (AnnexinV-/PI-negative, CD19-positive) was measured in mono-culture and co-culture with control-MSCs or leukemic-MSCs. Primary *BCR-ABL1*-positive and *TCF3-PBX1*-positive cells hardly survived in mono-culture conditions (<2% Annexin-/PI-negative, CD19-positive cells), but upon co-culture with leukemic-MSCs or control-MSCs survival was significantly increased ($p<0.05$, Figure 1A-B, Figure S2A-B). Control-MSCs and leukemic-MSCs did not differ in their effect on the survival of *BCR-ABL1*-positive (13% versus 16%, respectively) and *TCF3-PBX1*-positive cells (5% versus 5%, respectively). Survival of *ETV6-RUNX1*-positive and *KMT2A*-rearranged cells was relatively high in mono-culture compared to *BCR-ABL1*-positive and *TCF3-PBX1*-positive cells (56% and 23% Annexin/PI-negative CD19-positive cells, respectively), and was even more increased upon co-culture with

MSCs (Figure 1C-D, Figure S2C-D). Both control-MSCs and leukemic-MSCs provided a similar survival benefit for *ETV6-RUNX1*-positive (69% versus 70%, respectively) and *KMT2A*-rearranged cells (28% versus 25%, respectively). Taken together, the increased survival of primary BCP-ALL cells in co-culture with MSCs does not depend on the source of MSCs.

ALL cells induce an inflammatory-like signature in MSCs

Both leukemic-MSCs and control-MSC supported survival of BCP-ALL cells. To gain insight in the mechanism by which MSCs support leukemic cell survival, gene expression analyses were performed of MSCs upon co-culture with BCP-ALL cells. MSCs (n=6) were cultured for 40 hours in the presence of BCP-ALL cells (derived from 4 pediatric BCP-ALL patients). Microarray analyses were performed on sorted MSCs (Figure 2A, Figure S3).

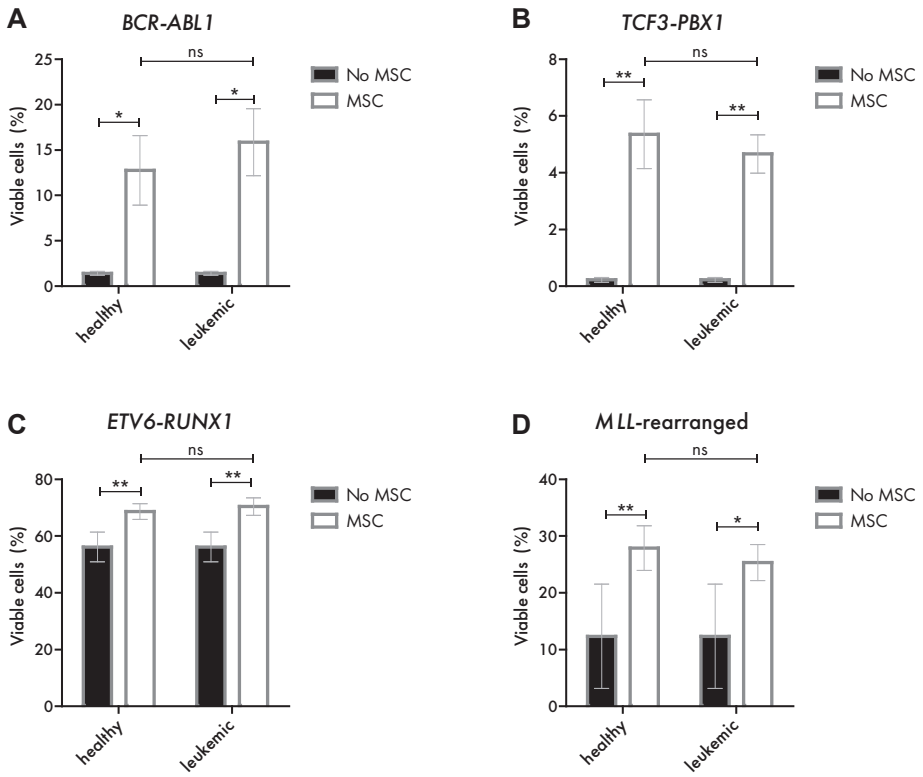

Figure 1. BCP-ALL cell survival is increased upon co-culture with MSCs obtained from leukemia patients and healthy donors.

The survival of primary CD19+ BCP-ALL cells in mono-culture (black) was compared to the survival in co-culture with two different control-MSCs or two different leukemic-MSCs (white). BCP-ALL cell survival was assessed after five days of culture using flow cytometry. Leukemic cell survival (AnnexinV$^-$/PI$^-$) was quantified in the CD19-positive fraction. Mean ± SEM of independent samples is shown. Paired Samples T-test. ** $p \leq 0.01$, * $p \leq 0.05$. (**A-D**) Percentage of viable primary leukemic cells (n=3 *BCR-ABL1*, n=3 *TCF3-PBX1*, n=3 *ETV6-RUNX1*, n=2 *KMT2A*-rearranged) in mono-culture or co-culture with control-MSCs (n=2) or leukemic-MSCs (n=2).

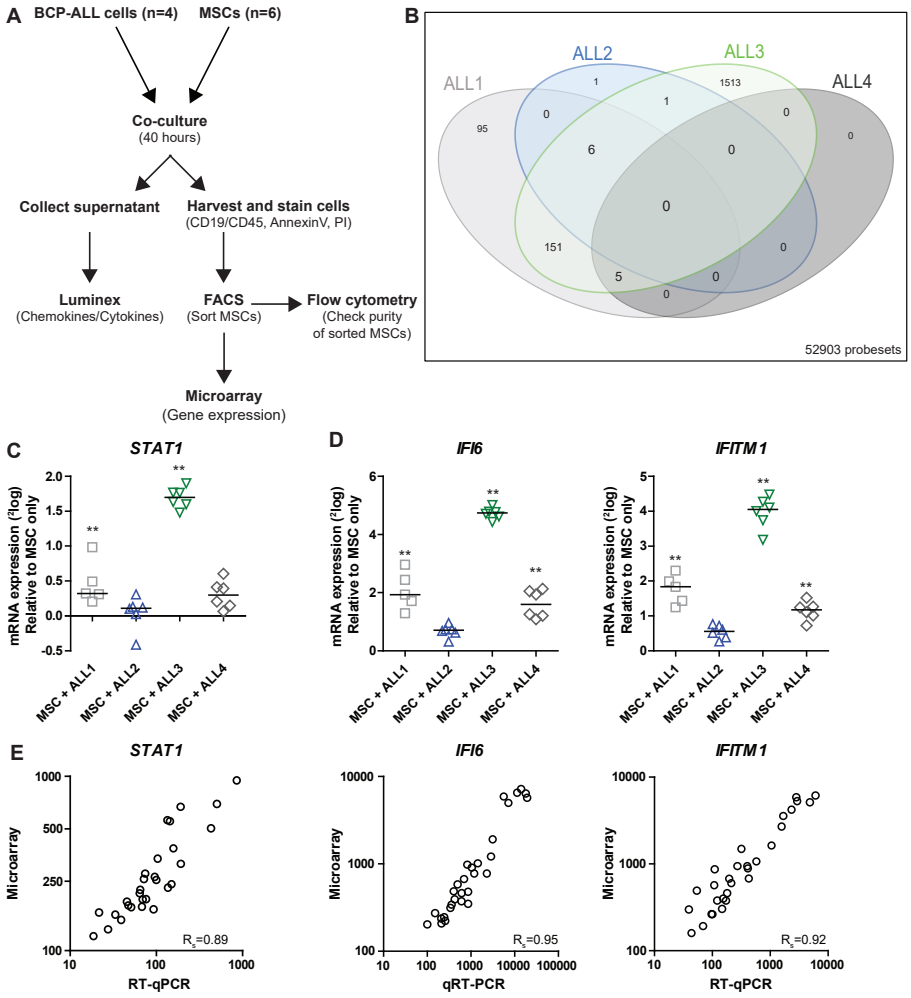

Figure 2. Gene expression profiles of MSC change after co-culture with leukemic cells.
(**A**) Primary BCP-ALL cells (n=2 B-other, n=2 *ETV6-RUNX1* samples) were co-cultured with six different primary MSCs (n=2 control-MSCs, n=4 leukemic-MSCs) for 40 hours. Supernatant was collected to determine the cytokine/chemokine profile. MSCs were separated from BCP-ALL cells using FACS. Purity of sorted samples was assessed afterwards by flow cytometry. RNA from the sorted MSCs was isolated and gene expression profiling was performed. (**B**) Limma analyses were performed to identify differentially expressed probesets (adj. $p < 0.05$) in MSCs upon co-culture with BCP-ALL cells. MSCs were compared to the mono-culture of the same MSCs. The Venn Diagram represents differentially expressed probesets (adj. $p < 0.05$). ALL1 (B-other), ALL2 (*ETV6-RUNX1*), ALL3 (*ETV6-RUNX1*) and ALL4 (B-other) altered expression of 257, 8, 1676, 5 probesets, respectively. (**C**) Increased expression levels of *STAT1* (probeset: AFFX-HUMISGF3a) in MSCs upon co-culture with primary BCP-ALL cells. Expression values in co-culture were normalized to expression values in mono-culture. ** adj. $p < 0.01$. (**D**) Increased expression levels of *IFI6* (probeset 204415_at), and *IFITM1* (probeset: 214022_at) in MSCs upon co-culture with primary BCP-ALL cells. Expression values in co-culture were normalized to expression values in mono-culture. ** adj. $p<0.001$. (**E**) Expression levels of *STAT1*, *IFI6*, and *IFITM1* determined by gene expression profiling was correlated with levels determined by RT-qPCR. Spearman correlation coefficients are shown. $p<0.0001$.

Limma analyses revealed multiple genes to be differentially expressed in MSCs upon co-culture with BCP-ALL cells compared to mono-cultures of these MSCs. Alterations were independent of the MSC source (leukemic-MSC or control-MSC), but most strikingly, the changed gene expression profile depended on the source of the leukemia sample. Co-culture of an identical BCP-ALL sample with six different MSCs induced similar changes in gene expression in all MSCs. Each BCP-ALL sample induced a specific profile, resulting into an altered expression ranging from 5 to 1676 probesets in MSCs (adj. $p<0.05$; Figure 2B). Although the number of probesets altered by ALL patient 2 (ALL2) and ALL patient 4 (ALL4) were low, differentially expressed genes overlapped with those induced by ALL patient 1 (ALL1) and ALL patient 3 (ALL3; 7/8 and 5/5, respectively). To study whether specific pathways were affected, Ingenuity pathway analysis was performed. Interestingly, the interferon pathway was significantly upregulated in MSCs after co-culture with ALL1, ALL3, and ALL4 ($p < 1E-07$; Figure S4). The inflammation-associated transcription factor *STAT1* was the most upstream gene in the pathway for which expression levels were changed (Figure 2C, Figure S4). In addition, also genes more downstream in the pathway were affected (e.g. IFI6 and IFITM1, Figure 2D, Figure S4). Upregulation of *STAT1*, *IFI6*, and *IFITM1* was validated using RT-qPCR (Figure 2E). Taken together, gene expression profiles of MSCs were significantly changed after co-culture with primary BCP-ALL cells. These results indicate that BCP-ALL cells drive gene expression changes in MSCs. Although induced changes were leukemia-sample specific, three out of the four ALL samples upregulated the interferon/STAT1 pathway in MSCs.

Gene expression profiles of MSCs from leukemia patients are comparable to control-MSCs

In order to study the persistence of the induced changes in the gene expression profile of MSCs, MSCs were cultured for approximately 14 days without leukemic cells. Microarray analyses were performed of primary MSCs derived from bone marrow samples collected at initial diagnose (n=35; leukemic-MSCs), after induction and consolidation therapy when patients are in remission of their leukemia (n=29; remission MSCs), and at relapse (n=6; relapse-MSCs). These profiles were compared to the gene expression profile of 16 control-MSCs. Limma analyses revealed 234 probesets to be differentially expressed between leukemic-MSCs and control-MSCs (adj. $p<0.05$; Figure 3A). Strikingly, only 27 probesets overlapped with the probesets induced in MSCs upon co-culture with BCP-ALL cells. In addition, none of the 234 differentially expressed probesets could classify MSCs as either healthy or leukemic. Variation between samples was large and fold-changes were low, as visualized in Figure 3B-C for the probesets with the highest and lowest fold change. Principal component analyses revealed that MSCs could not be classified by origin using this gene expression signature (Figure 3D). Additionally, pathway analysis revealed a low number of differentially expressed genes per pathway (≤ 5) between control-MSCs and leukemic-MSCs (overlap < 11%), suggesting no strong difference between leukemic-MSCs and control-MSCs. Furthermore, no overlap with pathways induced upon co-culture with BCP-ALL cells was observed (Figure S5A). In relapse MSCs, one probeset was significantly upregulated compared to control-MSCs, though this upregulation was only observed in two samples (Figure S5B). Most strikingly, remission-MSCs were similar to both control-MSCs and leukemic-MSCs (Figure 3A-B). As these MSCs were isolated after induction and consolidation therapy, these results suggest that gene expression changes

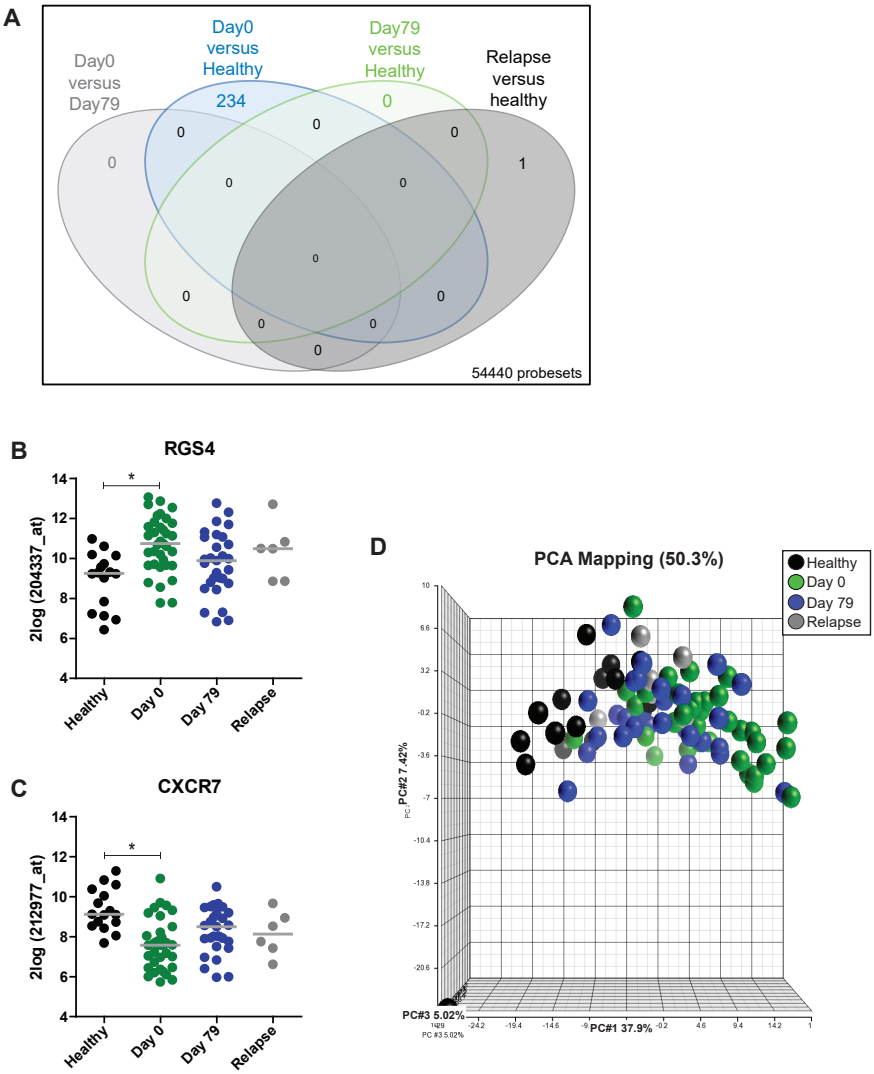

Figure 3. Gene expression signatures of MSCs derived at various time-point of leukemia or healthy controls.

Gene expression profiling of 86 primary MSCs isolated from 35 newly diagnosed BCP-ALL cases (leukemic-MSCs), 29 patients after 79 days of (induction and consolidation) therapy (remission-MSCs), 6 relapse patients (relapse-MSCs), and 16 MSCs healthy controls (control-MSCs). (**A**) Venn Diagram showing Limma results of significant differentially expressed probesets (adj. $p < 0.05$). 234 probesets were differentially expressed between leukemic-MSCs and control-MSCs. One probeset was differentially expressed between relapse-MSCs and control-MSCs. (**B**) Significant difference in *RGS4* expression levels between leukemic-MSCs and control-MSCs. RGS4 represents the probeset with the largest positive log fold change. * adj. $p < 0.05$. (**C**) Significant difference in *CXCR7* expression levels between leukemic-MSCs and control-MSCs. CXCR7 represents the probeset with the largest negative log fold change. * adj. $p < 0.05$. (**D**) PCA analyses of the 234 differentially expressed from panel A. Control-MSCs are depicted in black, leukemic-MSCs in green, remission-MSCs in blue, and relapse MSCs in grey.

between control-MSCs and leukemic-MSCs are transient. For example, the expression of *RGS4* was significantly higher in leukemic-MSCs compared to control-MSC, but reduced to almost normal levels after induction and consolidation therapy (remission-MSCs; Figure 3B). Taken together, changes induced in the gene expression profile of MSCs upon co-culture with BCP-ALL cells are not persistent. Furthermore, our results imply that only marginal differences exist in gene expression between leukemic-MSCs and control-MSCs. Changes are likely induced by the presence of leukemic cells, since elimination of leukemic cells (remission-MSCs) restores gene expression profiles.

Interference with the STAT1 pathway

Our results indicate that an increased survival of BCP-ALL cells, coincides with a changed gene expression profile in MSCs. These changes are not persistent, but rather restored upon elimination of leukemic cells and therefore indicate that BCP-ALL cells drive the altered gene expression program of MSCs. The interferon/STAT1 pathway was most frequently induced, suggesting importance of the pathway in the interaction between leukemic cells and MSCs. Interestingly, in mesenchymal progenitors activation of interferon/STAT1 responses regulate the differentiation and proliferation of hematopoietic stem cells (HSCs) and pathway activation is characterized by secretion of the pro-inflammatory CXC chemokine ligand 10 (CXCL10, IP-10).[8] In the leukemia-sample that most strongly induced *STAT1* and its downstream targets (ALL3), we also observed the secretion of IP-10 upon co-culture with MSCs (Figure 4A). As inflammatory signals have been reported to promote proliferation and differentiation of HSCs,[17, 18, 29, 30] we questioned whether BCP-ALL cells use similar features for their expansion. Activation of the interferon/STAT1 pathway in MSCs was mimicked by IFNα exposure, inducing expression of STAT1, IFI6 and IFITM1 mRNA expression levels (Figure 4B) and secretion of IP-10 (Figure 4C), suggesting that MSCs are the source of the chemokine. To further elucidate the therapeutic potential of interferon/STAT1 pathway, *STAT1* expression was silenced in three MSCs. Efficiency of gene silencing ranged between 60% and 80% (Figure 5A-B). Knockdown of *STAT1* in MSCs did not affect the increased survival of BCP-ALL cells upon co-culture with MSCs, demonstrated by a comparable survival of leukemic cells after two and five days of co-culture with *STAT1*-silenced-MSCs and scrambled-control-MSCs (Figure 5C). Secretion of IP-10 was only detected after co-culture of MSCs with ALL3. Although secretion was below limit of detection in MSCs transduced with shRNA-2, no effect on secretion levels was observed in MSCs transduced with shRNA-1 and shRNA 3 (Figure S6). Taken together, these preliminary results suggest that knockdown of STAT1 in MSCs does not affect the survival benefit of BCP-ALL cells induced by MSCs.

DISCUSSION

In recent years, it has been increasingly recognized that the tumor microenvironment has an essential role in cancer initiation and progression.[31] Tumor cells can take advantages of niche specific signaling, manipulate their microenvironment to promote survival, or cancer might even be the consequence of a disrupted microenvironment.[32-34] Unraveling the role of the bone marrow niche in pediatric BCP-ALL may provide novel options for therapeutic intervention. Results presented in this study indicate that leukemic-MSCs are not intrinsically different compared to control-MSCs. However, BCP-ALL cells instruct MSCs to change their phenotype.

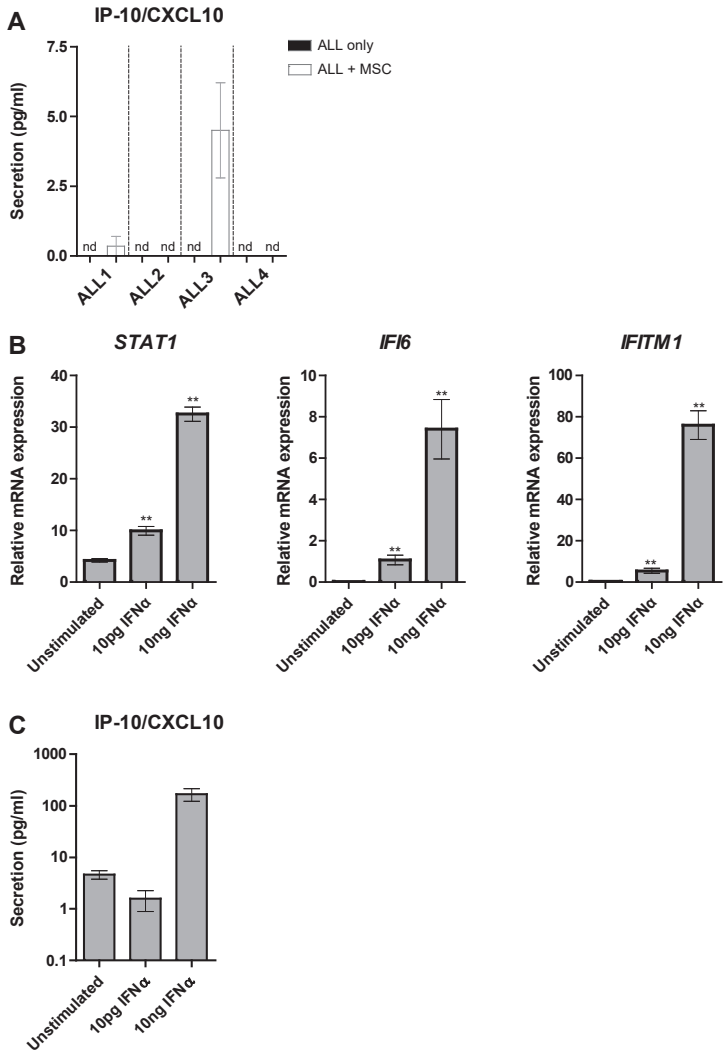

Figure 4. STAT1 signaling and IP-10 secretion.

(**A**) Levels of secreted chemokines/cytokines were determined in the supernatant of MSC and BCP-ALL after 40 hours of mono-culture (n=6 MSCs; n=4 ALL samples) or co-culture (n=24; see Figure 2A). Supernatant was removed from cell cultures and centrifuged to remove cell debris. IP-10 levels were determined using a multiplexed fluorescent bead-based immunoassay. Signal intensity values of MSC mono-culture samples was subtracted from corresponding ALL/MSC co-culture fractions. Mean ± SEM of IP-10 levels in ALL mono-cultures or ALL/MSC co-cultures is shown. nd=not detectable/ below limit of detection. (**B**) MSCs (n=8) were stimulated for 48 hours with 10 pg or 10 ng IFNα. Expression of *STAT1*, *IFI6*, and *IFITM1* was determined using RT-qPCR. Relative mRNA expression levels towards GAPDH are shown. Mean ± SEM of eight independent samples is shown. Paired Samples T-test. ** $p \leq 0.01$. (**C**) MSCs (n=8) were stimulated for 48 hours with 10 pg or 10 ng IFNα. Levels of IP-10 in the supernatant of (non-)IFNα-exposed MSC cultures were determined using ELISA. Mean ± SEM of eight independent samples is shown. Paired Samples T-test. ** $p \leq 0.01$.

Our data revealed that both control-MSCs and leukemic-MSCs promote the survival of primary BCP-ALL cells. No difference in support between both sources of MSCs was observed. Moreover, gene expression profiles of MSCs were significantly changed after co-culture with primary BCP-ALL cells. Each BCP-ALL sample induced a characteristic

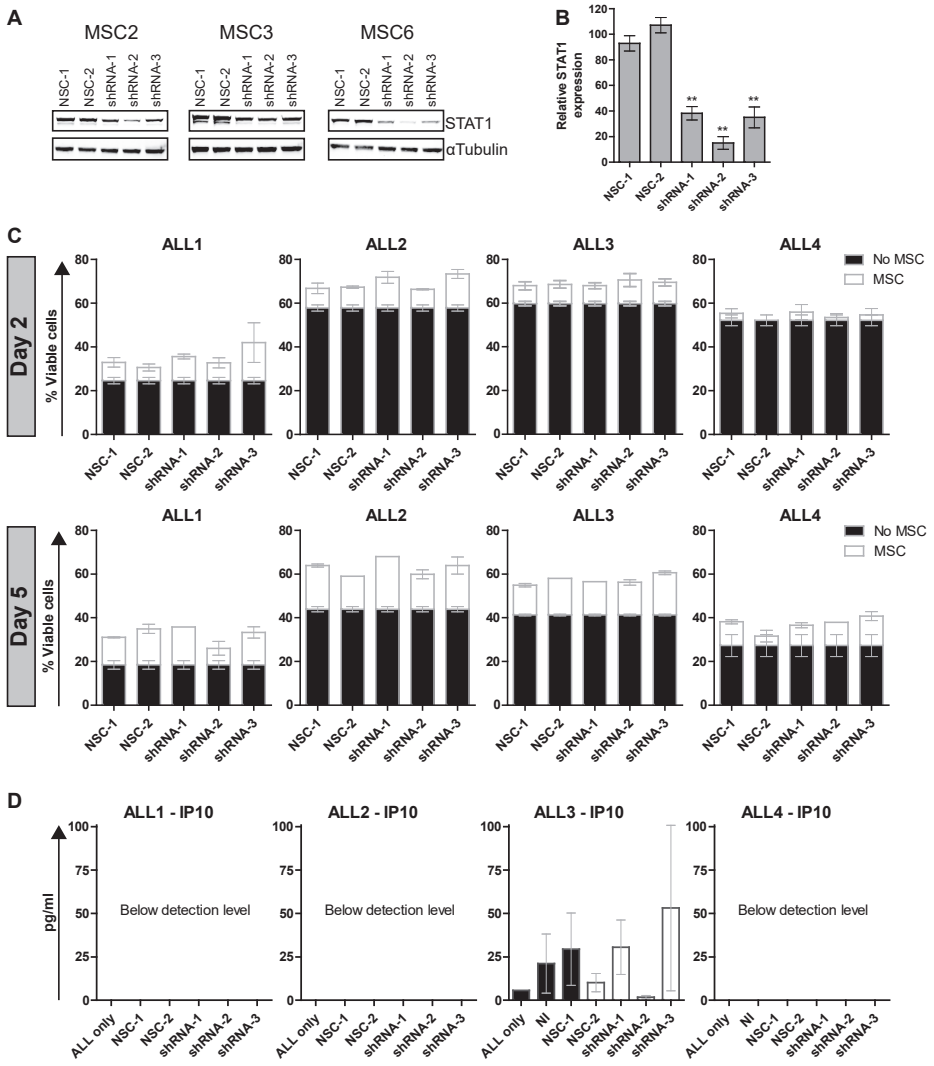

Figure 5. Knockdown of STAT1 in MSCs does not alter the survival benefit for BCP-ALL cells.
STAT1 was silenced in MSCs (n=3) using three different shRNAs against STAT1. (**A**) Western blot analyses of STAT1 and αTubulin expression levels in 15 µg lysate of the three MSCs. (**B**) Quantified protein expression levels of STAT1 relative to αTubulin. Mean ± SEM of three independent samples is depicted. (**C**) Percentage of viable primary leukemia cells (n=4) in mono-culture compared to the survival in co-culture with MSCs (n=3). BCP-ALL cell survival was assessed after two or five days of culture using flow cytometry. Leukemic cell survival (AnnexinV-/PI-) was quantified in the CD19+-positive fraction. Mean ± SEM of three independent samples is depicted.

gene expression change, which was consistent between different MSCs. These results suggest that BCP-ALL cells drive gene expression changes in MSCs. This change in gene expression was only transient, as elimination of leukemic cells (remission-MSCs) restored gene expression levels back to levels as observed in control-MSCs. Although conflicting results have been reported concerning the genetic background of MSCs in pediatric BCP-ALL,[21, 35, 36] our results indicate that MSCs derived from pediatric BCP-ALL cases are not abnormal. Rather BCP-ALL cells have a transient effect on the gene expression profile MSCs, which coincides with an increased survival of leukemia cells.

Dysfunction of the bone marrow has been reported to contribute to the development of myeloid malignancies and vice versa leukemogenesis can induce abnormal bone marrow niches.[37-41] Moreover, these niche supporting properties seem to be leukemia-type specific: osteoblastic cell-specific activation attenuated chronic myeloid leukemia (CML), but in turn enhanced acute myeloid leukemia progression.[41] In a T-cell ALL mice model, normal hematopoiesis was suppressed by leukemic cells that hijacked the proliferative vascular space and repressed the endosteal niche.[23] In addition, pro-inflammatory cytokines are responsible for the reinforcement of the leukemic niche in CML.[40] In line with these data, results obtained in the present study imply that MSCs are not actively involved in the initiation of BCP-ALL nor the induction of a relapse. Rather BCP-ALL cells manipulate the bone marrow niche. Further research is required to confirm our findings and unravel whether the altered gene expression profile of MSCs attenuates normal hematopoiesis and favors leukemogenesis.

The interferon/STAT1 pathway was the most commonly induced pathway in MSCs upon co-culture with primary BCP-ALL cells. Induction of a pro-inflammatory expression profile in MSCs is in concordance with a study focusing on the interaction between acute myeloid cell lines and MSCs.[22] The inflammation-associated transcription factor *STAT1* is involved in a variety of cellular processes and is generally considered as tumor suppressor.[42] However, emerging data suggest a role for STAT1 in tumorigenesis.[42, 43] In addition, inflammatory signals are reported to promote proliferation and differentiation of HSCs.[17, 18, 29, 30] To preserve self-renewing capacity and prevent stem cell exhaustion, HSCs generally remain in a quiescent, dormant state. Though, under certain conditions of stress, HSCs can be stimulated to proliferate and differentiate in order to replenish lineages which are lost.[17] It has been postulated that stress, e.g. inflammation, increases the risk of accumulation of genetic alterations in HSCs, which can facilitate leukomogenesis.[18, 32, 34] Moreover, activation of the interferon/STAT1 pathway in murine endosteal mesenchymal progenitors induced proliferation and differentiation of HSCs and resulted in an overproduction of IP-10.[8] BCP-ALL cells may use similar features as HSCs for their expansion, suggesting involvement of STAT1 in leukemogenic processes. Our preliminary data did not reveal that *STAT1* expression is essential for the viability of BCP-ALL cells. However, residual expression levels of *STAT1* or rescue via alternative pathways may have occurred and therefore the role of the interferon/STAT1 pathway in BCP-ALL remains elusive.[44]

To communicate, leukemic cells and MSCs need to signal, which can occur through soluble factors and cellular projections.[45] In the present study, we observed secretion of IP-10 upon co-culture of MSCs and BCP-ALL cells. IP-10 can be secreted from a variety of cells under pro-inflammatory conditions (e.g. stromal cells, monocytes) and has been implicated in several types of cancers.[46] Co-culture of primary BCP-ALL cells with monocytes also resulted in secretion of IP-10, which induced migration and invasion

of leukemic cells.[47] Our results point to a potential similar mechanism induced by the interaction between leukemic cells and MSCs. This is further strengthened by our recent study, in which we showed that co-culture of BCP-ALL cells and MSCs creates a niche that facilitates migration of additional leukemic cells, but not of healthy CD34+ cells.[48] Besides interaction via soluble factors, tunneling nanotubes can form a physical connection between ALL cells and MSCs.[14] These tunneling nanotubes can transfer various cargo, e.g. mitochondria and autophagosomes.[45, 49, 50] Autophagy is a known regulator of cytokine signaling and hence transfer of autophagosomes via these tunneling nanotubes might explain the release of CXCL10.[49, 51] In addition, transfer of structures via these tunneling nanotubes might be an explanation for the altered gene expression observed in MSCs in the present study. Targeting this direct communication between BCP-ALL cells and MSCs or downstream factors of these processes might offer alternative treatment approaches.
In conclusion, our results indicate that the gene expression profile of leukemic-MSCs is intrinsically not different from that of control-MSCs. However, BCP-ALL cells enforce changes in the gene expression profile of MSCS, which coincide with an increased viability of BCP-ALL cells. These changes are transient and are restored upon removal of leukemic cells. Therefore, our results suggest that the bone marrow microenvironment by itself is not leukemogenic, but is actively being hijacked by leukemic cells to support the pathogenesis of BCP-ALL. Targeting this interplay between leukemic cells and MSCs might represent a novel treatment approach.

Acknowledgements

We would like to thank Yun Lei Li for her support with the Partek software.
This work was supported by the VICI program grant 016.126.612 from Netherlands Organization for Scientific Research (NWO), the Dutch Cancer Society grants AMC 2008-4265 and EMCR 2014-6998, the Kika Foundation (grant 132) and the Pediatric Oncology Foundation Rotterdam.

Authorship Contributions

EMPS, R. Polak, and BR designed and performed experiments, and analyzed and interpreted data. LCJvdB isolated and characterized MSCs. EMPS and CvdV performed microarray experiments. EMPS and JMB analyzed gene expression data. FS and MB performed experiments. R. Pieters and MLdB conceptualized the study, and interpreted data. EMPS and MLdB drafted the manuscript. The manuscript was revised and approved by all authors.

Disclosure of Conflicts of Interest

The authors declare no conflicts of interest.

REFERENCES

1. Sun Z, Wang S, Zhao RC. The roles of mesenchymal stem cells in tumor inflammatory microenvironment. J Hematol Oncol. 2014;7:14.
2. Hong IS, Lee HY, Kang KS. Mesenchymal stem cells and cancer: friends or enemies? Mutat Res. 2014 Oct;768:98-106.
3. Calon A, Espinet E, Palomo-Ponce S, Tauriello DV, Iglesias M, Cespedes MV, et al. Dependency of colorectal cancer on a TGF-beta-driven program in stromal cells for metastasis initiation. Cancer Cell. 2012 Nov 13;22(5):571-84.
4. Koontongkaew S. The tumor microenvironment contribution to development, growth, invasion and metastasis of head and neck squamous cell carcinomas. J Cancer. 2013;4(1):66-83.
5. Pietras K, Ostman A. Hallmarks of cancer: interactions with the tumor stroma. Exp Cell Res. 2010 May 1;316(8):1324-31.
6. D'Souza N, Burns JS, Grisendi G, Candini O, Veronesi E, Piccinno S, et al. MSC and Tumors: Homing, Differentiation, and Secretion Influence Therapeutic Potential. Adv Biochem Eng Biotechnol. 2013;130:209-66.
7. Whiteside TL. The tumor microenvironment and its role in promoting tumor growth. Oncogene. 2008 Oct 6;27(45):5904-12.
8. Guarnerio J, Coltella N, Ala U, Tonon G, Pandolfi PP, Bernardi R. Bone marrow endosteal mesenchymal progenitors depend on HIF factors for maintenance and regulation of hematopoiesis. Stem Cell Reports. 2014 Jun 3;2(6):794-809.
9. Qi XF, Kim DH, Yoon YS, Jin D, Huang XZ, Li JH, et al. Essential involvement of cross-talk between IFN-gamma and TNF-alpha in CXCL10 production in human THP-1 monocytes. J Cell Physiol. 2009 Sep;220(3):690-7.
10. Pui CH, Evans WE. A 50-year journey to cure childhood acute lymphoblastic leukemia. Semin Hematol. 2013 Jul;50(3):185-96.
11. Colmone A, Amorim M, Pontier AL, Wang S, Jablonski E, Sipkins DA. Leukemic cells create bone marrow niches that disrupt the behavior of normal hematopoietic progenitor cells. Science. 2008 Dec 19;322(5909):1861-5.
12. McMillin DW, Delmore J, Weisberg E, Negri JM, Geer DC, Klippel S, et al. Tumor cell-specific bioluminescence platform to identify stroma-induced changes to anticancer drug activity. Nat Med. 2010 Apr;16(4):483-9.
13. Lane SW, Scadden DT, Gilliland DG. The leukemic stem cell niche: current concepts and therapeutic opportunities. Blood. 2009 Aug 6;114(6):1150-7.
14. Polak R, de Rooij B, Pieters R, den Boer ML. B-cell precursor acute lymphoblastic leukemia cells use tunneling nanotubes to orchestrate their microenvironment. Blood. 2015 Nov 19;126(21):2404-14.
15. Iwamoto S, Mihara K, Downing JR, Pui CH, Campana D. Mesenchymal cells regulate the response of acute lymphoblastic leukemia cells to asparaginase. J Clin Invest. 2007 Apr;117(4):1049-57.
16. Vianello F, Villanova F, Tisato V, Lymperi S, Ho KK, Gomes AR, et al. Bone marrow mesenchymal stromal cells non-selectively protect chronic myeloid leukemia cells from imatinib-induced apoptosis via the CXCR4/CXCL12 axis. Haematologica. 2010 Jul;95(7):1081-9.
17. Baldridge MT, King KY, Goodell MA. Inflammatory signals regulate hematopoietic stem cells. Trends Immunol. 2011 Feb;32(2):57-65.
18. Takizawa H, Boettcher S, Manz MG. Demand-adapted regulation of early hematopoiesis in infection and inflammation. Blood. 2012 Mar 29;119(13):2991-3002.
19. Cai J, Wang J, Huang Y, Wu H, Xia T, Xiao J, et al. ERK/Drp1-dependent mitochondrial fission is involved in the MSC-induced drug resistance of T-cell acute lymphoblastic leukemia cells. Cell death & disease. 2016 Nov 10;7(11):e2459.
20. Fei F, Joo EJ, Tarighat SS, Schiffer I, Paz H, Fabbri M, et al. B-cell precursor acute lymphoblastic leukemia and stromal cells communicate through Galectin-3. Oncotarget. 2015 May 10;6(13):11378-94.
21. Conforti A, Biagini S, Del Bufalo F, Sirleto P, Angioni A, Starc N, et al. Biological, functional and genetic characterization of bone marrow-derived mesenchymal stromal cells from pediatric patients affected by acute lymphoblastic leukemia. PLoS One. 2013;8(11):e76989.
22. Civini S, Jin P, Ren J, Sabatino M, Castiello L, Jin J, et al. Leukemia cells induce changes in human bone marrow stromal cells. J Transl Med. 2013;11:298.
23. Wang W, Zimmerman G, Huang X, Yu S, Myers J, Wang Y, et al. Aberrant Notch Signaling in the Bone Marrow Microenvironment of Acute Lymphoid Leukemia Suppresses Osteoblast-Mediated Support of Hematopoietic Niche Function. Cancer Res. 2016 Mar 15;76(6):1641-52.
24. Den Boer ML, Harms DO, Pieters R, Kazemier KM, Gobel U, Korholz D, et al. Patient stratification based on prednisolone-vincristine-asparaginase resistance profiles in children with acute lymphoblastic leukemia. J Clin Oncol. 2003 Sep 01;21(17):3262-8.
25. Den Boer ML, van Slegtenhorst M, De Menezes RX, Cheok MH, Buijs-Gladdines JG, Peters ST, et al. A subtype of childhood acute lymphoblastic leukaemia with poor treatment outcome: a genome-wide classification study. Lancet Oncol. 2009 Feb;10(2):125-34.
26. van den Berk LC, van der Veer A, Willemse ME, Theeuwes MJ, Luijendijk MW, Tong WH, et al. Disturbed CXCR4/CXCL12 axis in paediatric precursor B-cell acute lymphoblastic leukaemia. Br J Haematol. 2014 Jul;166(2):240-9.
27. Huber W, von Heydebreck A, Sultmann H, Poustka A, Vingron M. Variance stabilization applied to microarray data calibration and to the quantification of differential expression. Bioinformatics. 2002;18 Suppl 1:S96-104.
28. Edgar R, Domrachev M, Lash AE. Gene Expression Omnibus: NCBI gene expression and hybridization array data repository. Nucleic acids research. 2002 Jan 01;30(1):207-10.

29. King KY, Goodell MA. Inflammatory modulation of HSCs: viewing the HSC as a foundation for the immune response. Nat Rev Immunol. 2011 Sep 09;11(10):685-92.
30. Schuettpelz LG, Link DC. Regulation of hematopoietic stem cell activity by inflammation. Front Immunol. 2013;4:204.
31. Li L, Neaves WB. Normal stem cells and cancer stem cells: the niche matters. Cancer Res. 2006 May 1;66(9):4553-7.
32. Raaijmakers MH. Niche contributions to oncogenesis: emerging concepts and implications for the hematopoietic system. Haematologica. 2011 Jul;96(7):1041-8.
33. Schepers K, Campbell TB, Passegue E. Normal and leukemic stem cell niches: insights and therapeutic opportunities. Cell stem cell. 2015 Mar 05;16(3):254-67.
34. Sneddon JB, Werb Z. Location, location, location: the cancer stem cell niche. Cell stem cell. 2007 Dec 13;1(6):607-11.
35. Menendez P, Catalina P, Rodriguez R, Melen GJ, Bueno C, Arriero M, et al. Bone marrow mesenchymal stem cells from infants with MLL-AF4+ acute leukemia harbor and express the MLL-AF4 fusion gene. Journal of Experimental Medicine. 2009 Dec 21;206(13):3131-41.
36. Shalapour S, Eckert C, Seeger K, Pfau M, Prada J, Henze G, et al. Leukemia-associated genetic aberrations in mesenchymal stem cells of children with acute lymphoblastic leukemia. Journal of Molecular Medicine. 2010 Mar;88(3):249-65.
37. Walkley CR, Shea JM, Sims NA, Purton LE, Orkin SH. Rb regulates interactions between hematopoietic stem cells and their bone marrow microenvironment. Cell. 2007 Jun 15;129(6):1081-95.
38. Walkley CR, Olsen GH, Dworkin S, Fabb SA, Swann J, McArthur GA, et al. A microenvironment-induced myeloproliferative syndrome caused by retinoic acid receptor gamma deficiency. Cell. 2007 Jun 15;129(6):1097-110.
39. Raaijmakers MH, Mukherjee S, Guo S, Zhang S, Kobayashi T, Schoonmaker JA, et al. Bone progenitor dysfunction induces myelodysplasia and secondary leukaemia. Nature. 2010 Apr 8;464(7290):852-7.
40. Schepers K, Pietras EM, Reynaud D, Flach J, Binnewies M, Garg T, et al. Myeloproliferative neoplasia remodels the endosteal bone marrow niche into a self-reinforcing leukemic niche. Cell stem cell. 2013 Sep 05;13(3):285-99.
41. Krause DS, Fulzele K, Catic A, Sun CC, Dombkowski D, Hurley MP, et al. Differential regulation of myeloid leukemias by the bone marrow microenvironment. Nat Med. 2013 Nov;19(11):1513-7.
42. Avalle L, Pensa S, Regis G, Novelli F, Poli V. STAT1 and STAT3 in tumorigenesis: A matter of balance. Jak-Stat. 2012 Apr 01;1(2):65-72.
43. Alvaro T, Lejeune M, Camacho FI, Salvado MT, Sanchez L, Garcia JF, et al. The presence of STAT1-positive tumor-associated macrophages and their relation to outcome in patients with follicular lymphoma. Haematologica. 2006 Dec;91(12):1605-12.
44. Blaszczyk K, Nowicka H, Kostyrko K, Antonczyk A, Wesoly J, Bluyssen HA. The unique role of STAT2 in constitutive and IFN-induced transcription and antiviral responses. Cytokine & growth factor reviews. 2016 Jun;29:71-81.
45. Abounit S, Zurzolo C. Wiring through tunneling nanotubes--from electrical signals to organelle transfer. J Cell Sci. 2012 Mar 01;125(Pt 5):1089-98.
46. Liu M, Guo S, Stiles JK. The emerging role of CXCL10 in cancer (Review). Oncology letters. 2011 Jul;2(4):583-9.
47. Lee Y, Chittezhath M, Andre V, Zhao H, Poidinger M, Biondi A, et al. Protumoral role of monocytes in human B-cell precursor acute lymphoblastic leukemia: involvement of the chemokine CXCL10. Blood. 2012 Jan 05;119(1):227-37.
48. de Rooij B, Polak R, van den Berk LCJ, Stalpers F, Pieters R, den Boer ML. Acute lymphoblastic leukemia cells create a leukemic niche without affecting the CXCR4/CXCL12 axis. Haematologica. 2017 Jun 15.
49. de Rooij B, Polak R, Stalpers F, Pieters R, Boer MLD. Tunneling nanotubes facilitate autophagosome transfer in the leukemic niche. Leukemia. 2017 Jul;31(7):1651-4.
50. Saenz-de-Santa-Maria I, Bernardo-Castineira C, Enciso E, Garcia-Moreno I, Chiara JL, Suarez C, et al. Control of long-distance cell-to-cell communication and autophagosome transfer in squamous cell carcinoma via tunneling nanotubes. Oncotarget. 2017 Mar 28;8(13):20939-60.
51. Mathew R, Karantza-Wadsworth V, White E. Role of autophagy in cancer. Nat Rev Cancer. 2007 Dec;7(12):961-7.

SUPPLEMENTAL DATA

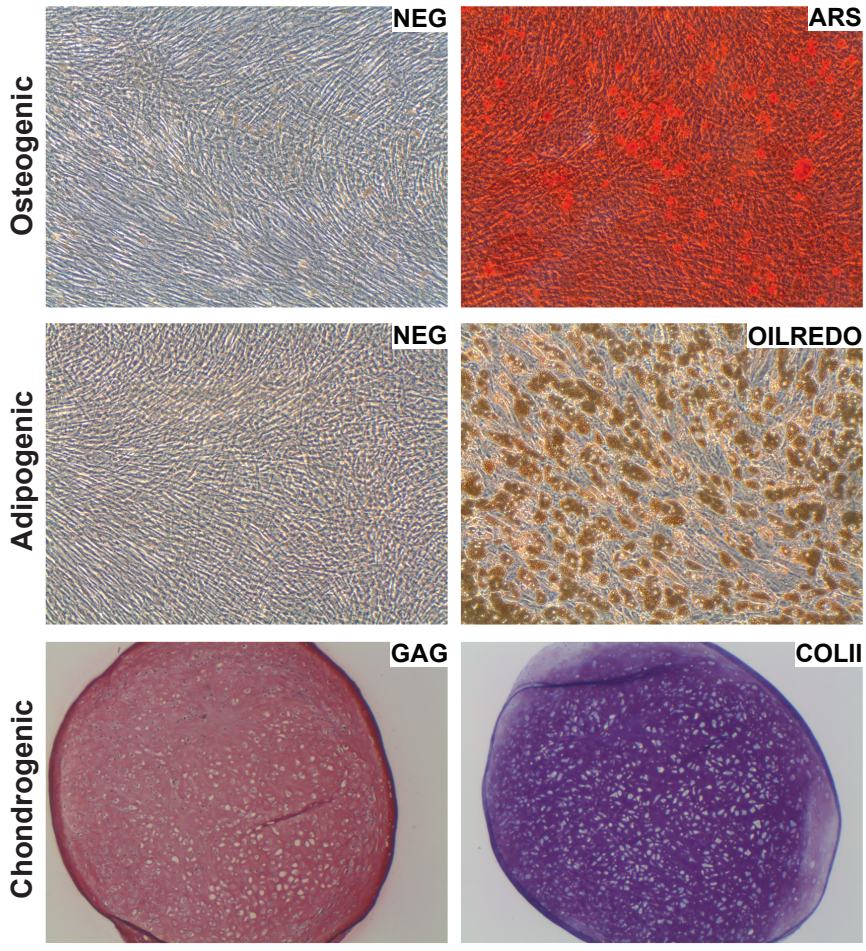

Supplementary Figure 1. Multi-lineage potential of MSCs.
Multi-lineage potential of isolated primary MSCs was confirmed for adipocyte (Oil Red O staining), osteocyte (Alizarin Red S staining), and chondrocyte (glycosaminoglycan (GAG) staining and Col2a/Thionine/Alcian Blue staining) differentiation. A representative experiment is shown, which equals the patterns seen for all leukemic-MSCs and control-MSCs used in this study.

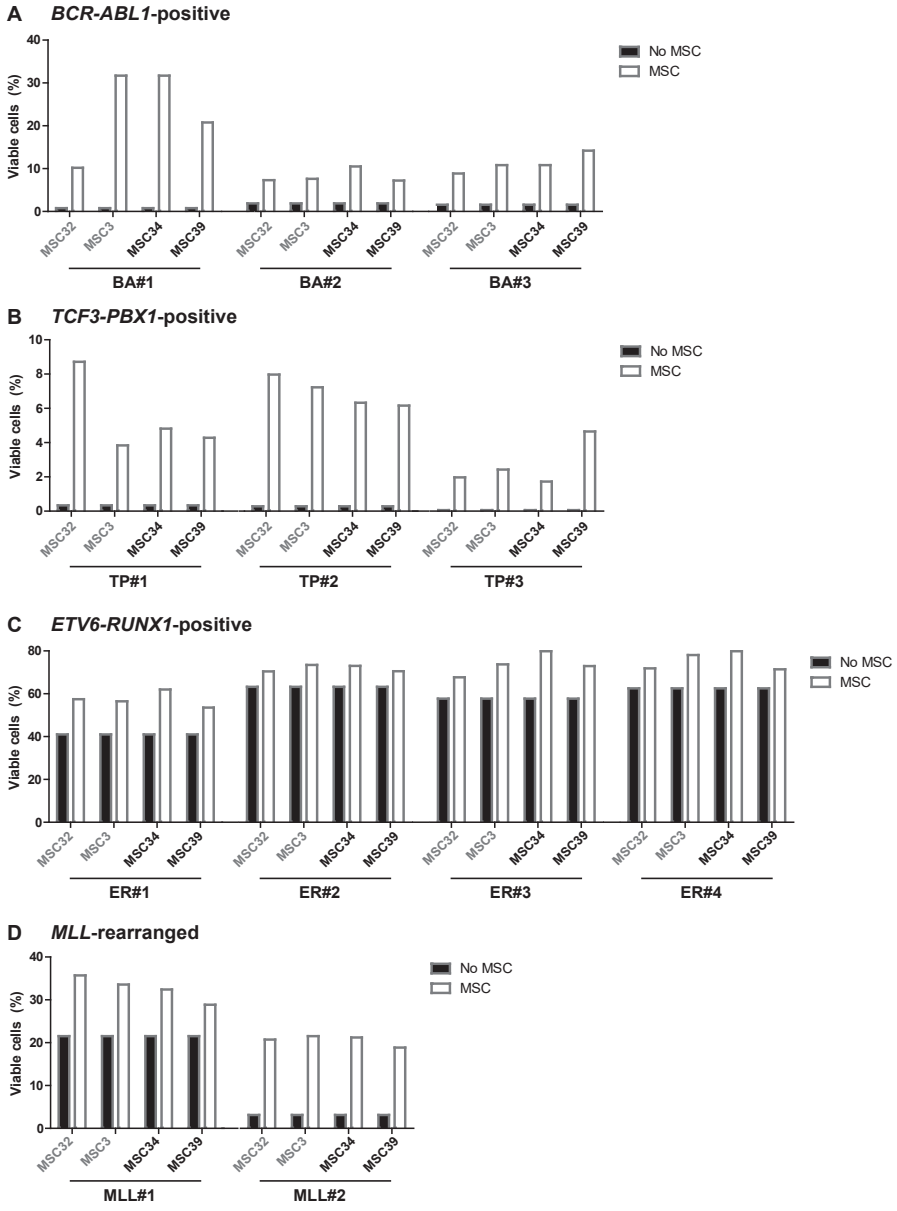

Supplementary Figure 2. BCP-ALL cell survival is supported by control-MSCs and leukemic-MSCs.

Survival of primary CD19+ BCP-ALL cells, co-cultured with two different sources of control-MSCs and leukemic-MSCs (CD19-). BCP-ALL cell survival was assessed after five days of culture using flow cytometry. Leukemic cell survival (AnnexinV-/PI-) was quantified in the CD19+-positive fraction. MSCs depicted in grey represent control-MSCs. MSCs depicted in black represent leukemic-MSCs. (**A-D**) Survival of three *BCR-ABL1*-positive (A), three *TCF3-PBX1*-positive (**B**), four *ETV6-RUNX1*-positive (**C**), and two *KMT2A*-rearranged (**D**) samples on two different sources of control-MSCs and two different sources of leukemic-MSCs. Values of each individual sample are shown.

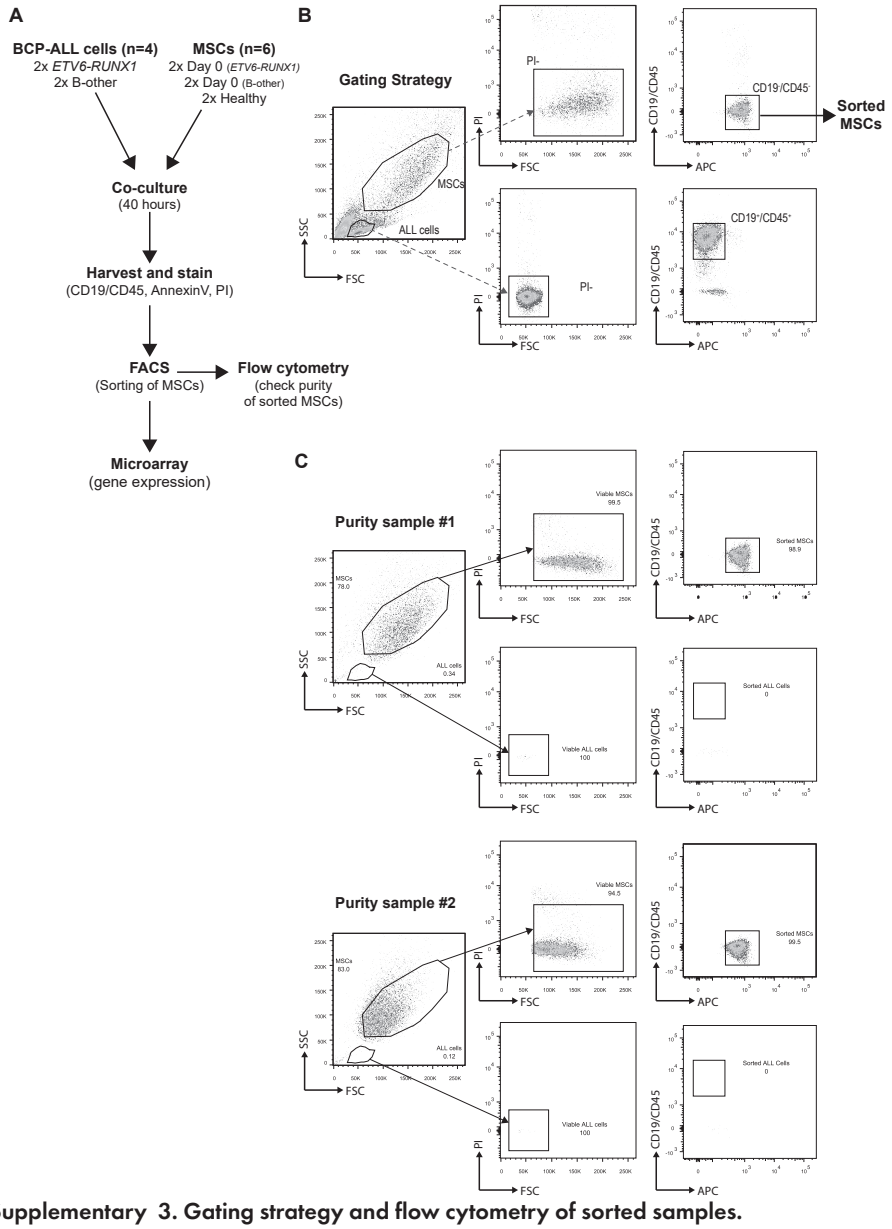

Supplementary 3. Gating strategy and flow cytometry of sorted samples.

(**A**) Primary BCP-ALL cells (n=2 B-other, n=2 *ETV6-RUNX1* samples) were co-cultured for 40 hours with six different sources of primary MSCs (n=2 control-MSCs, n=4 leukemic-MSCs) for 40 hours. MSCs were separated from BCP-ALL cells using FACS. Purity of sorted samples was assessed by flow cytometry. RNA from the sorted MSCs was isolated and gene expression profiling was performed. RNA quality of one sample was poor (RIN<6) and therefore excluded from analysis. (**B**) Gating strategy of FACS experiment. A pre-separation was made based on FSC/SSC. Subsequently, we selected for viable (PI-) cells, and CD19- and CD45 cells. MSCs are slightly autofluorescent in the APC channel, which was also used to separate BCP-ALL cells and MSCs. (**C**) Purity of two sorted MSCs samples was examined using flow cytometry.

Summary of Analysis - ALL1

Top canonical pathways	P-value	Overlap
Interferon Signaling	1.71E-14	30.6% (11/36)
Retinoic acid Mediated Apoptosis Signaling	2.20E-05	9.8% (6/61)
Mitotic Roles of Polo-Like Kinase	3.47E-05	9.1% (6/66)
Death Receptor Signaling	2.23E-04	6.5% (6/92)
Activation of IRF by Cytosolic Pattern Recognition Receptors	2.81E-04	8.1% (5/62)

Top upstream regulators	P-value	Predicted activation
IFNL1	7.36E-34	Activated
IFNA2	5.08E-31	Activated
IRF7	1.11E-28	Activated
PRL	2.15E-27	Activated
MAPK1	3.81E-24	Inhibited

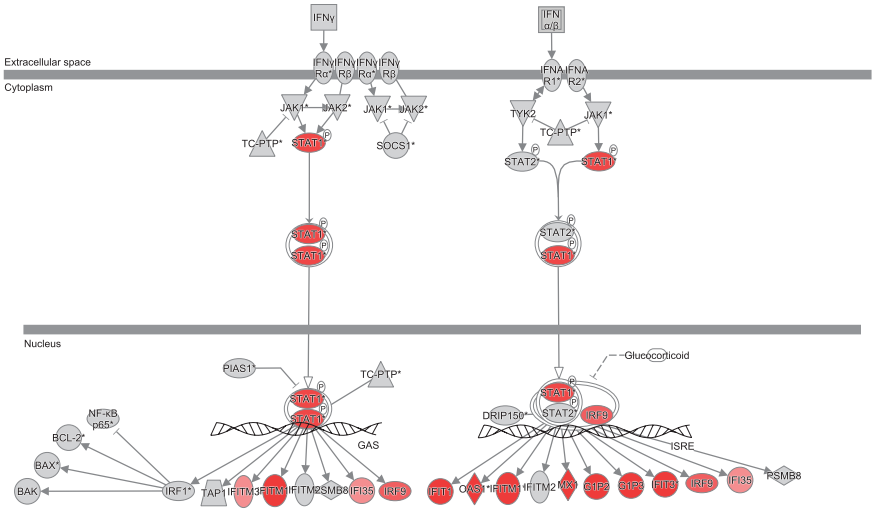

Supplementary Figure 4A. Ingenuity Pathway Analyses results. changes in MSCs induced by ALL1.

(**A-D**) The probesets, which were differentially expressed (Limma; adj. $p < 0.05$) in MSCs (n=6) after co-culture with primary leukemic samples (n=4) compared to MSC monocultures were analyzed using Ingenuity Pathway Analysis. Top 5 most significant canonical pathways and upstream regulators are shown per BCP-ALL sample (ALL1-ALL4). In the interferon/STAT1 pathway, significantly altered genes are depicted in red. *(Figure continued on the next pages)*

Summary of Analysis - ALL2

Top canonical pathways	P-value	Overlap
Pyrimidine Deoxyribonucleotides De Novo Biosynthesis I	5.46E-03	4.3% (1/23)
Glycolysis I	5.93E-03	4.0% (1/25)
Glyconeogenesis I	5.93E-03	4.0% (1/25)
Pyrimidine Ribonucleotides Interconversion	7.59E-03	3.1% (1/32)
Pyrimidine Ribonucleotides De Novo Biosynthesis	8.06E-03	2.9% (1/34)

Top upstream regulators	P-value
NEDD9	3.42E-03
salirasib	1.06E-03
paroxetine I	9.37E-03
COMMD1	1.02E-03
HIF1A	4.11E-03

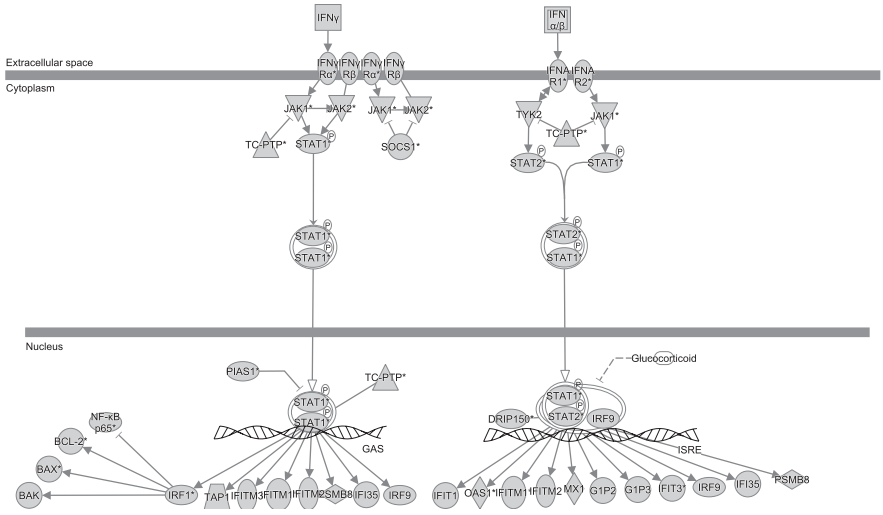

Supplementary Figure 4B. Ingenuity Pathway Analyses results. changes in MSCs induced by ALL2.

(**A-D**) The probesets, which were differentially expressed (Limma; adj. $p < 0.05$) in MSCs (n=6) after co-culture with primary leukemic samples (n=4) compared to MSC monocultures were analyzed using Ingenuity Pathway Analysis. Top 5 most significant canonical pathways and upstream regulators are shown per BCP-ALL sample (ALL1-ALL4). In the interferon/STAT1 pathway, significantly altered genes are depicted in red.

Summary of Analysis - ALL3

Top canonical pathways	P-value	Overlap
Antigen Presentation Pathway	3.64E-11	43.2%% (16/37)
Interferon Signaling I	2.85E-10	41.7% (15/36)
Glycolysis I	3.54E-08	44.0% (11/25)
Cell Cycle Control of Chromosomal Replication	9.34E-08	40.7% (11/27)
Cell Cycle: G2/M DNA Damage Checkpoint regulation	2.99E-07	28.6% (14/49)

Top upstream regulators	P-value	Predicted activation
NKX2-3	8.83E-55	Inhibited
IFNA2	7.98E-54	Activated
TP53	1.11E-49	Inhibited
IFNL1	5.76E-45	Activated
MAPK1	8.03E-44	Inhibited

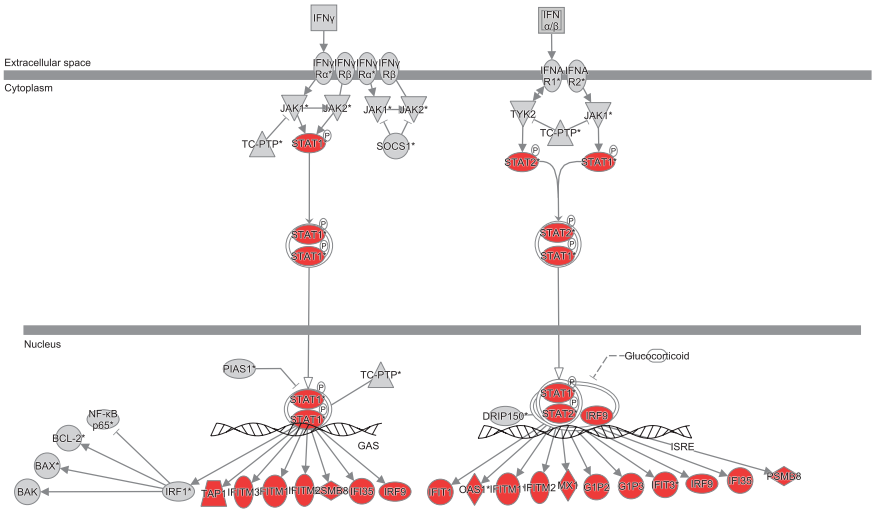

Supplementary Figure 4C. Ingenuity Pathway Analyses results. changes in MSCs induced by ALL3.

(**A-D**) The probesets, which were differentially expressed (Limma; adj. p < 0.05) in MSCs (n=6) after co-culture with primary leukemic samples (n=4) compared to MSC monocultures were analyzed using Ingenuity Pathway Analysis. Top 5 most significant canonical pathways and upstream regulators are shown per BCP-ALL sample (ALL1-ALL4). In the interferon/STAT1 pathway, significantly altered genes are depicted in red.

Summary of Analysis - ALL4

Top canonical pathways	P-value	Overlap
Interferon Signaling	1.84E-08	8.3% (3/36)
Extrinsic Prothrombin Activation Pathway	3.04E-03	6.2% (1.16)
Coagulation System	6.64E-03	2.9% (1/35)
Activation of IRF by Cytosolic Pattern Recognition Receptors	1.17E-02	1.6% (1/62)

Top upstream regulators	P-value
CNOT7	8.62E-09
IFNAR2	2.54E-08
stallimycin	2.91E-08
STAT2	3.11E-08
bromodeoxyuridine	4.49E-08

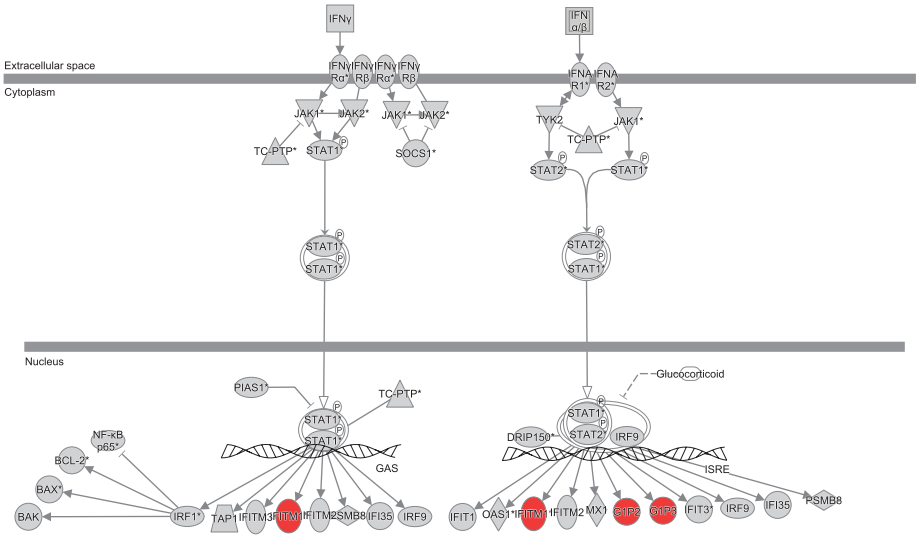

Supplementary Figure 4D. Ingenuity Pathway Analyses results. changes in MSCs induced by ALL4.

(**A-D**) The probesets, which were differentially expressed (Limma; adj. $p < 0.05$) in MSCs (n=6) after co-culture with primary leukemic samples (n=4) compared to MSC monocultures were analyzed using Ingenuity Pathway Analysis. Top 5 most significant canonical pathways and upstream regulators are shown per BCP-ALL sample (ALL1-ALL4). In the interferon/STAT1 pathway, significantly altered genes are depicted in red.

A

Top canonical pathways	P-value	Overlap
Hematopoiesis from Pluripotent Stem Cells	3.59E-05	10.6% (5/47)
Primary Immunodeficiency Signaling	3.98E-05	10.4% (5/48)
B Cell Development	2.29E-03	9.1% (3/33)
Atherosclerosis Signaling	3.56E-03	3.9% (5/127)
PI3K Signaling in B Lymphocytes	3.69E-03	3.9% (5/128)

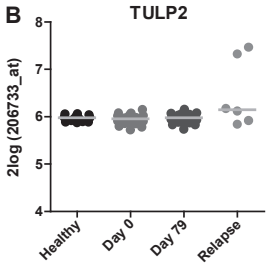

Supplementary Figure 5. Gene expression profiling of leukemic-MSCs and control-MSCs.
Gene expression profiling of 86 primary MSCS isolated from 35 newly diagnosed BCP-ALL cases (leukemic-MSCs), 29 patients after 79 days of (induction) therapy (remission-MSCs), 6 relapse patients (relapse-MSCs), and 16 MSCs healthy controls (control-MSCs).

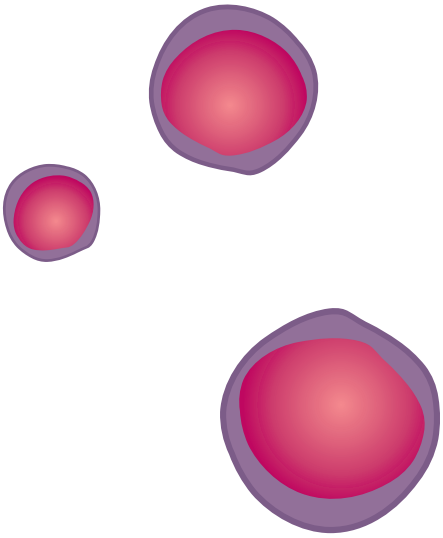

Chapter 7

GENERAL DISCUSSION

Carcinogenesis is a multi-dynamic process, depending on numerous variables. During the last decades, insights increased in the biology of cancer cells. In 2000 Hanahah and Weinberg proposed six hallmarks of cancer cells: sustaining proliferative signaling, evading growth suppressors, resisting cell death, enabling replicative immortality, inducing angiogenesis, activating invasion and metastasis.[1] In 2011 two additional hallmark were added: reprogramming of energy metabolism, and evading immune destruction.[2] Genomic instability and inflammation underlie these hallmarks. In addition, the tumor microenvironment provides another dimension of complexity.[1,2] These hallmarks of cancer cells are key elements for therapeutic intervention.
Normal cells evolve to malignant lesions by acquiring a series of mutations over time. Mutations occur as random events in cells, both in normal and cancer cells. However, only lesions that provide a growth advantage will drive the formation of cancer. A typical tumor contains two to eight of these driver mutations. The remaining mutations that are detected within these tumor samples are passengers, which do not confer a selective growth advantage.[3] It is important to distinguish driving lesions from passenger mutations, as targeting passenger mutations most likely will not be effective in the elimination of cancer cells. Across all different cancer types, numerous driving mutations have been identified. Strikingly, the number of cellular signaling pathways that are affected by these mutations is more limited and can even be reduced to three core cellular processes: cell fate determination, cell survival, and genome maintenance.[3] It is our scientific challenge to determine which mutations are good targets for therapeutic intervention.

Pediatric cancer

Pediatric cancers differ from adult tumors, especially by their very low mutational rate. This low mutational burden might be explained by the origin of pediatric cancers: these cells have not yet been able to renew themselves as often as in adults.[3-6] In addition, leukemias may require fewer rounds of clonal expansion compared to solid tumors.[7,8] Pediatric leukemias are often characterized by chromosomal translocations and therefore less likely arise from small point mutational events.[9] These chromosomal rearrangements result in the formation of fusion genes, which result in activation of proto-oncogenes (e.g. *ABL1*). However, to induce an overt leukemia additional cooperating lesions are required.[10,11]
Acute lymphoblastic leukemia (ALL) is the most common childhood malignancy.[12] During the last decades, outcome of patients improved enormously: in the early 1960 cure rate was approximately 10% whereas nowadays approximately 90% of the patients survives the disease.[13] This remarkable increase in survival was achieved by improved risk stratification, stem cell transplantations and therapy intensification.[14] However, still one out of the ten children diagnosed with ALL in the Netherlands dies due to the consequences of leukemia. Strikingly, the improvement in outcome of ALL cases was achieved without addition of new chemotherapeutic agents, with the exception of the ABL-kinase inhibitor Imatinib for *BCR-ABL1*-positive ALL. The traditional chemotherapeutic agents are already used for decades and are not specific for leukemia. Consequently, survivors of childhood ALL are at risk to develop long-term side effects due to aspecificity of these chemotherapeutic agents.[15] To further improve outcome and reduce side effects new treatment options are warranted. Ideally, unraveling the molecular pathobiology underlying ALL enables specific targeting of oncogenic lesions by precision medicines and thereby improves outcome and reduces side effects.

The treatment of cancer

During the past decades an incredible progress in the field of genomics was made. This resulted in increased knowledge of the pathobiology of diseases and identification of (new) genomic aberrations.[16] In addition, targeted therapies, including kinase inhibitors and therapeutic antibodies, are transforming the field of oncology.[17] Pharmaceutical companies rapidly developed a scale of anti-cancer drugs, which specifically target signaling pathways involved in the survival and expansion of cancer cells. Matching the appropriate targeted therapy to molecular tumor profiles showed successful treatment responses. Among the earliest targeted therapies are imatinib (leukemia), herceptin (breast cancer), and cetuximab (colorectal cancer).[18-20]

Current targeted treatment strategies are predominantly focused on the inactivation of oncogenes that have kinase activity. Unfortunately it remains a challenge to restore the function of tumor suppressors genes, to interfere with transcription factors, or to target the tumor microenvironment. These three important determinants of cancer should also be addressed in the hunt for new druggable targets.

Pathobiology of B-cell precursor acute lymphoblastic leukemia and targeted therapies

Pediatric ALL is a heterogeneous disease, caused by the malignant transformation of either T-cell (T-ALL,~15% of the cases) or B-cell (~85% of the cases) progenitors. The focus of this thesis was on B cell precursor ALL (BCP-ALL). Based on genomic aberrations BCP-ALL can be subdivided in subtypes with different long-term clinical outcome, including the favorable prognostic subtypes *ETV6-RUNX1*, high hyperdiploid, *TCF3*-rearranged, and the poor prognostic subtypes *BCR-ABL1*, and *KMT2A*-rearranged BCP-ALL. However, approximately 25% of the BCP-ALL patients has a genetically unclassified disease and are defined as 'B-other'. The past decade, unraveling the genetic landscape of B-other ALL has been the main focus of many research projects. These genetically unclassified cases can be subdivided in *BCR-ABL1*-like and non-*BCR-ABL1*-like B-other BCP-ALL.[21,22] Whole genome sequencing and RNAseq analyses revealed presence of activating tyrosine kinase lesions in a subgroup of *BCR-ABL1*-like patients, including chromosomal translocations involving ABL class kinases (ABL1, ABL2, PDGFRB, CFS1R) or JAK class kinases (JAK2, CRLF2, EPOR), as shown in literature and **Chapter** 2 of this thesis.[15,23,24] Furthermore, point mutations in tyrosine kinases (e.g. *JAK2*) and cytokine receptors (e.g. *CRLF2*, *IL7R*) were observed in another subgroup of *BCR-ABL1*-like cases.[15,23,24] These observations indicate that *BCR-ABL1*-like cases are characterized by genetic aberrations, resulting in activation of tyrosine kinases. The success story of imatinib in *BCR-ABL1*-positive BCP-ALL cases[25] provides a strong rationale for its implementation in the treatment of ABL class rearranged BCP-ALL. Indeed, case reports have shown that refractory/relapsed patients harboring ABL class fusion genes respond successfully to imatinib.[26-28] Therefore, in the current DCOG-ALL11 study newly diagnosed ABL class rearranged ALL cases with a poor response to induction therapy receive imatinib on top of the treatment protocol.

The COG-study group in the USA initiated a trial to add the JAK1/2 inhibitor ruxolitinib to the treatment protocol of pediatric BCP-ALL patients harboring *JAK2* lesions (*JAK2* translocations and *JAK2* point mutations) or *CRLF2* rearrangements. Although *JAK2* point mutations and *JAK2* translocations represent biologically distinct entities, both may be

targetable by JAK inhibitors. However, results presented in **Chapter 3** of this thesis imply that further optimization and evaluation of JAK inhibitor treatment is necessary prior to its clinical integration in pediatric BCP-ALL. We showed that JAK inhibitors have a high efficacy in *JAK2* mutated and *JAK2* translocated cells. Despite these promising findings, at least three limitations of momelotinib and ruxolitinib were identified. The two JAK inhibitors induced accumulation of phosphorylated JAK2^{Y1007}, which eventually resulted in a profound re-activation of JAK2 signaling upon release of the inhibitors. As these type I inhibitors bind JAK2 in its active conformation, reactivation of JAK2 may be overcome by type II inhibitors, which bind JAK2 in its inactive conformation.[29,30] Preclinical and clinical data of these novel inhibitors (e.g. CHZ868) are therefore warranted.[30] In addition, *JAK2* point mutations are likely secondary aberrations, since we observed that that these mutations occur at subclonal levels of in our pediatric BCP-ALL cohort (**Chapter 3**). Consequently, the effect of JAK inhibition may be compromised in *JAK2* mutated cells by alternative pathway activation. Heterogeneity of the leukemic cell population suggests that mutations in alternative survival pathways (e.g. KRAS mutations) may provide a way for these cells to escape JAK inhibitor treatment.[31] In fact, this is what we observed in NSG mice injected with primary *JAK2*-mutated BCP-ALL cells: a KRAS-mutated subclone grew out at the expense of the major *JAK2*-mutated clone (**Chapter 3**). The third limitation of JAK inhibitor therapy that we observed is micro-environmental-induced resistance. Microenvironment-induced resistance of leukemic cells has also been reported before for conventional drugs, e.g. prednisolone and asparaginase, and for imatinib in *BCR-ABL1*-positive cells.[32-36] These findings highlight that the micro-environmental protection should be taken into account for the evaluation of therapeutic agents. While we specifically analyzed the potential of JAK inhibitor treatment in this thesis, these limitations exemplify the major challenges for the clinical implementation of precision medicines in general.

Regardless of imatinib targeting the driving lesion, approximately 30% of the *BCR-ABL1*-positive BCP-ALL cases develop resistance and relapse.[25,37] A variety of mechanisms can underlie this resistance, e.g. activation of alternate survival pathways, down-regulation of drug influx transporters, or mutations at the inhibitor-binding domains (e.g. *ABL*^{T315I}).[38-42] Mutations at the inhibitor-binding domain can be overcome with inhibitors that bind the kinases via different domains. However, in time resistance against these new inhibitors will also develop.[41,43,44] Current knowledge implies that imatinib itself selects for pre-existing subclones, which gradually outgrowth the drug sensitive cells.[45] Similar observations have been reported in solid tumors.[46-51] These observations indicate the importance to screen for resistance-mutations in time and expose the cancer cells to alternative tyrosine kinase inhibitors that still target these cancer cells (e.g. dasatinib).

Non-tyrosine kinase activating lesions

Although a subgroup of *BCR-ABL1*-like B-other patients is characterized by kinase activating lesions, the pathobiology of the remaining *BCR-ABL1*-like and non-*BCR-ABL1*-like B-other cases remains poorly understood. Only very recently, chromosomal translocations involving *DUX4*, *ZNF384*, and *MEF2D* were identified in non *BCR-ABL1*-like B-other cases.[52-54] The pro-apoptotic gene *DUX4* is located within the D4Z4 macrosatellite repeat array on chromosome 4 and 10 and encodes a double homeobox transcription factor. *DUX4* is normally expressed in germline and testis cells, but epigenetically silenced in somatic cells.[55,56] Loss of function of the differentiation factor

ERG is an important secondary event in *DUX4*-rearranged cases.[54] Interestingly, *DUX4*-rearrangements and *ERG* deletions are associated with a favorable prognosis.[53,54,57,58] Therefore, *DUX4*-rearrangement can be used to a identify a favorable prognostic group within the B-other subtype. Despite this favorable prognosis, a targeted treatment for these cases is warranted to reduce side effects of therapy. As specific targeting of transcription factors remains a challenge, it is important to identify dysregulated signaling pathways downstream of *DUX4*. We show in **Chapter 4** that high expression of *STAP1* is a hallmark of *DUX4*-rearranged BCP-ALL cases. However, STAP1 is not a likely target for precision medicines in these cases, since silencing of *STAP1* did not induce death of leukemic cells. Therefore, the search to downstream factors and affected signaling pathways in *DUX4*-rearranged cells needs to be continued.

Cooperating lesions in B-cell development genes and risk stratification

BCP-ALL is often characterized by chromosomal rearrangements. These chromosomal rearrangements induce a pre-leukemic state, but additional events are required to develop leukemia.[10,11,59,60] Deletion of *IKZF1* is an example of a cooperating lesion in *BCR-ABL1*-positive leukemia. Loss of *IKZF1* circumvents the necessity to acquire additional pro-oncogenic hits, resulting in an accelerated onset of leukemia, as shown in a *BCR-ABL1*-positive mouse model.[61] The leukemia that developed in these mice was characterized by a polyclonal nature and few additional chromosomal abnormalities. In contrast, *BCR-ABL1*-positive mice without loss of *IKZF1* developed a monoclonal leukemia, in which leukemic cells harbored more chromosomal abnormalities.[61] Besides *IKZF1*, deregulation of other B-cell development regulators (e.g. *EBF1*, *PAX5*, ERG, *ETV6*), cell cycle and proliferations (*CDKN2A/B*, *RB1*), and apoptosis (*BTG1*) is often observed in BCP-ALL.[6,62,63] Lineage-specific transcription and fragility of highly transcribed loci are a major cause for enrichment of these lesions in BCP-ALL cells.[63]

Current research is focused on the implementation of copy number aberrations (CNAs) in B-cell development genes in risk factor stratification.[64,65] *IKZF1* was shown to predict a poor clinical outcome,[22,66,67] and therefore implemented as risk factor in the ongoing Dutch Childhood Oncology Group (DCOG) ALL11 protocol. Associations between CNAs and an unfavorable prognosis suggest that lesions in these differentiation factors and cell cycle regulators might cause cellular drug resistance. Indeed, *IKZF1* deletions were reported to mediate resistance towards glucocorticoids.[68-70] However, the relationship between remaining CNAs and cellular drug resistance is yet unknown. In **Chapter 5** we show that, with the exception of an *IKZF1* deletion, none of the remaining CNAs associated as single marker both with an unfavorable clinical prognosis and cellular drug resistance. The biological and clinical importance of CNAs in these eight genes appeared to be highly context dependent and differed between the diverse oncogenic drivers of pediatric BCP-ALL. For example, the relation between cellular drug resistance and *IKZF1* deletions differed per cytogenetic subtype: in high hyperdiploid cases loss of *IKZF1* was associated with >1500 fold resistance to prednisolone, whereas in *BCR-ABL1*-like and non-*BCR-ABL1*-like B-other cells deletion of *IKZF1* was associated with thiopurine resistance. In contrast to the prognostic value in the above mentioned groups, loss of *IKZF1* does not reverse the favorable outcome of *ETV6-RUNX1*, *DUX4*-rearranged, and ERG-deleted cases, indicating that these genomic lesions negate the effect of *IKZF1* deletions.[53,54,57,58,71] Context-dependency is also shown by deletions of the *BTG1* gene: loss

of *BTG1* only does not affect cellular drug resistance or the prognosis of BCP-ALL cases, while presence of *BTG1* deletions in *IKZF1*-deleted cases strongly enhanced the risk for a relapse and glucocorticoid resistance.[69] Taken together, these observations imply that the genetic context (e.g. oncogenic driver, cell type, differentiation stage) contributes to which intracellular pathways are activated and thereby affect carcinogenesis and/or the response to chemotherapeutic agents. This theory is supported by diverse consequences of genetic aberrations in different cancer types. For example, a deletion of *ERG* is an important secondary event for leukemogenesis in *DUX4*-rearranged ALL, whereas *ERG* expression is essential for leukemogenesis in *AML1-ETO* rearranged acute myeloid leukemia.[54,72,73] Moreover, the importance of the genetic background for the response to anti-cancer therapy is illustrated by findings in solid tumors: $BRAF^{V600E}$ mutations are reported both in melanoma and colorectal cancer patients, but BRAF inhibitors (e.g. Vemurafenib) only induce a tumor response in melanoma patients.[74,75] Absence of a response in colorectal patient is caused by feedback activation of EGFR upon BRAF inhibition, which is not induced in melanoma patients.[76]

In conclusion, the genetic context determines which intracellular pathways are activated and thereby affects carcinogenesis and cellular drug response. Consequently, efficient targeting of a genetic aberration in a specific cancer might not be effective in another cancer type. These findings indicate the importance to evaluate the efficacy of potential treatment strategies the correct cellular and genetic context in preclinical studies, which will facilitate more efficient clinical studies.

Cooperating lesions and opportunities for therapeutic intervention

During the last decade *IKZF1* was one of the main focusses for research. Deletions of the gene were reported to confer resistance to prednisolone and tyrosine kinase inhibitors.[37,77,78] Though imatinib directly targets the BCR-ABL1 fusion protein, deletion of *IKZF1* causes an aberrant stem cell phenotype and deregulates cellular adhesion, which enables BCP-ALL cells to evade cytotoxicity of imatinib and other tyrosine kinase inhibitors.[78] Combination therapy directed against both the *BCR-ABL1* oncogene and the consequences of *IKZF1* deletions might be an attractive treatment strategy for these cases and is currently being explored.[78]

In addition, *IKZF1* was recently shown to be a regulator of energy and glucose metabolism.[77] During normal B-cell development, *IKZF1* prevents malignant transformation by limiting the supply of glucose and energy. Deletion of the gene hinders this tumor suppressive function and consequently ATP and glucose levels increase. Besides enabling malignant transformation, these increased glucose levels cause glucocorticoid resistance.[77] Interestingly, we previously observed an association between increased glucose consumption and glucocorticoid resistance in primary BCP-ALL cells.[79] Inhibition of glycolysis by 2-deoxyglucose (2-DG) restored prednisolone efficacy in primary pediatric BCP-ALL cells.[79,80] Therefore, this role of *IKZF1* as energy regulator might potentially offer an alternative treatment strategy for *IKZF1*-deleted prednisolone resistant BCP-ALL cells. This hypothesis should be further explored in *in vitro* assays.

The bone marrow microenvironment

Oncology research is often focused on the cancer cell as a single entity. However, the tumor microenvironment has a profound effect in the initiation and progression of cancer.[81] This tumor niche consists of cancer cells and a supporting framework, including mesenchymal stromal cells (MSCs), fibroblasts, endothelial cells, pericytes and a variety of immune-regulatory cells.[82,83] Leukemic cells reside in the bone marrow, where they hijack the normal hematopoietic stem cell niches to create a leukemic niche.[84] In this thesis, the importance of the bone marrow niche for BCP-ALL cell survival was demonstrated by microenvironment-induced resistance to JAK inhibitors (**Chapter 3**). Unraveling the mechanism of protection may provide novel options for therapeutic intervention.

Tumor cells can take advantages of niche specific signaling, manipulate their microenvironment to promote survival, or cancer might even be the consequence of a disrupted microenvironment.[85-87] In myeloid malignancies, dysfunction of the bone marrow has been reported to contribute to the development of the disease and vice versa leukemogenesis can induce abnormal bone marrow niches.[88-92] Conflicting results have been reported concerning the genetic background of mesenchymal stromal cells (MSCs) in pediatric BCP-ALL.[93-95] Therefore, we studied in **Chapter 6** of this thesis whether MSCs obtained from pediatric BCP-ALL patients (leukemic-MSCs) are different compared to MSCs obtained from healthy pediatric controls (control-MSCs). Our results indicate that leukemic-MSCs are intrinsically not different compared to control-MSCs. Instead, BCP-ALL cells induce gene expression changes in MSCs, which coincide with an increased survival of BCP-ALL cells. Each BCP-ALL sample induced a characteristic gene expression change, which was consistent between different MSCs. This change in expression was only transient, as elimination of leukemic cells reversed gene expression changes. The interferon/STAT1 pathway was the most commonly induced pathway, suggesting a central role of STAT1 in the interaction between MSCs and BCP-ALL cells. However, knockdown of *STAT1* in our MSCs did not reduce the survival benefit of BCP-ALL cells upon co-culture with MSCs. Residual expression levels of *STAT1* or rescue via alternative pathways may have occurred and therefore the role of the interferon/STAT1 pathway in BCP-ALL remains elusive.[96] Taken together, our finding indicate that MSCs are not actively involved in the initiation of pediatric BCP-ALL or a relapse. Rather BCP-ALL cells manipulate MSCs to support leukemogenesis. Targeting the direct interaction between BCP-ALL cells and MSCs or downstream factors of these processes might offer alternative treatment approaches.

In order to support BCP-ALL cell survival and vice versa induce changes in the gene expression profile of MSCs, MSCs and BCP-ALL cells need to interact. Interaction can occur through soluble factors (e.g. chemokines and cytokines) and cellular projections (e.g. tunneling nanotubes).[97] Tunneling nanotubes (TNTs) can transfer various cargo, e.g. mitochondria and autophagosomes, which will affect with ongoing cellular processes.[97-99] Previously we showed that TNT signaling induces secretion of pro-survival cytokines. Like gene expression profiles, these cytokine secretion patterns are leukemia-specific, again suggesting that BCP-ALL cells, but not MSCs, are responsible for the active modulation of the tumor microenvironment.[100] Combining results from this study and **Chapter 6** indicate that there are at least three different approaches to interfere with the ALL-MSC interaction: 1) TNT signaling, 2) ALL-induced signaling pathways in MSCs, and 3) cytokine signaling. Results presented in this thesis show the variety of effects induced in MSCs by leukemic samples. Interference with a common mechanism of the ALL-MSC interaction, like TNT

inhibition, would be an attractive treatment approach. Unfortunately, no specific TNT inhibitors are available yet. Since our results show that MSCs are not actively involved in leukemogenesis, therapeutic interference should preferentially target leukemic cells and/or factors that are released upon co-culture of BCP-ALL cells and MSCs.

Immunotherapy

Targeted treatment strategies will be of great importance to improve the prognosis and reduce sight effect in pediatric BCP-ALL patients. In this thesis, we show promising results for the implementation of JAK inhibitor therapy in the treatment of BCP-ALL, but also identified important limitations (accumulation of phosphorylated JAK2, tumor heterogeneity, micro-environmental induced resistance) of these type of inhibitors. These limitations should be taken into account during treatment and provide directions for future research.

Besides targeted therapies, immunotherapy includes a promising new treatment approach against leukemia. High remission rates were achieved in relapsed and refractory BCP-ALL patients by bispecific antibodies, immunotoxins, and chimeric antigen receptor T cell therapy.[101-107] CD19 and CD22 are the main targets for these treatment strategies. Both proteins are expressed exclusively on B-cell lineage cells.[101] Blinatumomab is a bispecific antibody that simultaneously binds to CD19-positive cells and to endogenous cytotoxic T cells. This binding enables recognition and elimination of CD19-positive cells by these cytotoxic T cells.[101-103] Immunotoxins use the rapid internalization of CD22 upon antibody binding to mediate intracellular delivery of cytotoxic agents.[104,108] Inotuzumab ozogamicin is an anti-CD22 monoclonal antibody that is conjugated to the cytotoxic antibiotic agent calicheamicin.[109] The intracellular release of calicheamicin induces cells death in CD22-positive cells.[109] Chimeric antigen receptor T cell therapy involves the *ex vivo* modification of cytotoxic T cells. Expression of chimeric antigen receptors against CD19 or CD22 directs these T cells towards the leukemic cells.[105-107] Unfortunately, severe side effect are reported (e.g. severe cytokine release syndrome) and in time leukemic cells can also develop resistance against these immunotherapeutic approaches.[103,105,106] Leukemic cells can evade these therapies via different mechanisms, e.g. loss of CD19 expression, increased regulatory T-cells, or immunosuppressive cytokines.[110] Cells that acquired resistance due to loss of CD19 might be targeted by CD22-directed approaches.[107] In addition, blockade of T cell activation through high expression levels of inhibitory ligands on tumor cells (i.e. PD-L1) was proposed to be one of the main contributors of resistance.[111] Combined treatment with blinatumomab and antibodies that block the binding of PD-L1 on tumor cells to the PD-1 inhibitory T cell receptor (e.g. nivolumab) might increase the cytotoxicity of T cells. Indeed, promising results were obtained by combination therapy in a pediatric patient with refractory BCP-ALL.[112] The potency of this combination therapy will be studied in more detail in a phase I study for relapsed or refractory CD19+ BCP-ALL (NCT02879695).

Taken together, targeted therapies and immunotherapy have a high potential in the treatment of leukemia. However, the ability of leukemic cells to acquire resistance against different types of therapies suggests that future treatment approaches may need to combine different strategies.

Concluding remarks

The aim of this thesis was to gain insight in pathobiology of high risk BCP-ALL cases. In this journey we explored the potential of new targets for therapeutic intervention (i.e. *JAK2* and *STAP1*), the association between CNAs in B-cell development genes, long-term prognosis and cellular drug resistance, and the involvement the bone marrow niche in leukemogenesis. Our results show the efficacy of new precision medicines, i.e. JAK inhibitors, in BCP-ALL therapy, but we also identified important limitations that should be overcome. Moreover, we show that the genetic context matters and that the effect of anti-cancer drugs should be studied in the proper genetic context. Lastly, we show that MSCs are not actively involved in BCP-ALL leukemogenesis. Instead leukemic cells actively modulate signaling pathways in MSCs to support BCP-ALL cell survival. Targeting this interaction between BCP-ALL cells and MSCs might be an attractive alternative treatment strategy and will therefore be further explored in our future studies.

REFERENCES

1. Hanahan D, Weinberg RA. The hallmarks of cancer. Cell 2000;100:57-70.
2. Hanahan D, Weinberg RA. Hallmarks of cancer: the next generation. Cell 2011;144:646-74.
3. Vogelstein B, Papadopoulos N, Velculescu VE, Zhou S, Diaz LA, Jr., Kinzler KW. Cancer genome landscapes. Science 2013;339:1546-58.
4. Zhang J, Ding L, Holmfeldt L, et al. The genetic basis of early T-cell precursor acute lymphoblastic leukaemia. Nature 2012;481:157-63.
5. Lilljebjorn H, Rissler M, Lassen C, et al. Whole-exome sequencing of pediatric acute lymphoblastic leukemia. Leukemia 2012;26:1602-7.
6. Mullighan CG, Goorha S, Radtke I, et al. Genome-wide analysis of genetic alterations in acute lymphoblastic leukaemia. Nature 2007;446:758-64.
7. Nowell PC. The clonal evolution of tumor cell populations. Science 1976;194:23-8.
8. Laurenti E, Dick JE. Molecular and functional characterization of early human hematopoiesis. Annals of the New York Academy of Sciences 2012;1266:68-71.
9. Dupain C, Harttrampf AC, Urbinati G, Geoerger B, Massaad-Massade L. Relevance of Fusion Genes in Pediatric Cancers: Toward Precision Medicine. Mol Ther Nucleic Acids 2017;6:315-26.
10. Mori H, Colman SM, Xiao Z, et al. Chromosome translocations and covert leukemic clones are generated during normal fetal development. Proceedings of the National Academy of Sciences of the United States of America 2002;99:8242-7.
11. Cazzaniga G, van Delft FW, Lo Nigro L, et al. Developmental origins and impact of BCR-ABL1 fusion and IKZF1 deletions in monozygotic twins with Ph+ acute lymphoblastic leukemia. Blood 2011;118:5559-64.
12. de Ridder-Sluiter H, Kollen WJW. Jaarverslag SKION 2015. . 2016.
13. Pui CH, Evans WE. A 50-year journey to cure childhood acute lymphoblastic leukemia. Semin Hematol 2013;50:185-96.
14. Pieters R, de Groot-Kruseman H, Van der Velden V, et al. Successful Therapy Reduction and Intensification for Childhood Acute Lymphoblastic Leukemia Based on Minimal Residual Disease Monitoring: Study ALL10 From the Dutch Childhood Oncology Group. J Clin Oncol 2016;34:2591-601.
15. Robison LL, Hudson MM. Survivors of childhood and adolescent cancer: life-long risks and responsibilities. Nature reviews Cancer 2014;14:61-70.
16. Heard E, Tishkoff S, Todd JA, et al. Ten years of genetics and genomics: what have we achieved and where are we heading? Nature reviews Genetics 2010;11:723-33.
17. Dietel M, Johrens K, Laffert MV, et al. A 2015 update on predictive molecular pathology and its role in targeted cancer therapy: a review focussing on clinical relevance. Cancer gene therapy 2015;22:417-30.
18. Zardavas D, Tryfonidis K, Goulioti T, Piccart M. Targeted adjuvant therapy in breast cancer. Expert review of anticancer therapy 2016;16:1263-75.
19. Chen G, Yang Z, Eshleman JR, Netto GJ, Lin MT. Molecular Diagnostics for Precision Medicine in Colorectal Cancer: Current Status and Future Perspective. BioMed research international 2016;2016:9850690.
20. Druker BJ, Talpaz M, Resta DJ, et al. Efficacy and safety of a specific inhibitor of the BCR-ABL tyrosine kinase in chronic myeloid leukemia. N Engl J Med 2001;344:1031-7.
21. Den Boer ML, van Slegtenhorst M, De Menezes RX, et al. A subtype of childhood acute lymphoblastic leukaemia with poor treatment outcome: a genome-wide classification study. Lancet Oncol 2009;10:125-34.
22. Mullighan CG, Su X, Zhang J, et al. Deletion of IKZF1 and prognosis in acute lymphoblastic leukemia. N Engl J Med 2009;360:470-80.
23. Roberts KG, Morin RD, Zhang J, et al. Genetic alterations activating kinase and cytokine receptor signaling in high-risk acute lymphoblastic leukemia. Cancer Cell 2012;22:153-66.
24. Reshmi SC, Harvey RC, Roberts KG, et al. Targetable kinase gene fusions in high-risk B-ALL: a study from the Children's Oncology Group. Blood 2017;129:3352-61.
25. Schultz KR, Bowman WP, Aledo A, et al. Improved early event-free survival with imatinib in Philadelphia chromosome-positive acute lymphoblastic leukemia: a children's oncology group study. J Clin Oncol 2009;27:5175-81.
26. Lengline E, Beldjord K, Dombret H, Soulier J, Boissel N, Clappier E. Successful tyrosine kinase inhibitor therapy in a refractory B-cell precursor acute lymphoblastic leukemia with EBF1-PDGFRB fusion. Haematologica 2013;98:e146-8.
27. Schwab C, Ryan SL, Chilton L, et al. EBF1-PDGFRB fusion in pediatric B-cell precursor acute lymphoblastic leukemia (BCP-ALL): genetic profile and clinical implications. Blood 2016;127:2214-8.
28. Weston BW, Hayden MA, Roberts KG, et al. Tyrosine kinase inhibitor therapy induces remission in a patient with refractory EBF1-PDGFRB-positive acute lymphoblastic leukemia. J Clin Oncol 2013;31:e413-6.
29. Meyer SC, Levine RL. Molecular pathways: molecular basis for sensitivity and resistance to JAK kinase inhibitors. Clin Cancer Res 2014;20:2051-9.
30. Wu SC, Li LS, Kopp N, et al. Activity of the Type II JAK2 Inhibitor CHZ868 in B Cell Acute Lymphoblastic Leukemia. Cancer Cell 2015;28:29-41.
31. Tannock IF, Hickman JA. Limits to Personalized Cancer Medicine. N Engl J Med 2016;375:1289-94.
32. Polak R, de Rooij B, Pieters R, den Boer ML. B-cell precursor acute lymphoblastic leukemia cells use tunneling nanotubes to orchestrate their microenvironment. Blood 2015;126:2404-14.
33. Iwamoto S, Mihara K, Downing JR, Pui CH, Campana D. Mesenchymal cells regulate the response of acute lymphoblastic leukemia cells to asparaginase. The Journal of clinical investigation 2007;117:1049-57.
34. Vianello F, Villanova F, Tisato V, et al. Bone marrow mesenchymal stromal cells non-selectively protect chronic myeloid leukemia cells from imatinib-induced apoptosis via the CXCR4/CXCL12 axis. Haematologica 2010;95:1081-9.

35. Ehsanipour EA, Sheng X, Behan JW, et al. Adipocytes cause leukemia cell resistance to L-asparaginase via release of glutamine. Cancer research 2013;73:2998-3006.
36. Feldhahn N, Arutyunyan A, Stoddart S, et al. Environment-mediated drug resistance in Bcr/Abl-positive acute lymphoblastic leukemia. Oncoimmunology 2012;1:618-29.
37. van der Veer A, Zaliova M, Mottadelli F, et al. IKZF1 status as a prognostic feature in BCR-ABL1-positive childhood ALL. Blood 2014;123:1691-8.
38. Ottmann OG, Wassmann B. Treatment of Philadelphia chromosome-positive acute lymphoblastic leukemia. Hematology Am Soc Hematol Educ Program 2005:118-22.
39. Mian AA, Oancea C, Zhao Z, Ottmann OG, Ruthardt M. Oligomerization inhibition, combined with allosteric inhibition, abrogates the transformation potential of T315I-positive BCR/ABL. Leukemia 2009;23:2242-7.
40. Ramchandren R, Schiffer CA. Dasatinib in the treatment of imatinib refractory chronic myeloid leukemia. Biologics 2009;3:205-14.
41. Weisberg E, Manley PW, Cowan-Jacob SW, Hochhaus A, Griffin JD. Second generation inhibitors of BCR-ABL for the treatment of imatinib-resistant chronic myeloid leukaemia. Nature reviews Cancer 2007;7:345-56.
42. Gross S, Rahal R, Stransky N, Lengauer C, Hoeflich KP. Targeting cancer with kinase inhibitors. The Journal of clinical investigation 2015;125:1780-9.
43. Wei G, Rafiyath S, Liu D. First-line treatment for chronic myeloid leukemia: dasatinib, nilotinib, or imatinib. J Hematol Oncol 2010;3:47.
44. Sirvent A, Benistant C, Roche S. Cytoplasmic signalling by the c-Abl tyrosine kinase in normal and cancer cells. Biol Cell 2008;100:617-31.
45. Shah NP, Nicoll JM, Nagar B, et al. Multiple BCR-ABL kinase domain mutations confer polyclonal resistance to the tyrosine kinase inhibitor imatinib (STI571) in chronic phase and blast crisis chronic myeloid leukemia. Cancer Cell 2002;2:117-25.
46. Manzano JL, Layos L, Buges C, et al. Resistant mechanisms to BRAF inhibitors in melanoma. Annals of translational medicine 2016;4:237.
47. Khattak M, Fisher R, Turajlic S, Larkin J. Targeted therapy and immunotherapy in advanced melanoma: an evolving paradigm. Therapeutic advances in medical oncology 2013;5:105-18.
48. Hammond WA, Swaika A, Mody K. Pharmacologic resistance in colorectal cancer: a review. Therapeutic advances in medical oncology 2016;8:57-84.
49. Morgillo F, Della Corte CM, Fasano M, Ciardiello F. Mechanisms of resistance to EGFR-targeted drugs: lung cancer. ESMO open 2016;1:e000060.
50. Liegl B, Kepten I, Le C, et al. Heterogeneity of kinase inhibitor resistance mechanisms in GIST. The Journal of pathology 2008;216:64-74.
51. Barouch-Bentov R, Sauer K. Mechanisms of drug resistance in kinases. Expert opinion on investigational drugs 2011;20:153-208.
52. Lilljebjorn H, Henningsson R, Hyrenius-Wittsten A, et al. Identification of ETV6-RUNX1-like and DUX4-rearranged subtypes in paediatric B-cell precursor acute lymphoblastic leukaemia. Nature communications 2016;7:11790.
53. Yasuda T, Tsuzuki S, Kawazu M, et al. Recurrent DUX4 fusions in B cell acute lymphoblastic leukemia of adolescents and young adults. Nat Genet 2016;48:569-74.
54. Zhang J, McCastlain K, Yoshihara H, et al. Deregulation of DUX4 and ERG in acute lymphoblastic leukemia. Nat Genet 2016;48:1481-9.
55. van Geel M, Dickson MC, Beck AF, et al. Genomic analysis of human chromosome 10q and 4q telomeres suggests a common origin. Genomics 2002;79:210-7.
56. Kowaljow V, Marcowycz A, Ansseau E, et al. The DUX4 gene at the FSHD1A locus encodes a pro-apoptotic protein. Neuromuscular disorders : NMD 2007;17:611-23.
57. Harvey RC, Mullighan CG, Wang X, et al. Identification of novel cluster groups in pediatric high-risk B-precursor acute lymphoblastic leukemia with gene expression profiling: correlation with genome-wide DNA copy number alterations, clinical characteristics, and outcome. Blood 2010;116:4874-84.
58. Clappier E, Auclerc MF, Rapion J, et al. An intragenic ERG deletion is a marker of an oncogenic subtype of B-cell precursor acute lymphoblastic leukemia with a favorable outcome despite frequent IKZF1 deletions. Leukemia 2014;28:70-7.
59. Morrow M, Horton S, Kioussis D, Brady HJ, Williams O. TEL-AML1 promotes development of specific hematopoietic lineages consistent with preleukemic activity. Blood 2004;103:3890-6.
60. Wiemels JL, Cazzaniga G, Daniotti M, et al. Prenatal origin of acute lymphoblastic leukaemia in children. Lancet 1999;354:1499-503.
61. Virely C, Moulin S, Cobaleda C, et al. Haploinsufficiency of the IKZF1 (IKAROS) tumor suppressor gene cooperates with BCR-ABL in a transgenic model of acute lymphoblastic leukemia. Leukemia 2010;24:1200-4.
62. Rosenbauer F, Tenen DG. Transcription factors in myeloid development: balancing differentiation with transformation. Nat Rev Immunol 2007;7:105-17.
63. Boulianne B, Robinson ME, May PC, et al. Lineage-Specific Genes Are Prominent DNA Damage Hotspots during Leukemic Transformation of B Cell Precursors. Cell reports 2017;18:1687-98.
64. Moorman AV, Enshaei A, Schwab C, et al. A novel integrated cytogenetic and genomic classification refines risk stratification in pediatric acute lymphoblastic leukemia. Blood 2014;124:1434-44.
65. Gupta SK, Bakhshi S, Kumar L, Kamal VK, Kumar R. Gene copy number alteration profile and its clinical correlation in B-cell acute lymphoblastic leukemia. Leukemia & lymphoma 2017;58:333-42.
66. van der Veer A, Waanders E, Pieters R, et al. Independent prognostic value of BCR-ABL1-like signature and IKZF1 deletion, but not high CRLF2 expression, in children with B-cell precursor ALL. Blood 2013;122:2622-9.
67. Kuiper RP, Waanders E, van der Velden VH, et al. IKZF1 deletions predict relapse in uniformly treated pediatric precursor B-ALL. Leukemia 2010;24:1258-64.

68. Marke R, Havinga J, Cloos J, et al. Tumor suppressor IKZF1 mediates glucocorticoid resistance in B-cell precursor acute lymphoblastic leukemia. Leukemia 2016;30:1599-603.
69. Scheijen B, Boer JM, Marke R, et al. Tumor suppressors BTG1 and IKZF1 cooperate during mouse leukemia development and increase relapse risk in B-cell precursor acute lymphoblastic leukemia patients. Haematologica 2017;102:541-51.
70. Imamura T, Yano M, Asai D, et al. IKZF1 deletion is enriched in pediatric B-cell precursor acute lymphoblastic leukemia patients showing prednisolone resistance. Leukemia 2016;30:1801-3.
71. Enshaei A, Schwab CJ, Konn ZJ, et al. Long-term follow-up of ETV6-RUNX1 ALL reveals that NCI risk, rather than secondary genetic abnormalities, is the key risk factor. Leukemia 2013;27:2256-9.
72. Mandoli A, Singh AA, Prange KHM, et al. The Hematopoietic Transcription Factors RUNX1 and ERG Prevent AML1-ETO Oncogene Overexpression and Onset of the Apoptosis Program in t(8;21) AMLs. Cell reports 2016;17:2087-100.
73. Martens JH, Mandoli A, Simmer F, et al. ERG and FLI1 binding sites demarcate targets for aberrant epigenetic regulation by AML1-ETO in acute myeloid leukemia. Blood 2012;120:4038-48.
74. Barras D. BRAF Mutation in Colorectal Cancer: An Update. Biomarkers in cancer 2015;7:9-12.
75. Mao M, Tian F, Mariadason JM, et al. Resistance to BRAF inhibition in BRAF-mutant colon cancer can be overcome with PI3K inhibition or demethylating agents. Clin Cancer Res 2013;19:657-67.
76. Prahallad A, Sun C, Huang S, et al. Unresponsiveness of colon cancer to BRAF(V600E) inhibition through feedback activation of EGFR. Nature 2012;483:100-3.
77. Chan LN, Chen Z, Braas D, et al. Metabolic gatekeeper function of B-lymphoid transcription factors. Nature 2017;542:479-83.
78. Churchman ML, Mullighan CG. Ikaros: Exploiting and targeting the hematopoietic stem cell niche in B-progenitor acute lymphoblastic leukemia. Experimental hematology 2017;46:1-8.
79. Hulleman E, Kazemier KM, Holleman A, et al. Inhibition of glycolysis modulates prednisolone resistance in acute lymphoblastic leukemia cells. Blood 2009;113:2014-21.
80. Aries IM, Hansen BR, Koch T, et al. The synergism of MCL1 and glycolysis on pediatric acute lymphoblastic leukemia cell survival and prednisolone resistance. Haematologica 2013;98:1905-11.
81. Nombela-Arrieta C, Pivarnik G, Winkel B, et al. Quantitative imaging of haematopoietic stem and progenitor cell localization and hypoxic status in the bone marrow microenvironment. Nature cell biology 2013;15:533-43.
82. Hong IS, Lee HY, Kang KS. Mesenchymal stem cells and cancer: friends or enemies? Mutat Res 2014;768:98-106.
83. D'Souza N, Burns JS, Grisendi G, et al. MSC and Tumors: Homing, Differentiation, and Secretion Influence Therapeutic Potential. Adv Biochem Eng Biotechnol 2013;130:209-66.
84. Colmone A, Amorim M, Pontier AL, Wang S, Jablonski E, Sipkins DA. Leukemic cells create bone marrow niches that disrupt the behavior of normal hematopoietic progenitor cells. Science 2008;322:1861-5.
85. Raaijmakers MH. Niche contributions to oncogenesis: emerging concepts and implications for the hematopoietic system. Haematologica 2011;96:1041-8.
86. Schepers K, Campbell TB, Passegue E. Normal and leukemic stem cell niches: insights and therapeutic opportunities. Cell stem cell 2015;16:254-67.
87. Sneddon JB, Werb Z. Location, location, location: the cancer stem cell niche. Cell stem cell 2007;1:607-11.
88. Walkley CR, Shea JM, Sims NA, Purton LE, Orkin SH. Rb regulates interactions between hematopoietic stem cells and their bone marrow microenvironment. Cell 2007;129:1081-95.
89. Walkley CR, Olsen GH, Dworkin S, et al. A microenvironment-induced myeloproliferative syndrome caused by retinoic acid receptor gamma deficiency. Cell 2007;129:1097-110.
90. Raaijmakers MH, Mukherjee S, Guo S, et al. Bone progenitor dysfunction induces myelodysplasia and secondary leukaemia. Nature 2010;464:852-7.
91. Schepers K, Pietras EM, Reynaud D, et al. Myeloproliferative neoplasia remodels the endosteal bone marrow niche into a self-reinforcing leukemic niche. Cell stem cell 2013;13:285-99.
92. Krause DS, Fulzele K, Catic A, et al. Differential regulation of myeloid leukemias by the bone marrow microenvironment. Nat Med 2013;19:1513-7.
93. Conforti A, Biagini S, Del Bufalo F, et al. Biological, functional and genetic characterization of bone marrow-derived mesenchymal stromal cells from pediatric patients affected by acute lymphoblastic leukemia. PLoS One 2013;8:e76989.
94. Menendez P, Catalina P, Rodriguez R, et al. Bone marrow mesenchymal stem cells from infants with MLL-AF4+ acute leukemia harbor and express the MLL-AF4 fusion gene. Journal of Experimental Medicine 2009;206:3131-41.
95. Shalapour S, Eckert C, Seeger K, et al. Leukemia-associated genetic aberrations in mesenchymal stem cells of children with acute lymphoblastic leukemia. Journal of Molecular Medicine 2010;88:249-65.
96. Blaszczyk K, Nowicka H, Kostyrko K, Antonczyk A, Wesoly J, Bluyssen HA. The unique role of STAT2 in constitutive and IFN-induced transcription and antiviral responses. Cytokine & growth factor reviews 2016;29:71-81.
97. Abounit S, Zurzolo C. Wiring through tunneling nanotubes--from electrical signals to organelle transfer. Journal of cell science 2012;125:1089-98.
98. de Rooij B, Polak R, Stalpers F, Pieters R, Boer MLD. Tunneling nanotubes facilitate autophagosome transfer in the leukemic niche. Leukemia 2017;31:1651-4.
99. Saenz-de-Santa-Maria I, Bernardo-Castineira C, Enciso E, et al. Control of long-distance cell-to-cell communication and autophagosome transfer in squamous cell carcinoma via tunneling nanotubes. Oncotarget 2017;8:20939-60.

100. Polak R, de Rooij B, Pieters R, den Boer ML. B-cell precursor acute lymphoblastic leukemia cells use tunneling nanotubes to orchestrate their microenvironment. Blood 2015.
101. von Stackelberg A, Locatelli F, Zugmaier G, et al. Phase I/Phase II Study of Blinatumomab in Pediatric Patients With Relapsed/Refractory Acute Lymphoblastic Leukemia. J Clin Oncol 2016;34:4381-9.
102. Kantarjian H, Stein A, Gokbuget N, et al. Blinatumomab versus Chemotherapy for Advanced Acute Lymphoblastic Leukemia. N Engl J Med 2017;376:836-47.
103. Topp MS, Kufer P, Gokbuget N, et al. Targeted therapy with the T-cell-engaging antibody blinatumomab of chemotherapy-refractory minimal residual disease in B-lineage acute lymphoblastic leukemia patients results in high response rate and prolonged leukemia-free survival. J Clin Oncol 2011;29:2493-8.
104. Kantarjian HM, DeAngelo DJ, Stelljes M, et al. Inotuzumab Ozogamicin versus Standard Therapy for Acute Lymphoblastic Leukemia. N Engl J Med 2016;375:740-53.
105. Maude SL, Frey N, Shaw PA, et al. Chimeric antigen receptor T cells for sustained remissions in leukemia. N Engl J Med 2014;371:1507-17.
106. Grupp SA, Kalos M, Barrett D, et al. Chimeric antigen receptor-modified T cells for acute lymphoid leukemia. N Engl J Med 2013;368:1509-18.
107. Fry TJ, Shah NN, Orentas RJ, et al. CD22-targeted CAR T cells induce remission in B-ALL that is naive or resistant to CD19-targeted CAR immunotherapy. Nat Med 2018;24:20-8.
108. Daver N, O'Brien S. Novel therapeutic strategies in adult acute lymphoblastic leukemia--a focus on emerging monoclonal antibodies. Current hematologic malignancy reports 2013;8:123-31.
109. DiJoseph JF, Armellino DC, Boghaert ER, et al. Antibody-targeted chemotherapy with CMC-544: a CD22-targeted immunoconjugate of calicheamicin for the treatment of B-lymphoid malignancies. Blood 2004;103:1807-14.
110. Park JA, Cheung NV. Limitations and opportunities for immune checkpoint inhibitors in pediatric malignancies. Cancer Treat Rev 2017;58:22-33.
111. Krupka C, Kufer P, Kischel R, et al. Blockade of the PD-1/PD-L1 axis augments lysis of AML cells by the CD33/CD3 BiTE antibody construct AMG 330: reversing a T-cell-induced immune escape mechanism. Leukemia 2016;30:484-91.
112. Feucht J, Kayser S, Gorodezki D, et al. T-cell responses against CD19+ pediatric acute lymphoblastic leukemia mediated by bispecific T-cell engager (BiTE) are regulated contrarily by PD-L1 and CD80/CD86 on leukemic blasts. Oncotarget 2016;7:76902-19.

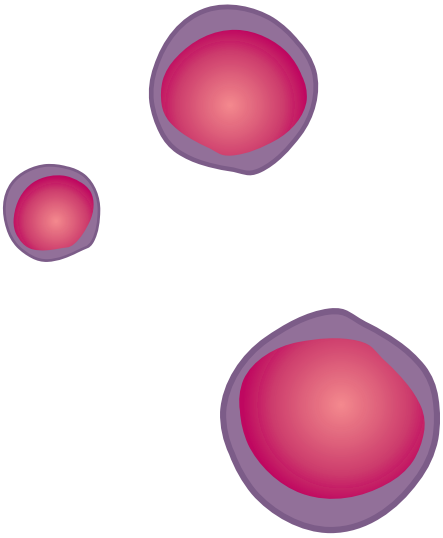

Chapter 8

SUMMARY

Summary

To improve the prognosis of children with B-cell precursor acute lymphoblastic leukemia (BCP-ALL), new targeted approaches are needed. Therefore, it is essential to unravel the underlying pathobiology. For *BCR-ABL1*-like and non-*BCR-ABL1*-like B-other patients the driving oncogenic lesions and mechanisms of therapy failure are poorly understood.

In the past decade, the genetic landscape of *BCR-ABL1*-like and non-*BCR-ABL1*-like B-other ALL has been intensively studied. Whole genome sequencing and RNA sequencing in USA patient cohorts identified activating tyrosine kinase lesions in a subgroup of *BCR-ABL1*-like patients.[1-3] The frequency of genetic lesions in ALL is linked to the genetic background (ancestry) of patients.[4-6] In **Chapter 2**, we therefore examined the prevalence of tyrosine kinase fusions in a Caucasian cohort of Dutch and German children with *BCR-ABL1*-like and non-*BCR-ABL1*-like ALL, using RT-PCR and targeted-locus-amplification. Tyrosine kinase fusions were solely detected in *BCR-ABL1*-like cases. These tyrosine kinase positive *BCR-ABL1*-like patients often harbored deletions of *IKZF1* and showed an unfavorable treatment outcome. Tyrosine kinase fusions involved either ABL class (ABL1, ABL2, PDGFRB, CFS1R) or JAK class (JAK2, CRLF2) kinases. The success of the ABL tyrosine kinase inhibitor imatinib in the treatment of *BCR-ABL1*-positive cases,[7] provides a strong rationale for the introduction of tyrosine kinase inhibitor treatment in patients carrying these new type of ABL fusion genes. Currently the first *BCR-ABL1*-like patients harboring ABL class tyrosine kinase fusions are being treated with imatinib.[8-10]

To gain insight in the clinical potential of JAK inhibitors in pediatric BCP-ALL, we determined the occurrence of *JAK2* aberrations, i.e. mutations and translocations, in different subtypes of childhood BCP-ALL. Results of this study are described in **Chapter 3**. *JAK2* translocations were a hallmark of *BCR-ABL1*-like ALL (6.5%). In contrast, *JAK2* point mutations were detected in three subtypes of BCP-ALL, i.e. *BCR-ABL1*-like (7.6%), B-other (11.9%) and high hyperdiploid (1.6%). Although *JAK2* point mutations and *JAK2* translocations represent genetically distinct entities, both may be targetable by JAK inhibitors. Therefore we examined the efficacy of the JAK inhibitors momelotinib and ruxolitinib in these cells. Momelotinib and ruxolitinib were cytotoxic in both *JAK2* translocated and *JAK2* mutated cells, although efficacy in *JAK2* mutated cells highly depended on cytokine receptor activation by TSLP. Despite these promising findings, we identified certain limitations of both JAK inhibitors. The inhibitors induced accumulation of phosphorylated JAK2^{Y1007}, which resulted in a profound re-activation of JAK2 signaling upon release of the inhibitors. In addition, we showed that the effect of JAK inhibition may be compromised by mutations in alternative survival pathways and microenvironment-induced resistance. Therefore, our results indicate that further optimization and evaluation of JAK inhibitor treatment is necessary prior to its clinical integration in pediatric BCP-ALL.

In **Chapter 4** we studied the signaling molecule STAP1, which may serve as new therapeutic target for *DUX4*-rearranged BCP-ALL. Only very recently, chromosomal translocations involving *DUX4* were identified in non-*BCR-ABL1*-like B-other cases.[11-13] Loss of function of the transcription factor *ERG* is proposed to be a direct consequence of *DUX4* deregulation.[13] Precision medicines mainly target kinase pathways and cell surface proteins, whereas transcription factors remain difficult to target. Therefore, it is important to identify signaling pathways that are affected by these transcription factors. We identified *STAP1* to be highly expressed in *BCR-ABL1*-like and non-*BCR-ABL1*-like B-other cases that often harbored *ERG* deletions. High expression of *STAP1* associated with high expression levels of genes

that are involved in the precursor B-cell receptor (pre-BCR) signaling pathway, which is an attractive pathway for therapeutic intervention. However, upregulation of pre-BCR signaling could not be confirmed in cases with high expression of *STAP1*. In addition, knockdown of *STAP1* did not induce cell death nor block the proliferation rate of these cells. These results indicate that *STAP1* is not a likely candidate for precision medicines. Therefore, the search for downstream factors and affected signaling pathways in *DUX4*-rearranged cells needs to be continued.

Besides chromosomal rearrangements, additional genetic aberrations such as mutations and copy-number alterations (CNAs) have been observed in BCP-ALL. Especially CNAs in genes that are involved in B-cell development and cell cycle progression are often detected in children with BCP-ALL.[5,6] In **Chapter 5** we showed that CNAs in B-cell development-associated genes occur in 71% of BCP-ALL cases and are not equally distributed across cytogenetic subtypes: the frequency was above 75% in *BCR-ABL1*-positive, *BCR-ABL1*-like, non-*BCR-ABL1*-like B-other, and *ETV6-RUNX1*-positive patients, but below 40% in *KMT2A*-rearranged, high hyperdiploid and *TCF3-PBX1*-positive cases. A deletion in *IKZF1* was the only risk factor that associated with both adverse clinical outcome and cellular drug resistance. However, associations with cellular drug resistance depended on the genetic context: extreme high prednisolone resistance (~1500-fold, $p<0.01$) was found in *IKZF1*-deleted high hyperdiploid cells, whereas thiopurine resistance (~1.7-fold, $p<0.05$) was predominantly detected in *BCR-ABL1*-like and B-other *IKZF1*-deleted cells. These results indicate that distinct combinations of genetic aberrations may have different effects on cellular drug resistance and therefore emphasize that the genetic context should be taken into account for functional studies that focus on cellular drug resistance.

In **Chapter 6** we gained insight in the interaction between leukemic cells and mesenchymal stromal cells (MSCs). MSCs are key components of the process of hematopoiesis through both cytokine secretion and direct cell-to-cell communication.[6,14,15] Furthermore, MSCs protect BCP-ALL cells against chemotherapeutic agents, including JAK inhibitors as demonstrated in **Chapter 3**.[16-20] Unraveling the role of the bone marrow microenvironment in leukemia may provide novel options for therapeutic intervention. Therefore, it was studied whether MSCs derived from leukemia patients at initial diagnosis (leukemic-MSCs) are different from MSCs isolated from healthy donors (control-MSCs). A significant increase in survival of BCP-ALL cells was observed if these cells were co-cultured with MSCs compared to the survival of BCP-ALL cells in mono-culture. Both control-MSCs and leukemic-MSCs provided a similar survival benefit and hence, the source of MSCs was not causing the increase in survival of leukemic cells. Strikingly, the gene expression profiles of MSCs did significantly change upon co-culture with primary BCP-ALL cells. Each BCP-ALL sample induced a specific change in gene expression profiles of MSCs, which was consistent between different MSCs. These changes were transient and were restored upon removal of leukeic cells. Taken together our results indicate that leukemic-MSCs are not intrinsically different from control-MSCs. Instead, BCP-ALL cells alter the transcriptome of MSCs, which coincides with an increased survival of BCP-ALL cells. Therefore our findings suggest that the bone marrow microenvironment by itself is not leukemogenic, but is actively being hijacked by leukemic cells to support the pathogenesis of BCP-ALL. Further knowledge about this interaction between BCP-ALL cells and MSCs may provide clues to target leukemic cells more specifically.

Leukemia is a multi-dynamic process, depending on numerous variables. Full understanding of the pathobiology of BCP-ALL is essential for the identification of new therapies. In this thesis, potential targets for therapeutic intervention were studied. In addition, our results show an important role for the bone marrow microenvironment in therapy resistance. The interaction between leukemic cells and the niche should be a central topic for future research.

REFERENCES

1. Roberts KG, Morin RD, Zhang J, et al. Genetic alterations activating kinase and cytokine receptor signaling in high-risk acute lymphoblastic leukemia. Cancer Cell. 2012;22(2):153-166.
2. Robison LL, Hudson MM. Survivors of childhood and adolescent cancer: life-long risks and responsibilities. Nat Rev Cancer. 2014;14(1):61-70.
3. Reshmi SC, Harvey RC, Roberts KG, et al. Targetable kinase gene fusions in high-risk B-ALL: a study from the Children's Oncology Group. Blood. 2017;129(25):3352-3361.
4. Boer JM, Marchante JR, Evans WE, et al. BCR-ABL1-like cases in pediatric acute lymphoblastic leukemia: a comparison between DCOG/Erasmus MC and COG/St. Jude signatures. Haematologica. 2015;100(9):e354-357.
5. Den Boer ML, van Slegtenhorst M, De Menezes RX, et al. A subtype of childhood acute lymphoblastic leukaemia with poor treatment outcome: a genome-wide classification study. Lancet Oncol. 2009;10(2):125-134.
6. Mullighan CG, Su X, Zhang J, et al. Deletion of IKZF1 and prognosis in acute lymphoblastic leukemia. N Engl J Med. 2009;360(5):470-480.
7. Schultz KR, Bowman WP, Aledo A, et al. Improved early event-free survival with imatinib in Philadelphia chromosome-positive acute lymphoblastic leukemia: a children's oncology group study. J Clin Oncol. 2009;27(31):5175-5181.
8. Lengline E, Beldjord K, Dombret H, Soulier J, Boissel N, Clappier E. Successful tyrosine kinase inhibitor therapy in a refractory B-cell precursor acute lymphoblastic leukemia with EBF1-PDGFRB fusion. Haematologica. 2013;98(11):e146-148.
9. Schwab C, Ryan SL, Chilton L, et al. EBF1-PDGFRB fusion in pediatric B-cell precursor acute lymphoblastic leukemia (BCP-ALL): genetic profile and clinical implications. Blood. 2016;127(18):2214-2218.
10. Weston BW, Hayden MA, Roberts KG, et al. Tyrosine kinase inhibitor therapy induces remission in a patient with refractory EBF1-PDGFRB-positive acute lymphoblastic leukemia. J Clin Oncol. 2013;31(25):e413-416.
11. Lilljebjorn H, Henningsson R, Hyrenius-Wittsten A, et al. Identification of ETV6-RUNX1-like and DUX4-rearranged subtypes in paediatric B-cell precursor acute lymphoblastic leukaemia. Nat Commun. 2016;7:11790.
12. Yasuda T, Tsuzuki S, Kawazu M, et al. Recurrent DUX4 fusions in B cell acute lymphoblastic leukemia of adolescents and young adults. Nat Genet. 2016;48(5):569-574.
13. Zhang J, McCastlain K, Yoshihara H, et al. Deregulation of DUX4 and ERG in acute lymphoblastic leukemia. Nat Genet. 2016;48(12):1481-1489.
14. Zhang J, Niu C, Ye L, et al. Identification of the haematopoietic stem cell niche and control of the niche size. Nature. 2003;425(6960):836-841.
15. Nagasawa T. Microenvironmental niches in the bone marrow required for B-cell development. Nature Reviews Immunology. 2006;6(2):107-116.
16. Polak R, de Rooij B, Pieters R, den Boer ML. B-cell precursor acute lymphoblastic leukemia cells use tunneling nanotubes to orchestrate their microenvironment. Blood. 2015.
17. Iwamoto S, Mihara K, Downing JR, Pui CH, Campana D. Mesenchymal cells regulate the response of acute lymphoblastic leukemia cells to asparaginase. J Clin Invest. 2007;117(4):1049-1057.
18. Vianello F, Villanova F, Tisato V, et al. Bone marrow mesenchymal stromal cells non-selectively protect chronic myeloid leukemia cells from imatinib-induced apoptosis via the CXCR4/CXCL12 axis. Haematologica. 2010;95(7):1081-1089.
19. Baldridge MT, King KY, Goodell MA. Inflammatory signals regulate hematopoietic stem cells. Trends Immunol. 2011;32(2):57-65.
20. Takizawa H, Boettcher S, Manz MG. Demand-adapted regulation of early hematopoiesis in infection and inflammation. Blood. 2012;119(13):2991-3002.

Nederlandse samenvatting voor niet ingewijden

Een cel moet een aantal eigenschappen verwerven om kanker te veroorzaken. Zo moet een kankercel oneindig kunnen delen, ongeremd kunnen groeien en celdood voorkomen. Bovendien speelt de interactie van deze cel met de omgeving een belangrijke rol: een kankercel moet voorkomen dat hij wordt opgeruimd door het immuunsysteem, of niet meer kan delen als gevolg van omgevingsfactoren. Normale cellen kunnen in kankercellen veranderen door het verwerven van mutaties. Dit is een dynamisch proces dat veel tijd in beslag neemt. Zowel in gezonde cellen als kankercellen ontstaan spontaan mutaties. Echter alleen mutaties die een groei- en overlevingsvoordeel met zich meebrengen, dragen bij aan het ontstaan van kanker. Deze mutaties worden ook wel driver mutaties genoemd. Een tumor bevat normaal gesproken twee tot acht van deze driver mutaties. De andere mutaties zijn later ontstaan (passenger mutaties) of zijn zelfs helemaal niet betrokken bij het ontstaan van de ziekte. Bij de behandeling van kanker is het belangrijk om op deze driver mutaties te focussen, omdat deze belangrijk zijn voor de overleving van de kankercellen.

Leukemie

Leukemie is een verzamelnaam voor een vorm van kanker die wordt veroorzaakt door een ongeremde groei van witte bloedcellen. Bloedcellen ontwikkelen zich in het beenmerg uit één voorloper cel: de bloedstamcel of ook wel de hematopoietische stamcel (HSC) genoemd. Deze HSC kan zich ontwikkelen tot drie typen bloedcelen: witte bloedcellen, rode bloedcellen en bloedplaatjes. De verschillende typen bloedcellen hebben ieder een specifieke functie. Zo zijn de witte bloedcellen belangrijk voor de afweer van ons lichaam tegen virussen, zijn rode bloedcellen verantwoordelijk voor zuurstoftransport en zorgen bloedplaatjes voor stolling. Ontwikkeling en rijping van bloedcellen, ook wel hematopoïese genoemd, vindt in het beenmerg plaats. De HSC heeft de bijzondere eigenschap dat deze, naast de ontwikkeling in specifieke bloedcellen, zichzelf ook kan vernieuwen. Op deze manier is er een 'eindeloze' voorraad van bloedcellen. Hoe ontwikkelder en volgroeider een bloedcel raakt, hoe beperkter de levensduur en de mogelijkheid tot celdeling. Volgroeide, rijpe bloedcellen verlaten het beenmerg en gaan de bloedbaan in. Op deze manier wordt de hoeveelheid bloedcellen in ons lichaam continue gereguleerd, vernieuwd en aangevuld. Echter een fout in de rijping van witte bloedcellen kan tot een blokkade in de ontwikkeling leiden, waardoor deze cel het beenmerg niet kan verlaten. Gecombineerd met ongeremde celdeling kan deze bloedcel leukemie veroorzaken: de leukemiecel verdringt en overgroeit gezonde bloedcellen. Dit heeft tot gevolg dat patiënten met leukemie een verminderde weerstand hebben (tekort aan gezonde witte bloedcellen), bloedarmoede hebben (tekort aan rode bloedcellen) en er gemakkelijk blauwe plekken en bloedingen ontstaan (tekort aan bloedplaatjes).
Er zijn verschillende vormen van leukemie. Zo kan leukemie acuut of chronisch zijn. Een acute leukemie ontwikkelt zich relatief snel uit niet gerijpte, voorloper, witte bloedcellen. Bij een chronische leukemie is de bloedcel beter ontwikkeld, maar kan deze niet geheel normaal functioneren. Dit heeft tot gevolg dat de leukemie zich wat langzamer ontwikkelt. Een verdere onderverdeling van leukemie vindt plaats aan de hand van het type witte bloedcel dat de leukemie veroorzaakt, namelijk een myelöide cel of lymfocyt. Deze cellen behoren tot de twee verschillende immuunsystemen. Myeloïde cellen zijn onderdeel van

het aangeboren immuunsysteem, de algemene afweer van ons lichaam. Lymfocyten zijn onderdeel van het verworven immuunsysteem. Dit immuunsysteem ontwikkelt zich gedurende ons leven en heeft een geheugen: nadat je eenmalig in aanraking bent geweest met ziekteverwekkers, kan je immuunsysteem de infectie bij een nieuwe infectie sneller onderdrukken.

Acute lymfatische leukemie

Acute lymfatische leukemie (ALL) is de meest voorkomende vorm van kanker bij kinderen. Jaarlijks worden er in Nederland zo'n 125 kinderen gediagnostiseerd met de ziekte. ALL kan worden onderverdeeld in voorloper B-cel of T-cel ALL; de verschillende typen lymfocyten. In 85% van de gevallen wordt ALL veroorzaakt door een fout in de ontwikkeling van de B-cellen, ook wel B-cel precursor ALL (BCP-ALL) genoemd. In deze thesis is gefocust op dit type leukemie.

De overlevingskans van kinderen met ALL is de afgelopen jaren enorm toegenomen: in de jaren 60 overleefde ongeveer 10% van de kinderen de ziekte, maar hedendaags is de overlevingskans ongeveer 90%.[1] Alhoewel dit een enorme stijging is, betekent dit helaas nog steeds dat 1 op de 10 kinderen met leukemie overlijdt aan de gevolgen van de ziekte. Daarnaast hebben overlevenden van kinderkanker vaak te maken bijwerkingen en nare (late) effecten als gevolg van de behandeling van hun ziekte. Om de prognose van deze kinderen te verbeteren en gevolgen van de behandeling te verminderen zijn nieuwe therapeutische opties nodig.

Pathobiologie van B-cell Precursor Acute Lymfatische Leukemie

De ontwikkeling (differentiatie) van B cellen heeft als doel om een volwassen (mature) B-cel met unieke B-cel receptor te creëren, waarmee ziekteverwekkers worden herkend. Dit ontwikkelingsproces verloopt gefaseerd, waarbij de cel vanuit het diepe beenmerg richting de bloedvaten migreert. Regulatie van dit differentiatieproces vindt plaats door factoren in de cel (intracellulair), maar ook door andere factoren in het beenmerg (extracellulair). Intracellulaire regulatie vindt plaats door transcriptiefactoren, die ervoor zorgen dat de juiste processen in de cel actief zijn.[2] Voorbeelden van deze transcriptiefactoren zijn *ERG*, *IKZF1*, *EBF1* en *PAX5*. Naast transcriptiefactoren wordt de ontwikkeling van B-cellen gecontroleerd door andere niet-hematopoietische cellen uit het beenmerg, o.a. mesenchymale stroma cellen (MSCs). MSCs scheiden groeifactoren uit en activeren signaleringscascades in B-cellen door direct cel-cel contact.[3-5]

BCP-ALL is een heterogene ziekte die door een spectrum van genetische afwijkingen kan worden veroorzaakt. Een veelvoorkomend mechanisme dat betrokken is bij het ontstaan van leukemie zijn chromosomale translocaties. Bij een translocatie worden DNA segmenten van twee chromosomen 'uitgewisseld', wat leidt tot (twee) nieuwe chromosomen. Zo kan een chromosomale translocatie tot gevolg hebben dat het *BCR* gen op chromosoom 22 doormidden wordt gebroken en fuseert met een deel van het *ABL1* gen op chromosoom 9. Dit *BCR-ABL1* fusiegen verstoort de normale signaleringsprocessen in de cel en activeert groei- en overlevingsprocessen. Andere voorbeelden van fusiegenen in BCP-ALL zijn *ETV6-RUNX1*, *TCF3-PBX1* en *KMT2A-AF4*. Naast fusiegenen wordt de leukemiecel bij een ander groot deel (~30%) van de kinderen gekarakteriseerd door een afwijkend aantal chromosomen. Indien er meer dan 50 chromosomen aanwezig zijn in de leukemiecel

spreekt men over hoog hyperdiploïde leukemie. Met de onderverdeling in fusiegenen en chromosoom aantallen, blijft ongeveer 25% van de leukemiepatiënten over met een genetisch ongekarakteriseerde ziekte. Opmerkelijk is dat het genexpressie profiel van de leukemiecellen van een deel van deze patiënten sterk lijkt op het genexpressieprofiel van *BCR-ABL1*-positieve cellen. Echter is het *BCR-ABL1* fusiegen niet aanwezig in deze cellen. Deze vorm van leukemie wordt daarom *BCR-ABL1*-like leukemie genoemd. De overige patiënten worden gekarakteriseerd als hebbende een 'overige' vorm van leukemie, ook wel 'B-other' leukemie genoemd.
De verschillende subtypen van leukemie zijn ieder geassocieerd met een specifieke prognose. Zo hebben kinderen met de *ETV6-RUNX1* translocatie of hoog hyperdiploïde leukemie een relatief goede prognose. *TCF3-PBX1* en 'B-other' leukemie zijn geassocieerd met een intermediaire prognose en kinderen met *KMT2A*-herschikte, *BCR-ABL1*, of *BCR-ABL1*-like hebben een relatief slechte prognose. Behalve het feit dat deze genetische afwijkingen voorspellend zijn voor de prognose, kunnen ze ook een doel (target) vormen voor doelgerichte therapie. Patiënten met *BCR-ABL1*-positieve leukemie worden behandeld met een specifiek middel, imatinib, dat de signalering van het *BCR-ABL1* oncogen remt. In Nederland is *BCR-ABL1*-positieve leukemie het enige subtype van BCP-ALL dat met een doelgerichte therapie (=precisiemedicijn) wordt behandeld.

De behandeling van kinderleukemie

De enorme stijging in de overleving van kinderen met leukemie, die de afgelopen decennia heeft plaatsgevonden, is niet veroorzaakt door de introductie van nieuwe geneesmiddelen. De middelen die worden gebruikt voor de behandeling van leukemie zijn namelijk al jaren in de kliniek en alles behalve specifiek voor de leukemiecel, met de uitzondering van imatinib. De toename in overleving is met name te danken aan een verbeterde risico-indeling van leukemiepatiënten met daarbij horende behandeling, en stamcel transplantaties bij kinderen met een slechte prognose.
De afgelopen jaren is het inzicht in genetische afwijkingen die bijdragen aan het ontstaan van kanker toegenomen. Bovendien vormen precisiemedicijnen een doorbraak in de behandeling van kanker. Precisiemedicijnen zijn gericht tegen een specifieke genetische afwijking in de kankercel. Voor een succesvolle behandeling is het daarom van groot belang om het juiste moleculaire tumorprofiel te koppelen aan het juiste precisiemedicijn. Het aantal bekende DNA afwijkingen groeit snel, maar er valt nog veel inzicht te winnen in klinisch relevante combinaties van DNA afwijkingen en precisiemedicijnen. Het vergroten van de kennis van genetische afwijkingen die betrokken het ontstaan van kinderleukemie zal hier aan bijdragen. Daarnaast bevordert het bestuderen van potentiële targets en precisiemedicijnen in preklinische modellen succesvolle implementatie in de kliniek. Om hieraan bij te dragen, is in deze thesis gefocust op de pathobiologie van pediatrische BCP-ALL, met name de genetisch ongeclassificeerde *BCR-ABL1*-like en B-other BCP-ALL.

De biologie van *BCR-ABL1*-like leukemie

Het afgelopen decennium is het genetische landschap van *BCR-ABL1*-like leukemie intensief bestudeerd. De gelijkenis in de genexpressieprofielen met *BCR-ABL1*-positieve leukemie impliceert dat een vergelijkbaar mechanisme verantwoordelijk is voor het ontstaan de leukemie. Recente studies en **hoofdstuk** 2 van deze thesis laten zien dat dat een

deel van deze patiënten gekenmerkt wordt door zeldzame chromosomale translocaties.[6-8] Deze translocaties kunnen worden onderverdeeld in ABL klasse translocaties en JAK klasse translocaties. Aangezien imatinib naast ABL1 ook andere ABL familieleden remt, wordt de effectiviteit van imatinib in de behandeling van deze patiënten momenteel onderzocht. Daarnaast wordt geïmpliceerd om de JAK klasse fusiegenen met specifieke JAK remmers te behandelen, zoals bijvoorbeeld ruxolitinib of momelotinib. In **hoofdstuk 3** van deze thesis hebben we ons verdiept in de therapeutische potentie van deze JAK remmers. Naast de JAK translocaties, wordt een deel van de kinderen met BCP-ALL namelijk ook gekenmerkt door puntmutaties in het *JAK2* gen. Deze puntmutaties zijn niet beperkt tot het *BCR-ABL1*-like subtype, maar worden ook in B-other en hoog hyperdiploïde leukemie patiënten gevonden. Alhoewel de biologie van de *JAK2* translocaties en *JAK2* mutaties anders is, kunnen beiden mogelijk worden geremd door JAK remmers. Onze resultaten laten zien dat deze JAK remmers inderdaad effectief zijn in het doden van cellen met een *JAK2* translocatie of *JAK2* puntmutatie. Helaas laten onze resultaten ook een aantal limitaties zien:

1. De huidige remmers (ruxolitinib en momelotinib) binden de mutant *JAK2* en *JAK2* fusiegenen in een actieve conformatie. Opheffing van deze binding (bijvoorbeeld als gevolg van instabiliteit/afbraak van de remmer) resulteert in hypersignalering. Om re-activatie van de JAK2 signalering te voorkomen, dient er een JAK remmer te worden ontwikkeld die de *JAK2* mutanten en fusiegenen in een inactieve toestand kan binden.
2. Leukemiecellen met *JAK2* puntmutaties kunnen ontsnappen aan het effect van JAK remmers d.m.v. alternatieve signaleringspathways. Naast *JAK2* puntmutaties, zijn er namelijk ook andere puntmutaties in de leukemiecellen aanwezig (bijv. *KRAS*). In een muismodel observeerden we een heterogeen uitgroeipatroon van deze mutaties, waarin de *JAK2* mutaties zelfs kon verdwijnen. Deze observaties suggereren dat *JAK2* mutaties, geen drivers maar passenger mutaties zijn.
3. De beenmerg micro-omgeving speelt een belangrijke rol in de bescherming van leukemiecellen tegen JAK remmers. MSCs blijken niet alleen belangrijk voor de ontwikkeling van bloedcellen; ze kunnen leukemiecellen ook beschermen tegen JAK remmers.

Deze resultaten laten zien dat JAK remmers veel potentie bieden, maar verdere optimalisatie nodig is voor hun implementatie in de kliniek.

De biologie van 'B-other' leukemie

Recente publicaties hebben het inzicht in de onderliggende mechanismen van B-other leukemie vergroot. Een deel van deze B-other patiënten blijkt namelijk een genetische translocatie van het *DUX4* gen te bevatten.[9-11] Helaas is er momenteel nog geen doelgerichte therapie tegen *DUX4* beschikbaar. Om toch een precisiemedicijn te kunnen geven aan deze patiënten is het van belang om volledig inzicht te verkrijgen in de signaleringscascade van *DUX4* in leukemiecellen. Op deze manier kan therapie eventueel worden gericht op een belangrijke factor voor *DUX4* signalering. In **hoofdstuk 4** van de thesis ontdekten we dat een deel van de B-other en *BCR-ABL1*-like patiënten een verhoogde expressie van het *STAP1* gen hebben, wat een specifiek kenmerk bleek van leukemiepatiënten met een *DUX4*-translocatie. Onderzoek naar de therapeutische potentie van *STAP1* bleek helaas niet veelbelovend. Verlaging van *STAP1* expressie levels resulteerde niet in celdood, noch

maakte het cellen gevoeliger voor chemotherapeutische middelen. Dit betekent dat de zoektocht naar targets voor therapie in deze *DUX4*-rearranged patiënten vervolgd dient te worden.

Coöperatieve genetische afwijkingen

Chromosomale translocaties alleen zijn niet voldoende om leukemie te veroorzaken; ze hebben een meewerkende, coöperatieve, genetische aberratie nodig. De frequentie waarmee de *ETV6-RUNX1* translocatie wordt gedetecteerd in navelstrengbloed ligt bijvoorbeeld 100 keer hoger dan de incidentie van deze vorm van leukemie.[12] Daarnaast laat een studie in een eeneiige tweelingen zien dat de *BCR-ABL1* translocatie ook afhankelijk is van een additionele aberratie. In de navelstrengbloedsamples werd bij beide kinderen de *BCR-ABL1* translocatie geïdentificeerd. Echter alleen het kind waar ook een deletie van het *IKZF1* gen aanwezig was, ontwikkelde een leukemie.[13] Deze voorbeelden suggereren dat naast een initiële hit, coöperatieve genetische afwijkingen nodig zijn voor het ontstaan van leukemie. De afgelopen jaren is er veel onderzoek gedaan naar additionele afwijkingen bij kinderleukemie en het belang van deze afwijkingen voor risicostratificatie.[14,15]

Opvallend worden in BCP-ALL patiënten vaak deleties gedetecteerd in genen die van belang zijn voor de regulatie van de B cel ontwikkeling (*IKZF1*, *EBF1*, *PAX5*, *ETV6*), celdeling (*CDKN2A/B*, *RB1*) of celdood (*BTG1*). In **hoofdstuk 5** detecteerden we in 71% van de kinderen met leukemie een deletie in een van deze genen. Echter verschilde de verdeling van deze deleties per subtype. Zo ligt de frequentie van één of meer deleties in *BCR-ABL1*, *BCR-ABL1*-like, B-other en *ETV6-RUNX1* patiënten boven de 75%. In *KMT2A*-herschikte, hoog hyperdiploid en *TCF3-PBX1* leukemie ligt deze frequentie beneden de 40%. Verder onderzoek naar de relaties van deleties van deze genen met chemotherapieresistentie en een slechte prognose, toonde alleen een associatie aan met *IKZF1* deleties. Deze associatie was afhankelijk van het BCP-ALL subtype, oftewel de genetische context van de leukemiecel. Zo bleken hoog hyperdiploïde cellen met een *IKZF1* deletie extreem resistent tegen prednisolon, terwijl *BCR-ABL1*-like en B-other cellen resistent bleken tegen thiopurines. Deze resultaten laten zien dat het van groot belang is om studies naar chemotherapieresistentie en prognose te verrichten in de juiste genetische context.

De beenmergmicro-omgeving

MSCs zijn een belangrijke factor voor de ontwikkeling van bloedcellen, zowel door secretie van groeifactoren als direct cel-cel contact.[3-5] In **hoofdstuk 3** van deze thesis hebben we gezien dat MSCs leukemiecellen beschermen tegen het effect van JAK remmers. Vergelijkbare observaties zijn gerapporteerd voor andere middelen die worden gebruikt in de behandeling van leukemie.[16-20] Deze observaties laten het belang van MSCs voor de overleving van de leukemiecel zien. Daarom stond in **hoofdstuk 6** van deze thesis de vraag centraal of MSCs van kinderen met leukemie (leukemie-MSCs) verschillen van MSCs van gezonde kinderen (controle-MSCs). Om dit te onderzoeken zijn ondersteunende eigenschappen voor leukemieceloverleving van deze MSCs vergeleken. De overleving van leukemiecellen is namelijk verhoogd als deze in de aanwezigheid van MSCs worden gekweekt. Onze resultaten laten zien dat zowel leukemie-MSCs

als controle-MSCs de overleving van BCP-ALL cellen verhogen en er werd geen verschil gedetecteerd in ondersteuning tussen leukemie-MSCs en controle-MSCs. Een opmerkelijke bevinding was echter dat het genexpressieprofiel van MSCs verandert als deze samen met leukemiecellen worden gekweekt. Elk leukemie sample induceerde een karakteristieke verandering in het genexpressie profiel van MSCs, die consistent was tussen verschillende MSCs. Deze veranderingen in het genexpressie profiel van de MSCs bleken niet permanent, maar verdwenen in afwezigheid van de leukemiecellen. Er werden namelijk kleine verschillen geobserveerd tussen de genexpressieprofielen van leukemie-MSCs en controle-MSC, maar deze verschillen waren verdwenen in MSCs die tijdens de behandeling van leukemie werden geïsoleerd. Samengenomen laten deze resultaten zien dat leukemie-MSCs intrinsiek niet verschillen van controle-MSCs. Echter manipuleren leukemiecellen het genexpressieprofiel van MSCs, wat samenvalt met een verhoogde overleving van deze BCP-ALL cellen. Daarmee is de interactie tussen leukemiecellen en MSCs mogelijk een belangrijk target voor de behandeling van leukemie. Deze interactie dient dan ook verder bestudeerd te worden in toekomstig onderzoek.

Leukemie is een dynamisch proces dat afhankelijk is van verscheidene variabelen. Volledig inzicht in de pathobiologie van BCP-ALL is essentieel voor de identificatie voor nieuwe therapeutische targets. In deze thesis, zijn een aantal potentiële targets bestudeerd. Daarnaast laten onze resultaten een belangrijke rol zien van de beenmerg micro-omgeving in therapieresistentie. Deze interactie tussen BCP-ALL cellen en MSCs staat centraal in ons vervolg onderzoek.

REFERENTIES

1. Pui CH, Evans WE. A 50-year journey to cure childhood acute lymphoblastic leukemia. Semin Hematol 2013;50:185-96.
2. Somasundaram R, Prasad MA, Ungerback J, Sigvardsson M. Transcription factor networks in B-cell differentiation link development to acute lymphoid leukemia. Blood 2015;126:144-52.
3. Zhang J, Niu C, Ye L, et al. Identification of the haematopoietic stem cell niche and control of the niche size. Nature 2003;425:836-41.
4. Nagasawa T. Microenvironmental niches in the bone marrow required for B-cell development. Nature Reviews Immunology 2006;6:107-16.
5. Lilly AJ, Johnson WE, Bunce CM. The haematopoietic stem cell niche: new insights into the mechanisms regulating haematopoietic stem cell behaviour. Stem Cells International 2011;2011:274564.
6. Roberts KG, Morin RD, Zhang J, et al. Genetic alterations activating kinase and cytokine receptor signaling in high-risk acute lymphoblastic leukemia. Cancer cell 2012;22:153-66.
7. Robison LL, Hudson MM. Survivors of childhood and adolescent cancer: life-long risks and responsibilities. Nature reviews Cancer 2014;14:61-70.
8. Reshmi SC, Harvey RC, Roberts KG, et al. Targetable kinase gene fusions in high-risk B-ALL: a study from the Children's Oncology Group. Blood 2017;129:3352-61.
9. Lilljebjorn H, Henningsson R, Hyrenius-Wittsten A, et al. Identification of ETV6-RUNX1-like and DUX4-rearranged subtypes in paediatric B-cell precursor acute lymphoblastic leukaemia. Nature communications 2016;7:11790.
10. Yasuda T, Tsuzuki S, Kawazu M, et al. Recurrent DUX4 fusions in B cell acute lymphoblastic leukemia of adolescents and young adults. Nature genetics 2016;48:569-74.
11. Zhang J, McCastlain K, Yoshihara H, et al. Deregulation of DUX4 and ERG in acute lymphoblastic leukemia. Nature genetics 2016;48:1481-9.
12. Mori H, Colman SM, Xiao Z, et al. Chromosome translocations and covert leukemic clones are generated during normal fetal development. Proceedings of the National Academy of Sciences of the United States of America 2002;99:8242-7.
13. Cazzaniga G, van Delft FW, Lo Nigro L, et al. Developmental origins and impact of BCR-ABL1 fusion and IKZF1 deletions in monozygotic twins with Ph+ acute lymphoblastic leukemia. Blood 2011;118:5559-64.
14. Den Boer ML, van Slegtenhorst M, De Menezes RX, et al. A subtype of childhood acute lymphoblastic leukaemia with poor treatment outcome: a genome-wide classification study. Lancet Oncol 2009;10:125-34.
15. Mullighan CG, Su X, Zhang J, et al. Deletion of IKZF1 and prognosis in acute lymphoblastic leukemia. N Engl J Med 2009;360:470-80.
16. Polak R, de Rooij B, Pieters R, den Boer ML. B-cell precursor acute lymphoblastic leukemia cells use tunneling nanotubes to orchestrate their microenvironment. Blood 2015.
17. Iwamoto S, Mihara K, Downing JR, Pui CH, Campana D. Mesenchymal cells regulate the response of acute lymphoblastic leukemia cells to asparaginase. J Clin Invest 2007;117:1049-57.
18. Vianello F, Villanova F, Tisato V, et al. Bone marrow mesenchymal stromal cells non-selectively protect chronic myeloid leukemia cells from imatinib-induced apoptosis via the CXCR4/CXCL12 axis. Haematologica 2010;95:1081-9.
19. Baldridge MT, King KY, Goodell MA. Inflammatory signals regulate hematopoietic stem cells. Trends Immunol 2011;32:57-65.
20. Takizawa H, Boettcher S, Manz MG. Demand-adapted regulation of early hematopoiesis in infection and inflammation. Blood 2012;119:2991-3002.

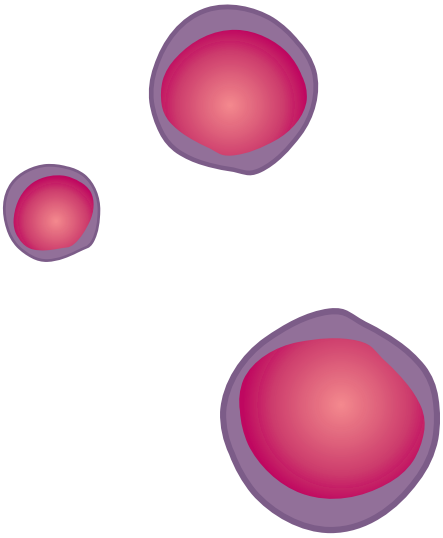

Chapter 9

ABOUT THE AUTHOR

Biografie

Lieneke Steeghs werd op 30 mei 1989 geboren te Oirlo. Nadat ze in 2007 haar Gymnasium diploma behaalde, startte ze met de Bachelor Biomedische Wetenschappen aan de Faculty of Health, Medicine and Life Science van de Universiteit Maastricht. Voor de afronding van haar Bachelor liep ze een wetenschappelijk stage op de afdeling Gastroenterology and Hepatology aan de Universiteit Maastricht. Haar interesse in oncologie uitte zich in het vervolg van haar studie met de Master Oncology and Developmental Biology in 2010. Als onderdeel van deze master onderzocht ze op de afdeling Tumor Immunologie aan de Universiteit Maastricht het effect van hypoxie op chemo-immunotherapy voor multiple myeloma. Voor de afronding van de master deed ze onderzoek op de afdeling Pathologie van het UMC Utrecht. Hier bestudeerde ze de rol van humane granzymen in de verdediging van het immuun systeem tegen kanker. Na voltooiing van de master, starte ze in 2012 een promotieonderzoek op de afdeling kinderoncologie/-hematologie in het Sophia kinderziekenhuis - Erasmus MC te Rotterdam. Onder de begeleiding van Prof. dr. Monique den Boer en Prof. dr. Rob Pieters deed ze gedurende een periode van 4 jaar onderzoek naar de pathobiologie van voorloper B-cel acute lymfatische leukemie bij kinderen. De resultaten van dit onderzoek zijn beschreven in dit proefschrift.
Lieneke vervolgt haar carrière in het Radboudumc op de afdeling Pathologie. Hier werkt ze aan een landelijke project dat als doel heeft om de moleculaire predictieve diagnostiek ten behoeve van therapiekeuze bij patiënten met kanker te optimaliseren.

List of publications

***Steeghs EMP**, Bakker M, Hartman Q, Stalpers F, Pieters R, den Boer ML. High STAP1 expression in DUX4-rearranged cases is not suitable as therapeutic target in pediatric B-cell precursor acute lymphoblastic leukemia. Scientific reports. 2018 Jan 12;8(1):693.*

Steeghs EMP, Jerchel IS*, de Goffau-Nobel W, Hoogkamer AQ, Boer JM, Boeree A, van de Ven C, Koudijs MJ, Besselink NJM, de Groot-Kruseman HA, Zwaan CM, Horstmann MA, Pieters R, den Boer ML. JAK2 aberrations in B-cell precursor acute lymphoblastic leukemia. Oncotarget. 2017 Sep 16;8(52):89923-89938.*

*Boer JM, **Steeghs EMP**, Marchante JM, Boeree A, Beaudoin JJ, Beverloo HB, Kuiper RP, Escherich G, van der Velden VHJ, van der Schoot E, de Groot-Kruseman HA, Pieters R, den Boer ML. Tyrosine kinase fusion genes in pediatric BCR-ABL1-like acute lymphoblastic leukemia. Oncotarget. 2017 Jan 17;8(3):4618-4628.*

***Steeghs EMP**, Boer JM, Hoogkamer AQ, Boeree A, Escherich G. de Haas V, de Groot-Kruseman HA, Pieters R, den Boer ML. CNAs in B-cell development genes, drug resistance, and clinical outcome of pediatric BCP-ALL. Submitted.*

***Steeghs EMP**, Polak R, de Rooij B, van den Berk LCJ, van de Ven C, Stalpers F, Boer JM, Pieters R, den Boer ML. B-cell precursor acute lymphoblastic leukemia cells manipulate mesenchymal stromal cells. Work in progress.*

*Jerchel IS, Hoogkamer AQ, Aries IM, **Steeghs EMP**, Boer JM, Besselink NJM, Boeree A, van de Ven C, de Groot-Kruseman HA, de Haas V, Horstmann MA, Escherich G, Stam RW, Zwaan CM, Cuppen EPJG, Koudijs MJ, Pieters R, den Boer ML. Ras pahtway mutations as predictive biomarker for treatment adaptation in pediatric B-cell precursor acute lymphoblastic leukemia. Leukemia. 2018 Apr;32(4):931-940.*

*de Poot SA, van Erp EA, Meeldijk J, Broekhuizen R, Goldschmeding R, Olthof MC, **Steeghs EMP**, Bovenschen N. Bioluminescent reporters to monitor killer cell-mediated delivery of granzymes inside target cells. Blood. 2015 Dec 24;126(26):2893-5.*

*Sarkar S, Germeraad WT, Rouschop KM, **Steeghs EMP**, van Gelder M, Bos GM, Wieten L. Hypoxia induced impairment of NK cell cytotoxicity against multiple myeloma can be overcome by IL-2 activation of the NK cells. PLoS One. 2013 May 28;8(5):e64835.*

PhD portfolio

Surname	: Steeghs
Cristian names	: Elisabeth, Maria, Petronella
First name	: Lieneke
Erasmus MC department	: Pediatric Oncology/Hematology
Research school	: MolMed
PhD period	: 15th September 2012 – 14th September 2016
Promotors	: Prof. dr. M.L. den Boer, Prof. dr. R. Pieters

Seminars/ Courses/ Workshops	**Year**	**ECTS**
Basic Course on R *Postgraduate School Molecular Medicine, Erasmus MC*	2013	0.7
Course on R *Postgraduate School Molecular Medicine, Erasmus MC*	2013	0.7
Course on the Analysis of microarray and RNA seq expression data using R/BioC and web tools *Postgraduate School Molecular Medicine, Erasmus MC*	2013	2
Biostatistical Methods I: Basic Principles (CC02) *NIHES, Erasmus MC*	2013	5.7
Course and master classes on molecular aspects of hematological disorders *Postgraduate School Molecular Medicine, Erasmus MC*	2014	1
BD Flow Course, Basis and Advanced Course *Department of Immunology, Erasmus MC*	2015	0.7
Research Integrity *Department Medical Ethis and Philosophy of Medicine, Erasmus MC*	2016	0.3
National Conferences		
• 17th and 18th Molecular Medicine Day, *Eraasmus*	2013-2014	1
• Ceremony Tom Voûte Award, *KiKa, Utrecht*	2013-2016	2
• Research Retraite, *SKION-Princes Máxima Centrum, De Bilt*	2013, 2015	1

International conferences and Presentations	**Year**	**ECTS**
Oral presentation at the KiKa Research day (Nominee Tom Voûte award)	2017	2
Oral presentation at the Daniel den Hoed day, *Erasmus MC*	2017	2
Oral presentation at the American Society of Hematology (ASH) Annual Meeting 2016, *San Diego, CA, USA*	2016	2
Presentation at the Research Meeting of the Laboratory of Pediatrics, *Erasmus MC*	2015	0.5
Presentations at the Pediatric Oncology Research Meetings, *Erasmus MC*	2012-2016	8

Training and Supervising	**Year**	**ECTS**
Supervising Marjolein Bakker Final year student HLO, seven months internship, *Biology and Medical Laboratory Research, Hogeschool Rotterdam*	2015-2016	10
Supervising Quirine Hartman First year master student, seven months internship *Molecular Medicine Master, Erasmus MC*	2015-2016	10
Lecture for Erasmus University Medicine Students *Minor Pediatric Oncology, Erasmus MC*	2016	1

Total ECTS: 50.6

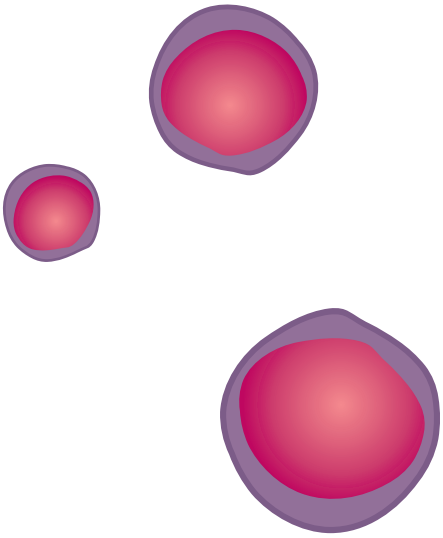

DANKWOORD

Dankwoord

Eindelijk is het tijd voor het dankwoord! Ik wil iedereen ontzettend bedanken die mijn onderzoek mogelijk heeft gemaakt en betrokken is de geweest de afgelopen tijd.

In het bijzonder wil ik de leukemiepatiënten en hun ouders bedanken. Jullie keuze om materiaal beschikbaar te stellen, maakt wetenschappelijk onderzoek naar deze ziekte en verbetering van de behandeling mogelijk. Dank voor deze moelijke, maar belangrijke beslissing.

Prof. dr. M. den Boer, beste Monique, bedankt voor het bieden van deze kans en al je vertrouwen. Onze wegen kruisten voor het eerst in de zomer van 2012. Zowel Rotterdam als het Erasmus MC waren toen nog onbekend terrein voor mij, maar daar was die interessante vacature. Ik ben nog steeds erg blij en dankbaar voor alles wat het heeft gebracht. Het TYK2 project liep anders dan we beiden hoopten, maar vormde uiteindelijk een goede start voor de weg die we hebben afgelegd. Je gaf me een ongekende vrijheid en veel ruimte om me verder te ontwikkelen, zowel op het lab als in persoonlijk opzicht. Daaraast heeft deze vrijheid unieke kansen gebracht, waar het laatste hoofdstuk een mooi resultaat van is. Bedankt voor je kritisch blik, sturing en alle feedback.

Prof. dr. Pieters, beste Rob, toen ik in het Erasmus MC begon, was jij al druk bezig met het verwezenlijken van de komst van het Prinses Máxima Centrum en nu zijn de deuren dan echt geopend. Ik heb ontzettend veel respect voor al je plannen, visie, passie en toewijding. Naast dit alles bleef je geïnteresseerd en betrokken bij mijn onderzoek. Je klinische blik was belangrijk om bevinden in perspectief te plaatsen. Bedankt voor je betrokkenheid, al je feedback en suggesties.

Een grote dankjewel voor de samenwerkingspartners van binnen en buiten het Erasmus MC. De mensen van het SKION, Hester de Groot, Valerie de Haas, en Edwin Sonneveld, en de COALL studiegroep, Martin Horstmann and Gaby Escherich: thank you very much for the convenient collaboration and providing the material and clinical data for the studies described in this thesis. Het hematologisch laboratorium specieel, alle kinderartsen, verpleegkundigen en andere betrokkenen: bedankt voor de verzameling van het onderzoeksmateriaal. De gegevens van het cytogenetisch en immunologisch lab zijn van onmisbare waarde voor dit proefschrift. Bedankt voor jullie adequate analyses en het beschikbaar stellen van jullie resultaten. Ook wil ik stichting KOCR bedanken, zowel voor de financiering van de onderzoeken als voor het faciliteren van het drukwerk.

Mijn dank gaat uit ook naar prof. dr. Marc Raaijmakers, prof. dr. Michel Zwaan en prof. dr. Sjaak Neefjes voor deelname aan de kleine commissie en het kritisch nalezen van mijn proefschrift. Daarnaast wil ik dr. Frank van Leeuwen, prof. dr. André Uitterlinden en prof. dr. Jolanda de Vries bedanken voor het zitting nemen in de grote commissie.

Het laboratorium kindergeneeskunde stond centraal bij de vier jaar van m'n onderzoek. Ik heb hier met veel plezier gewerkt en wat heb ik daarbij geluk gehad met jullie als collega's. Veel mooie momenten hebben we gedeeld. Femke, ik had de eer om jou welkom te heten

op de afdeling en een rondleiding te geven, terwijl het voor mij ook nog allemaal nieuw was. Je steun op het lab, maar vooral ook daarbuiten heeft erg veel voor me betekend. Ik ben ontzettend trots dat je mijn paranimf wilt zijn. Isabel, we got to known each other better during the last two years of our PhD projects. You were a great colleague and friend. I am very happy that you found a nice job and great life in Berlin. Aurélie, jij kwam het B-ALL team in het tweede jaar van m'n promotie versterken en al snel bleek dat we het goed konden vinden. Dat uitte zich niet alleen op het werk, maar ook daarbuiten hebben we samen veel lol gehad. De mooie mountainbike uitjes, je aanmoedigingen tijdens de halve marathon, escape rooms en ook je hulp bij de verhuizing. Bedankt voor alles. Mijn kamergenoten: Bob, dank voor je altijd nuchtere blik, eerlijkheid en oprechtheid. Het was erg fijn je als collega te hebben, die nergens omheen draaide, maar gewoon oprechte feedback gaf. Mark, wij begonnen ons PhD avontuur bijna tegelijk. Je hebt heel wat afgereisd qua woningen die vier jaar, maar bent maar één keer van werkkamer gewisseld. Zo zijn we bijna atijd kamergenootjes geweest. Je humor en vriendschap hebben veel voor me betekend. Heel veel succes in de toekomst met je nieuwe baan! Roel, de initiatiefnemer van het jaarlijkse mountainbikeweekend. Bedankt hiervoor! En daarnaast ook bedankt voor de fijne collega die je bent geweest. Naast je vriendelijkheid, heb je ook een belangrijke rol gespeeld in mijn onderzoek. João, thank you very much for you happiness, but also your willingness to help other people. Your R-skills helped me a lot! Judith, ook jij was er altijd om me wegwijs te maken in R. Daarnaast was je een erg fijne collega die altijd een luisterend oor bood. Zowel voor experimenten als voor privé adviezen kon ik op je rekenen. Priscilla, de escaperoomuitjes die je organiseerde waren altijd een succes of we nu wel of niet wisten te ontsnappen. Succes met het afronden van jouw promotieonderzoek. Alex, je passie voor handboogschieten was groot en dat leverde mooie verhalen op na het weekend. Daarnaast stond je altijd klaar om een helpende hand te reiken bij mijn onderzoek. Cesca, jij was de persoon die mij opwachtte op m'n eerste dag en me wegwijs heeft gemaakt op de afdeling. Bovendien had je veel geduld bij de muizen en heb je me daarmee veel geleerd. Heel erg bedankt hiervoor. Lieke, we zijn maar kort collega's geweest, maar toch heb je ontzettend veel voor m'n onderzoek betekend: zonder jou waren al die experimenten met de MSCs niet mogelijk geweest. Willemieke, een jaar lang hebben we mogen samenwerken. Het JAK2 stuk was nooit zo'n succes geweest zonder jou. Bedankt voor de fijn samenwerking! Iris, onze samenwerking was maar kort, maar je was een hele fijne collega. Ik ben blij dat je zo je plek hebt gevonden. De overige leden van de B-ALL groep: Myrthe, Rosanna, Ingrid, Farhad, Diana: bedankt voor jullie betrokkenheid bij m'n onderzoek, feedback tijdens de werkbesprekingen en gezelligheid daarbuiten. Mijn eerste kamergenoten Arian, Sylvia, Dicky, Lisette, Roelien, Ytje en Malou, bedankt voor de fijne start die ik bij jullie heb mogen maken. Marcel, jij was een onmisbare schakel op het lab en zorgde dat alle gestroomlijnd kon verlopen. Daarnaast was je ook altijd erg betrokken en bij iedere borrel aanwezig. Bedankt voor alles! Linda, we deelden onze passie voor hardlopen. Ik ben nog altijd trots op die CPC-loop voor crocokids! Succes met het afronden van je promotieonderzoek en in de toekomst! Sanne en Ruben, jullie hebben allebei mooie projecten en al veel bereikt. Succes met de laatste loodjes. M'n medelabdag organisatoren: Judith, Lea, Priscilla en Theo, ik heb het erg leuk gehad om met jullie de labdag te organiseren, die een groot succes was. Bedankt hiervoor! Daarnaast wil ik ook alle andere collega's van het lab bedanken. De analisten van de patiëntendienst: Pauline, Merel, Susan, Lonneke, Jessica en Wilco.

Dank voor jullie adequate werk van het isoleren en opwerken van de leukemiecellen. De patiëntensample database die jullie hebben opgebouwd is de drijvende kracht achter de onderzoeken op de afdeling. Sandra, Eddy, Noorie, Nicole, Celia, Kirsten, Dirk, Yun Lei, Ad, Sharon, en Patrick, het was fijn om jullie als collega te hebben. Rui, it was very nice that we could share the experience of half a marathon in Dordrecht. It is still a very grateful memory. Jessica, dank voor al je attendheid, begrip en goede gesprekken. Ik ben blij dat ik je heb kunnen aanmoedigen bij de Vierdaagse. Patricia, I admire your drive for research a lot. Besides that you were always interested in how life was going. I am still grateful that you adviced me to visit your physiotherapist. I wish you all the best for the future.
Quirine en Marjolein, het was erg leuk om jullie stagebegeleidster te zijn en om jullie te zien groeien op het lab. Bedankt voor al jullie hulp bij het STAP1 project en heel veel succes voor de toekomst!

Daarnaast wil ik ook overige groepsleiders van het laboratorium Kindergeneeskunde bedanken: Jules, Ronald, Maarten, Janneke en Wendy, bedankt voor alle jullie feedback en suggesties tijdens de werkbesprekingen en daarbuiten. Veel succes in de toekomst.

Mijn nieuwe collega's uit het Radboudumc. Marjolijn en Katrien, ik ben jullie ontzettend dankbaar voor het vertrouwen en de kansen die jullie me nu al hebben gegeven. Simone, bedankt voor al je hulp, samenwerking, maar vooral ook vaak je luisterende oor. Daarnaast wil ik ook m'n collega's van de moleculaire diagnostiek bedanken. Het is fijn hoe jullie me hebben opgenomen in jullie team: Leonie, Astrid, Mandy, Patricia, Riki, Annemiek, Greet, Jeroen, Jos, Marjan, Monique, Monique, Paul, Sandra. En natuurlijk mijn kamergenoten, Annemieke, Lisa en Robbert: we werken aan heel verschillende projecten, maar voelen elkaar goed aan. Helaas kan ik hier geen appel stickertje plakken;)

Naast het lab, heb ik veel afleiding gehad en inspiratie gevonden in mijn vrije tijd. Korfbal speelde hierin een grote rol. RSKV Erasmus bedankt voor jullie alle mooie momenten die we hebben gedeeld. Natuurlijk was er die gezamenlijke passie voor sport, maar er was veel meer dan alleen dat.
Eveline, via korfbal leerden wij elkaar kennen. Toen bleek je vlakbij me in de buurt te wonen en ook nog eens een enthousiaste hardloopster te zijn. Samen hebben we al veel moois bereikt en ik hoop er nog een paar leuke wesdtrijden aankomen! Heel erg bedankt voor je fijne vriendschap en alle steun en afleiding die je hebt gegeven. Ik wens je veel geluk in de toekomst samen met je mannen.
Jacoline, ook wij kennen elkaar via het korfbal. Niet uit Rotterdam, maar al uit Maastricht. Van korfbalgenootje werd je m'n huisgenootje. Tijdens mijn stage in Utrecht hielden we contact en uiteindelijk bleek dat we beiden een baan in Rotterdam hadden gevonden! Wat was het fijn dat er iemand die ik zo goed kende ook naar die vreemde stad ging. Ik ben je heel erg dankbaar voor al je steun en nuchterheid. Ook al zijn de wekelijkse etentjes er niet meer, we voelen elkaar nog steeds goed aan. Ik ben je heel erg dankbaar voor je vriendschap en het is een eer dat je mijn paranimf wilt zijn.
Elise, ik ben heel blij dat we contact hebben gehouden na de stage bij pathologie. Of we nu in Rotterdam, het mooie Gouda, of Utrecht afspreken, het is altijd goed. Heel veel succes met je avontuur in Canada!

Loes, we leerden elkaar eigenlijk pas goed kennen toen jij besloot Maastricht te verlaten. Het heeft onze vriendschap er niet minder sterk op gemaakt. Waar je ook woonde, je bent altijd erg belangrijk voor me geweest. Bedankt voor de bijzondere band die hebben en heel veel succes en geluk voor de toekomst.
Natuurlijk wil ik ook m'n vriendinnen uit Oirlo en omgeving bedanken. We kennen elkaar allemaal al erg lang en dat maakt het ook zo vertrouwd. Anne, Ilse, Lilian, Lonneke, Marieke, Sanne, Sandra en Sandra. Bedankt voor de gezelligheid, alle leuke uitjes, maar ook jullie luisterende oor en interesse in mijn promotie. Jolanda, Linda en Mariëlle, na de middelbare school zijn we allemaal in een ander deel van Nederland terecht gekomen, maar gelukkig zijn we elkaar nooit uit het oog verloren. De uitstapjes zijn altijd een groot succes en ik hoop dat we samen nog veel gaan ondernemen in de toekomst!

De familie Steeghs en Peters: alle ooms en tantes en neven en nichten die met me hebben meegeleefd de afgelopen jaren en altijd geïnteresseerd waren: heel erg bedankt voor jullie steun! Jullie interesse voor m'n onderzoek was altijd groot en dat was erg fijn. Mijn peetoom en peettante: Pieter, jij bent erg intensief bij alles betrokken geweest. Iedere verhuizing heb je meegemaakt en altijd stond je weer klaar om me te helpen. Daarnaast hebben we in Rotterdam ook kunnen genieten van heel wat etentjes. Bedankt voor alles! Ria, jij ook bedankt voor al je interesse, betrokkenheid en steun.

Elvire, Walter, Anne-Hilde en Wouter: bedankt voor de warme ontvangst die jullie me in jullie gezin hebben gegeven. Daarnaast heeft jullie interesse en steun veel voor me betekend de afgelopen tijd.

Lieve mam en pap, de afgelopen jaren zijn voor jullie niet makkelijk geweest. Ook mijn keuzes waren daarbij niet altijd de meest voor de hand liggende en makkelijkste voor jullie. Toch hebben jullie altijd iedere keuze gerespecteerd en gesteund. Ik ben jullie erg dankbaar voor jullie positiviteit en hoop dat de komende jaren veel moois voor jullie in petto hebben. Anne-Mieke, jij bent er altijd voor me geweest. We zijn het lang niet altijd eens, maar je bent wel altijd bereid om me te helpen. Of het nu is om nieuwe woonruimte te zoeken, afleiding tijdens een leuke vakantie, winkelen, een goed telefoongesprek, of gezelligheid, ik kan altijd op je rekenen. Ik ben erg blij dat je m'n zus bent! Silke, voor jou is er de afgelopen tijd veel veranderd. Ik ben blij dat je zo je draai hebt gevonden, zowel op het werk als in jullie eigen huis. Het is fijn dat we elkaar zo makkelijk snappen. Peter-Jan, jij was nog zo jong toen ik ging studeren, maar inmiddels ben je zo volwassen geworden! Ik ben trots op m'n kleine broertje! Jij hebt je draai helemaal gevonden in Nijmegen. Geniet nog lekker van deze mooie periode! Ruud en Rob, jullie ook bedankt voor alle steun en heel veel succes en geluk voor de toekomst!

Lieve Vincent, bedankt voor al je liefde en toeverlaat. Het is zeker niet altijd makkelijk voor je geweest. Toch hielden je goede adviezen en geduld nooit op, en bleef je me onvoorwaardelijk steunen. Je creativiteit heeft zelfs een belangrijke rol gespeeld bij het ontwerp van de cover. En zeker niet minder belangrijk: alle mooie momenten die we samen hebben beleefd zijn een bron van inspiratie geweest voor de afronding van dit proefschrift. Bedankt voor alles en ik kijk uit naar onze toekomst samen.